Czech University of Life Sciences

Faculty of Forestry and Wood Sciences

Department of Forest Genetics and Physiology

Ph.D. Thesis

The effect of drought on soil microbial community dynamics in Norway spruce seed orchards

Author: Ing. Dagmar Zádrapová

Supervisor: doc. Ing. Ivana Tomášková, Ph.D.

Consultants: Dr. Amrita Chakraborty & Dr. Amit Roy

2024

CZECH UNIVERSITY OF LIFE SCIENCES PRAGUE

Faculty of Forestry and Wood Sciences

Ph.D. THESIS ASSIGNMENT

Ing. Dagmar Zádrapová

Forestry Engineering

Forest Biology

Thesis title

The effect of drought on soil microbial community dynamics in Norway spruce seed orchards

---

Objectives of thesis

1. Determination of soil quality parameters in forest soils under different precipitation regimes.
2. Exploring the bacterial and fungal diversity in forest soils under different precipitation regimes.
3. Understanding the bacterial and fungal community structure in the rhizosphere soil at two clonal seed orchards of Norway spruce (Picea abies) under different precipitation regimes.

Methodology

The study took place in two Norway spruce (Picea abies) clonal seed orchards located in south-west of the Czech Republic, namely Prenet (P-site) (49.2354172N, 13.2112808E, 970 m above sea level) and Lipová Lhota (L-site) (49.2816108N, 13.5515606E, 560 m above sea level). The seed orchards were selected for their remarkable long-term differences in the precipitation regime despite their geographical proximity. Both bulk soil and rhizospheric soil samples will be collected at a depth of 10-15cm from the soil surface. Rhizospheric soil will be collected from five Norway spruce clonal tree varieties from each site in replicates. The soil samples will be stored at 4°C to measure soil physicochemical and biochemical properties. The remaining soil samples will be stored at -80°C for PLFA analysis, soil metabolite profiling, and DNA extraction to determine microbial community composition using the next-generation sequencing method. The soil physicochemical properties will cover soil pH, electrical conductivity (EC), total organic carbon (TOC), and total nitrogen (TN) using standard procedures. Selected extracellular enzymes (cellobiohydrolase, b-galactosidase, a-glucosidase, b-glucosidase, b-xylosidase, chitinase and acid phosphatase) present in the soil samples will be measured using microplate-based fluorometric and photometric assays. The metabolite profiling of the soil samples will be analysed using a two-dimensional comprehensive gas chromatography with mass detection (GCxGC-MS). The bacterial and fungal community structure in the forest soils will be determined using Illumina paired-end amplicon sequencing targeting the bacterial 16S and the fungal ITS region. The paired-end reads generated from Illumina sequencing will be further analysed using bioinformatic pipelines such as QIIME. Alpha and beta diversity of the microbial communities present in the two sites will be determined. Furthermore, the putative functional predictions of the bacterial communities in the two sites will be performed using PICRUSt software, while the ecological guild of the fungal communities will be determined using FunGuild software to predict the functional variability of mycobiome on both sites.

The proposed extent of the thesis

100 pages

Keywords

precipitation, climate change, bacterial diversity, fungal diversity, microbiome, amplicon sequencing, PLFA analysis, soil metabolites, rhizosphere

---

Recommended information sources

Baldrian, P. (2017). Forest microbiome: diversity, complexity and dynamics. FEMS Microbiology reviews, 41(2), 109-130.

De Vries, F. T., & Shade, A. (2013). Controls on soil microbial community stability under climate change. Frontiers in microbiology, 4, 52465.

Fierer, N. (2017). Embracing the unknown: disentangling the complexities of the soil microbiome. Nature Reviews Microbiology, 15(10), 579-590.

Chodak, M., Klimek, B., & Niklińska, M. (2016). Composition and activity of soil microbial communities in different types of temperate forests. Biology and Fertility of Soils, 52, 1093-1104.

Nielsen, U. N., & Ball, B. A. (2015). Impacts of altered precipitation regimes on soil communities and biogeochemistry in arid and semi-arid ecosystems. Global change biology, 21(4), 1407-1421.

Rousk, J., Smith, A. R., & Jones, D. L. (2013). Investigating the long-term legacy of drought and warming on the soil microbial community across five European shrubland ecosystems. Global Change Biology, 19(12), 3872-3884.

Schimel, J. P. (2018). Life in dry soils: effects of drought on soil microbial communities and processes. Annual review of ecology, evolution, and systematics, 49, 409-432.

Torsvik, V., & Øvreås, L. (2002). Microbial diversity and function in soil: from genes to ecosystems. Current opinion in microbiology, 5(3), 240-245.

Uroz, S., Buée, M., Deveau, A., Mieszkin, S., & Martin, F. (2016). Ecology of the forest microbiome: highlights of temperate and boreal ecosystems. Soil Biology and Biochemistry, 103, 471-488.

Uroz, S., Ioannidis, P., Lengelle, J., Cébron, A., Morin, E., Buée, M., & Martin, F. (2013). Functional assays and metagenomic analyses reveals differences between the microbial communities inhabiting the soil horizons of a Norway spruce plantation. PloS one, 8(2), e55929.

Expected date
2023/24 SS – FFWS – State Doctoral Examinations

The Dissertation Thesis Supervisor
doc. Ing. Ivana Tomášková, Ph.D.

Supervising department
Department of Forest Genetics and Physiology

Electronic approval: 05. 09. 2024
doc. Ing. Ivana Tomášková, Ph.D.
Head of department

Electronic approval: 05. 09. 2024
prof. Ing. Milan Lstibůrek, MSc, Ph.D.
Chairperson of Field of Study Board

Electronic approval: 05. 09. 2024
prof. Ing. Róbert Marušák, PhD.
Dean

Prague on 06. 09. 2024

Declaration

I hereby declare that this Ph.D. thesis, titled "The effect of drought on soil microbial community dynamics in Norway spruce seed orchards," was independently developed, utilizing appropriately cited literature, and in accordance with the guidance and recommendations provided by my supervisor and consultants.

I consent to the publication of this Ph.D. thesis in accordance with Czech Law (Act No. 111/1998 Coll. Act on Higher Education, as amended). This consent is given regardless of the outcome of the thesis defence.

Prague, September 13th, 2024

Acknowledgement

First and foremost, I would like to thank to my supervisor, doc. Ing. Ivana Tomášková, Ph.D., for her kindness and for offering a helping hand when I needed it the most.

I would also like to express my deepest gratitude to my consultants, Dr. Amrita Chakraborty and Dr. Amit Roy. They are not only exceptional scientists but also some of the kindest people I have had the honour to work with. I am especially grateful to Amit for his vision, determination, and trust in allowing me to be part of this project, as well as for his continual encouragement and motivating words. And to Amrita, for her dedication, wisdom, and patience. She has taught me so much, guiding me through the entire process of writing our publications and this dissertation thesis. I am incredibly proud to share first co-authorship with her on our publications.

I would also like to acknowledge the people without whom none of this would have been possible. Jiří Breitkopf, who showed that Friday the 13th does not have to bring necessarily only bad luck. Arnau Sanz, who has always been there for me and proved that the Erlenmeyer flask can also be used as a rose vase. Jakub Dvořák, for not only sharing the office but also all the highs, lows, and everything in between that comes with pursuing a Ph.D. Shuran Zhao and Liz Vargas, who made the student years at Suchdol truly unforgettable. Petra Kasnarová, for being my trusted companion for more than a quarter of a century. And Jakub Málek, for sharing his passion for lichens with me.

My thanks go to the Czech University of Life Sciences for allowing me to pursue higher education, from my bachelor's degree through to my postgraduate studies, and for providing me with knowledge, experiences, and many great memories. I am also grateful to the Estonian University of Life Sciences for hosting me during my Erasmus program and for letting me be part of their team during my Erasmus+ internship. I also extend my appreciation to the laboratory of Petr Baldrian (Institute of Microbiology, The Czech Academy of Sciences) for their support during the soil enzymatic activity study.

A special note of appreciation goes to Alexandra Elbakyan for her unwavering contributions to academia. This thesis is just one of many that would not exist without her dedication to making science accessible for all.

Finally, and most importantly, I would like to thank my parents. They have supported me from the very first day of elementary school until the last day of my postgraduate studies. Without their unconditional love, support, and encouragement, I would not have achieved what I have today. So, Mom and Dad, thank you for everything.

Dedication

This project was funded by the Internal Grant Agency (IGA) from the Faculty of Forestry and Wood Sciences, Czech University of Life Sciences.

List of publications

Chakraborty, A.*, **Zádrapová, D.***, Dvořák, J., Faltinová, Z., Žáček, P., Cajthaml, T., ... & Roy, A. (2023). Impact of 30 years precipitation regime differences on forest soil physiology and microbial assemblages. *Frontiers in Forests and Global Change*, 6, 1142979. (* Equal contribution)

Author contribution

DZ conducted fieldwork and lab experiments, manuscript writing, read and contributed to the final version of the manuscript.

Zádrapová, D.*, Chakraborty, A.*, Žáček, P., Korecký, J., Bhar, A., & Roy, A. (2024). Exploring the Rhizospheric Microbial Communities under Long-Term Precipitation Regime in Norway Spruce Seed Orchard. *International Journal of Molecular Sciences*, 25(17), 9658. (* Equal contribution)

Author contribution

DZ conducted methodology, fieldwork, manuscript writing, read and agreed to the published version of the manuscript.

Abstract

Climate change profoundly impacts both abiotic and biotic environmental factors in forest ecosystems. Rising temperatures and shifting precipitation patterns alter soil moisture content, which in turn influences the diversity, abundance, and functions of soil microbial communities. However, research on the long-term effects of precipitation variability on forest soil microfauna remains surprisingly limited.

In this study, we investigated the impact of long-term precipitation variation on soil quality parameters and microbial community dynamics in the two Norway Spruce (*Picea abies*) clonal seed orchards: Lipová Lhota (L-site) and Prenet (P-site). Over three decades, precipitation data revealed that the P-site received nearly twice the amount of rainfall compared to the L-site. We analysed the effects of precipitation on both rhizospheric soil and the surrounding bulk soil. By integrating traditional methods with modern multi-omics approaches, we aimed to assess soil texture, physicochemical properties (pH, EC), biochemical parameters (total organic carbon (TOC), total nitrogen (TN)), phospholipid fatty acid (PLFA) content, extracellular enzyme activities, metabolic profiles, along with microbial community structure in the two forest soils.

Our results revealed a positive correlation between TOC, TN, extracellular enzyme activities, and phospholipid fatty acid (PLFA) content in the soil with increased precipitation, while microbial diversity exhibited an opposite trend. The soil metabolite profiles showed distinct variations between the two sites, with a higher abundance of metabolite at the P-site, which receives greater precipitation. Additionally, the rhizospheric soul at the P-site had elevated levels of Aluminium (Al), Iron (Fe), Phosphorus (P), and Sulphur (S) compared to the L-site. Variance partitioning canonical correspondence analysis (VPA) further demonstrated that TOC and TN played a greater role in shaping soil microbial communities compared to soil pH and electrical conductivity. Clear microbiome differences were also observed between the sites. The P-site rhizospheric soil exhibited a higher abundance of Proteobacteria, Acidobacteriota, Ascomycota, and Mortierellomycota, while the L-site showed a higher prevalence of Bacteroidota, Actinobacteria, Chloroflexi, Firmicutes, Gemmatimonadota, and Basidiomycota. A higher clustering coefficient in the P-site rhizospheric soil microbial network indicated a more interconnected and closely clustered microbial community structure.

Overall, our study unveiled the impact of precipitation variability on microbial communities and functions in bulk soil and the rhizospheric microbial associations of two Norway spruce stands. The generated field data provided valuable insights for modelling the effects of long-term precipitation changes on forest ecosystems, offering new perspectives for understanding how the global climate change affects soil microbial associations in forest tree species.

Key words: precipitation, climate change, bacterial diversity, fungal diversity, microbiome, amplicon sequencing, PLFA analysis, soil metabolites, rhizosphere, bulk soil

Table of contents

List of tables, figures, and equations

List of used symbols and abbreviations

16S rRNA	Component of the 30S subunit of a prokaryotic ribosome
ACE	Abundance-based Coverage Estimator
ADONIS	The Analysis of Dissimilarities
AMF	Arbuscular Mycorrhizal Fungi
AMOVA	Analysis of Molecular Variance
ANOSIM	Analysis of Similarity
ANOVA	Analysis of Variance
ASV	Amplicon Sequence Variant
CCA	Canonical Correspondence Analysis
DAA	Differential Abundance Analysis
EC	Electrical Conductivity
EAA	Environmental Association Analysis
FDR	False Discovery Rate
G^+	Gram-positive bacteria
G^-	Gram-negative bacteria
GCxGC-MS	Two-dimensional Comprehensive Gas Chromatography–Mass Spectrometry
GC-MS	Gas Chromatography–Mass Spectrometry
GC-TOF-MS	Gas Chromatography–Time-of-Flight–Mass Spectrometry
ICP-OES	Inductively Coupled Plasma Optical Emission Spectrometry
ITS	Internal Transcribed Spacer
KEGG	The Kyoto Encyclopedia of Genes and Genomes database
LDA	Linear Discriminant Analysis
LEfSe	Linear Discriminant Analysis Effect Size
MD	Modularity
MHB	Mycorrhizae Helper Bacteria
MRPP	Multi-Response Permutation Procedure
NMDS	Non-metric Multidimensional Scaling

OTU	Operational Taxonomic Unit
PCoA	The Principal Coordinates Analysis
PCR	Polymerase Chain Reaction
PICRUSt	Phylogenetic Investigation of Communities by Reconstruction of Unobserved States
PGPR	Plant Growth-Promoting Rhizobacteria
PLFA	Phospholipid Fatty Acids Analysis
rRNA	Ribosomal RNA
SCC	The Spearman Correlation Coefficient
SEM	Standard Error of the Mean
SOM	Soil organic matter
sPLS-DA	Sparse Partial Least Square Discriminant Analysis
SWC	Soil water content
T_m	Melting temperature
TN	Total nitrogen
TOC	Total organic carbon
UniFrac	Unique Fraction Distance
UPGMA	Unweighted Pair-group Method with Arithmetic Means
VPA	Variance Partitioning Canonical Correspondence Analysis

1. Introduction

Ongoing global climate change is significantly affecting the functioning of forest ecosystems. One of the primary consequences of climate change is the shift in precipitation patterns (Ault, 2020; Stocker, 2014), which impacts not only life above ground but also the microbial communities within the soil (Hu et al., 2023).

Soil microbes, particularly bacteria and fungi, play essential roles in maintaining forest ecosystem health. They are crucial for processing of organic matter, driving biogeochemical cycles, and contributing to carbon turnover and sequestration. Microbial activity is especially pronounced in the rhizosphere—a narrow soil zone surrounding plant roots that acts as a microbial hotspot. In this zone, microbes closely interact with plants, aiding in nutrient uptake, producing plant growth hormones, and even protecting plants from pathogens (Philippot et al., 2013).

In addition to factors like temperature, pH, and soil texture, soil moisture is one of the primary determinants of soil microbial community structure and function (Li et al., 2016), influencing nutrient availability in the soil. Consequently, changes in soil moisture resulting from shifts in precipitation patterns can directly or indirectly affect ecosystem functions and processes (Sorensen et al., 2013; Patel et al., 2021).

This study aims to investigate how precipitation and varying soil moisture levels influence edaphic factors and the structure of soil microbial communities in two clonal Norway spruce (*Picea abies*) seed orchards: Prenet (P-site) and Lipová Lhota (L-site). Over the past three decades, the P-site has experienced nearly twice the annual precipitation of the L-site. The study also seeks to characterize the bacterial and fungal microbiota inhabiting the rhizosphere associated with clonal Norway spruce individuals in these genetically identical stands. To achieve this, we used high-throughput sequencing and multi-omics approaches, combined with extensive statistical analysis. Ultimately, this research aims to assess the impact of reduced precipitation on forest soil microbial communities and provide insights into the potential consequences of climate change.

2. Aims and objectives

The research aims to investigate the effect of drought on soil microbial community dynamics in two Norway spruce (*Picea abies*) seed orchards under significantly different precipitation regime. Three main objectives were formulated:

1) Determination of soil quality parameters in forest soils under different precipitation regimes.
2) Exploring the bacterial and fungal diversity in forest soils under different precipitation regimes.
3) Understanding the bacterial and fungal community structure in the rhizosphere soil at two clonal seed orchards of Norway spruce (*Picea abies*) under different precipitation regimes.

3. Literature review

3.1 Forest ecosystems and climate change

Forests cover an estimated area of 38–40 million square kilometres on Earth, thus they present one third of total global land area (Baldrian, 2017). Forest ecosystems are found in majority Earth's biomes and harbour a large proportion of the global diversity (Lladó et al., 2017). Furthermore, forests are involved in many environmental processes of global importance. They take part in carbon sequestration (thus they are an important carbon sink) (Pan et al., 2011), erosion control, biodiversity conservation, and geochemical cycles of elements, such as nitrogen or phosphorus (Bonan, 2008).

Forests, through their many ecological functions, take part in global climate control (Crowther et al., 2015; Pan et al., 2011). However, ironically, it is the climate and its rapid changes that threatens the forests nowadays immensely (Bonan, 2008; Seppälä, 2009; Khaine and Woo, 2015). Global climate change alters the environmental conditions in a rapid speed and threatens even the well-adapted tree stands. Between 1850 and 2019, the global surface temperature has increased by 1.07 °C and is expected to further rise (IPCC, 2023). Consequentially, shifts in total precipitation amount and its interannual distribution (Held and Sonen, 2000; Han et al., 2024), large increases in mean temperature, and pronounced heat waves intensify the chronic forest stress, vulnerability and mortality (Khaine and Woo, 2015). Alterations in precipitation associated with rising temperatures may lead to drought and decreased soil moisture content (Dai et al., 2018; Cook et al., 2018).

Forzieri et al. (2022) estimate that approximately 23% of the world's forests—primarily tropical, temperate, and arid forests—have already reached a critical threshold of resilience against disturbances caused by climate variability and increasing water limitations. And further decline in resilience is expected. Moreover, according to IPCC (2023), global warming of 1.5 °C may lead to near-term high risks for biodiversity loss in forest ecosystems. Due to the strong connections within forest ecosystems, these risks might also be threatening to forest soils and their associated microbial communities.

3.2 Forest soil

Forest soils differ from other soil types, such as grasslands or agricultural soils. Trees largely contribute to the spatial heterogeneity of forest soil by multiple means, including the penetration of soils by the roots, generation of patches of litter and ground vegetation, and changes of the morphology of the terrain during uprooting or the production of deadwood (Hardoim et al., 2015; Štursová et al., 2016).

Residual components from the decomposition of litter and deadwood are accumulated in form of soil organic matter (SOM) further to be transformed by soil microorganisms, mainly fungi and bacteria (Clemmensen et al., 2013).

In forests, unlike in other ecosystems, the identity of the dominant tree species affects both the community composition of soil microorganisms and their enzymatic activity (Baldrian, 2014). It is caused among others by amount of photosynthetic production of the dominant tree taxa or rooting depth of the particular tree individuals (Baldrian and Štursová, 2011). Consequently, the composition of forest soil microbiome differs from that of other soils. For instance, forest soils tend to have a higher fungal biomass and a greater abundance of root-associated ectomycorrhizal fungi compared to agricultural and grassland soils (Baldrian, 2014). Additionally, fungal mycelia growing in forest soils play a crucial role in immobilizing carbon derived from photosynthesis (Clemmensen et al. 2013).

Consequently, forest soils exhibit spatial (both vertical and horizontal) and temporal heterogeneity. They are characterized by strong physicochemical gradients (Huhta and Setälä, 1990), which offer a mosaic of microhabitats for a diverse spectrum of microorganisms, including bacteria, archaea, and fungi. The accumulation of aboveground litter leads to the vertical layering of forest soils. The build-up of recalcitrant organic matter, along with the absence of roots near the soil surface, leads to the formation of a distinct litter layer. This layer is characterized by elevated extracellular enzyme activity of bacterial and fungal decomposers, resulting in higher rates of heterotrophic respiration and rapid decomposition (Žifčáková et al., 2016; Baldrian et al., 2012). Vertical stratification is largely driven by the decline in soil organic matter (SOM) content with increasing soil depth (Šnajdr et al., 2008), which also causes shifts in microbial community composition (O'Brien et al., 2005; López-Mondéjar et al., 2015). Whereas saprotrophs are common in the upper soil layers, bacterial relative abundance tends to increase with depth (Lindahl et al. 2007; Šnajdr et al., 2008). Moreover, microorganisms in the soil are not evenly distributed. As Raynaud and Nunan (2014) point out, bacterial cells tend to form aggregates at the scale of a few micrometres, most likely due to soil structure and bacterial reproduction patterns. This spatial distribution regulates the interactions among microbial individuals.

3.3 Rhizosphere

The understanding of the rhizosphere dates back over a century, when it was first defined as the zone surrounding plant roots that is inhabited by a distinct population of microorganisms, shaped by the chemicals released from the roots (Hiltner, 1904). Indeed, rhizosphere forms the interface between living roots and the bulk soil and is considered a microbial hotspot, because each gram of soil in this

narrow zone can host up to 10^{11} microbial cells (Berendsen et al., 2012). Similarly to bulk soil microbial communities, the rhizospheric microbes also contribute to various ecosystem processes, including soil organic matter decomposition, biogeochemical cycling, and carbon sequestration (Mohanram and Kumar, 2019). Moreover, diverse microbial communities inhabiting the rhizospheric microenvironment play a key role in plant growth and health by enhancing nutrient acquisition from the soil, producing growth-promoting plant hormones, protecting against pathogen infection, and conferring tolerance to abiotic stress (Philippot et al., 2013). These functions are especially important for plants growing in nutrient-poor soils, where nutrients are limited and not easily accessible to roots, which is often the case of forests developed on acidic and nutrient-deficient soils (Uroz et al., 2016). Hence, the rhizospheric microbial communities influence the plant growth and overall ecosystem functioning (Berendsen et al., 2012).

Figure 1 (Lladó et al., 2017) illustrates the key forest soil niches and highlights the main characteristics of their microbial diversity. It provides a comprehensive overview of the spatial distribution of microbial communities across different soil layers and their functional roles within the forest ecosystem.

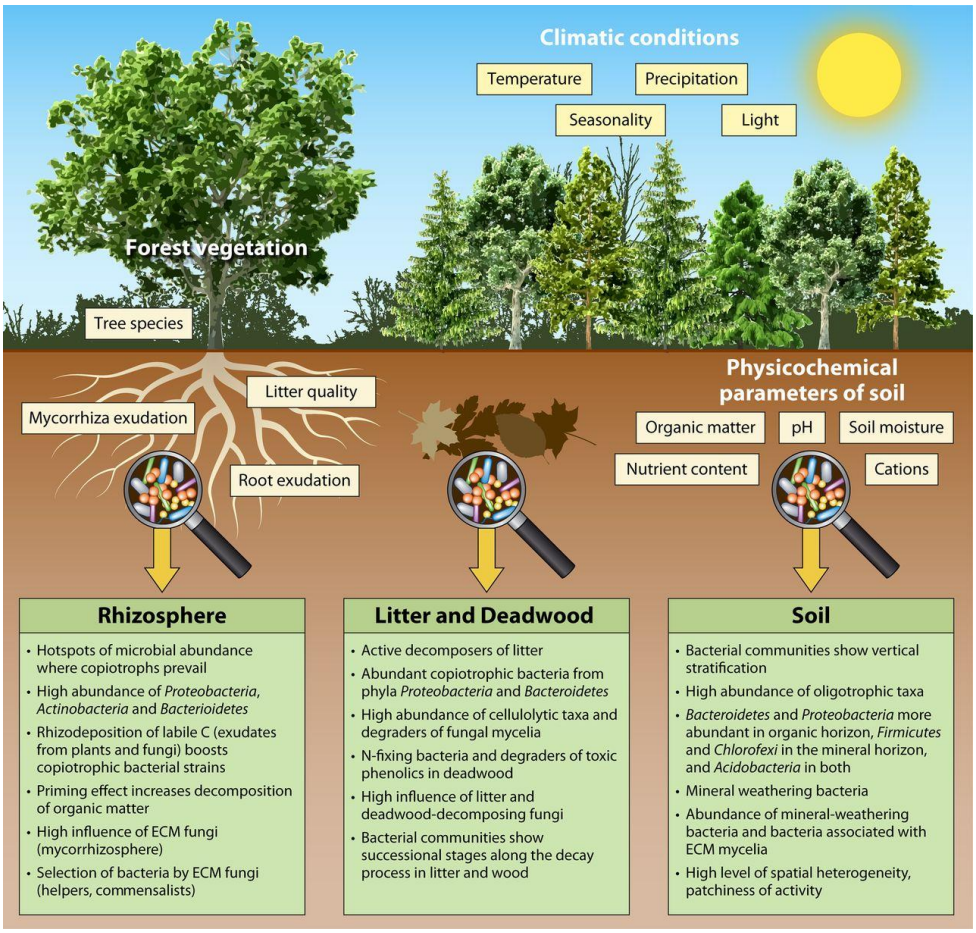

Figure 1 – Spatial distribution of microbial communities in forest soil

Source: Lladó et al., 2017

3.4 Soil microbial communities

Soil microbes represent an immense reservoir of biodiversity in terrestrial ecosystems and are largely responsible for the maintenance of soil quality and functioning (Philippot et al., 2013). The diversity of soil microbial communities directly influences forest health and productivity, contributing to the long-term sustainability of forest ecosystems (Chernov et al., 2021; Mishra et al., 2022). Quite literally, soil microbes bridge the gap between above-ground and below-ground processes in forests, significantly shaping the overall structure of the whole ecosystem (Chang et al., 2017).

More specifically, microbes contribute to soil organic matter processing, organic carbon turnover and sequestration, orchestration of the biogeochemical cycling of various essential elements (i.e., nitrogen, phosphorus, or sulphur), and contribute to soil structure formation and stabilization (Banerjee and Chapman, 1996; Li et al., 2015; Fang et al., 2016; De Feudis et al., 2017; Martinovič et al., 2022; He et al., 2017). In addition, microbes also enhance plant growth, fitness, and resistance by facilitating nutrient uptake, thereby contributing to forest ecosystem productivity and fertility (Uroz et al., 2013; Chodak et al., 2016; Chang et al., 2017; Haas et al., 2018). Figure 2 (Fierer, 2017) highlights a selection of soil biogeochemical processes that are directly modulated by soil microorganisms.

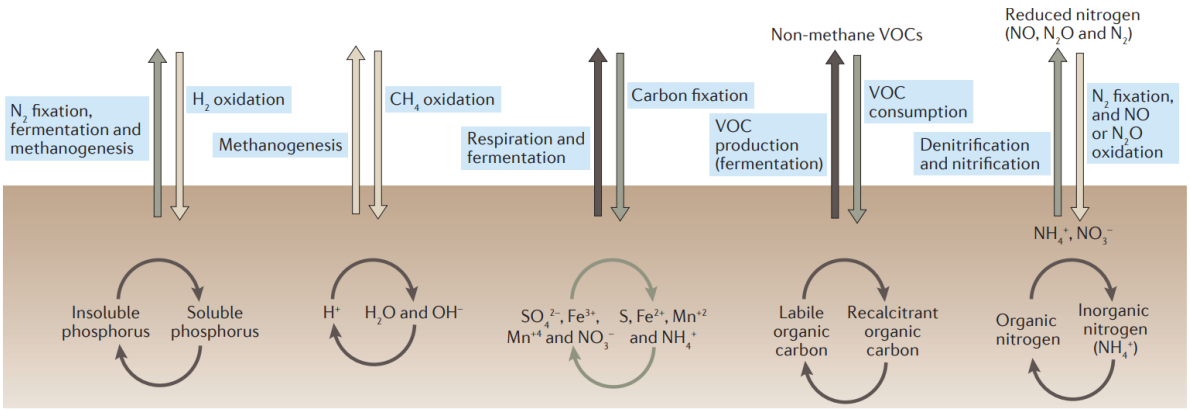

Figure 2 – Soil biogeochemical processes regulated by microorganisms

Source: Fierer, 2017

Several studies have investigated the main biotic and abiotic factors determining the structure and functioning of soil microbial communities. In addition to impacts of soil type, age, mineralogy, and pH, several studies have highlighted the strong link between plants and soil microorganisms (Yu et al., 2014; Jeanbille et al., 2016). Indeed, through litter degradation and the production of nutrients and in their rhizodeposits, plants modify the physical, chemical, and biological properties of their soil environment

(Uroz et al., 2016). In the context of forests, studies investigating the relationship between trees and the adjacent soil microbiome have been conducted on species such as *Populus tremuloides*, *Pinus contorta*, and *Picea engelmannii* (Ayres et al., 2009), and common European forest tree species, including *Picea abies*, *Abies alba, Betula spp., Quercus spp.* (Augusto et al., 2002), as well as *Fagus sylvatica* and *Fraxinus excelsior* (Cezars et al., 2013).

Microbial-driven ecosystem processes are the sum of the activities of microbial cells, most of which are subject to cell-to-cell interactions (Raynaud and Nunan, 2014). Therefore, not only the amount but also the composition of the microbes and their interactions are likely to have significant effects on overall processes. Understanding of microbial composition, their interactions, and the drivers shaping them is therefore critical for maintaining the role of forests in the future (Baldrian, 2017).

The diversity and composition of the rhizospheric microbial community result from the collective influences of plant species (including its genotype and physiological stage), soil properties, and climate (Park et al., 2023; Bakker et al., 2013). Plant species or even specific genotypes tend to assemble relatively distinct rhizobacterial communities (Matthews et al., 2019), and these communities can be remarkably similar even in different environments across geographical regions (Trivedi et al., 2020; Xu et al., 2018). Moreover, rhizosphere microbiota exhibit succession patterns and phylogenetic conservation of rhizospheric competence characteristics, suggesting evolutionary adaptation to host plant species (Shi et al., 2015). Due to the intimate relationship between a plant and its microbiome, the microbiome is sometimes referred to as an extension of the plant genome or a form of the plant's 'genetic outsourcing' (Turner et al., 2013), greatly expanding the plant's functional repertoire (Bakker et al., 2013). A concrete example of a plant partially relying on its associated rhizospheric microorganisms was described by Cook et al. (1995), who observed a strain of *Pseudomonas fluorescens* in the rhizosphere of wheat (*Triticum*) that produced an enzyme similar to those in the plant's enzyme family involved in antibiotic production and defence against fungal diseases. This phenomenon is referred to as specific disease suppression, where certain microorganisms make soils particularly resistant to specific diseases, surpassing the general disease-suppressive properties of soils. In addition to *P. fluorescens*, other microorganisms contributing to suppressiveness have been identified within the *Proteobacteria* and *Firmicutes* bacterial phyla, as well as among fungi from the *Ascomycota* phylum (Berendsen et al., 2012).

The microbial community in the rhizosphere is primarily acquired from the surrounding bulk soil pool (Yan et al., 2017; Ling et al., 2022). Soil microorganisms are chemotactically attracted to plant root exudates, after which they proliferate in this carbon-rich environment (Lugtenberg and Kamilova, 2009). Furthermore, nutrients and signalling molecules present in the root exudates promote the

selection of particular taxa and functions within the vicinity of the root system (Marschner et al., 2004). One hypothesis to explain this selection, known as the 'rhizosphere effect' (Philippot et al., 2013), posits that plants recruit indigenous microbial communities from the soil that are beneficial for improving plant health and nutrition while also preventing the establishment of pathogens. An important aspect of the rhizosphere effect, as noted by Berendsen et al. (2012), is the significantly higher microbial population densities in the rhizosphere compared to the surrounding bulk soil. However, the overall diversity of these communities tends to be lower than that of bulk soil, as plants selectively recruit specific microorganisms from the larger microbial reservoir present in the surrounding soil (Berg et al., 2006).

The rhizosphere-associated microbiome not only tends to have lower diversity than the surrounding bulk soil, but it also differs in its composition. For instance, Ling et al. (2022) observed a 0.9–5.3% decrease in bacterial diversity in the rhizosphere compared to bulk soil, suggesting that the rhizosphere contains only a subset of the broader soil community. Additionally, certain bacterial phyla, such as Proteobacteria and Bacteroidetes, were more prevalent in the rhizosphere, while others, like Chloroflexi, Acidobacteria, and Nitrospirae were significantly reduced. This shift may be attributed to the higher availability of organic carbon and faster nutrient cycling in the rhizosphere, which favour fast-growing bacteria with functions related to carbon transformation and plant pathogenesis, while reducing the abundance of bacteria responsible for processes like nitrification. Figure 3 (Ling et al., 2022) illustrates these patterns of bacterial enrichment and depletion in the rhizosphere compared to bulk soil.

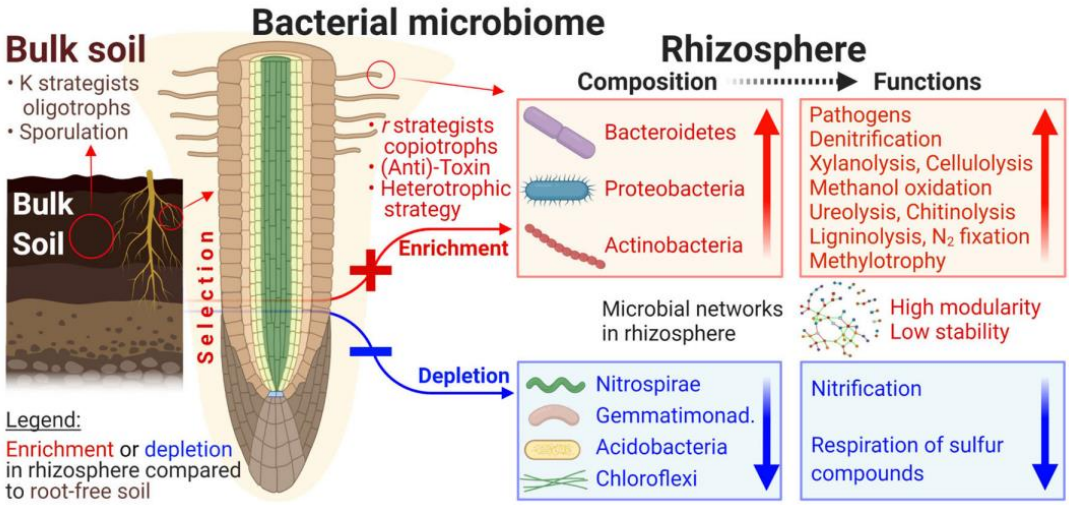

Figure 3 – Abundance and functionality of rhizospheric bacterial taxa

Source: Ling et al., 2022

Notably, the selection of microbes has been shown to shift throughout plant development and root growth, suggesting that this selection process adjusts based on the plant's changing nutritional needs or physiological state (DeAngelis et al., 2009; Chaparro et al., 2014). Given that root exudates vary between plant species, it is expected that the rhizosphere microbiomes of different plant species will also exhibit distinct differences (Bakker et al., 2013).

Due to its importance, the rhizosphere is the focus of many studies. However, despite the vast area covered by forests worldwide and their high importance for global ecosystem, most studies on the rhizospheric microbiome are limited to agricultural ecosystems. There, the in-depth understanding of the stable rhizosphere microbiota is restricted due to the short growth periods of crops (Smalla et al., 2001; Kokalis-Burelle et al., 2017). In contrast, conifers establish their rhizospheric microbial associations through prolonged interactions with the soil environment in forest ecosystems (Mercado-Blanco et al., 2018). Surprisingly, knowledge about the rhizosphere associated with forest trees remains rather limited to date.

3.5 Impact of precipitation on soil microbiota

The increase in the Earth's surface temperature intensifies the global hydrological cycle and alters precipitation patterns (Dietzen et al., 2019), leading to prolonged periods of drought (Dai et al., 2018; Cook et al., 2018). Consequently, shifts in precipitation may affect soil microbiota by altering soil moisture content, nutrient availability, and plant communities (Li et al., 2016; Wu et al., 2020). Water availability is essential for soil microbial growth, biomass, and optimal activity (Bian et al., 2022; Gomez et al., 2021). In the rhizosphere specifically, precipitation is a key abiotic driver influencing its microbial community (Mavrodi et al., 2018). As Bengough (2012) highlights, up to 40% of terrestrial precipitation passes through the small volume of soil surrounding plant roots before being transpired, making the rhizosphere one of the most hydrologically active zones in the biosphere. Hence, changes in precipitation patterns and global warming can alter the structure of soil microbial communities and their functions as a whole (Schimel, 2018).

Specifically, changes in precipitation and warming of the soil are expected to alter microbial community composition, the ratio of bacteria and fungi, and their functions. For instance, studies have shown that microbial activity is directly influenced by osmotic stress or limited substrate diffusion during short-term drought (Schimel, 2018). In contrast, long-term droughts modify soil microbial community composition and subsequently alter nutrient flow and strategies for carbon utilization (Su et al., 2020; Fang et al., 2016; Sridhar et al., 2022). Drought reduces movement of substrates in the soil, lowers the

activity of root-associated microbes, and stresses plants, leading to reduced photosynthesis and belowground carbon allocation (Suseela and Dukes, 2013). Furthermore, water availability, together with temperature, are major drivers of soil microbial respiration (Liu et al., 2016; Bowd et al., 2022). This is especially important because the rate of terrestrial carbon storage depends on the balance between carbon fixed through photosynthesis and that released into the atmosphere via plant and soil respiration (Suseela and Dukes, 2013).

Alternatively, higher precipitation can influence microbial activity by increasing the diffusion of soluble carbon substrates (Hungate et al., 2007; Yan et al., 2011), leading to enhanced plant growth and carbon allocation (Zak et al., 1993; Zak et al., 1994). Nevertheless, the positive correlation between water availability and microbial activity is valid only up to a certain threshold; beyond that, higher water availability can negatively affect microbial activity by reducing oxygen concentration (Horz et al., 2004; Linn and Doran, 1984). Therefore, accurate assessment and future predictions of the carbon budget require a better understanding of the impact of varying precipitation levels on microbe-mediated belowground processes (Nielsen and Ball, 2015; Schimel, 2016).

Over the last few decades, experiments based on altered precipitation have increased significantly (Zhou et al., 2017). While meta-analyses have successfully demonstrated a connection between changes in precipitation and the structure and function of belowground microbial communities, they often struggle to fully capture the extent and direction of these effects, which can vary depending on other climatic factors (Zhou et al., 2017). Unfortunately, most studies have been conducted over short periods of precipitation alteration, limiting their ability to capture the long-term effects of seasonal precipitation differences on the structure and function of forest soil microbial communities. Thus, research on the long-term effects of precipitation on soil physiology, microbial community structure, and function is crucial for addressing existing knowledge gaps and developing more accurate models to predict the impacts of climate change (Zhang et al., 2017).

Few studies have explored the microbial communities in the rhizosphere soil within forest ecosystems and their responses to climate change (Maitra et al., 2024; Fu et al., 2024; Zheng et al., 2020; Morales-Rodríguez et al., 2024). However, overall information on the ecological functions of rhizospheric microorganisms in forest soils under long-term differing precipitation regimes remains scarce. Gaining a deeper understanding of the dynamics and mechanisms governing these communities—particularly in response to changes in precipitation regime—is crucial for improving predictions of how climate change will impact the ecological functions of soil microbes.

3.6 Approaches to exploring soil properties and soil microbial communities

3.6.1 Soil physicochemical properties

The size, composition, and activity of soil microbial communities depend on various biotic and abiotic factors. Several studies have revealed a strong correlation between the structural and functional diversity of soil microbial communities and specific tree species composition (Li et al., 2014; Chodak et al., 2016), the amount of litter, and the quality of soil substrate (Haichar et al., 2008; He et al., 2017; Krashevska et al., 2015). Soil texture, moisture, and temperature are among the most crucial environmental drivers impacting microbial biomass (De Feudis et al., 2017).

Soil texture plays a vital role in carbon storage and strongly affects nutrient retention and availability in forest ecosystems (Silver et al., 2000). For instance, clay-rich soils tend to accumulate organic carbon more rapidly than sandy soils and delay the decomposition of organic matter (Six et al., 2000; Six et al., 2002). In addition, soil texture also influences soil moisture, which in turn impacts organic carbon accumulation by manipulating the quantity of carbon input from plants and the rate of their decomposition in the soil (Zhou et al., 2008; O'Brien et al., 2010).

Soil pH is another critical factor that influences microbial communities, particularly bacteria, due to the higher sensitivity of bacterial cells to narrow pH alterations (Chaparro et al., 2012; Lladó et al., 2017; Fierer and Jackson, 2006; Rousk et al., 2010). This is especially relevant for evergreen tree species, such as Norway spruce (*Picea abies*) and Scots pine (*Pinus sylvestris*), which are known to acidify soils (Uroz et al., 2016). Soil pH presumably also influences the bacterial-to-fungal ratio, as soil acidification can reduce the bacterial abundance while favouring fungal predominance (Coûteaux et al., 1998; Kennedy and Maillard, 2023). This phenomenon can be observed in acidic coniferous soils, where fungal biomass tends to exceed that of bacteria. Alternatively, elevated atmospheric nitrogen deposition causes a shift from fungal predominance to bacterial (Berg et al., 1998; Gao et al., 2016; Coûteaux et al., 1998; Frey et al., 2020).

3.6.2 Soil enzyme activities

Enzymes produced by soil microorganisms play a crucial role in wide range of biological processes, such as the degradation and mineralization of organic compounds, recycling of nutrients like nitrogen (N), phosphorus (P), and sulphur (S), and converting soil biopolymers into forms accessible to microorganisms and plants (Baldrian, 2009). As previously discussed, the dominant tree species in forests play a crucial role in shaping the microbial community composition (Baldrian, 2014). In mixed forests, the presence of different tree species can influence bacterial biomass and community

structure, likely due to factors such as differences in litter quality, rhizosphere effects, or soil moisture variations caused by differing levels of throughfall, as Saetre and Bååth (2000) demonstrated in a mixed stand of Norway spruce (*Picea abies*) and White birch (*Betula pubescens*). Interestingly, even in monoculture forests, soil enzymatic activity varies spatially. For example, Gömöryová (2004) found that catalase activity in a European beech (*Fagus sylvatica*) forest was unevenly distributed, with higher concentrations found near the edges of tree crowns.

In forests, especially, enzymes involved in lignin transformation (such as Mn-peroxidase or lignin peroxidase), cellulose degrading (such as cellobiohydrolase or β-glucosidase), and hemicelluloses degrading (such as β-glycosidases or various esterases) hold an important place. Some enzymes are produced by a wide range of soil microorganisms. For example, enzymes involved in cellulose degradation are produced both by bacteria (for example genera *Streptomyces, Micromonospora* or *Bacillus*) and fungi (such as Ascomycota and Basidiomycota). On the other hand, production of some other enzymes, such as peroxidases, are often associated predominantly with fungi (Boer et al., 2005; Hättenschwiller et al., 2005). Furthermore, some ligninolytic enzymes (namely Mn-peroxidase and lignin peroxidase) are produced exclusively by saprotrophic species of fungi from Basidiomycota (Baldrian, 2009). Thus, measurements of enzymatic activity can serve as an indirect indicator of the activity of specific groups of microorganisms in the soil (Hofrichter, 2002; Baldrian, 2008) and can be a useful approach how to evaluate soil processes in ecosystems with a high turnover of organic compounds, such as in forest (Baldrian, 2009).

Alterations in soil microbial community structure may affect the composition of enzyme production and thus impact the degradation of soil organic matter and other physiological processes in soil (Sinsabaugh, 2010; Fang et al., 2016; Borowik et al., 2022; Wu et al., 2022). Consequently, such shifts in the soil microbial equilibrium affect the energy and nutrients flow within the forest ecosystem and impact the aboveground life.

3.6.3 Phospholipid fatty acids (PLFAs)

Phospholipids are an integral component of the membranes in all living cells, forming a semi-permeable bilayer. Viable cells maintain intact membranes that contain fatty acids as part of their phospholipids. Furthermore, as noted by Lechevalier (1989), phospholipids represent a relatively stable proportion of an organism's biomass.

Phospholipid Fatty Acid (PLFA) analysis present an effective non-culture-based method to evaluate the soil microbial communities in environmental samples (Frostegård et al., 2011; Yao et al., 2015).

It has two main advantages for assessing microbial community structure over the nowadays most widely used DNA-based techniques, as pointed by Zhang Y. et al. (2019). PLFA analysis can provide accurate quantification of microbial biomass and can be therefore more sensitive in detecting shifts in microbial community structure. Another benefit is that phospholipid fatty acids are taken to be indicative of living organisms since phospholipids are assumed to rapidly degrade after cell death.

Consequently, PLFA analysis is a valuable method for detecting rapid changes in soil microbial community structure. Shifts in PLFA patterns can provide early insights into alterations within these communities. Since soil microbes play an essential role in various biogeochemical cycles, changes in their composition and activity are often among the first indicators of soil quality shifts (Zelles, 1999).

3.6.4 Metabolite profiling

Soil contains various chemical compounds produced by the metabolism of plants, microorganisms, and fauna. The range of metabolites found in soil includes low molecular weight (<1,000 Da) compounds such as fatty acids, amino acids, lipids, sterols, sugars, alcohols, organic phosphates, and purines (Withers et al., 2020; Rochfort et al., 2015). These metabolites appear in soil as a direct input or as a product of degradation and they are usually quickly processed by diverse microbial communities residing in soil (Song et al., 2024; Van Hees et al., 2005). Therefore, microbial metabolic activities play a crucial role in determining soil health, which in turn affects the overall health of the ecosystem.

Metabolomics aims to analyse the metabolomes of organisms (Fiehn, 2002) which includes dozens of metabolites originating from both primary metabolism (such as amino acids and sugars), and secondary metabolism (for example flavonoids and terpenoids). Metabolomics can be targeted, which focuses on highly specific detection and quantification of beforehand selected metabolites (Jones et al., 2014; Lu et al., 2008). In contrast, untargeted metabolomics is global and unspecific (Jones et al., 2014) and aims to simultaneously analyse as many metabolites as possible in a single analysis, yielding hundreds of metabolites (Tautenhahn et al., 2012; Rivas-Ubach et al., 2013). This approach enables a broad analysis of the metabolites present in a sample (Vinayavekhin and Saghatelian, 2010). As highlighted by Withers et al. (2020), recent advancements in spectroscopy technologies have made it possible identify and quantify the relative abundance of thousands of metabolites in biological samples (Patti et al., 2012).

Metabolomics has been widely used to analyse metabolic processes in plant physiology (Bundy et al., 2009; Shulaev et al., 2008) and microbiology (Koek et al., 2006). It offers a powerful tool not only for characterizing the structure of microbial communities (Abram, 2015; Graham et al., 2018),

but also for assessing their responses to environmental changes (Bundy et al., 2003; Jones et al., 2013; Jones et al., 2014; Viant, 2008). Metabolite production is regulated not only by gene expression, but it is further modulated by environmental factors (Jones et al., 2013). Furthermore, the metabolome is typically much more susceptible to environmental fluctuations than proteome or transcriptome (Peñuelas and Sardans, 2009). That makes metabolomics a useful method which provides valuable insights into how microbial communities respond to environmental changes (Riedl et al. 2012; Sardans et al., 2011). Additionally, the metabolic products generated by microbes can serve as biomarkers that reflect different soil conditions and shifts in the microbial communities (Jones et al., 2014; Bundy et al., 2009). However, the knowledge on soil microbial metabolome is limited. Untargeted metabolomics analysis may therefore provide an insight into the soil-specific microbial nutrient and cellular pathways and shed a light on how climate change affects soil health (Withers et al., 2020).

However, as White et al. (2017) highlights, it is important to acknowledge that the soil metabolites originate from numerous sources such as soil organic matter, plant exudates, and microbial metabolism. Ascertaining the source of metabolites is challenging, because it is difficult to differentiate the contribution of individual driving factors to the soil metabolite profiles.

3.6.5 High-throughput amplicon sequencing

Until recently, the knowledge of the structure of soil microbial communities was largely based on cultivation-dependent studies. However, nowadays it is recognized that these traditional cultivation-based methods considerably underestimate soil microbial diversity (Fierer, 2017). In fact, only about 1% of microorganisms on Earth can be cultured, while the remaining 99% are unculturable. However, advances in metagenomics, particularly in high-throughput sequencing technologies, now make it possible to analyse complex bacterial communities, including both culturable and unculturable species (Hongoh and Toyoda, 2011). Over the last decade, the development of high-density microarrays has resulted in major advancements in soil microbiome studies (Uroz et al., 2016). At the moment commonly applied DNA-based and RNA-based analyses of the soil microbiome have greatly expanded the knowledge on phylogenetic and taxonomic structure of soil microbial communities (Fierer, 2017). However, it is important to mention that soil contains a wide spectrum of microorganisms, the majority of which still stays uncharacterized (Torsvik and Øvreås, 2002).

High-throughput amplicon sequencing of marker genes has greatly expanded the knowledge of microorganisms living in soils (Lundberg et al., 2012). In most of the studies, 16S ribosomal RNA (rRNA) gene sequencing has been widely used for diversity analysis in the polymicrobial population (Kamble et al., 2020). The 16S rRNA, an approximately 1,600 base pairs long gene, is universally present

in all prokaryotes and includes nine hypervariable regions, namely V1–V9, which differ in the level of their conservation (Wang et al., 2009). Whereas more conservative regions are useful for determining the higher-ranking taxa, less conservative ones can help to identify genus or species (Bukin et al., 2019). Currently, primer sets targeting the V3–V4 hypervariable regions (Klindworth et al., 2013) and the V4–V5 hypervariable regions (Parada et al., 2016) are the most widely used for investigation of bacterial communities (Fadeev et al., 2021). Internal transcribed spacer (ITS) on the other hand, has been selected as the primary DNA barcode for fungi (Schoch et al. 2012). ITS (comprising of two sections: ITS1 and ITS2) is the spacer DNA situated between the small-subunit and the large-subunit of rRNA genes in the chromosome or the corresponding transcribed region (Lindahl et al. 2013).

Thanks to high-throughput amplicon sequencing, many studies have characterized root-associated microbial communities of plants, such as *Arabidopsis thaliana* (Lundberg et al., 2012), rice (Edwards et al., 2015), wheat (Donn et al., 2015), corn (Walters et al., 2018), citruses (Xu et al., 2018), and even some tree species such as *Populus deltoides* (Gottel et al., 2011) or *Fagus sylvatica* (Uroz et al., 2016).

3.6.5.1 Classification of microbial taxa

High-throughput amplicon sequencing generates reads which need to be further processed. Operational Taxonomic Units (OTUs) or Amplicon Sequence Variants (ASVs) are clusters with sequence similarity at the molecular level, and they are commonly used to classify microbial taxa. Both OTU and ASV analyses assume that the taxa clustered within the same OTU/ASV perform similar functions and share the same ecological roles, based on their genetic similarity (Beiko, 2015). A standard threshold for clustering of OTUs is 97% sequence similarity (He et al. 2015). Additionally, OTU can refer to a cluster of uncultivable microorganisms which are grouped according to their DNA sequence similarity detected by a specific taxonomic marker gene, such as 16S ribosomal RNA (rRNA) gene. ASV presents a modification of OTU. This denoising method creates an error model based on the quality of the sequencing run and uses it to differentiate between true biological variation and variations likely caused by sequencing errors. The remaining "true" sequences, which may differ by as little as a single nucleotide, are then classified as distinct ASVs (Chiarello, 2022). Despite this higher resolution up to 99% similarity, the ASV approach generally provides similar ecological insights as OTUs (Glassman and Martiny, 2018). The obtained OTUs and ASVs are then annotated by matching with specific databases such as SILVA[1] in case of bacterial 16S or UNITE[2] in case of fungal ITS.

[1] http://www.arb-silva.de/
[2] https://unite.ut.ee/

3.7 Microbial diversity

Although hidden beneath the surface, soil microbes represent a significant portion of global biodiversity, often rivalling the biomass of plants and animals aboveground. A hectare of soil can hold more than 1,000 kilograms of microbial biomass carbon (Fierer et al., 2009; Fierer, 2017). A single gram of soil may contain up to 10 billion microorganisms, potentially encompassing thousands of species (Torsvik and Øvreås, 2002). In the case of bacteria, a single gram can house up to 10^{10} bacterial cells, with species diversity estimates ranging from 4,000 (Torsvik et al., 1990) to 50,000 species (Roesch et al., 2007).

As outlined in previous chapters, these microorganisms play critical roles in nutrient cycling, carbon sequestration, and both directly and indirectly contribute to the health of aboveground ecosystems (Mohanram and Kumar, 2019). The abundance and composition of these microbes, along with their interactions, have substantial effects on microbe-driven processes. Consequently, various metrics are used to assess microbial richness and diversity within and across different sites. These microbial communities can be categorized at multiple levels using diverse indices, which will be discussed in further detail.

3.7.1 Alpha diversity

Alpha diversity estimates the diversity within a single community (within-sample). It reflects both the number of different species (species richness) and their distribution (species evenness). Therefore, alpha diversity metrics provide insight into the complexity and variability of the microbial community at a specific location, indicating how diverse the community is in terms of species presence and abundance. The selected alpha diversity indices characterizing the microbial community richness ($Chao_1$, Abundance-based Coverage Estimator), diversity (Shannon, Simpson), evenness (Pielou), and sequencing depth (Good's coverage) are detailed in the following chapters.

3.7.1.1 Good's coverage

The Good's coverage index (Chao et al., 1988) is a metric used to estimate the completeness of sampling (sequencing depth) in microbial diversity studies. It gives an indication of what proportion of the total population has been sampled, based on the number of singletons (species observed only once) in the sample. The higher the Good's coverage value (close to 1), the greater likelihood that the sequences present in the sample have been detected. Mathematically, Good's coverage (C) can be expressed as follows:

$$C = 1 - \frac{F_1}{N} \tag{1}$$

where:

- F_1 is the number of singletons (species observed only once),
- N is the total number of individuals or the sum of the abundances of all OTUs.

3.7.1.2 Chao$_1$ index

Chao$_1$ index (Chao, 1984) is a non-parametric estimator used to estimate the total species richness in a community, including unobserved species based on the number of rare species detected. Thus, it is an abundance-based estimator of species richness. A higher Chao$_1$ index denotes a larger quantity of species, suggesting a relatively higher species diversity within the sample. The equation defining the index is as follows:

$$S_{\text{Chao1}} = S_{\text{obs}} + \frac{F_1^2}{2F_2} \tag{2}$$

where:

- S_{Chao1} is the estimated total species richness,
- S_{obs} is the number of observed species in the sample,
- F_1 is the number of singletons (species observed only once),
- F_2 is the number of doubletons (species observed exactly twice).

3.7.1.3 Abundance-based Coverage Estimator (ACE)

ACE (Chao and Lee, 1992; Chao and Yang, 1993) is another richness index and is used to estimate species richness in a community, particularly focusing on rare species. It divides the species into "abundant" and "rare" groups and uses the frequency of the rare species to estimate the total species richness. ACE index is defined as:

$$S_{\mathrm{ACE}} = S_{\mathrm{abund}} + \frac{S_{\mathrm{rare}}}{C_{\mathrm{ACE}}} + \frac{F_1}{C_{\mathrm{ACE}}} \cdot \gamma^2_{\mathrm{ACE}} \quad (3)$$

where:

- S_{ACE} is the estimated species richness,
- S_{abund} is the number of abundant species,
- S_{rare} is the number of rare species ($S_{abund} + S_{rare} = S_{obs}$),
- F_1 is the number of singletons (species observed only once),
- γ^2_{ACE} is the estimated coefficient of variation for the rare species,
- C_{ACE} is the sample coverage estimator for rare species defined as:

$$C_{\mathrm{ACE}} = 1 - \frac{F_1}{N_{\mathrm{rare}}} \quad (4)$$

where:

- N_{rare} is the total number of individuals in the rare group.

3.7.1.4 Shannon and Simpson indices

The Shannon (Shannon, 1948) and Simpson (Simpson, 1949) indices are commonly used to estimate community diversity. These metrics account for both species abundance and their relative abundance (evenness), offering a more detailed understanding of community composition compared to basic species richness alone.

The Shannon index (or Shannon Entropy) is based on the idea that as the number of unique species increases and their relative abundance becomes more evenly distributed, predicting which species will appear next in a sequence becomes increasingly difficult. This concept therefore measures the uncertainty (entropy) in predicting the identity of a randomly selected individual from a dataset.

A higher Shannon index value indicates greater diversity within the community. The formula for the Shannon Index (H') is:

$$H' = -\sum_{i=1}^{S} p_i \ln(p_i) \quad (5)$$

where:

- S is the total number of species (species richness),
- p_i is the proportion of individuals or the relative abundance of species i.

The Simpson index reflects the probability that two entities, randomly selected from a dataset of interest, will belong to the same species. It emphasizes the dominance of species in a community, meaning it gives more weight to dominant species. Therefore, value closer to 1 indicates lower diversity. The formula of Simpson index (D) is given as below:

$$D = \sum_{i=1}^{S} p_i^2 \quad (6)$$

where:

- S is the total number of species,
- p_i is the proportion of individuals of species i relative to the total number of individuals in the community.

3.7.1.5 Pielou index

The Pielou's Evenness Index (Pielou, 1966) is used to measure the evenness of species distribution within a community. It compares the actual diversity (observed species abundance distribution) to the maximum possible diversity (where all species are equally abundant). It ranges from 0 (no evenness – one species dominates the community while the others are rare) to 1 (complete evenness – all species are equally abundant). The formula for Pielou index (J') is:

$$J' = \frac{H'}{\ln(S)} \quad (7)$$

where:

- H' is Shannon-Wiener diversity index,
- S is the total number of species in the community (species richness).

3.7.1.6 Rarefaction curve

A rarefaction curve (Sanders, 1968) is a graphical tool used to estimate species richness by analysing a random subset of individuals or samples from a population. The curve is plotted based on the association between the quantity of individuals and the number of represented species. This method allows for a standardized comparison of species diversity across different datasets by showing the cumulative number of species (or operational taxonomic units, OTUs) as more samples are collected. When the curve flattens, it indicates that most species in the community have been identified, meaning further sampling is unlikely to reveal many new OTUs. In contrast, if the curve remains steep, additional sampling may still uncover a significant number of new species (OTUs). Thus, rarefaction curves provide valuable insight into whether the sequencing depth is sufficient (Deng et al., 2021).

3.7.2 Beta diversity

Beta diversity quantifies the variation in species composition between different communities (between-sample), evaluating how similar or different two communities are in terms of species presence or abundance. To analyse beta diversity of communities, a distance (or dissimilarity) metric is first needed to quantify the distances or dissimilarities between microbial communities. The comparisons of these communities are then made based on these distance measurements. Common distance metrics include the Bray-Curtis index, Jaccard index, and UniFrac distances. UniFrac distances, the phylogenetic beta diversity measures, are particularly useful for microbiome data and are frequently employed to summarize overall microbiota variability (Lozupone et al., 2011; Xia and Sun, 2023). UniFrac distances incorporate the phylogenetic relationships between taxa by assessing the level of divergence between different sequences. Unweighted UniFrac (Lozupone and Knight, 2005) focuses on phylogenetic information and considers only the presence or absence of species, calculating the fraction of unique branch lengths between communities without accounting for species relative abundance. On the other hand, Weighted UniFrac (Lozupone et al., 2007) takes into account the relative abundance of each taxon, adding a proportional weighting to the branch length with abundance difference.

Out of many ordination techniques based on dissimilarity or distance matrix, the Non-metric Multidimensional Scaling (NMDS) is commonly regarded as the most robust unconstrained ordination method in community ecology (Minchin 1987). This indirect gradient analysis, creating an ordination based on a dissimilarity or distance matrix, is specifically useful method to analyse a large number of genes (Taguchi and Oono, 2005). Many studies have used NMDS in analysing microbial communities by constructing ordination plots of samples obtained through 16S rRNA gene sequencing (Che et al.,

2015; Sinclair et al., 2015; LeBrun et al., 2018). Another commonly used distance matrix-based method is the Unweighted Pair-group Method with Arithmetic Means (UPGMA) (Sokal and Michener, 1958) which uses hierarchical clustering to construct phylogenetic trees based on distance data. The closest pairs of taxa are grouped based on a distance matrix with the distances represented in the branch lengths. This method is often used in studies to visualise the phylogenetic relationships within microbial communities (Schreiter et al., 2014; Jovel et al., 2016).

Significant variation of the soil microbial communities can be determined by statistical methods, such as ADONIS (Anderson, 2001), Analysis of Similarity (ANOSIM) (Clarke, 1993), and Multi-Response Permutation Procedure (MRPP) analysis (Cai, 2006). ADONIS is a non-parametric multivariate test based on distance matrices that evaluates differences between sample groups and determines their significance through permutation tests (Stat et al., 2013). ANOSIM, utilizing the UniFrac distance matrix, provides a way to evaluate whether there is a significant difference in species composition between groups in sampling unit. Thus, it tests if the variation between groups is significantly greater than within groups (Chapman and Underwood, 1999). MRPP, on the other hand, assesses the strength and significance of sample clustering and explores associations between microbial communities and environmental factors by examining average distances (Mielke, 1991).

Another statistical tool often used in microbiome studies is Linear Discriminant Analysis Effect Size (LEfSe) (Segata et al., 2011). It is used in microbial ecology and bioinformatics to identify features (typically microbial taxa or genes) that are significantly different between the groups. It combines standard statistical tests with Linear Discriminant Analysis (LDA) to estimate the effect size of each feature, indicating how strongly it differentiates the groups. LEfSe is particularly popular in microbiome studies to identify specific microbes that are associated with different conditions (for example environmental factors) and these microbes can be used as biomarkers distinguishing between the groups (Chang et al., 2022).

3.7.3 Microbial functional prediction

Microbes perform a wide range of vital functions in soil ecosystems. While high-throughput amplicon sequencing can generate sequences and operational taxonomic units (OTUs) that reveal the richness and composition of microbial communities, this approach does not provide insight into the biological processes or functional roles of the identified microbes (Toole, 2021). To predict the metabolic functions of soil microbes, the microbial composition from amplicon sequencing can be mapped to reference databases of microbial genomes. For instance, bacterial 16S ASVs can be aligned with

functional databases like the Kyoto Encyclopedia of Genes and Genomes (KEGG)[3] (Kanehisa et al., 2012), PFAM[4] (Mistry et al., 2021), and Enzyme Commission (EC)[5] (Bairoch, 2000) to predict different potential functional roles of bacterial communities in soil samples. Similarly, the putative functions of the fungal communities in soil can be determined by categorizing fungal ASVs based on their ecological guilds using tools such as FUNGuild[6] (Nguyen et al., 2016).

Functional predictions are particularly valuable in complex environments like soils (Quince et al., 2017; Diamond et al., 2019), but it is important to note that these predictions are based on computational models and may not fully reflect the actual *in situ* scenario. Therefore, further experimental validations are often necessary to confirm these predicted functions.

3.7.4 Microbial co-occurrence networks

Soil is a complex habitat inhabited by numerous microbial taxa. Many studies examining soil microbial communities primarily focus on the diversity within individual samples (alpha diversity) or the relative abundance of taxa and the similarities between different communities (beta diversity). However, less attention has been given to using sequencing data to investigate the direct or indirect interactions between microbial taxa that coexist in environmental samples. This is significant because, as previously mentioned, ecosystem processes driven by microbes are a result of both individual microbial activities and their interactions with one another (Raynaud and Nunan, 2014). Microorganisms thrive within intricate association networks, rather than functioning in isolation. Species that are highly interconnected likely play critical roles within microbial communities (Liu et al., 2024). Therefore, both the quantity and composition of microbes, along with their interactions, can significantly influence overall ecological processes.

Network analysis provides a mathematical approach to uncover the complexity of relationships within a microbial community. In this framework, microbes are represented as nodes, while the interactions and associations between them are depicted as edges (Guseva et al., 2022). In microbial communities—particularly in environments as complex as soil—interactions between taxa are typically inferred indirectly through co-occurrence data, since these interactions are not directly observable *in situ*.

[3] http://www.genome.jp/kegg/
[4] http://pfam.xfam.org/
[5] https://enzyme.expasy.org/index.html
[6] https://github.com/UMNFuN/FUNGuild

As a result, network analysis relies on the observation of species co-occurrence patterns within molecular microbial datasets, such as those obtained from 16S rRNA amplicon sequencing (Röttjers and Faust, 2018), and this is commonly referred to as microbial co-occurrence network analysis.

Network analysis has become a well-established tool for examining species interactions within ecosystems (Bascompte, 2009; Poisot et al., 2016), as it goes beyond traditional measures of alpha and beta diversity (Chaffron et al., 2010; Barberán et al., 2012). By integrating diverse types of information, networks can reveal patterns at the systems level (Röttjers and Faust, 2018).

3.8 Environmental Association Analysis (EAA)

Environmental Association Analysis (EAA) is an approach used to identify links between microbial community structures and site-specific environmental factors. EAA provides insights into how environmental variables affect the composition, diversity, and functional potential of soil microbial communities, illustrating how these communities respond to environmental changes (Rellstab et al., 2015). Various methods are available to connect microbial communities with their environmental drivers.

One way to evaluate the relationship between microbial abundance and environmental factors is through Spearman's rank correlation (Spearman, 1904), a non-parametric statistical metric that measures the nonlinear monotonic relationship between two variables (Fujita et al., 2009). It identifies whether an increase (or decrease) in one variable tends to correspond to an increase (or decrease) in another. The correlation ranges from 1 (a perfect positive correlation, where both variables increase in a perfectly monotonic relationship) to −1 (a perfect negative correlation, where one variable increases while the other decreases in a perfectly monotonic way). A value of zero signifies no correlation and no monotonic relationship between the variables. Additionally, the Mantel test (Mantel, 1967) can be used to examine the correlation between two distance matrices, typically to assess whether spatial or environmental distances correlate with biological, genetic, or ecological distances. The Mantel test is commonly used to evaluate the relationship between geographic distance and genetic divergence (Diniz-Filho et al., 2013).

Another widely used method is Canonical Correspondence Analysis (CCA) (Ter Braak, 1986), which explores how soil microbial communities vary in response to environmental factors. CCA identifies key environmental factors shaping the composition and structure of microbial communities by comparing a matrix of species abundances with a matrix of environmental variables from the same site. An extension of CCA is Variance Partitioning Canonical Correspondence Analysis (VPA or VP-CCA) (Borcard et al., 1992; Legendre and Anderson, 1999), which partitions the variation in microbial community composition into components explained by different sets of environmental variables. The aim of variance partitioning is to determine how much variation in community composition can be attributed to distinct categories of environmental factors, as well as to quantify the relative importance of these factors. Any residual variation represents unexplained variance not accounted for by the included explanatory variables.

4. Materials and methods

4.1 Seed orchards

For this study, two Norway spruce (*Picea abies*) clonal seed orchards were selected: Prenet (P-site) (49.2354172N, 13.2112808E) and Lipová Lhota (L-site) (49.2816108N, 13.5515606E), both located in the southwest of the Czech Republic (Plzeň Region, Klatovy county). The maps in Figure 4 depict the locations of both sites on both a larger and smaller scale.

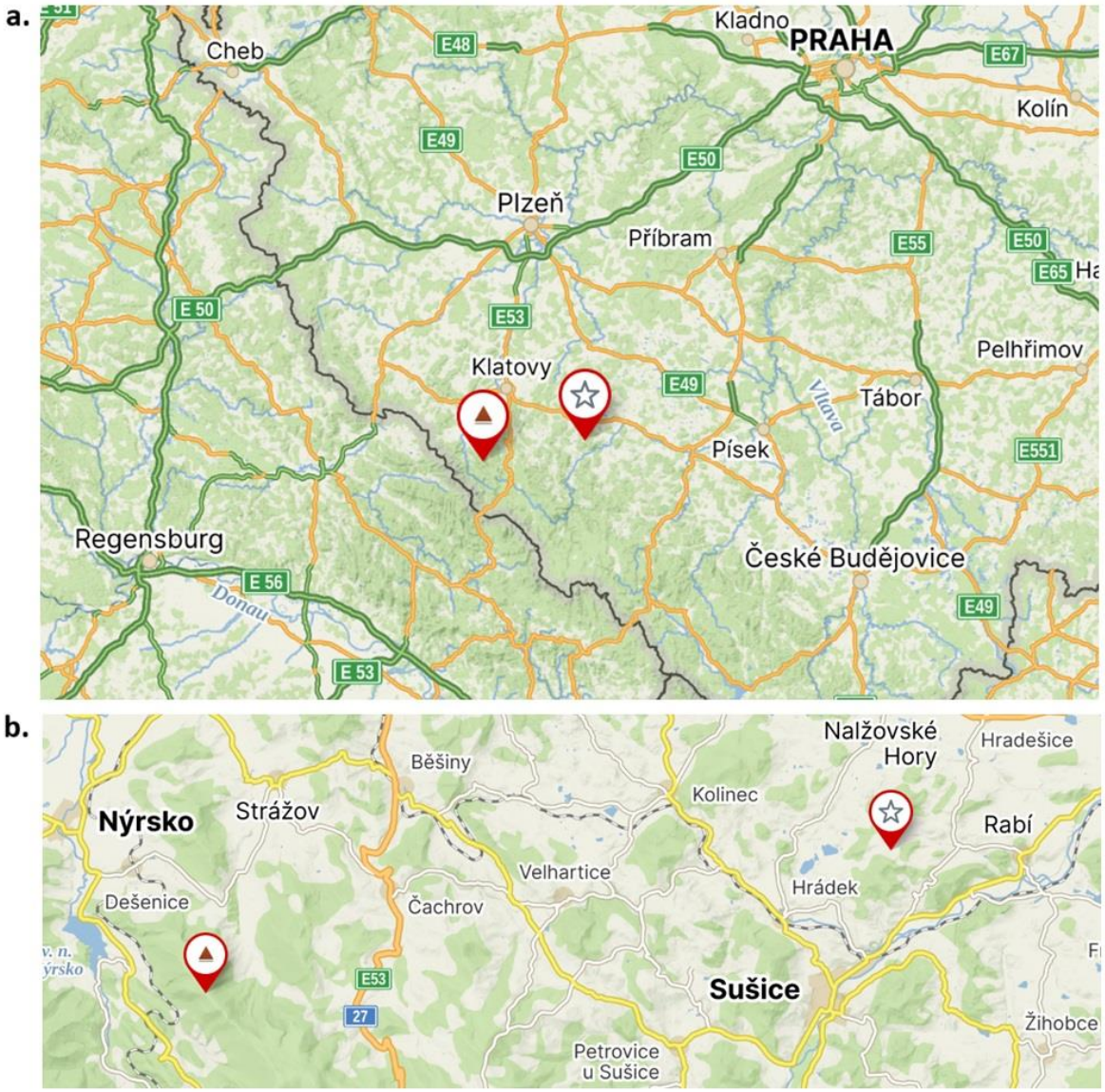

Figure 4 – Location of L-site and P-site seed orchards

Location of the Lipová Lhota and Prenet study sites on **(A)** larger and **(B)** smaller scale (Source: mapy.cz)

These orchards were established as part of a breeding program aimed at preserving the gene pool of Norway spruce from the Modrava region. The project's goal was to select indigenous Modrava Norway spruce individuals and create seed orchards that could produce seeds suitable for reforestation in the highest elevations of the Šumava Mountains.

The Lipová Lhota seed orchard was officially established in 1984, using ramets from 64 spruce individuals from the Modrava forest district (altitudes of 1180–1350 meters above sea level). The Prenet seed orchard followed five years later in 1989, utilizing the same ramets. The establishment of the second seed orchard at a higher altitude was due to concerns about the potential impact of long-distance pollen transfer from the lower altitudes in Lipová Lhota, which could compromise the use of seeds for reforestation in the highest elevations of the Šumava Mountains. Establishing two orchards with identical clones at different altitudes enables the investigation of growth variations and other characteristics among the clonal individuals. Additionally, it allows for comparative studies of the surrounding environment such as soil conditions.

4.2 Climatic data

Despite their geographical proximity of approximately 25 kms, the seed orchards display remarkably different environmental conditions, as highlighted in Table 1. Over the past 30 years, the recorded average annual temperature in Prenet was 1.56°C lower than in Lipová Lhota. In contrast, Prenet received more than twice the average annual precipitation compared to Lipová Lhota. Boxplots in Figure 5 visualise the significant variability in average annual precipitation (A) and temperature (B) between the study sites.

Table 1 – Selected environmental conditions in L-site and P-site

	Lipová Lhota (L)	**Prenet (P)**
Altitude [MASL]	560	970
Slope [%]	9	14
Tree spacing [m]	5 × 5	6 × 6
Average annual temperature [°C]	8.6	7.04
Average annual precipitation [mm]	633	1306.48

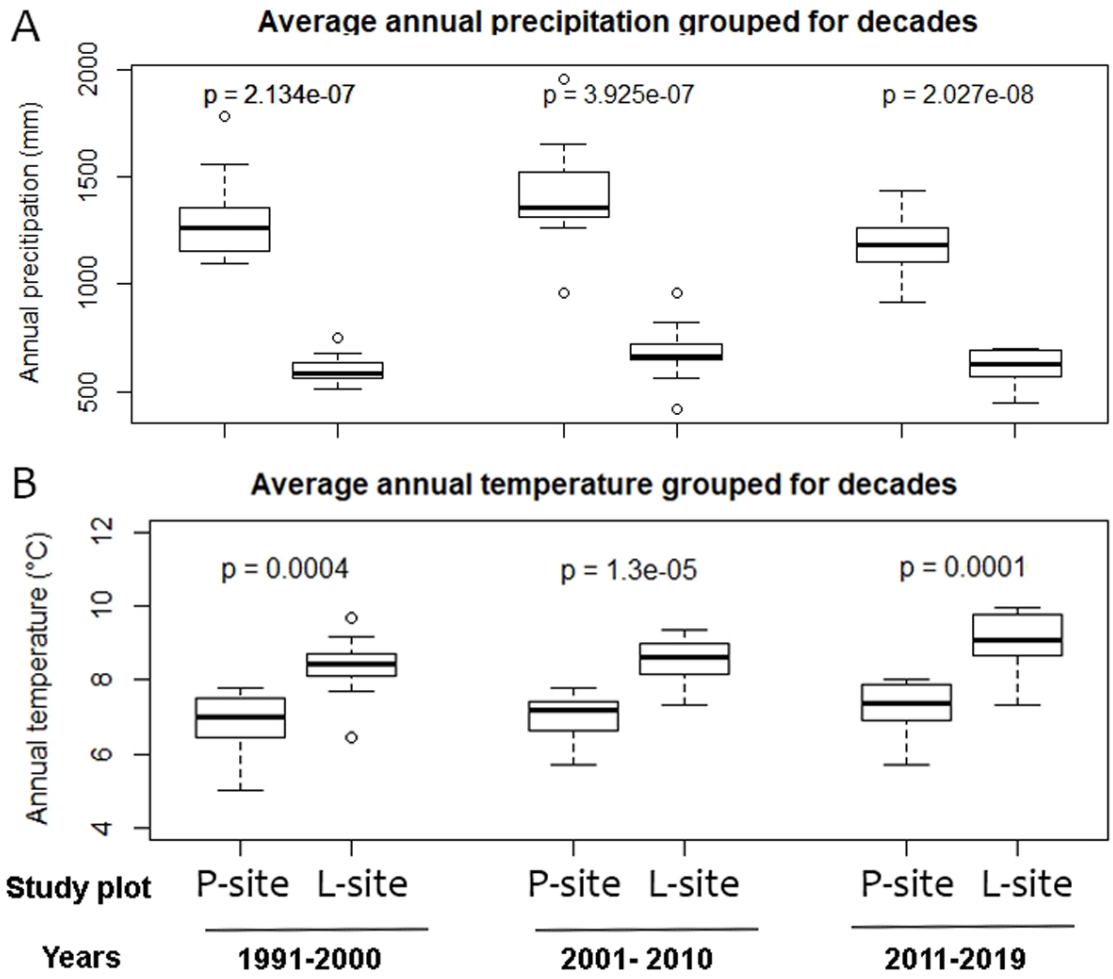

Figure 5 – Variability in selected environmental factors

Variation in **(A)** average annual precipitation and **(B)** average annual temperature between the L-site and P-site study sites recorded over a period of more than 30 years.

4.3 Sample collection

Sampling of soil and rhizosphere took place between October and November 2019.

4.3.1 Bulk soil sampling

Bulk soil samples were obtained at a depth of 10 cm below the surface using a root corer (Eijkelkamp, Netherlands). Six randomly chosen samples from Prenet and nine from Lipová Lhota were collected to account for the difference in land size between the two seed orchards (L-site > P-site). In total, 15 samples were placed in sterile plastic zip-lock bags and transported to the laboratory for further analysis. The samples were first sieved using a 2.0 mm screen sieve. Some were kept at 4°C for later analysis of soil physicochemical and biochemical properties, while the rest were frozen at –80°C

for PLFA analysis, soil metabolite profiling, and DNA extraction to investigate microbial communities through next-generation sequencing. Physicochemical properties were measured using air-dried soil samples, whereas enzyme activity assays were conducted on moist field samples. All results were reported based on the soil's dry weight.

4.3.2 Rhizosphere sampling

For the sampling of rhizospheric soil, five Norway spruce clonal tree varieties (1901, 1902, 1908, 1941, and 1950) were selected. Each of these grafted clonal tree varieties had five tree replicates as shown in detail in Table 2.

Table 2 – Rhizosphere sampling details

Grafted clonal Spruce variety	Trees	L-site	P-site
1901	A	L1901_A	P1901_A
	B	L1901_B	P1901_B
	C	L1901_C	P1901_C
	D	L1901_D	P1901_D
	E	L1901_E	P1901_E
1902	A	L1902_A	P1902_A
	B	L1902_B	P1902_B
	C	L1902_C	P1902_C
	D	L1902_D	P1902_D
	E	L1902_E	P1902_E
1908	A	L1908_A	P1908_A
	B	L1908_B	P1908_B
	C	L1908_C	P1908_C
	D	L1908_D	P1908_D
	E	L1908_E	P1908_E
1941	A	L1941_A	P1941_A
	B	L1941_B	P1941_B
	C	L1941_C	P1941_C
	D	L1941_D	P1941_D
	E	L1941_E	P1941_E
1950	A	L1950_A	P1950_A
	B	L1950_B	P1950_B
	C	L1950_C	P1950_C
	D	L1950_D	P1950_D
	E	L1950_E	P1950_E

Rhizospheric soil samples were gathered from a depth of 15 cm for each clonal tree replicate from the two sites. Since the trees were grafted and have different root systems, the variations in the rhizosphere microbiome among the clonal tree varieties were not considered. For each clonal tree variety, five rhizosphere soil samples were randomly taken from a distance of 20–30 cm from the trunk and approximately 10 mm from the roots. In total, 50 soil samples (25 from each site) were collected in sterile plastic zip-lock bags, transported to the laboratory, and sieved through a 2.0 mm screen sieve. Similarly to bulk soil samples, part of the samples was stored at 4°C for analysis of soil properties, while the remaining samples were frozen at –80°C for soil metabolite profiling and DNA extraction. These samples were used to assess microbial community structure through amplicon sequencing, targeting the bacterial 16S rRNA gene and the fungal ITS2 region.

4.4 Soil texture and water content determination

The soil particle size distribution was determined using a laser granulometer (CILAS 1190 LD) to measure particle sizes from 0.04 to 2,500 mm in wet mode. The soil samples were pretreated following the method outlined by Lisá et al. (2017). Three separate measurements were conducted: the first was taken after the sample had reacted with a KOH solution for 10 minutes to ensure proper dispersion. The second measurement was performed on the same sample after carbonates were removed through a 10-minute reaction with 35% concentrated HCl. The third dispersion aimed to eliminate any organic matter using the reaction with H_2O_2. The soil texture was classified into three fractions: clay (<2 µm), silt (2–63 µm), and sand (63–2,000 µm), according to Wentworth (1922). Soil water content (SWC, %) was determined by oven-drying 5 g of soil at 105°C for 24 hours, and the results were reported based on the soil's dry weight.

4.5 Trace elements in soil

Presence of the trace elements (Al, Ca, Fe, K, Mg, Mn, Na, P, S, Si, Zn) in the rhizospheric soil was determined following the Mehlich 3 (M3) extraction procedure (Mehlich, 1984). The M3 extraction solution consisted of 0.2M acetic acid (CH_3COOH), 0.25M ammonium nitrate (NH_4NO_3), 0.015M ammonium fluoride (NH_4F), 0.013M nitric acid (HNO_3), and 0.001M ethylenediaminetetraacetic acid (EDTA) [$(HOOCCH_2)_2\ NCH_2CH_2N(CH_2COOH)_2$] at pH 2.5±0.1. The air-dried soil was extracted with 1:10 (m/v) soil: M3 solution for 10 min, and the extract was measured by ICP-OES using ICP-OES Agilent 5100 (Zbíral, 2016). All the results were reported based on the soil's dry weight. The level of significance was determined using the student’s t-test ($p < 0.05$).

4.6 Soil physicochemical and biochemical properties

Soil physicochemical and biochemical properties, including soil pH, electrical conductivity (EC), total organic carbon (TOC), and total nitrogen (TN), were analysed following standard procedures. Soil pH (in a 1:5 H_2O ratio, w/v) was measured using an ISFET electrode (Sentron, Netherlands) after the equilibrium between hydrogen ions in the solution and hydrogen ions bonded to the sorption complex of the sample was established. EC was determined based on the increase in the specific electrical conductivity of the extracted infusion (water-soluble electrolytes were extracted in a 1:25 H_2O m/V) after filtration. TOC was calculated from total carbon by subtracting the correction for carbonates present in the sample[7]. TOC was quantified using the dry oxidative combustion method to CO_2 at 1,250°C with a TOC analyser (SSM-5000A; Shimadzu Corp., Kyoto, Japan) as described by Nelson and Sommers (1982). TN content in the soil was determined using the Kjeldahl method (Bremner, 1996). Statistical significance was evaluated using the Kruskal-Wallis test.

4.7 Extracellular enzyme activities in soil

A total of seven hydrolytic soil extracellular enzymes were assessed using microplate-based fluorometric and photometric assays as outlined by Baldrian (2009). The enzymes cellobiohydrolase, β-galactosidase, α-glucosidase, β-glucosidase, and β-xylosidase are involved in the degradation of organic carbon, whereas chitinase and acid phosphatase catalyse nitrogen and phosphorous transformation in the soil (Bell et al., 2013).

To measure enzyme activity, 1 g of moist field soil was suspended in 100 ml of distilled water and subjected to sonication for 4 min. A 200 µl aliquot of this soil suspension was then added to a 50 µl solution of methylumbelliferyl (MUF, pH 7.0) in a 96-well plate and incubated at 40°C. Fluorescence readings were taken at 5 and 125 min using a fluorescence reader (Infinite, TECAN, Austria), with excitation at 355 nm and emission at 460 nm (Baldrian, 2009). A standard curve was created from serial dilutions of 4-methylumbelliferone (MUF) (Vepsäläinen et al., 2001). Enzyme activity was calculated from the fluorescent readings using the standard curve and expressed as nmol g^{-1} soil × h^{-1} after correcting for dry weight.

[7] If the carbonates in the sample are removed beforehand, the organic carbon is determined directly.

4.8 Phospholipid fatty acids (PLFA) analysis

The PLFAs were extracted using the protocols previously described by Stella et al. (2015) and Šnajdr et al. (2008). Phospholipids were extracted from 1 g of freeze-dried soil using a mixture of chloroform-methanol-phosphate buffer (1:2:0.8), purified using a solid-phase extraction cartridge (LiChrolut Si-60, Merck, White House Station, NJ, USA), and subjected to mild alkaline methanolysis. The free methyl esters of PLFAs were then analysed by gas chromatography-mass spectrometry (GC-MS) (450-GC, 240-MS ion trap detector, Varian, Walnut Creek, CA, USA).

The fungal biomass in the soil samples was determined based on 18:2ω6,9 fatty acid content, while the bacterial biomass was estimated as the sum i14:0, i15:0, a15:0, 16:1ω5, 16:1ω7, 16:1ω9, 10Me-16:0, i16:0, i17:0, a17:0, cy17:0, 17:0, 10Me-17:0, 18:1ω7, 10Me-18:0, 15:0, and cy19:0. Actinobacteria biomass was quantified according to 10Me-16:0, 10Me-17:0, and 10-Me18:0. The sum of all the identified lipids was used to estimate the total microbial biomass (total PLFAs). Different microbial ratios such as fungal:bacteria biomass, actinobacteria:bacteria, and G^+ bacteria:G^- bacteria were also calculated (Moore-Kucera and Dick, 2008).

4.9 Metabolite profiling

For the extraction of soil metabolites, freeze-dried samples stored at –80°C were homogenized using a mortar and pestle. The extraction process followed a protocol by Song et al. (2020), which was modified from Swenson and Northen (2019). Homogenized soil (500 mg) was mixed with 600 µl of a methanol solution (H_2O 3:1, v/v) and 600 µl ethyl acetate, along with 10 µl of adonitol [0.5 mg/ml, internal standard A (IS_A)]. The mixture was sonicated with an ultrasonic rod homogenizer (30 s, 50%, 30 kHz) and incubated in a thermoshaker for 15 min at 10°C and 2,000 rpm, followed by centrifugation at 16,000 g for 15 min at 4°C. The supernatant was collected, and the extraction steps were repeated for the soil pellet. All supernatants were pooled and vacuum-dried using a vacuum concentrator without heating (Modul 4080C, Hanil Science Industrial). The dried samples were resuspended in 50 µl of anhydrous pyridine and 50 µl of methoxyamine hydrochloride in pyridine (25 mg/ml) and incubated at 40°C for 90 min at 1,700 rpm. To this solution, 100 µl of N,O-Bis(trimethylsilyl)trifluoroacetamide with trimethylchlorosilane (BSTFA + TMSC) was added and incubated at 40°C for 30 min. Finally, 10 µl of 1-bromoeicosane [0.52 mg/ml in hexane, internal standard B (IS_B)] was added, mixed, and centrifuged for 5 min and 3,000 rpm. The supernatant was transferred for analysis in a GCxGC-MS.

The samples were analysed using a two-dimensional comprehensive gas chromatography with mass detection (GCxGC-MS; Pegasus 4D, Leco Corporation) controlled by ChromaTOF v4.5. The gas chromatograph is coupled with a time-of-flight mass spectrometer (GC-TOF-MS, Pegasus 4D, Leco corporation). A combination of non-polar and polar separation columns was used for the GCxGC analyses: Primary column; Rxi-5SilMS (29.5 m 0.25 mm, Restek); Secondary column BPX-50 (1.44 m 0.1 mm, SGE). Other parameters were set as follows: inlet temperature 300°C, injection volume 1 ml in split 10 mode, constant He flow 1 ml/min, modulation time 3 s (hot pulse 1 s), modulation temperature offset to the secondary oven 15°C, transfer line temperature 280°C, ion source temperature 220°C, mass range m/z 85–1,000. Temperature program applied to the primary oven: 50°C (hold 1 min) with a gradual increase to 190°C (8°C/min) followed by an increase to 220°C (4°C/min) and then to 320°C (8°C/min) with 12 min hold. The same program was applied to the secondary oven with a temperature offset of +5°C. Two-dimensional chromatograms of the analyses were aligned and processed in Statistical Compare, an in-build module of ChromaTOF v4.5 software.

Metabolites were analysed as trimethylsilyl derivatives and normalized according to the weight taken to the extraction and internal standards IS_A and IS_B. The metabolites were identified by comparing their mass spectra with those available in NIST Library, Fiehn Library, and the in-house-built mass library. If available in the mass databases, retention indices were determined using linear hydrocarbons with the retention indexes (based on linear hydrocarbons). Statistical analysis included a sparse PLS discriminant plot using the sPLS-DA algorithm (Lê Cao et al., 2011) and normalized data evaluation in MetaboAnalyst 5.01 (Chong et al., 2019). Soil samples were clustered using Euclidean distance, and metabolites were grouped using Ward's Clustering Algorithm. T-tests and ANOVA were used to assess the significance of metabolite differences across the soils.

4.10 DNA extraction

For sequencing, soil DNA was extracted from all samples of biological replicates that had been stored at –80°C. Around 250–300 mg (depending on the soil texture) of soil was used for each extraction, utilizing the Nucleospin Soil DNA Purification Kit (Macherey Nagel, Germany) according to the manufacturer’s protocol (minor protocol modifications are listed in footnotes).

Approximately 250 mg of fresh sample material was transferred into a NucleoSpin Bead Tube Type A containing the ceramic beads and 700 µL of Buffer SL1 or Buffer SL2[8] was added. Then, lysis conditions

[8] Buffer SL1 proved to be more effective than SL2 for soil DNA extraction.

were adjusted by adding 150 µL of Enhancer SX[9] into the tubes with pre-prepared samples. Afterwards, sample lysis was secured by vortexing the samples at full speed and room temperature (18–25 °C) for 5 min. To precipitate the contaminants, samples were then centrifugated for 2 min at 11,000 x g in order to eliminate the foam caused by the detergent. Afterwards, 150 µL of Buffer SL3 was added and samples were vortexed for 5 s, followed by 5 min incubation at 0–4°C and then the samples were centrifuged for 1 min at 11,000 x g. To filtrate the lysate, NucleoSpin Inhibitor Removal Column was placed in a Collection Tube (2 mL, lid). 700 µL of clear supernatant from the previous step was loaded into the filter and then centrifuged for 1 min at 11,000 x g. In case of visible pellet in the flow through, clear supernatant was transferred to a new collection tube. To adjust the binding conditions, 250 µL of Buffer SB was added and the sample was vortexed for 5 s[10] with a closed lid. In the DNA binding step, the NucleoSpin Soil Column was placed in a Collection Tube (2mL), 550 of µL the sample was loaded into the column and then the sample was centrifuged for 1 min at 11,000 x g. The flow-through was discarded and the column was placed back into the Collection tube. Remaining sample was loaded into the column and centrifuged for 1 min at 11,000 x g. Again, the flow-through was discarded and the column was placed back into the Collection tube. Afterwards, the washing of the silica membrane with bound DNA was performed by four consecutive washings. In the first washing, 500 µL of Buffer SB was added into the NucleoSpin Soil Column and the sample was centrifuged for 30 s at 11,000 x g. The flow-through was discarded and the column was placed back into the Collection tube. In the second washing, 550 µL of Buffer SW1 was added into the NucleoSpin Soil Column and the sample was centrifuged for 30 s at 11,000 x g. Again, the flow-through was discarded and the column was placed back into the Collection tube. In the third washing, 700 µL of Buffer SW2 was added into the NucleoSpin Soil Column. Sample was then vortexed with the closed lid for 2 s and then centrifuged for 30 s at 11,000 x g. Again, the flow-through was discarded and the column was placed back into the Collection tube. Lastly, in the fourth wash, 700 µL of Buffer SW2 was added into the NucleoSpin Soil Column, vortexed with the closed lid 2 s, and then centrifuged for 30 s at 11,000 x g. The flow-through was discarded and the column was placed back into the Collection tube. To dry the silica membrane with bound DNA, the sample was centrifuged for 2 min at 11,000 x g. The last step was the DNA elution when the NucleoSpin Soil Column was placed into a new microcentrifuge tube. 50 µL[11] of Buffer SE was added into the column and the sample was incubated for 1 min at room temperature (18–25 °C) with opened lid. Afterwards, the lid was closed, and the sample was centrifuged for another 30 s at 11,000 x g.

[9] This step was omitted, because Enhancer SX did not have an impact on soil DNA yield.

[10] Short spin was added after the vortexing to ensure the complete passage of the solution.

[11] To maximize DNA yield, two consecutive elutions (2×25 µL) into the same microcentrifuge tube were performed.

The extracted soil DNA was quantified using a Qubit 2.0 Fluorometer with a Qubit 2.0 High Sensitivity dsDNA Assay Kit. The DNA integrity was then assessed by electrophoresis on a 1% agarose gel. Finally, the isolated DNA samples were sent to Novogene (Beijing, China) for high-throughput amplicon sequencing, which was conducted following their standardized protocol.

4.11 DNA amplification and amplicon sequencing

The purified DNA (1 ng/µl) was used for amplification with a specific set of universal primers with unique barcodes. These primers targeted the bacterial 16S rRNA gene region (341F/806R) as described by Klindworth et al. (2013) and the fungal ITS2 domain (ITS3, ITS4) according to White et al. (1990). The primer sequences are provided in Table 3.

Table 3 – Primers targeting 16S rRNA and ITS2 domain

	Region	Fragment lenght [bp]	Primer	Primer sequences (5' - 3')	T_m [°C]	Reference
Bacterial 16S	V3–V4	466	341F	CCTAYGGGRBGCASCAG	57.5	Klindworth et al., 2013
			806R	GGACTACNNGGGTATCTAAT	50.2	Klindworth et al., 2013
Fungal ITS	ITS2	386	ITS3	GCATCGATGAAGAACGCAGC	57	White et al., 1990
			ITS4	TCCTCCGCTTATTGATATGC	52.1	White et al., 1990

The PCR reactions (including the negative control with no template DNA for contamination control) were performed using Phusion High-Fidelity PCR Master Mix (New England Biolabs, Ipswich, MA, USA). Amplification was performed in a thermal cycler with optimized PCR protocol. Initial denaturation at 95°C for 5 min, denaturation at 95°C for 30 s, primer annealing at T_m (melting temperature) for 30 s, extension at 72°C for 30 s, and final extension at 72°C for 1 min. Total of 30 cycles of amplification were performed.

The equi-density of PCR amplicons was then pooled, and gel purified (Qiagen Gel Extraction Kit, Germany) before the library preparation. The sequencing library, with index codes, was prepared using the NEBNext Ultra DNA Library Prep Kit from Illumina. Following preparation, the library was quantified using a Qubit 2.0 Fluorometer (Thermo Scientific, Waltham, MA, USA), and its quality was assessed using the Agilent Bioanalyzer 2100 system. Sequencing was then carried out on the Illumina NovaSeq 6000 platform, producing 250 bp paired-end reads.

4.12 Sequencing data analysis

4.12.1 Data filtering

The paired-end reads generated from Illumina sequencing of soil DNA samples were assembled using FLASH (V1.2.7) (Magoč and Salzberg, 2011) following the removal of barcode and primer sequences. High-quality clean tags were then obtained by filtering the assembled reads based on pre-set parameters (Bokulich et al., 2013) in QIIME (V1.7.0) (Caporaso et al., 2010). Chimeric sequences were detected using the UCHIME algorithm (Edgar et al., 2011) by comparing the reads to reference databases: the SILVA database for bacterial 16S sequences (Wang et al., 2007) and the UNITE database for fungal ITS sequences (Nilsson et al., 2019). Any identified chimeras were removed, resulting in the final effective tags (Haas et al., 2011).

For the rhizosphere DNA samples, data filtering and analysis were conducted using QIIME2 software (version 2022.2) (Bolyen et al., 2019). Similar to the soil samples, the Illumina paired-end reads assigned to each sample were assembled based on their unique barcodes after the removal of the barcode and primer sequence and merged to get raw reads using FLASH (V1.2.11) (Magoč and Salzberg, 2011). Quality control of the raw tags was carried out using fastp software (version 0.23.0) (Chen et al., 2018), discarding any reads with a Phred Quality score below 30, resulting in high-quality clean tags. Chimeric sequences were then identified and removed using VSEARCH software (version 2.7.1) (Rognes et al., 2016), yielding effective tags for further downstream bioinformatic analysis.

4.12.2 Operational Taxonomic Units (OTUs) and Amplicon Sequence Variants (ASVs)

For soil samples, OTU clustering was performed using UPARSE software (UPARSE v7.0.1001) (Edgar, 2013) and all sequences with ≥97% similarity were assigned to the same OTU. Each OTU was then searched for the representative species annotation against the respective reference databases. Bacterial species annotation was done against the SILVA database (Release v138.1) (Wang et al., 2007), while the UNITE database was used for the annotation of fungal species (Nilsson et al., 2019). The phylogenetic relationship of different OTUs was explored by the Multiple sequence alignment using MUSCLE software (Version 3.8.31) (Edgar, 2004). Additionally, the singletons obtained during the analysis were removed, and the normalized OTU abundance table was calculated using the number of sequences corresponding to the sample with the lowest reads.

For the rhizosphere samples, the updated ASV approach using QIIME2 was employed. The effective tags were denoised using the DADA2 module (Callahan et al., 2016) in QIIME2 software (version 2022.2), and the sequence abundance of less than 5 reads was discarded to obtain the final

ASVs (Li M. et al., 2020) along with the feature table. The species annotation for each ASV was performed by comparing the ASVs against the SILVA database (Release v138.1) for bacterial sequences (Quast et al., 2012) and the UNITE database (version 9.0) for fungal sequences (Nilsson et al., 2019), using the Classify-sklearn module (version 2020.6) (Bokulich et al., 2018) in QIIME2.

4.12.3 Alpha diversity

Alpha diversity indices were calculated to assess the microbial diversity within each site, considering both the number of distinct species (species richness) and their relative abundance (species evenness). The selected alpha diversity indices used to characterize the richness ($Chao_1$, ACE), diversity (Shannon, Simpson), evenness (Pielou), and sequencing depth (Good's coverage) of the soil and rhizospheric microbial communities were applied for analysis.

The alpha diversity of bacterial and fungal species in bulk soil was calculated using normalized OTU abundance. These alpha diversity indices were estimated with QIIME (Version 1.7.0) (Caporaso et al., 2010) and visualized using R software (Version 2.15.3; R Core Team, 2013, Vienna, Austria) (R Core Team, 2013). Similarly, the alpha diversity indices for rhizospheric microbial communities were calculated using QIIME2. The statistical significance of the indices was assessed using the Wilcoxon test to compare the two seed orchards.

4.12.4 Beta diversity

Beta diversity metrics were evaluated to examine the variation in species composition between the sites, determining the degree of similarity or dissimilarity between two microbial communities based on species presence or abundance.

Beta diversity, representing the variation in microbial diversity between bulk soil samples from two different sites, was measured using QIIME software (Version 1.7.0) (Caporaso et al., 2010). Pairwise dissimilarity between samples was calculated using Unweighted (Lozupone and Knight, 2005) and Weighted (Lozupone et al., 2007) UniFrac distance matrices. To visualize the complex multidimensional data, Non-metric Multidimensional Scaling (NMDS) analysis was conducted (Oksanen et al., 2010). Hierarchical clustering using the Unweighted Pair-group Method with Arithmetic Means (UPGMA) (Lozupone et al., 2011) was also performed to analyse the distance matrix using average linkage.

Statistical methods such as ADONIS (Anderson, 2001), Analysis of Similarity (ANOSIM) (Clarke, 1993), and Multi-Response Permutation Procedure (MRPP) analysis (Cai, 2006) were used to determine the significant variation of the microbial communities in the soils of two different sites.

Additionally, differences in microbial species abundance between bulk soil samples from the two sites were analysed using a t-test (D'Argenio et al., 2014) and MetaStats (Paulson et al., 2011). The significance of these differences was evaluated through p-values, determined using the permutation method, and q-values, calculated using the Benjamini and Hochberg False Discovery Rate (FDR) correction method (White et al., 2009).

The presence of microbial communities showing significant intra-group variation among the soil samples was assessed using Linear Discriminant Analysis Effect Size (LEfSe) with LEfSe software (Segata et al., 2011). A Linear Discriminant Analysis (LDA) score threshold of [log10]>4 was set to identify high-dimensional biomarkers, distinguishing between two sample groups. This approach highlighted both statistical significance and biological consistency, facilitating the detection of important biomarkers and distinguishing features, such as genes, metabolites, or taxa, based on their abundance across the samples.

In a similar manner to the bulk soil samples, the beta diversity microbial variation between the rhizospheric soil samples was assessed using QIIME2 software (Version 2022.2) (Bolyen et al., 2019) and the Unweighted UniFrac distance metric. The Principal Coordinates Analysis (PCoA) (Minchin, 1987) was then performed and visualized in R software, where samples with comparable species compositions were grouped closer together, while those with distinct compositions were farther apart. Significant differences in the overall microbial community structure between the rhizospheric soils from the two sites were evaluated using ADONIS and ANOSIM functions. To determine the significant differences in microbial species abundance, a t-test was applied. Additionally, MetaStats analysis was used to detect significant differences in species abundance between groups, incorporating multiple hypothesis-testing and false discovery rate (FDR) corrections. Further analysis with LEfSe was conducted, setting the threshold at a linear discriminant analysis (LDA) score [log10] >4.

4.12.5 Functional prediction

Functional prediction of bulk soil microbial communities was carried out using PICRUSt analysis (Phylogenetic Investigation of Communities by Reconstruction of Unobserved States, version 1.0.0) (Douglas et al., 2018) on the bacterial 16S OTU table generated with QIIME (Version 1.7.0) (Caporaso et al., 2010). The Kyoto Encyclopedia of Genes and Genomes (KEGG) database (Kanehisa et al., 2012) was utilized to predict the abundance of various gene families within the microbial communities.

The metabolic functions of rhizospheric microbes derived from amplicon sequencing were predicted by mapping the microbial composition to various databases. For bacterial communities, functional predictions were made using the PICRUSt2 software (version 2.3.0) (Douglas et al., 2020) and the abundance of bacterial 16S ASVs was aligned with the KEGG database (Kanehisa et al., 2012) to infer potential functions associated with the bacterial communities in the rhizospheric soil samples. The KEGG functional annotations were visualized using Principal Component Analysis (PCA), and significant KEGG orthologs (KOs) were identified through a t-test. Similarly, the predicted functions of fungal communities in the rhizospheric soil were identified using the FUNGuild annotation tool (version 1.0), which classifies fungal ASVs by their ecological guild (Nguyen et al., 2016). Differentially abundant fungal guilds were also determined using a t-test.

4.12.6 Network analysis

Network analysis was employed to better grasp the complexity of soil environment and to reveal the microbial associations and interactions among dominant species (Guseva et al., 2022). Rhizospheric microbial abundance data (ASV table) were converted into a co-occurrence network using Graphviz-2.38.0 software to explore the interactions among microbial communities. Microbial species with an average relative abundance below 0.005% were excluded. The Spearman Correlation Coefficient (SCC) was calculated for all samples, and effective connections with a correlation coefficient cutoff of ±0.6 and $p < 0.05$ were selected for network construction. Various network parameters, including nodes, links (positive and negative), network density, diameter, average degree, modularity degree, clustering coefficients, and average path length, were estimated using the igraph package (version 2.0.2) (Csardi and Nepusz, 2006). Basic principles of network analysis are illustrated in Figure 6 (Guseva et al., 2022) and they are further explained below.

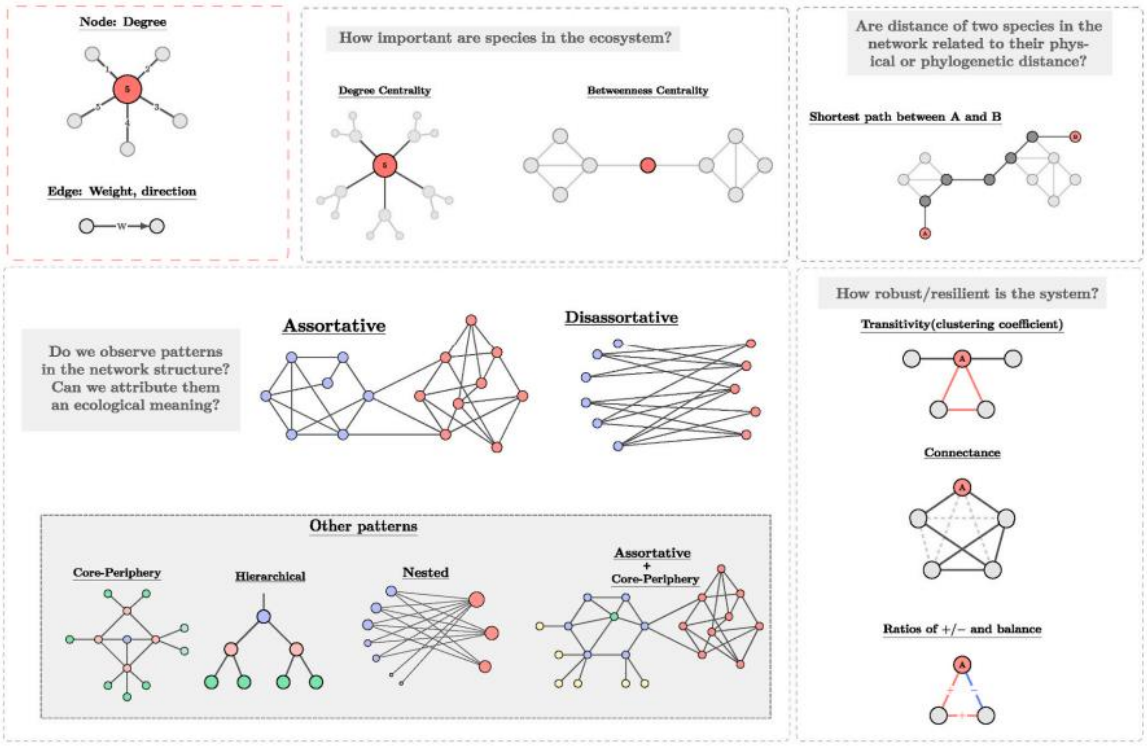

Figure 6 – Network properties to characterise microbial communities

source: Guseva et al., 2022

In this context, nodes represent microbial genera, and links (edges) depict interactions (either positive or negative) between microbial taxa. Network density reflects the proximity of the overall microbial community, with a higher density indicating a more interconnected network. Modularity (MD) measures the strength of divisions within the community. MD value ranges from 1 to −1 and values close to 1 signify a strong community structure (Clauset et al., 2004). The average degree indicates the average number of links per node, representing the average number of neighbours in the network.

Network diameter measures the shortest distance between the two most distant nodes, while average path length identifies the shortest average distance between nodes. Clustering coefficients reflect the proportion of actual links compared to possible links, with higher values indicating more tightly connected communities, which suggest greater network robustness (Iyer et al., 2013; Shang, 2014). Networks with short average path lengths and high clustering coefficients are considered efficient and are often referred to as "small world" networks, characterized by high network efficiency (Watts and Strogatz, 1998).

4.12.7 Environmental association analysis

Environmental association analysis (EAA) was applied to explore the relationship between soil microbial species abundance (alpha diversity) and site-specific environmental factors (such as soil pH, EC, TOC, and TN) in the two seed orchards. This relationship was assessed using the Spearman rank correlation (Algina and Keselman, 1999) and the Mantel test (Yang et al., 2007). Additionally, Canonical Correspondence Analysis (CCA) was conducted in R using the vegan package (Sheik et al., 2012) to identify the key environmental factors that shape the composition and structure of specific microbial communities.

Furthermore, Variance Partitioning Canonical Correspondence Analysis (VPA) was used to quantify the relative contributions of selected environmental variables in explaining the structure of the microbial community (Peres-Neto et al., 2006). VPA enabled the partitioning of beta diversity variation across environmental and spatial factors, helping to determine whether the same factors influenced the spatial distribution of different organisms (Legendre, 2008). The analysis was carried out in R using the "varpart" function within the vegan package. The various components of variance were estimated following the methodology outlined by Borcard et al. (1992).

5. Results

This section presents our findings on the physiology, enzymatic activity, metabolic profile, and microbial population structure of forest bulk and rhizospheric soils in two Norway spruce (*Picea abies*) seed orchards, which differ significantly in long-term precipitation patterns. Our study highlights how variation in precipitation, along with soil physicochemical properties, influence belowground microbial communities over the long term. These results offer an insight into the functioning of forest soil ecosystems under different precipitation regimes and provide field data for modelling microbial responses to future global climate change scenarios.

The results are divided into two sections: one focusing on bulk soil and the other on rhizospheric soil, summarizing the outcomes of the methods and techniques described in the Materials and Methods section.

For clarity, the Prenet seed orchard is referred to as the P-site, and Lipová Lhota as the L-site.

All values are reported as means ± Standard Error of the Mean (SEM).

5.1 Impact of long-term precipitation regime differences on bulk soil

5.1.1 Soil texture, physicochemical, and biochemical properties

The soil texture, physicochemical, and biochemical properties are summarized in Table 4. Granulometric analysis revealed that the soil at the P-site was classified as sandy loam (0.8% clay, 28.3% silt, 70.8% sand), whereas the soil at the L-site was categorized as loamy sand (0.6% clay, 24.9% silt, 74.3% sand). The P-site soil exhibited a significantly higher water content (32%) compared to the L-site soil (9%), likely due to its texture and the greater long-term average annual precipitation (1,306 mm at the P-site versus 633 mm at the L-site).

The soil pH (measured in a 1:5 ratio with water) ranged from extremely acidic at the P-site (pH 4.45 ± 0.06) to strongly acidic at the L-site (pH 5.06 ± 0.24) (Burt, 2014). Both soils were non-saline, with low electrical conductivity (P-site: 0.04 ± 0.001 mS/cm; L-site: 0.03 ± 0.005 mS/cm).

Additionally, notable differences in total organic carbon (TOC) and nitrogen (TN) content were observed. The P-site, with its higher annual precipitation, had significantly higher TOC (6.79% ± 0.14) and TN (0.51% ± 0.01) levels compared to the L-site soils (TOC: 3.27% ± 0.13; TN: 0.25% ± 0.01) ($p < 0.05$), which experienced considerably lower precipitation.

Table 4 – Soil texture, physicochemical, and biochemical soil properties

Soil properties	L-site	P-site	p-value
Soil texture	Loamy sand (0.6% clay, 24.9% silt, 74.3% sand)	Sandy loam (0.8% clay, 28.3% silt, 70.8% sand)	NA
Soil water content [%]	9	32	<0.0001
EC [mS/cm]	0.03 ± 0.005	0.04 ± 0.001	0.198
pH [1:5 H_2O, v/v]	5.06 ± 0.24	4.45 ± 0.06	0.069
TN [%]	0.25 ± 0.01	0.51 ± 0.01	0
TOC [%]	3.27 ± 0.13	6.79 ± 0.14	<0.0001

5.1.2 Extracellular enzyme activities

The extracellular enzyme activities in the bulk soil (Table 5) showed notable differences between the two sites. The P-site exhibited significantly higher activity levels for all the measured enzymes—cellobiohydrolase, β-galactosidase, α-glucosidase, β-glucosidase, β-xylosidase, chitinase, and acid phosphatase—compared to the L-site ($p < 0.05$, Kruskal-Wallis test). These elevated enzyme activities at the P-site are consistent with its higher precipitation levels and the greater availability of nutrients (TOC, TN), both of which likely play a role in enhancing soil enzyme activity at this location.

Table 5 – Extracellular enzyme activities

Enzyme	L-site [nmol·g^{-1}·h^{-1}]	P-site [nmol·g^{-1}·h^{-1}]	p-value
cellobiohydrolase	28.7 ± 0.12	234.6 ± 0.72	0
β-galactosidase	55.2 ± 0.18	337.5 ± 0.52	0.001
α-glucosidase	40.3 ± 0.17	148.8 ± 0.57	0.008
β-glucosidase	563.5 ± 1.44	1833 ± 5.00	0.001
β-xylosidase	141.9 ± 0.41	1853 ± 3.37	0
chitinase	116.3 ± 0.27	499.5 ± 1.38	0.001
acid phosphatase	1056.8 ± 2.49	2988.6 ± 5.10	0.001

The results are expressed as the dry weight of the soil. p-value denotes the significance level between the two sites ($p < 0.05$, Kruskal-Wallis test).

5.1.3 Soil metabolomics

The two bulk soil samples contained 183 metabolites, including alcohols, carbohydrates, amino acids, fatty acids, and organic acids. Fatty acids were the most prevalent, accounting for 26.2% of the total metabolites, followed by carbohydrates (25.6%), alcohols (12.5%), and organic acids (6.5%).

Component analysis revealed a clear distinction between the soil metabolite profiles of the L-site and P-site, as shown by their separate clustering (Figure 7A). A heatmap (Figure 7B) highlights the top 70 metabolites that differed significantly between the two sites. The P-site soil displayed a higher

abundance of fatty acids, carbohydrates, and alcohols than the L-site. These metabolites largely originated from the decomposition of organic matter, plant exudates, and microbial by-products. The high organic carbon content (TOC) at the P-site aligns with the increased concentration of soil metabolites. However, it is important to note that distinguishing the contribution of microbial metabolites from other influencing factors in the soil remains challenging (White et al., 2017).

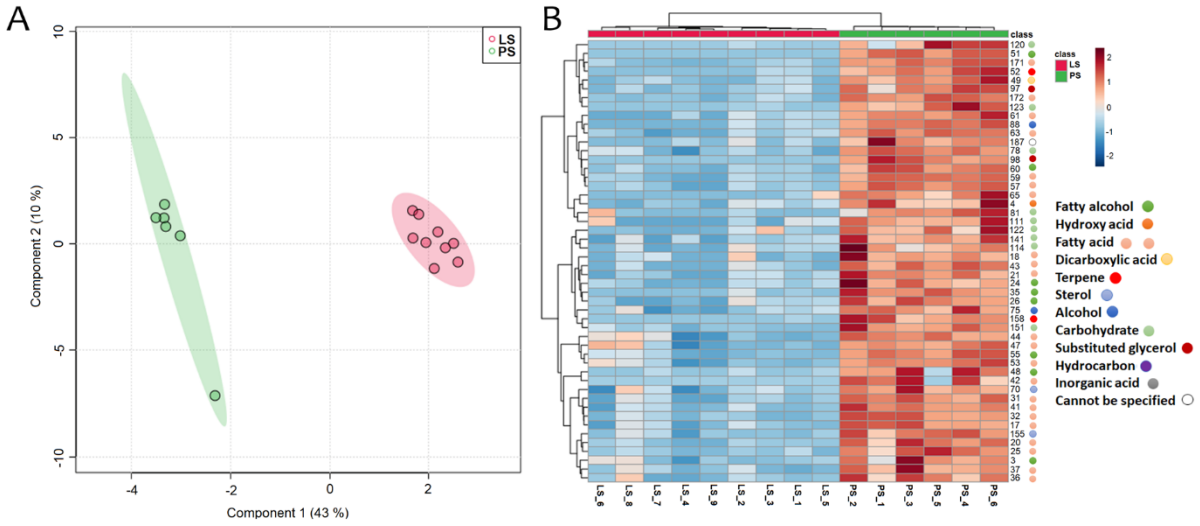

Figure 7 – Bulk soil metabolite profile

(A) Sparse Partial Least Square Discriminant Analysis (sPLS-DA) plot representing the differences in the metabolite profiles in soil samples. **(B)** Heatmap showing 70 most significant metabolites between the two soil samples from L-site and P-site in replicates based on t-test and ANOVA (Source: Chakraborty et al., 2023).

5.1.4 Phospholipid fatty acids (PLFAs) analysis

Phospholipid fatty acid (PLFA) analysis revealed notable differences in microbial cell membrane composition, used to assess the presence of functionally active microbial communities in the soil (Table 6) (Cavigelli et al., 1995; Torsvik and Øvreås, 2002). The P-site soil had significantly higher viable microbial biomass (71.7 ± 1.74 mg PLFA g^{-1} soil, $p < 0.05$) compared to the L-site soil (22.7 ± 2.01 mg PLFA g^{-1} soil), indicating a greater abundance of active microbial communities, likely supported by higher levels of TOC and TN.

While both bacterial (59.5 ± 1.34 mg PLFA g^{-1} soil, $p < 0.05$) and fungal (1.1 ± 0.09 mg PLFA g^{-1} soil, $p < 0.05$) biomass were greater in the P-site soil, the bacteria-to-fungi ratio showed no significant difference between the two locations (P-site: 51.5 ± 3.77 mg PLFA g^{-1} soil; L-site: 57.3 ± 4.21 mg PLFA g^{-1} soil; $p > 0.05$). Additionally, the amounts of G^+ bacteria (7.83 ± 0.32 mg PLFA g^{-1} soil, $p < 0.05$), G^- bacteria (37.8 ± 1.08 mg PLFA g^{-1} soil, $p < 0.05$), and actinobacteria (13.4 ± 0.28 mg PLFA g^{-1} soil, $p < 0.05$) were significantly higher in P-site soil compared to L-site.

Table 6 – PLFA analysis

PLFA analysis [µg PLFA · g^{-1} soil]	L-site	P-site	p-value
$PLFA_{total}$	22.7 ± 2.01	71.7 ± 1.74	0
$PLFA_{bacteria}$	19.2 ± 1.75	59.5 ± 1.34	0
$PLFA_{fungi}$	0.35 ± 0.04	1.2 ± 0.09	0
$PLFA_{G+}$	2.09 ± 0.29	7.8 ± 0.32	0
$PLFA_{G-}$	12.0 ± 1.30	37.8 ± 1.08	0
$PLFA_{actinobacteria}$	5.0 ± 0.40	13.4 ± 0.28	0
$PLFA_{bacteria:fungi}$	57.3 ± 4.21	51.5 ± 3.77	0.346
$PLFA_{fungi:bacteria}$	0.02 ± 0.001	0.02 ± 0.001	0.346

Significant difference between the two sites is denoted by p-value ($p < 0.05$, Mann-Whitney test of significance).

5.1.5 Soil microbial community composition and diversity

5.1.5.1 Quality control

The structure of the soil microbial communities was assessed using Illumina paired-end amplicon sequencing, specifically targeting the bacterial 16S rRNA gene and the fungal ITS region. The bulk soil samples from the two different sites generated a total of 2,026,594 reads for bacterial diversity and 1,932,039 reads for fungal diversity (Table 7 and Table 8). An initial quality check was applied with a Phred Quality score threshold of >30. Reads falling below this threshold were discarded, and the high-quality reads for both bacterial 16S and fungal ITS regions were processed using bioinformatics pipelines for further analysis.

Table 7 – Illumina paired-end amplicon sequencing of bacterial 16S in bulk soil

Sample name	Raw PE reads	Combined reads	Uncombined reads	Percent combined [%]	Combined base [bp]	Min lenght [bp]	Max lenght [bp]	Average lenght [bp]	Qualified reads	Nochimera	Base [nt]	Q20	Q30	GC [%]	Effective [%]
L01	139 568	123 739	15 829	88.66	51 260 154	44	441	414	120 358	115 737	47 935 493	97.55	92.83	56.85	82.93
L02	134 505	120 660	13 845	89.71	50 174 371	44	441	416	117 733	113 465	47 157 103	97.54	92.72	56.76	84.36
L03	136 839	122 844	13 995	89.77	50 840 729	44	441	414	119 580	114 889	47 524 490	97.52	92.77	56.54	83.96
L04	139 907	126 084	13 823	90.12	52 379 250	64	441	415	122 960	118 499	49 219 271	97.6	92.9	56.5	84.7
L05	138 364	125 208	13 156	90.49	51 781 288	51	441	414	122 123	117 514	48 594 817	97.73	93.11	56.63	84.93
L06	147 510	134 328	13 182	91.06	55 879 188	44	441	416	131 031	126 025	52 398 217	97.62	92.96	57.08	85.43
L07	142 309	127 945	14 364	89.91	53 275 091	44	441	416	124 396	119 234	49 661 949	97.6	92.93	56.51	83.79
L08	148 735	133 801	14 934	89.96	55 729 463	44	441	417	130 550	125 437	52 223 278	97.51	92.73	56.44	84.34
L09	130 873	120 133	10 740	91.79	50 004 616	44	441	416	117 347	110 900	46 161 316	97.71	93.07	56.68	84.74
P01	131 057	118 105	12 952	90.12	48 551 100	101	441	411	115 341	111 586	45 843 576	97.6	92.93	56.69	85.14
P02	114 742	105 362	9 380	91.83	43 235 663	51	441	410	102 979	99 673	40 879 029	97.79	93.32	56.87	86.87
P03	138 481	126 725	11 756	91.51	52 117 697	109	441	411	123 535	120 024	49 351 092	97.72	93.22	56.57	86.67
P04	128 540	117 762	10 778	91.62	48 361 932	153	441	411	114 977	112 099	46 025 261	97.8	93.36	56.66	87.21
P05	119 819	108 145	11 674	90.26	44 341 949	53	441	410	105 362	101 452	41 615 725	97.76	93.29	56.76	84.67
P06	135 345	124 086	11 259	91.68	50 822 129	51	441	410	121 133	117 638	48 177 737	97.86	93.44	56.63	86.92

Table 8 – Illumina paired-end amplicon sequencing of fungal ITS in bulk soil

Sample name	Raw PE reads	Combined reads	Uncombined reads	Percent combined [%]	Combined base [bp]	Min lenght [bp]	Max lenght [bp]	Average lenght [bp]	Qualified reads	Nochimera	Base [nt]	Q20	Q30	GC [%]	Effective [%]
L01	147 788	138 652	9 136	94	48 211 880	47	437	348	137 060	117 706	41 181 168	98	95	44	80
L02	134 494	125 760	8 734	94	42 644 923	47	438	339	124 094	97 596	33 354 042	98	94	48	73
L03	148 009	140 038	7 971	95	47 016 485	47	438	336	138 792	122 661	41 362 355	98	95	47	83
L04	136 353	128 991	7 362	95	43 350 477	23	438	336	128 197	107 643	36 494 396	98	95	50	79
L05	147 678	140 458	7 220	95	45 666 574	43	438	325	139 354	112 916	37 125 101	98	95	49	76
L06	145 675	139 586	6 089	96	44 210 268	42	438	317	138 784	101 655	32 314 649	98	95	51	70
L07	130 362	120 156	10 206	92	42 597 438	47	438	355	118 767	105 089	37 620 539	98	94	51	81
L08	142 594	133 488	9 106	94	44 970 804	48	438	337	116 548	100 271	34 693 042	98	95	50	70
L09	131 442	124 375	7 067	95	39 374 958	42	438	317	102 434	89 633	29 133 741	98	95	52	68
P01	135 539	128 963	6 576	95	45 684 897	48	438	354	125 413	113 892	40 685 087	98	94	50	84
P02	103 120	97 434	5 686	94	33 921 675	39	438	348	96 765	84 542	29 558 459	98	94	46	82
P03	125 048	118 722	6 326	95	41 772 148	52	438	352	117 789	105 705	37 187 334	98	94	44	85
P04	94 649	89 190	5 459	94	31 867 902	48	438	357	83 878	71 759	26 046 905	98	94	45	76
P05	79 350	74 788	4 562	94	27 341 088	48	438	366	74 063	64 674	23 807 931	98	94	44	82
P06	129 938	124 748	5 190	96	42 289 642	48	438	339	124 007	104 786	35 815 139	98	95	49	81

5.1.5.2 Operational Taxonomic Units (OTUs) abundance

Illumina sequencing of the bulk soil samples revealed a total of 6,389 bacterial OTU clusters at a 97% similarity threshold. Out of these, 2,426 unique bacterial OTUs were identified in the L-site soil, while only 382 unique OTUs were found in the P-site soil (Figure 8A).

The relative abundance of the top 10 bacterial orders detected in the soil samples is shown in Figure 8B. P-site soil exhibited a higher proportion of Rhizobiales (36.2%), Acidobacteriales (10.9%), Chthoniobacterales (7.3%), Rhodospirillales (6.8%), Ktedonobacterales (4.2%), and Frankiales (4.1%). In contrast, L-site soil had a greater presence of Gaiellales (6.6%), Solirubrobacterales (5.3%), Solibacterales (4.9%), and Xanthomonadales (3.7%).

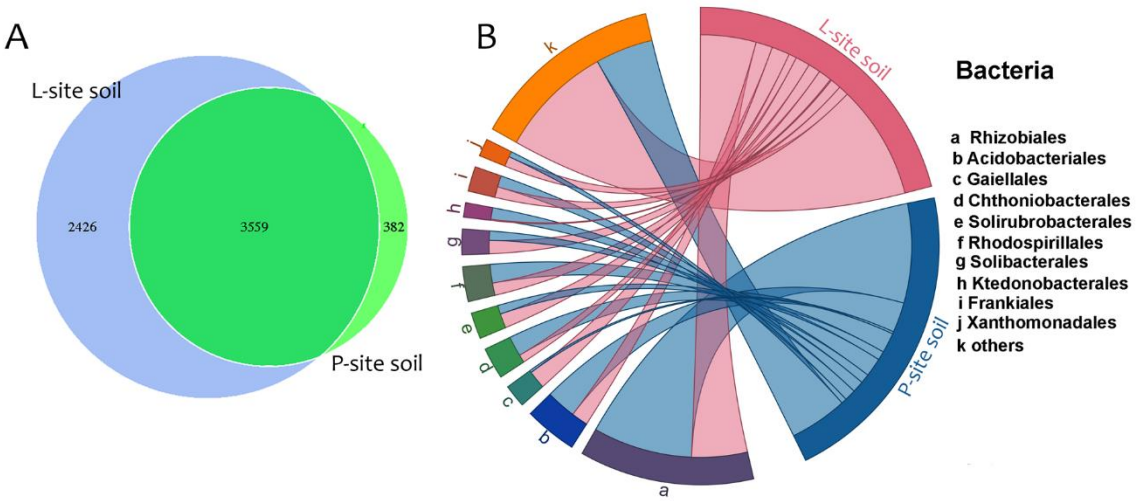

Figure 8 – Bacterial Operational Taxonomic Units (OTUs) abundance

(A) Venn diagram showing the distribution of unique and common bacterial OTUs. **(B)** Relative abundance of the top 10 bacterial orders observed in L-site and P-site soil. "Others" denote the relative abundance of the rest of the bacterial orders present in the soil (Source: Chakraborty et al., 2023).

Illumina sequencing also identified 2,288 fungal OTU clusters at a 97% similarity threshold. Similar to the bacterial findings, the L-site soil exhibited a higher number of unique fungal OTUs (1,313) compared to the P-site, which had only 256 unique OTUs (Figure 9A). The top 10 fungal orders present in the soil samples are displayed in Figure 9B. In the P-site soil, Mortierellales (39.2%), Incertae-sedis-Leotiomycetes (7.7%), and Entorrhizales (5.1%) were the most dominant orders. Conversely, the L-site soil had a higher prevalence of Russulales (12.9%), Tremellales (13.3%), Thelephorales (9.8%), Atheliales (10.9%), Hypocreales (6.3%), Hysteriales (4.5%), and Eurotiales (4.7%).

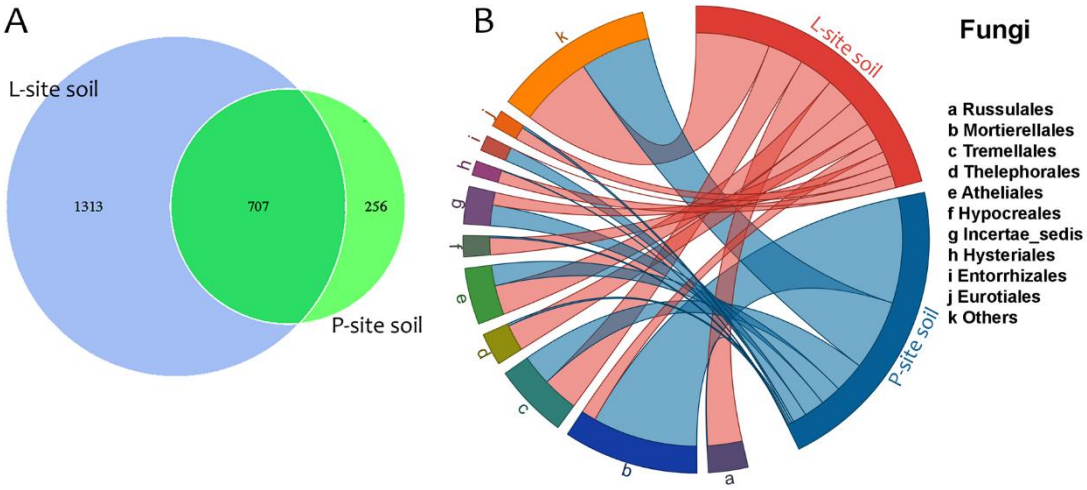

Figure 9 – Fungal Operational Taxonomic Units (OTUs) abundance

(A) Venn diagram showing the distribution of unique and common fungal OTUs. **(B)** Relative abundance of the top 10 fungal orders observed in L-site and P-site soil. "Others" denote the relative abundance of the rest of the fungal orders present in the soil (Source: Chakraborty et al., 2023).

Comparison of biological replicates within each site is visualized by Flower diagram (Figure 10). Within the site, the L-site soil replicates shared a total of 1,511 core bacterial OTUs and 127 core fungal OTUs (Figure 10A and Figure 10C). In contrast, the P-site soil replicates shared 944 core bacterial OTUs and 160 core fungal OTUs (Figure 10B and Figure 10D).

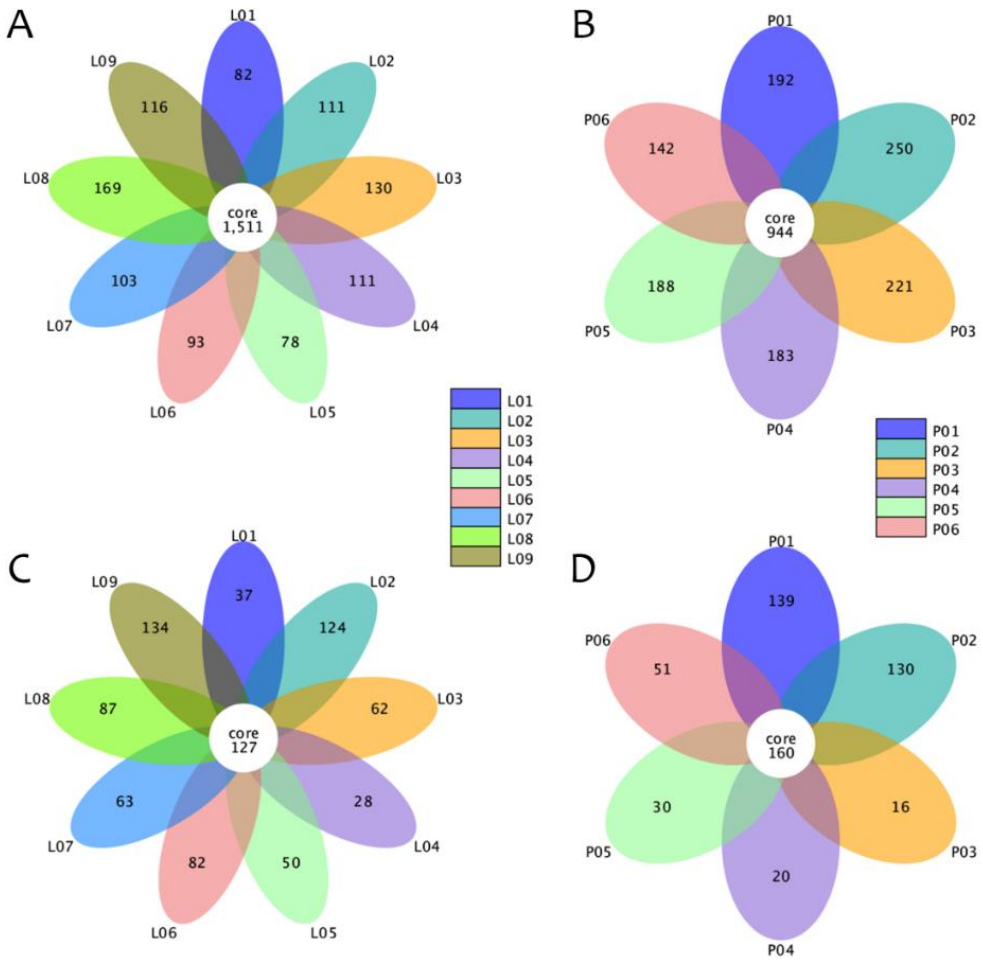

Figure 10 – Flower diagram

A comparison of biological replicates within the sites revealed the L-site unique and core **(A)** bacterial and **(C)** fungal OTUs, as well as P-site unique and core **(B)** bacterial and **(D)** fungal OTUs (Source: Chakraborty et al., 2023).

The bacterial communities in the bulk soil were classified into 41 different phyla. In the L-site soil, the Graphlan visualization highlighted the dominance of five key phyla: Proteobacteria, Firmicutes, Actinobacteria, Bacteroidetes, and Acidobacteria (Figure 11A). In contrast, the P-site soil displayed a similar predominance of Proteobacteria, Firmicutes, Acidobacteria, and Actinobacteria, but also showed a significant presence of the Chloroflexi and Verrucomicrobia phyla (Figure 11B).

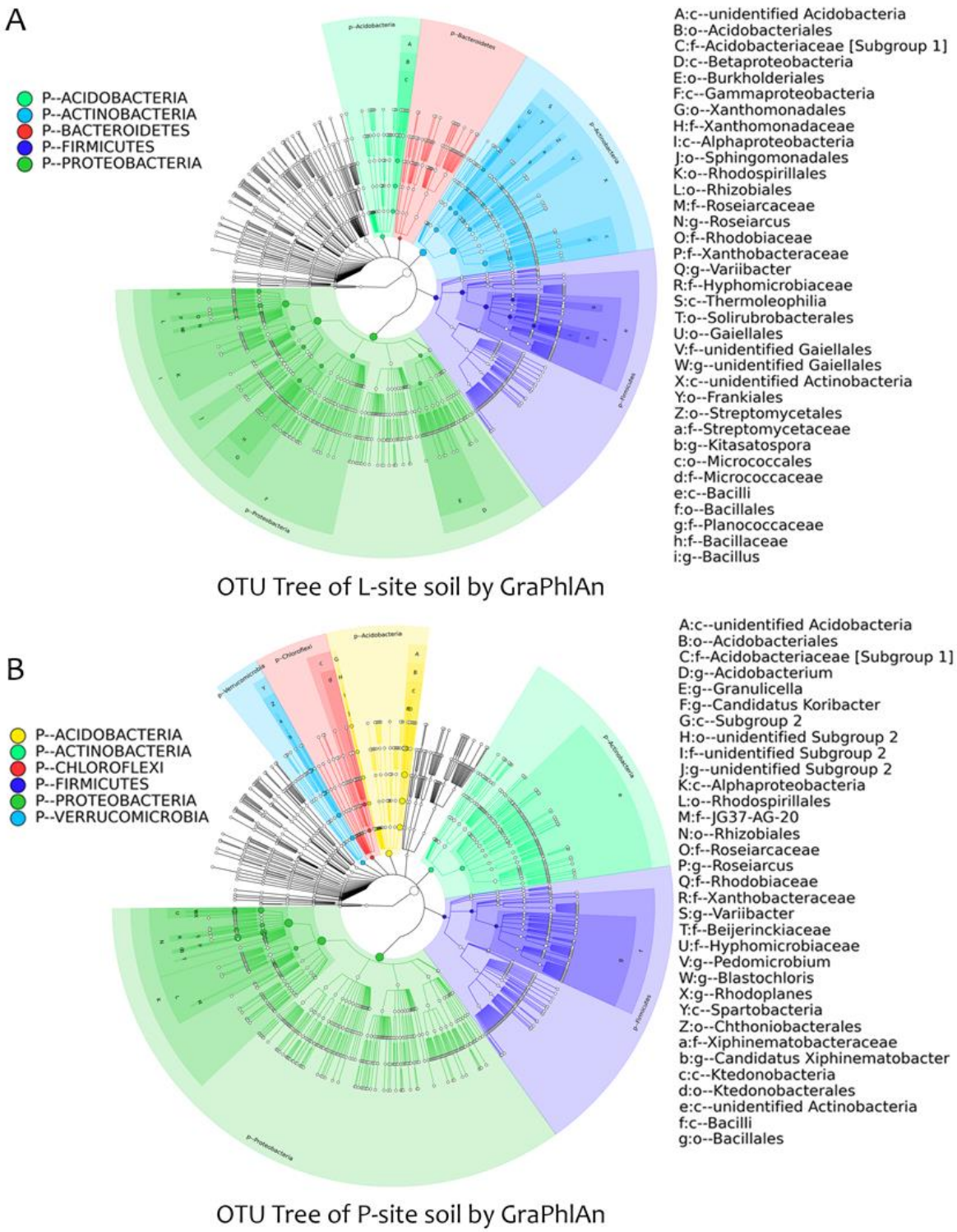

Figure 11 – Cladogram of bacterial phyla

Bacterial OTU tree of **(A)** L-site and **(B)** P-site soil visualized by Graphlan (Source: Chakraborty et al., 2023).

The fungal communities in the bulk soil were categorized into 6 distinct phyla. The OTU tree visualization via Graphlan revealed that Ascomycota, Basidiomycota, and Zygomycota were the predominant fungal phyla. In contrast to the bacterial phyla, these dominant fungal phyla were present in equal proportions in both L-site (Figure 12A) and P-site (Figure 12B) soils.

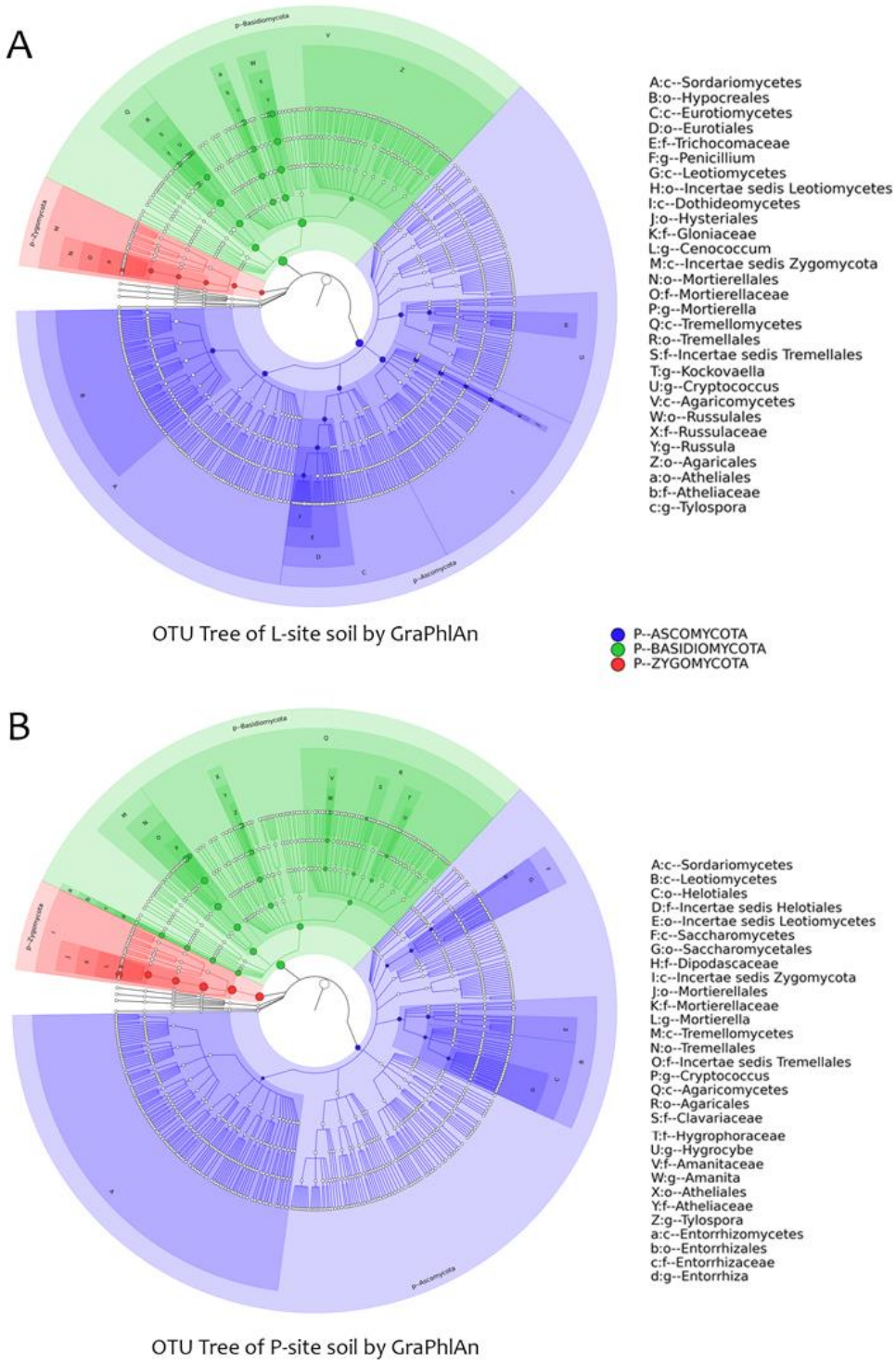

Figure 12 – Cladogram of fungal phyla

Fungal OTU tree of **(A)** L-site and **(B)** P-site soil visualized by Graphlan (Source: Chakraborty et al., 2023).

The evolutionary tree illustrated the relative abundance of the top 100 bacterial (Figure 13A) and fungal (Figure 13B) genera observed in the two soils.

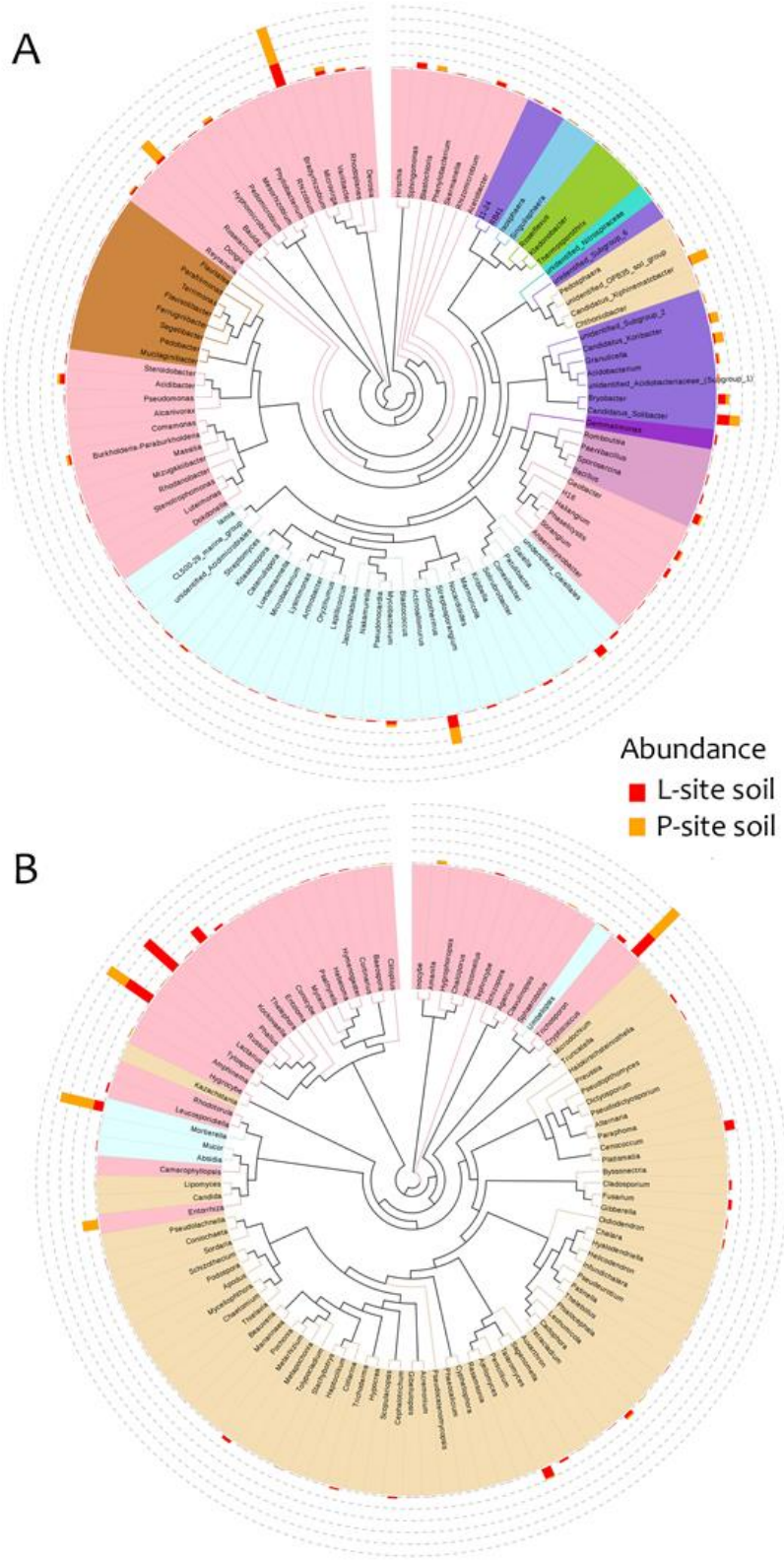

Figure 13 – Evolutionary tree

Relative abundance of top 100 **(A)** bacterial and **(B)** fungal genera in bulk soil (Source: Chakraborty et al., 2023).

Finally, the heatmap illustrates the relative abundance of 35 predominant bacterial (Figure 14A) and fungal (Figure 14B) genera found in the bulk soils of both the L-site and P-site.

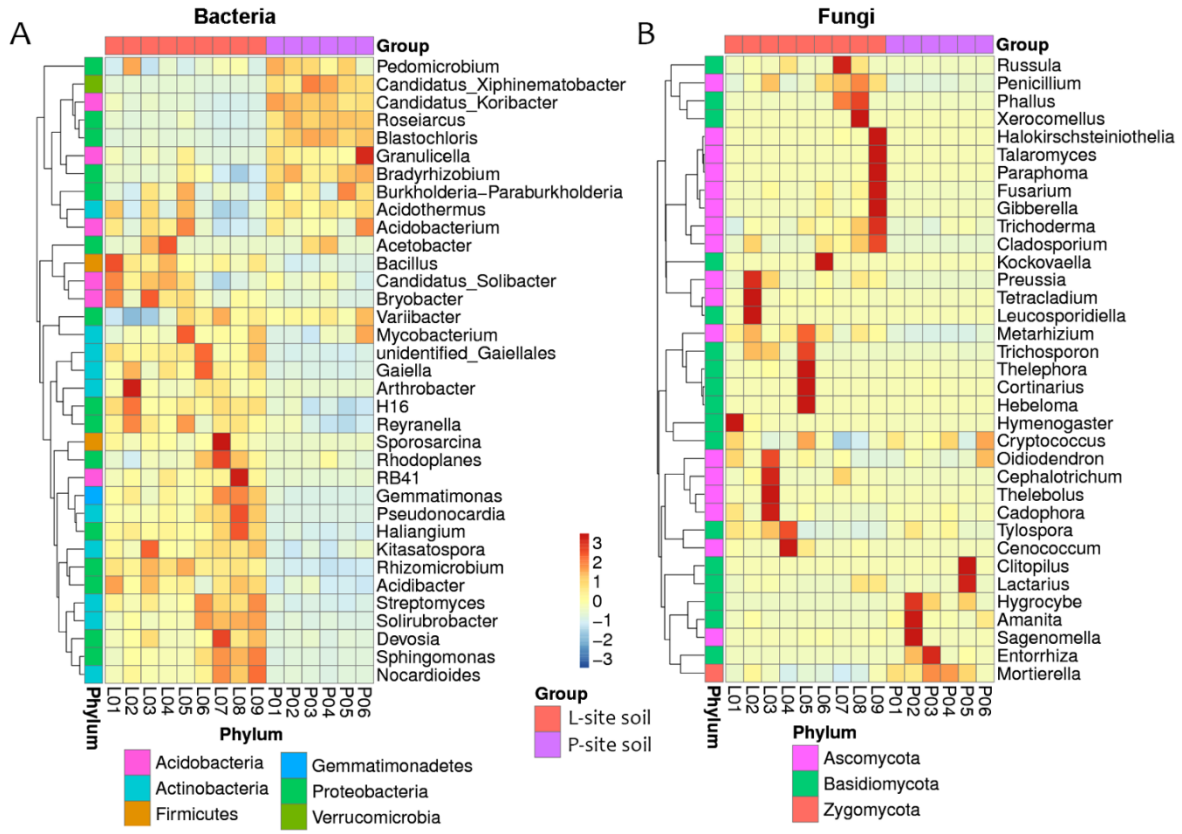

Figure 14 – Heatmap of 35 predominant bacterial and fungal genera

(A) The relative abundance of 35 predominant bacterial genera in bulk soil samples from the L-site and P-site, with six replicates each. **(B)** The relative abundance of 35 prevalent fungal genera in the bulk soil samples, with nine replicates each. The colour gradient indicates the relative OTU abundance for each soil sample, where darker colours denote higher abundance, and lighter colours represent lower abundance (Source: Chakraborty et al., 2023).

5.1.5.3 Alpha diversity

The rarefaction curves and Good's coverage index (>99%) confirm that the sequencing effectively captured the full microbial diversity present in the soil samples (Figure 15). Good's coverage index, along with other alpha diversity metrics that reflect microbial richness and evenness, are detailed in Table 9.

For bacterial species, the L-site bulk soil revealed a total of 3,375 ± 89.23 species, while the P-site soil had 2,117 ± 62.61 species. Similarly, the observed fungal species were 743 ± 45.70 in L-site soil and 429 ± 45.70 in P-site soil, indicating a lower number of both bacterial and fungal species at the P-site.

L-site soil exhibited greater bacterial community richness, with ACE (Abundance-based Coverage Estimator) of 3,778 ± 127.30 and $Chao_1$ estimates of 3,926 ± 304.89, compared to P-site soil, which had ACE of 2,421 ± 75.58 and $Chao_1$ of 2,375 ± 78.42 (Wilcoxon test, p <0.01). A similar pattern was observed for fungal richness, with L-site soil showing higher values (ACE: 933 ± 30.77; $Chao_1$: 916 ± 32.17) compared to P-site soil (ACE: 508 ± 62.64; $Chao_1$: 499 ± 60.38) (Wilcoxon test, p <0.01).

Additionally, bacterial diversity, as indicated by Shannon and Simpson indices, was significantly higher in L-site soil (Shannon index: 9.14 ± 0.14; Simpson index: 0.99) compared to P-site soil (Shannon: 7.12 ± 0.04; Simpson: 0.97) (Wilcoxon test, p <0.01). Interestingly, fungal diversity did not show significant differences between L-site (Shannon: 4.79 ± 0.41; Simpson: 0.85 ± 0.05) and P-site (Shannon: 4.40 ± 0.18; Simpson: 0.88 ± 0.02).

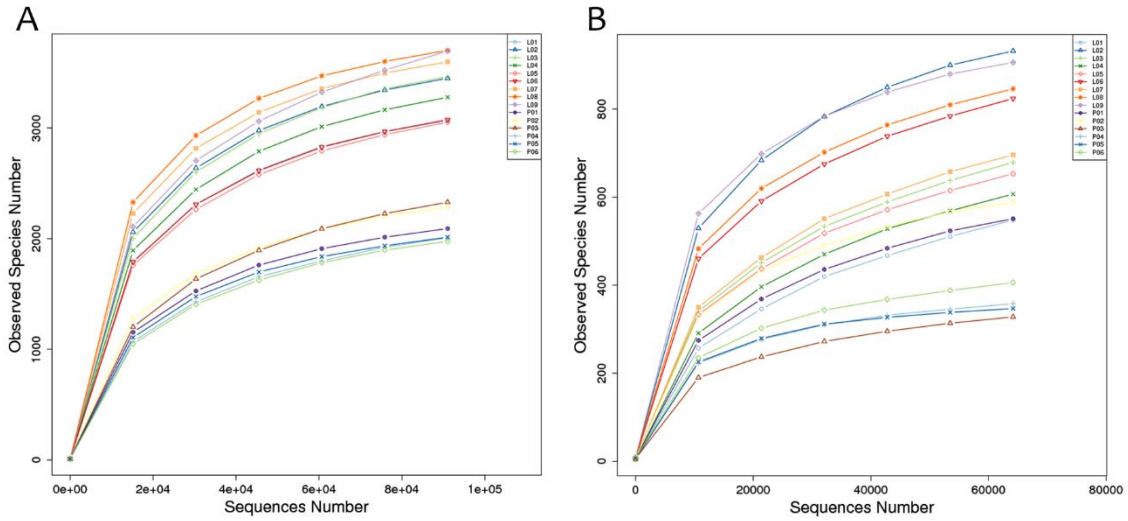

Figure 15 – Bulk soil rarefaction curves

(A) Bacterial 16S amplicon sequencing and **(B)** fungal ITS sequencing of bulk soil samples from L-site and P-site. Different colours and symbols denote different samples (Source: Chakraborty et al., 2023).

Table 9 – Alpha diversity indices

	Bacterial diversity			Fungal diversity		
Indices	**L-site**	**P-site**	**p-value**	**L-site**	**P-site**	**p-value**
Good's coverage [%]	99.3	99.5	-	99.7	99.8	-
Observed species	3375 ± 89.23	2117 ± 62.61	<0.001	743 ± 45.70	429 ± 45.70	<0.01
$Chao_1$	3926 ± 304.89	2375 ± 78.42	<0.001	916 ± 32.17	499 ± 60.38	<0.001
ACE	3778 ± 127.30	2421 ± 75.58	<0.001	933 ± 30.77	508 ± 62.64	<0.001
Shannon	9.14 ± 0.14	7.12 ± 0.04	<0.001	4.79 ± 0.41	4.40 ± 0.18	0.45
Simpson	0.99	0.97	<0.001	0.85 ± 0.05	0.88 ± 0.02	0.9

Significant difference between the L-site and P-site soil is denoted by p-value (p <0.01, Wilcoxon test)

5.1.5.4 Beta diversity

The beta diversity analysis, utilizing both Unweighted (Figure 16A and Figure 16C) and Weighted (Figure 17B and Figure 17E) UniFrac distances, revealed significant differences in microbial diversity between the soil samples.

The unweighted pair group method with arithmetic mean (UPGMA) hierarchical clustering analysis based on Unweighted UniFrac distances demonstrated that soil samples from the two sites formed two distinct clusters, highlighting the considerable differences in bacterial (Figure 16B) and fungal (Figure 16D) communities between the sites. Similar result was obtained for bacterial community using Weighted UniFrac distance (Figure 17C).

However, when clustering fungal communities based on Weighted UniFrac distances, the UPGMA analysis showed that the biological replicates from the L-site soil were divided into two separate clades, indicating some level of heterogeneity within the site (Figure 17F).

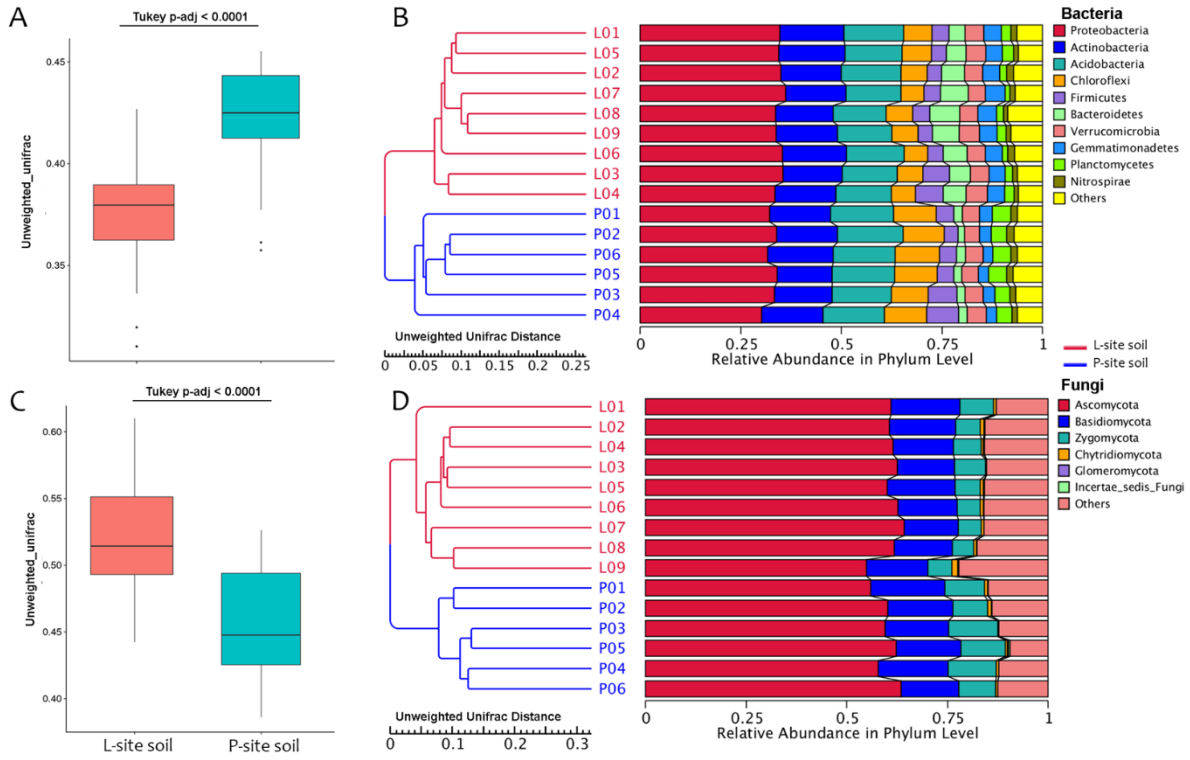

Figure 16 – Boxplot and UPGMA tree

A box plot based on Unweighted UniFrac distance representing the variation in **(A)** bacterial and **(C)** fungal communities. UPGMA tree clustering, also based on Unweighted UniFrac distance, illustrates differences in **(B)** bacterial and **(D)** fungal communities between the soil samples collected from the same site in replicates. The relative abundance of soil bacterial and fungal communities at the phylum level is displayed alongside the UPGMA tree (Source: Chakraborty et al., 2023).

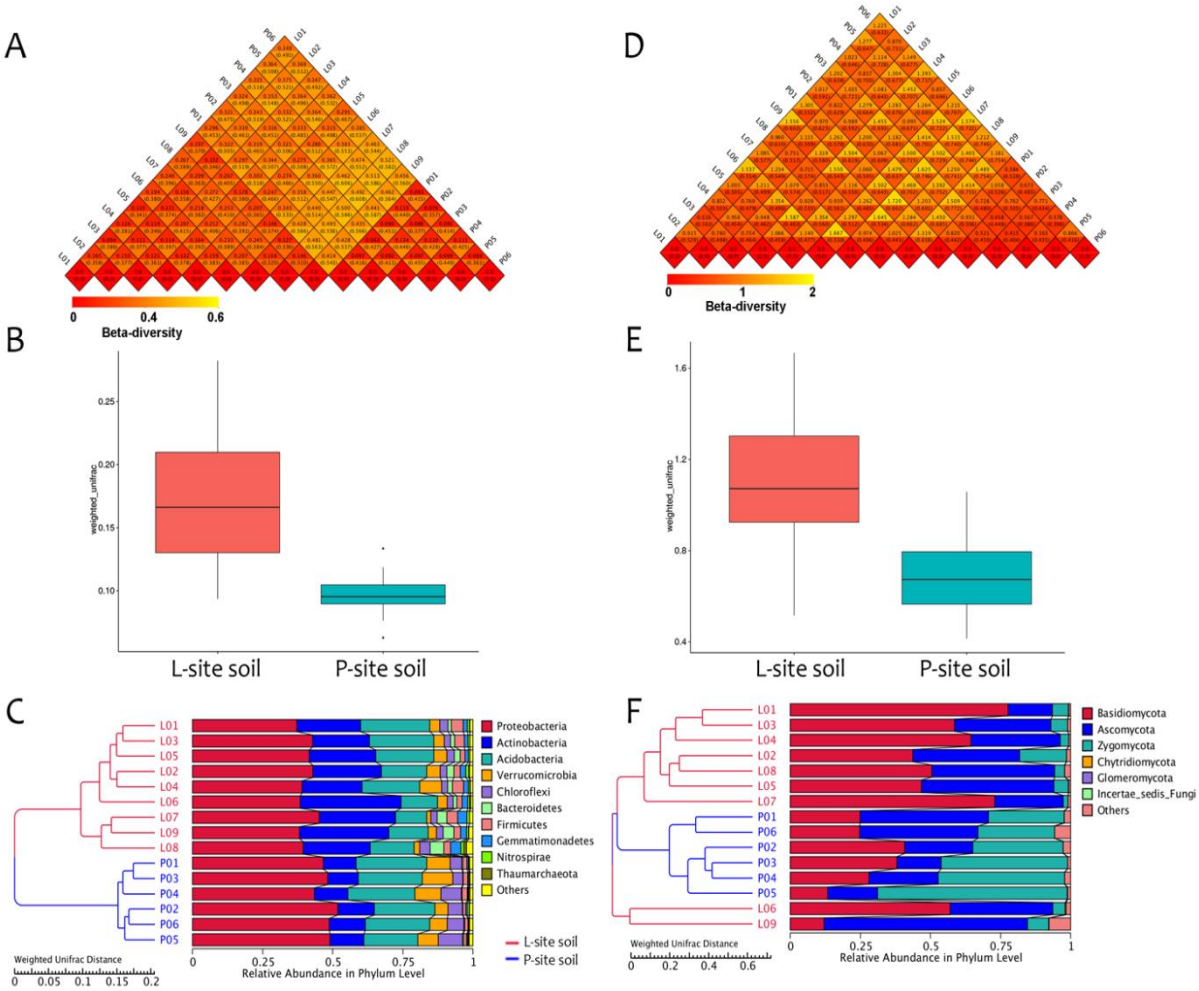

Figure 17 – Heatmap, boxplot, and UPGMA tree

Heatmap representation of Weighted and Unweighted UniFrac distance matrices showing the pairwise dissimilarity coefficient of **(A)** bacterial and **(D)** fungal communities between L-site and P-site soils, with Weighted UniFrac distance displayed above and Unweighted UniFrac distance below. Boxplots illustrate beta diversity variation based on Weighted UniFrac distance matrices for **(B)** bacterial and **(E)** fungal communities. The significance of differences between soils was assessed using the Wilcoxon signed-rank test. UPGMA tree clustering based on Weighted UniFrac distance shows the similarity in **(C)** bacterial and **(F)** fungal communities among the soil samples collected from the same site in replicates. The relative abundance of soil bacterial and fungal communities at the phylum level is represented alongside the UPGMA tree (Source: Chakraborty et al., 2023).

Additionally, the Non-Metric Multidimensional Scaling (NMDS) analysis revealed distinct differences in the soil microbiome between the two sites. The bacterial community structure formed two separate clusters (Figure 18A), indicating significant variation between the sites. A similar pattern of distinct clustering was observed for fungal communities as well (Figure 18B). These findings suggest that site-specific environmental factors have a notable impact on microbial communities. However, further validation is needed to confirm the extent of environmental influence on soil microbiota.

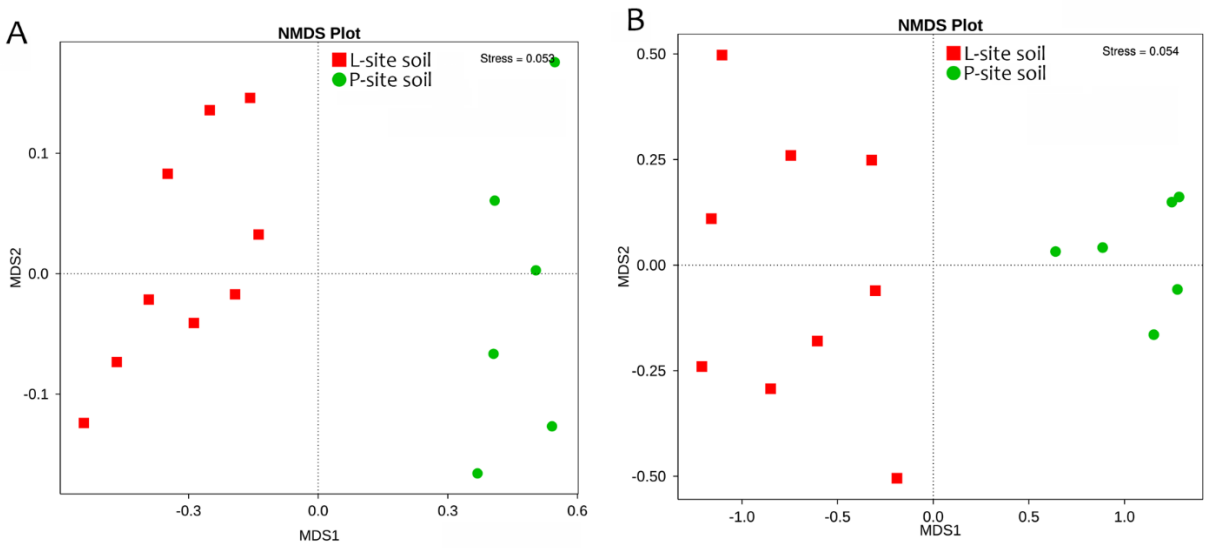

Figure 18 – NMDS analysis of bulk soil microbiota

Difference in **(A)** bacterial and **(B)** fungal communities in bulk soils from the L-site and P-site. Data points in the same colour represent soil samples from the same site, while different symbols indicate soil samples from different locations (Source: Chakraborty et al., 2023).

The MetaStats (Figure 19 and Figure 20) and t-test (Figure 21A and Figure 21B) analysis of differentially abundant microbes between the two soil samples highlighted a marked predominance of distinct bacterial and fungal groups at each site.

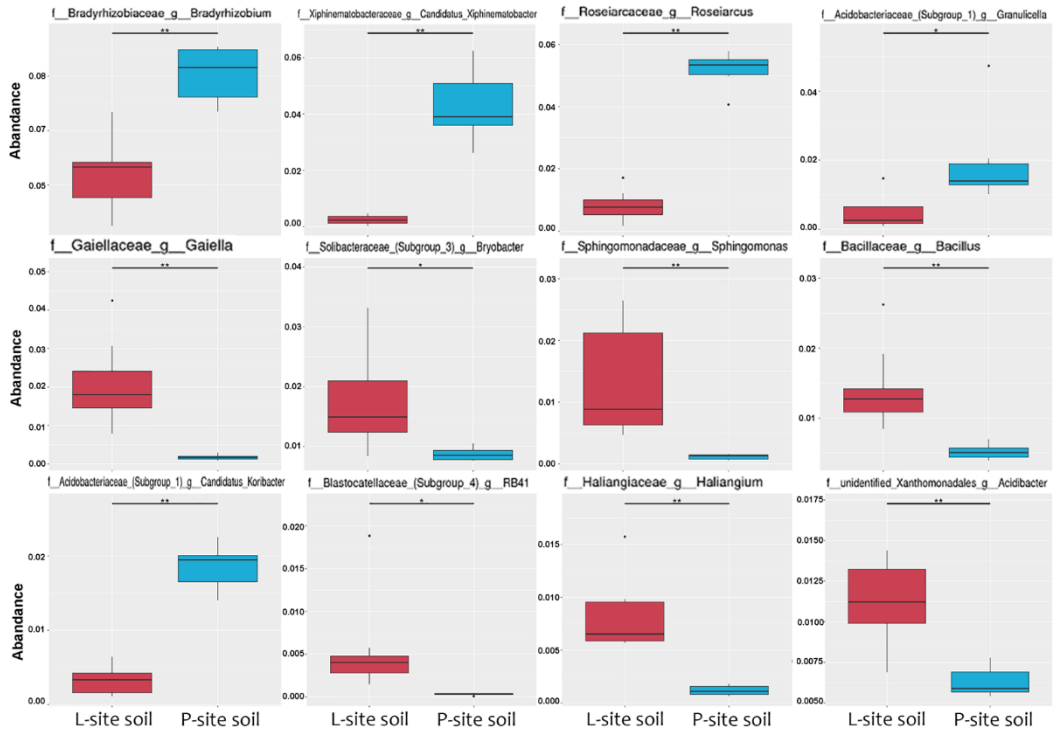

Figure 19 – Bacterial MetaStats analysis of bulk soil

Significant differences in relative abundance were evaluated using the FDR test where the "*" indicates significant variation at a q value <0.05, and "**" denotes high significance at a q value <0.01 (Source: Chakraborty et al., 2023).

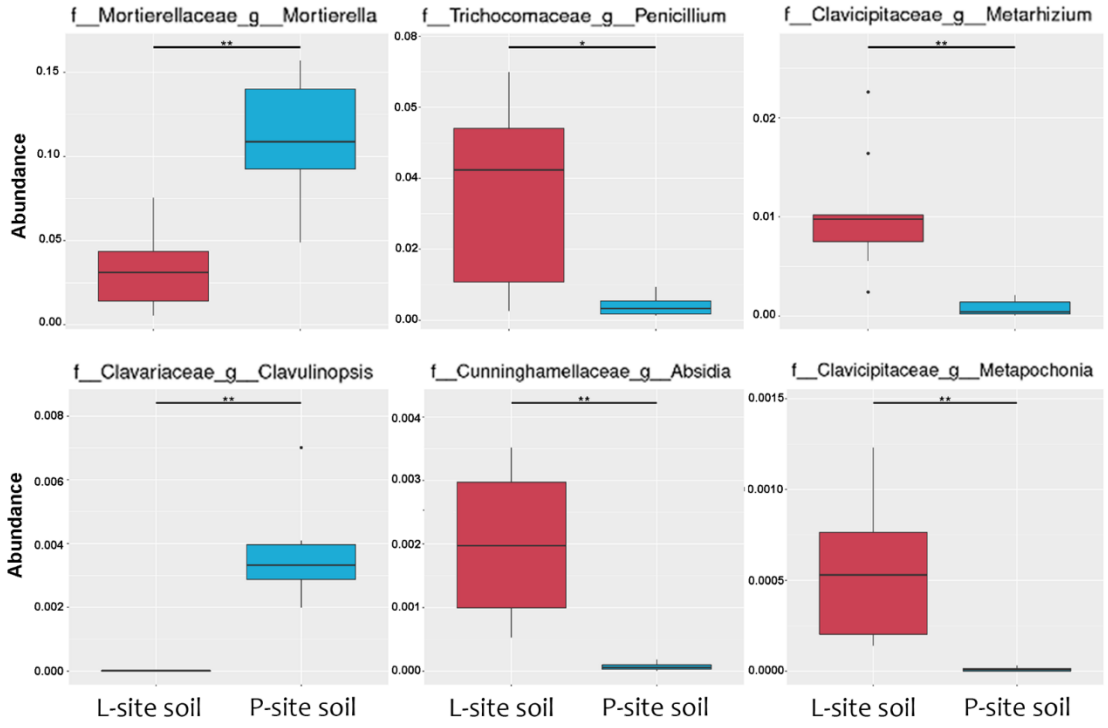

Figure 20 – Fungal MetaStats analysis of bulk soil

Significant differences in relative abundance were evaluated using the FDR test where the "*" indicates significant variation at a q value <0.05, and "**" denotes high significance at a q value <0.01 (Source: Chakraborty et al., 2023).

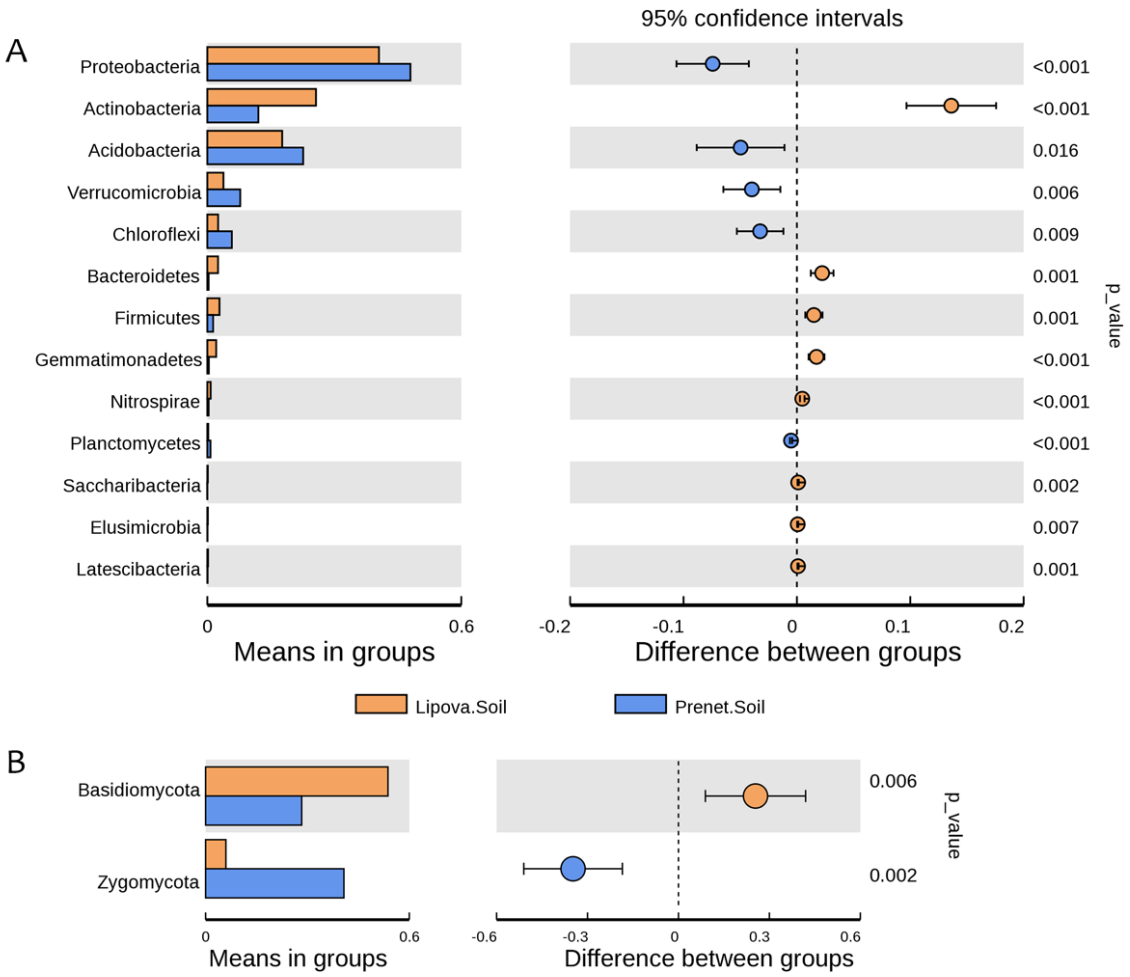

Figure 21 – t-test analysis of bulk soil

Significant variation in **(A)** bacterial and **(B)** fungal communities at the phylum level in the bulk soils from L-site and P-site. The last panel illustrates the abundance of phyla that significantly differ between the two soils. Each bar represents the mean abundance at the phylum level that is significantly different. The right panel displays the confidence intervals between the soils, where the leftmost part of each circle indicates the lower 95% confidence interval limit, the rightmost part represents the upper limit, and the centre of the circle indicates the difference in mean values. The colour of each circle reflects the soil sample with the higher mean value. The rightmost value represents the p-value from the significance test (Source: Chakraborty et al., 2023).

Statistical analyses were performed to evaluate the differences in microbial community structure between the L-site and P-site. The Analysis of Similarity (ANOSIM) (Table 10) revealed significant differences in the microbial community structure between the two soil types, compared to the variation observed within biological replicates. The positive R values indicate significant differences in the microbial communities in two different soils. P-value < 0.05 represents significant differences.

Similarly, the Multi-Response Permutation Procedure (MRPP) (Table 11) analysis confirmed substantial differences in microbial communities across the two soil samples. The low observed-δ values within

replicates indicate minimal variation within each soil type, while the higher expected-δ values point to larger differences between the two soil types. The positive A-value suggests that the distinction between soil types is greater than the variation within replicates, with p-values < 0.05 supporting the significance of these differences.

Consistent findings were also observed with other statistical methods, including The Analysis of Dissimilarities (ADONIS) (Table 12) and AMOVA (Table 13) (where Df stands for degree of freedom, F.Model stands for F-test value, and R2 is the ratio of grouping variance and total variance). Values in parentheses denote Residual Error. The Pr value in ADONIS and the p-value in AMOVA represent the significant variation in the microbial community structure.

These analyses collectively support the conclusion that environmental factors at the different sites have a substantial impact on microbial community composition.

Table 10 – ANOSIM bulk soil

ANOSIM				
Comparison	Bacterial diversity		Fungal diversity	
	R-value	p-value	R-value	p-value
P-site vs L-site	0.939	0.001	0.569	0.002

Table 11 – MRPP bulk soil

MRPP								
Comparison	Bacterial diversity				Fungal diversity			
	A	observed d	expected d	significance	A	observed d	expected d	significance
P-site vs L-site	0.3753	0.268	0.429	0.001	0.1517	0.6471	0.7628	0.001

Table 12 – ADONIS bulk soil

ADONIS						
P-site vs L-site	Df	Sum of Squares	Mean Square	F.Model	R2	Pr(>F)
Bacterial diversity	1(13)	0.93967(0.55824)	0.93967(0.04294)	21.883	0.62732(0.37268)	0.001
Fungal diversity	1(13)	1.2714(2.9741)	1.27140(0.22878)	5.5573	0.29947(0.70053)	0.001

Table 13 – AMOVA bulk soil

AMOVA					
P-site vs L-site	Df	Sum of Squares	Mean Square	F.Model	p-value
Bacterial diversity	1(13)	0.458513(0.160448)	0.458513(0.0123422)	37.1501	<0.001
Fungal diversity	1(13)	3.12511(6.47944)	3.131511(0.498418)	6.29012	<0.001

The study identified specific microbial biomarkers that are significantly abundant and consistently present in the soil samples. Using Linear Discriminant Analysis Effect Size (LEfSe), bacterial (Figure 22A) and fungal (Figure 22B) biomarkers were determined with an LDA score [log10] > 4, highlighting key differences between the sites. Figure 23 depicts a cladogram of bacterial (A) and fungal (B) biomarkers in soils evaluated by the LEfSe analysis.

For P-site bulk soil, the differentially abundant bacterial biomarkers included:

- Acidobacteria (class—Acidobacteria, order—Acidobacteriales, family—*Acidobacteriaceae_subgroup 1*; class—Subgroup_2)
- Proteobacteria (class—Alphaproteobacteria, order— Rhizobiales, family—*Bradyrhizobiaceae,* family—*Roseiarcaceae,* family—*Xanthobacteraceae*; order—Rhodospirillales)
- Chloroflexi (class—Ktedonobacteria, order—Ktedonobacterales, family—*HSB_OF53_F07*)
- Verrucomicrobia (class—Spartobacteria, order—Chthonlobacterales, family—*Xiphinematobacteraceae*)

In contrast, L-site soil was characterized by bacterial biomarkers including:

- Bacteroidetes (class—Sphingobacteriia, order—Sphingobacteriales)
- Actinobacteria (class—Thermoleophilla, order—Gaiellales; order—Soilrubrobacterales)
- Acidobacteria (class—Subgroup_6)
- Proteobacteria (class—Betaproteobacteria; class—Gammaproteobacteria; class—Deltaproteobacteria)

Fungal biomarkers in P-site soil included:

- Zygomycota (class—Incertae_sedis_Zygomycota; order—Mortierellales; family—*Mortierellaceae*)
- Basidiomycota (class—Entorrhizommycetes, order—Entorrhizales, family—*Entorrhizaceae*)

Fungal biomarkers in L-site soil were:

- class—Dothideomycetes
- class—Eurotiomycetes (order—Eurotiales, family—*Trichocomaceae*; order—Chaetothyriales, family—*Herpotrichlellaceae*)
- order—Hypocreales (family—*Nectriaceae*)
- order—Russulales (family—*Russulaceae*)

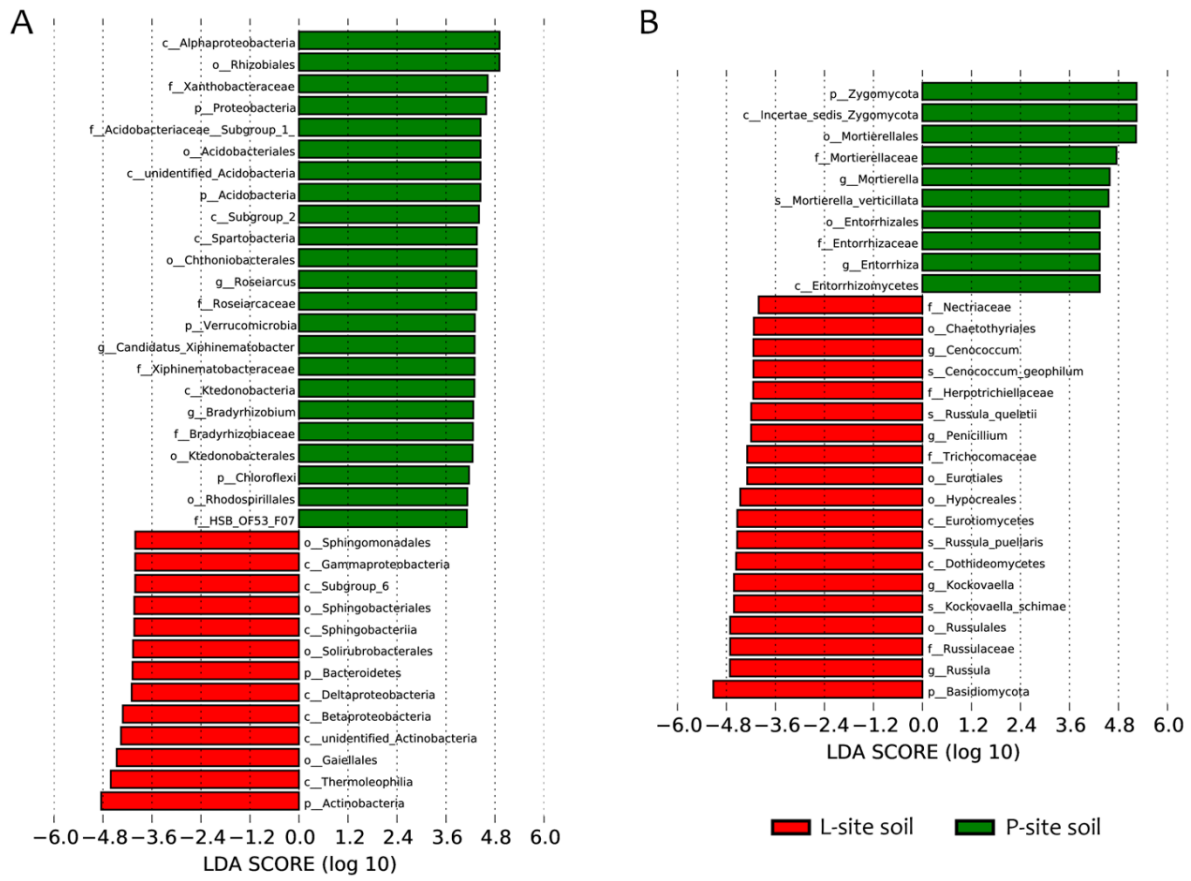

Figure 22 – LEfSe analysis of bulk soil

Presence of **(A)** bacterial and **(B)** fungal biomarker species with significantly different abundance between soils from the L-site and P-site. The length of each bin, represented by the LDA score, indicates the effect size (the extent to which a biomarker explains the differentiating phenotypes among groups) at the LDA score cutoff threshold of >4 (Source: Chakraborty et al., 2023).

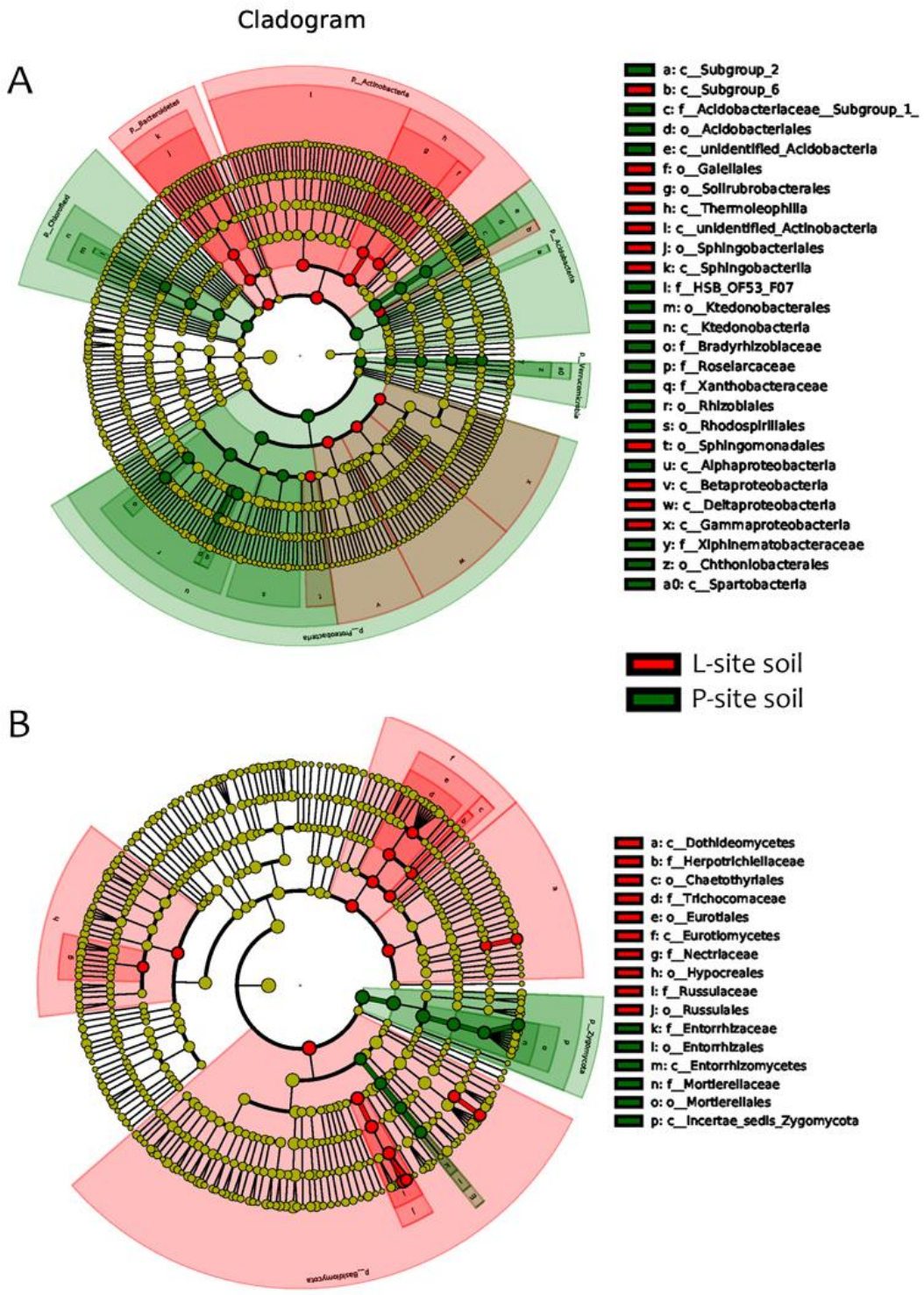

Figure 23 – Cladogram of bulk soil biomarkers obtained by LEfSe

(A) Bacterial and **(B)** fungal biomarkers in soils evaluated using LEfSe analysis. The circles, radiating from inside to outside, represent taxonomic level from phylum to genus. Each circle corresponds to a distinct taxon at its respective taxonomic level, with the size of each circle being proportional to the relative abundance of that taxon. Bacterial and fungal biomarkers that exhibit significant differences are coloured according to the corresponding soil samples, while yellowish-green circles indicate non-significant species. Red and green nodes represent species that contribute significantly to their respective groups. The letters above the circles identify the different biomarkers (Source: Chakraborty et al., 2023).

5.1.5.5 Functional composition

PICRUSt analysis of bacterial 16S gene sequences provided insights into the potential functional profiles of the soil bacterial communities, associating each OTU with specific functions.

The analysis revealed that L-site soil had a higher predicted abundance for functions related to amino acid metabolism, lipid metabolism, terpenoids and polyketides, carbohydrate metabolism, membrane transport, DNA replication and repair, nucleotide metabolism, xenobiotics biodegradation, and metabolism of cofactors and vitamins. In contrast, P-site soil exhibited a higher abundance of functions associated with signal transduction, genetic information processing, biosynthesis of secondary metabolites, glycan metabolism, energy metabolism, and transcription (Figure 24A). Despite these differences, the most abundant gene functions, as identified in the top 10 categories, did not show significant variation between the two sites. These top functions included membrane transport, amino acid metabolism, carbohydrate metabolism, replication and repair, energy metabolism, xenobiotic metabolism, lipid metabolism, translation, and metabolism of cofactors and vitamins (Figure 24B).

The Principal Component Analysis (PCA) plot based on PICRUSt data indicated that the predicted functional gene profiles of the two soil samples were distinct, clustering into two separate groups (Figure 24C).

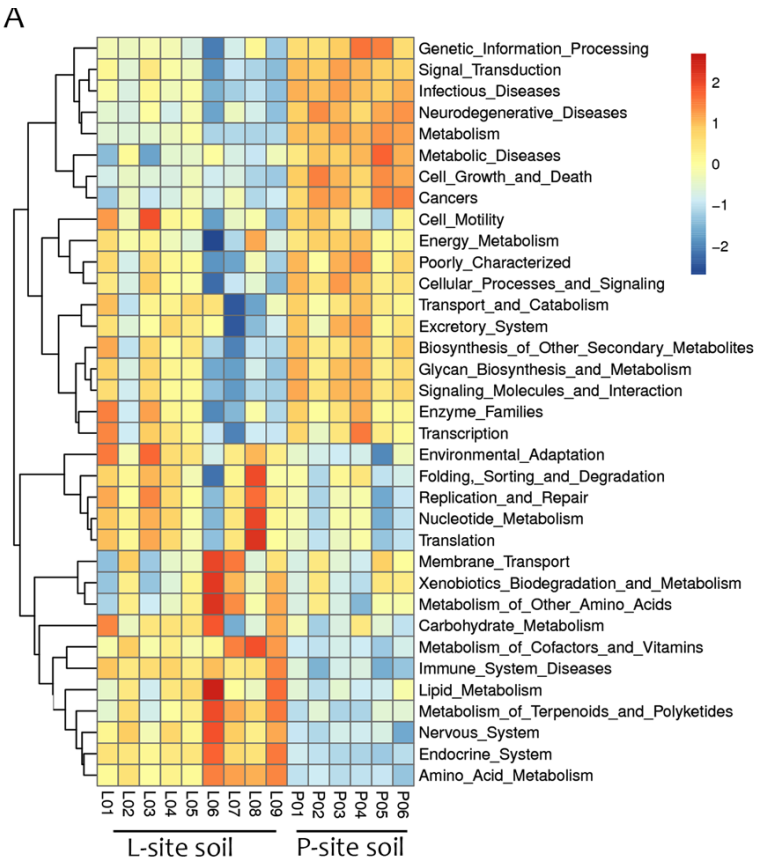

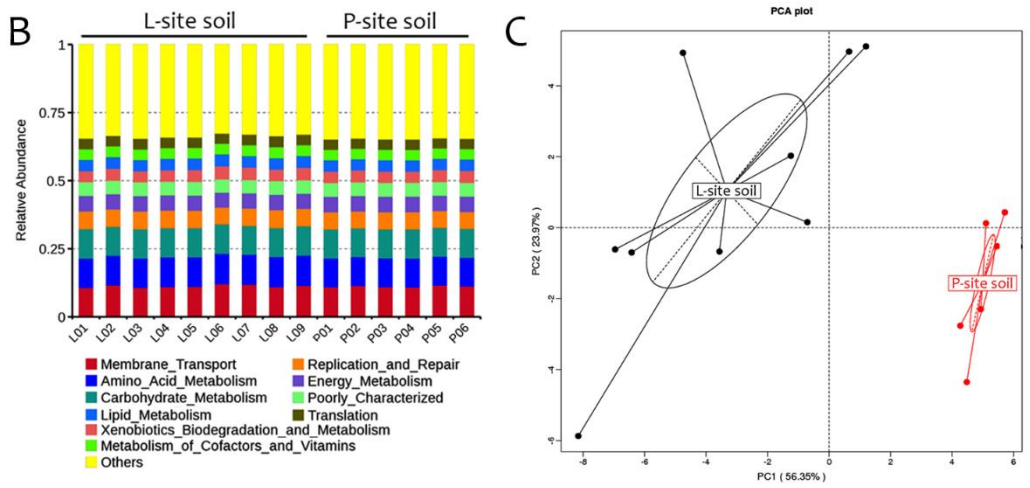

Figure 24 – PICRUSt analysis

(A) A heatmap illustrating the functional profile predicted at level 2 KEGGs Orthologs using PICRUSt analysis, which represents the overall functional contribution of bacterial communities present in two soil samples, each with replicates. **(B)** A bar plot displaying the relative OTU abundance contributing to the top 10 gene functions in soil, showing no significant differences. The "Others" category represents the relative OTU abundance for the remaining gene functions. **(C)** A PCA plot highlighting differences in the predicted functional contributions of the soil bacteriome between the two sites based on PICRUSt analysis (Source: Chakraborty et al., 2023).

5.1.5.6 Correlation between edaphic drivers and soil microbiota

The Spearman rank correlation analysis (Figure 25) demonstrated a significant association between microbial species abundance and environmental factors such as pH, electrical conductivity (EC), total organic carbon (TOC), and total nitrogen (TN) ($p < 0.05$). Bacterial communities were more strongly influenced by pH, TOC, and TN compared to fungal species. Several bacterial genera, including *Streptomyces*, *Kitasatospora*, *Devosia*, *Reyranella*, *Pseudonocardia*, *Gemmatimonas*, *Arthrobacter*, *Nocardioides*, *Solirubacter*, *Rhizomicrobium*, *Acidibacter*, *Haliangium*, *RB41*, *Sporosarcina*, *Bacillus*, *Sphingomonas*, *Bryobacter*, and *Gaiella*, showed negative correlations with TOC and TN. In contrast, *Blastochloris*, *Pedomicrobium*, *Candidatus Koribacter*, *Granulicella*, *Roseiarcus*, *Candidatus Xiphinematobacter*, and *Bradyrhizobium* displayed positive correlations with these factors (Figure 25A).

Soil pH had a significant positive correlation with genera such as *Streptomyces*, *Devosia*, *Pseudonocardia*, *Gemmatimonas*, *Nocardioides*, *Solirubacter*, *Haliangium*, *RB41*, *Sphingomonas*, and *Gaiella*, while *Granulicella*, *Acidothermus*, *Roseiarcus*, *Candidatus Xiphinematobacter*, and *Bradyrhizobium* were negatively correlated. EC had minimal influence, with only *Variibacter* and *Candidatus Solibacter* showing significant correlations (Figure 25A). Mantel test results further confirmed a strong correlation between bacterial community structure and environmental factors ($r = 0.7497$, $p = 0.001$).

Fungal species abundance was also significantly ($p < 0.05$) influenced by soil pH, with genera such as *Paraphoma*, *Phialosimplex*, *Preussia*, *Trichoderma*, *Oidiodendron*, *Hymenogaster*, *Cladosporium*, *Gibberella*, *Halokirschsteiniothelia*, *Fusarium*, *Cadophora*, *Entorrhiza*, and *Russula* showing strong correlations (Figure 25B). TOC and TN notably affected the abundance of fungal genera like *Clitopilus*, *Hygrocybe*, *Thelebolus*, *Preussia*, *Hymenogaster*, *Metarhizium*, *Cladosporium*, *Gibberella*, *Xerocomellus*, *Amanita*, *Fusarium*, *Mortierella*, *Russula*, and *Cenococcum*. Interestingly, only *Tylospora* was significantly influenced by soil EC. The Mantel test also demonstrated a significant correlation between fungal communities and environmental variables ($r = 0.4115$, $p = 0.002$).

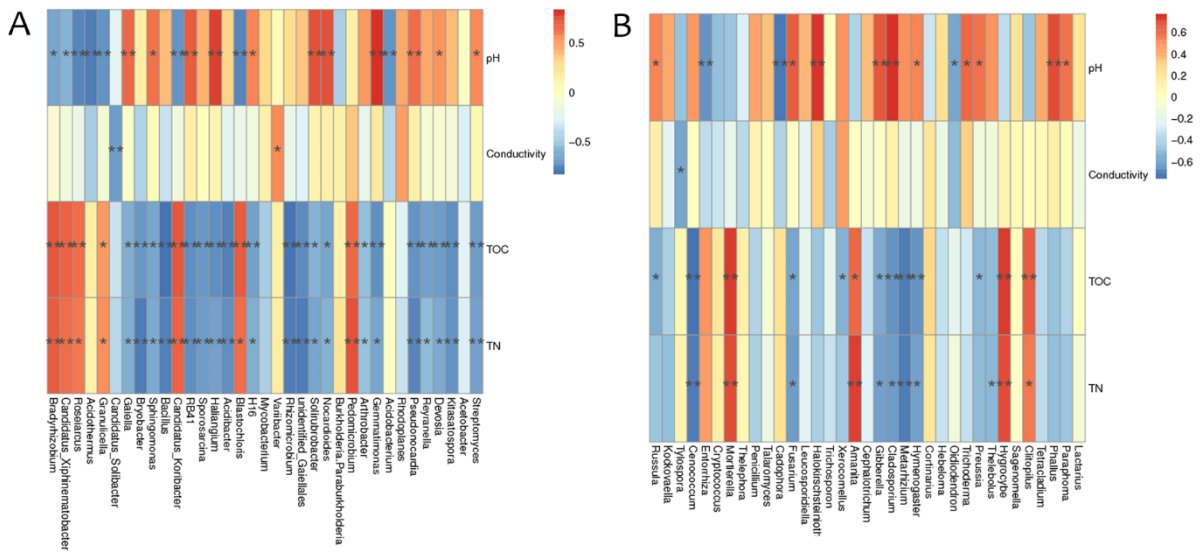

Figure 25 – Spearman rank correlation analysis

A heatmap illustrating the Spearman correlation between environmental factors such as pH, electrical conductivity (EC), total organic carbon (TOC), total nitrogen (TN) with **(A)** bacterial species abundance and **(B)** fungal species abundance. This analysis aims to assess the correlation and significance between the two variables. The columns represent the environmental factors, while the rows indicate the species. Coloured tiles correspond to the Spearman rank correlation coefficient (SCC) r values, which range from –1 to 1. An $r < 0$ indicates a negative correlation, while an $r > 0$ signifies a positive correlation. An asterisk '*' denotes significance at $p < 0.05$ (Source: Chakraborty et al., 2023).

The Canonical Correspondence Analysis (CCA) results illustrated the relationship between microbial communities and environmental factors, showing that soil pH, EC, TOC, and TN significantly influenced microbial development (Figure 26). For bacterial communities, the CCA accounted for 91% of the community variance, suggesting a strong association with these edaphic factors. The analysis revealed that the first canonical axis (CCA1) was positively correlated with TOC and TN, while the second canonical axis (CCA2) showed a negative correlation with soil pH and EC. This differentiation resulted in a clear clustering of L-site and P-site soils into distinct groups (Figure 26A).

Similarly, the fungal community variance explained by the soil parameters was 64.87%, with a distinct grouping for P-site soil, while the L-site soil samples were more dispersed (Figure 26B). In fungal communities, CCA1 was positively correlated with soil pH and EC, and CCA2 was negatively correlated with TOC and TN.

The length of the arrows representing soil pH, TOC, and TN indicated that these were the most influential factors shaping the soil microbial community structure across the two sites. This data highlights the significant role of these edaphic factors in driving microbial community composition and structure in different environments.

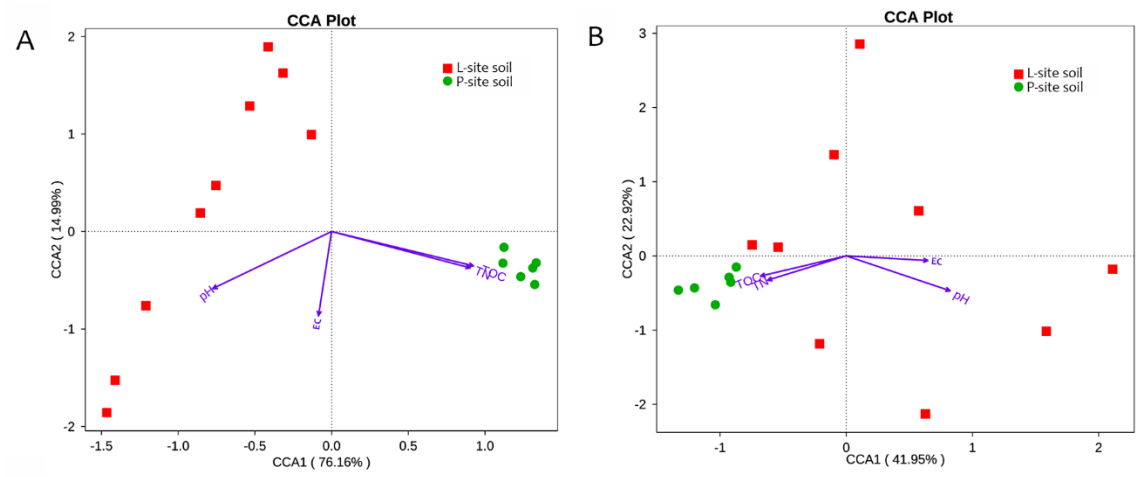

Figure 26 – Canonical Correspondence Analysis (CCA)

A Canonical Correspondence Analysis (CCA) plot representing the relationship between environmental factors (pH, EC, TOC, TN) and the distribution of **(A)** bacterial and **(B)** fungal communities in soil samples. The arrows indicate the association between environmental factors and microbial community distribution; longer arrows signify a stronger association, while shorter arrows indicate a weaker association. The angle between the arrows and the ordination axes reflects the relationship between each environmental factor and the ordination axes; a smaller angle indicates a stronger association, while a large angle indicates a weaker association. A positive relationship between two environmental factors is indicated by an acute angle, whereas a negative correlation is suggested when the angle is obtuse (Source: Chakraborty et al., 2023).

The Variation Partition Analysis (VPA) provided insights into the relative contributions of key edaphic factors (pH, EC, TOC, and TN) to the soil microbial diversity (Figure 27). For the bacterial communities, VPA revealed that soil physical characteristics, such as pH and EC, accounted for 6.5% of the total variation, while TOC and TN explained a significant 37.6% of the total variance (Figure 27A). This highlights the dominant role of organic carbon and nitrogen content in shaping bacterial diversity. Nevertheless, 20.7% of the variation in bacterial community structure remained unexplained, indicating the presence of other unidentified factors.

In contrast, for fungal communities, pH and EC contributed to 6.6% of the total variance, and TOC and TN accounted for 32.8% (Figure 27B). Interestingly, a much larger portion of the fungal community variance, around 52%, remained unexplained, suggesting that fungal diversity might be influenced by additional factors not captured in this analysis. This substantial unexplained variance reflects the complexity of fungal ecology in soil environments.

The partitioning of explained and unexplained variance in VPA was calculated following methods outlined by Legendre (2008), which emphasizes the differential impact of environmental factors on bacterial and fungal communities.

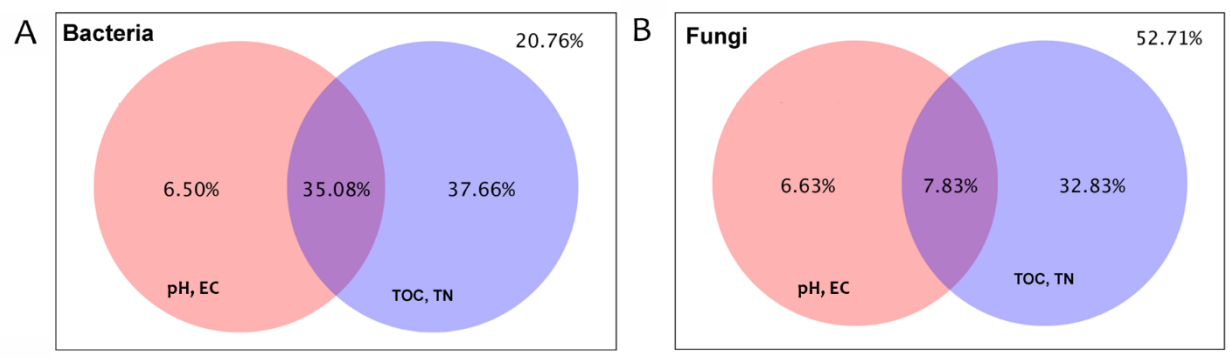

Figure 27 – Variation Partition Analysis (VPA)

Variance Partitioning Analysis (VPA) displaying the total variance in the distribution of **(A)** bacterial and **(B)** fungal communities, illustrating the respective contributions and covariations of each set of environmental variables. The outer value indicates the percentage of variance that remains explained (Source: Chakraborty et al., 2023).

5.2 Impact of long-term precipitation regime differences on rhizospheric soil

5.2.1 Soil texture and trace elements analysis

The analysis of soil texture based on particle size distribution confirmed that both L-site and P-site rhizospheric soils had a loamy sand texture. L-site soil contained 0.03% clay, 23.4% silt, and 76.5% sand, while P-site soil had 0.05% clay, 29.4% silt, and 70.4% sand. Despite the similar texture, P-site soil had a significantly higher moisture content (38%) compared to L-site soil (13%), likely due to increased precipitation at the P-site.

Physicochemical and biochemical parameters, including pH, electrical conductivity (EC), total organic carbon (TOC), and total nitrogen (TN), were assessed for bulk soil as previously outlined. These measurements were not repeated for rhizospheric soil, as the primary emphasis was placed on exploring the diversity of the rhizospheric microbial community.

Elemental analysis (Figure 28A and Figure 28B) indicated that Aluminium (Al), Iron (Fe), Phosphorous (P), and Sulphur (S) were present in significantly higher concentrations in P-site soil, whereas Calcium (Ca) was significantly more abundant in L-site soil (t-test, $p < 0.05$). There were no significant differences in the levels of Potassium (K), Magnesium (Mg), Manganese (Mn), Sodium (Na), Silicon (Si), or Zinc (Zn) between the two sites. This elemental abundance, particularly in P-site, could play a role in shaping the local soil microbial communities and overall soil fertility.

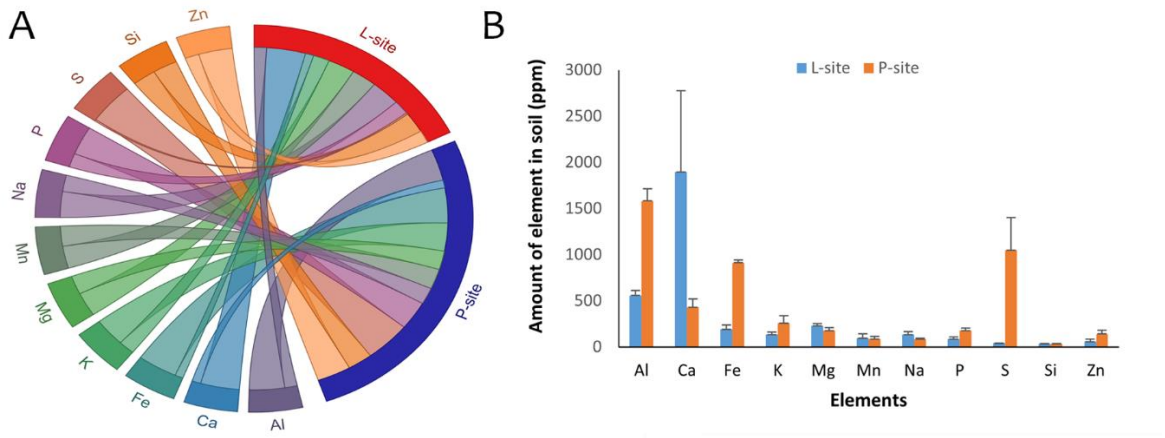

Figure 28 – Elemental analysis

(A) The relative abundance of various elements (expressed as percentages) present in the rhizospheric soil samples collected from the two sites. **(B)** A bar graph illustrating the differences in elemental content among the rhizospheric soil samples (Source: Zádrapová et al., 2024).

5.2.2 Metabolite profiling

A total of 204 metabolites were identified, primarily comprising acids and alcohols. The top 50 metabolites showed significant differences in abundance between the two sites (t-test, $p < 0.05$). The chordial plot illustrated the relative abundance of major metabolite classes in the rhizospheric soils from the L-site and P-site (Figure 29A). The L-site soil was enriched in carbohydrates (62.7%) and alcohols (17%), while the P-site had slightly lower carbohydrate content (55%) but higher alcohols (22%). Additionally, fatty acids (L-site: 2.5%; P-site: 4.5%), acids (L-site: 0.85%; P-site: 1.7%), and terpenes (L-site: 2.7%; P-site: 4.3%) were significantly more abundant in the P-site soil (t-test, $p < 0.05$). These differences suggest variations in soil organic matter composition, plant exudates, and microbial activity, although attributing the exact contribution of each factor to the metabolite profile remains challenging (White et al., 2017).

The Sparse partial least square discriminant analysis (sPLS-DA) plot (Figure 29B) revealed distinct clustering into two groups based on site, indicating the differences in the metabolite profiles of rhizospheric soil samples from L-site and P-site.

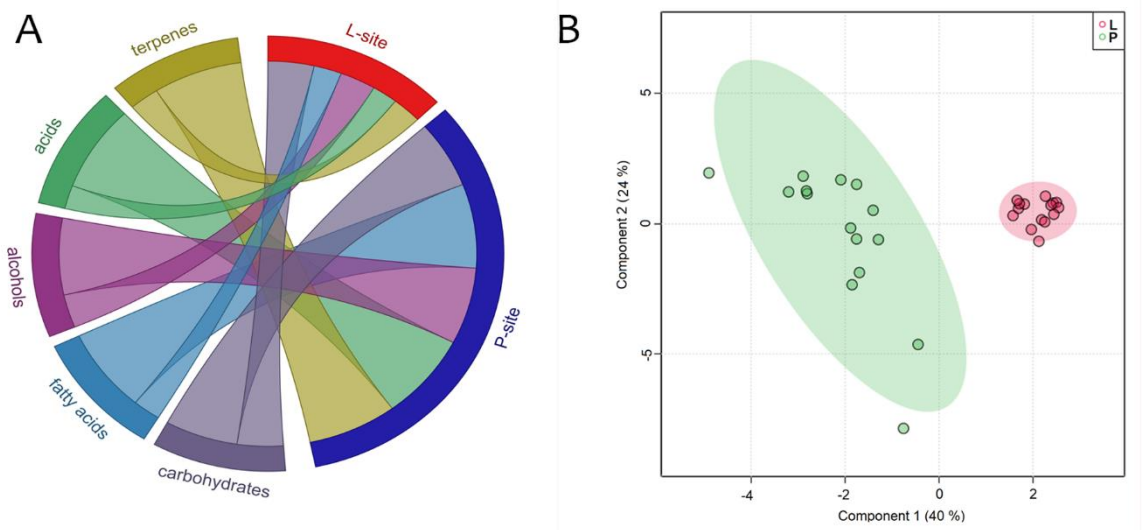

Figure 29 – Metabolite profiling

(A) The relative abundance of various classes of metabolites (expressed as percentages) present in the rhizospheric soil samples collected from the two sites. **(B)** An sPLS-DA plot illustrating the differences in metabolite profiles between rhizospheric soil samples from the two different sites (Source: Zádrapová et al., 2024).

Additionally, variation in the rhizospheric metabolic profiles among individual clonal tree varieties (1901, 1902, 1908, 1941, and 1950) from both L-site and P-site were depicted in a heatmap (Figure 30), highlighting the top 70 metabolites that exhibited significant differences.

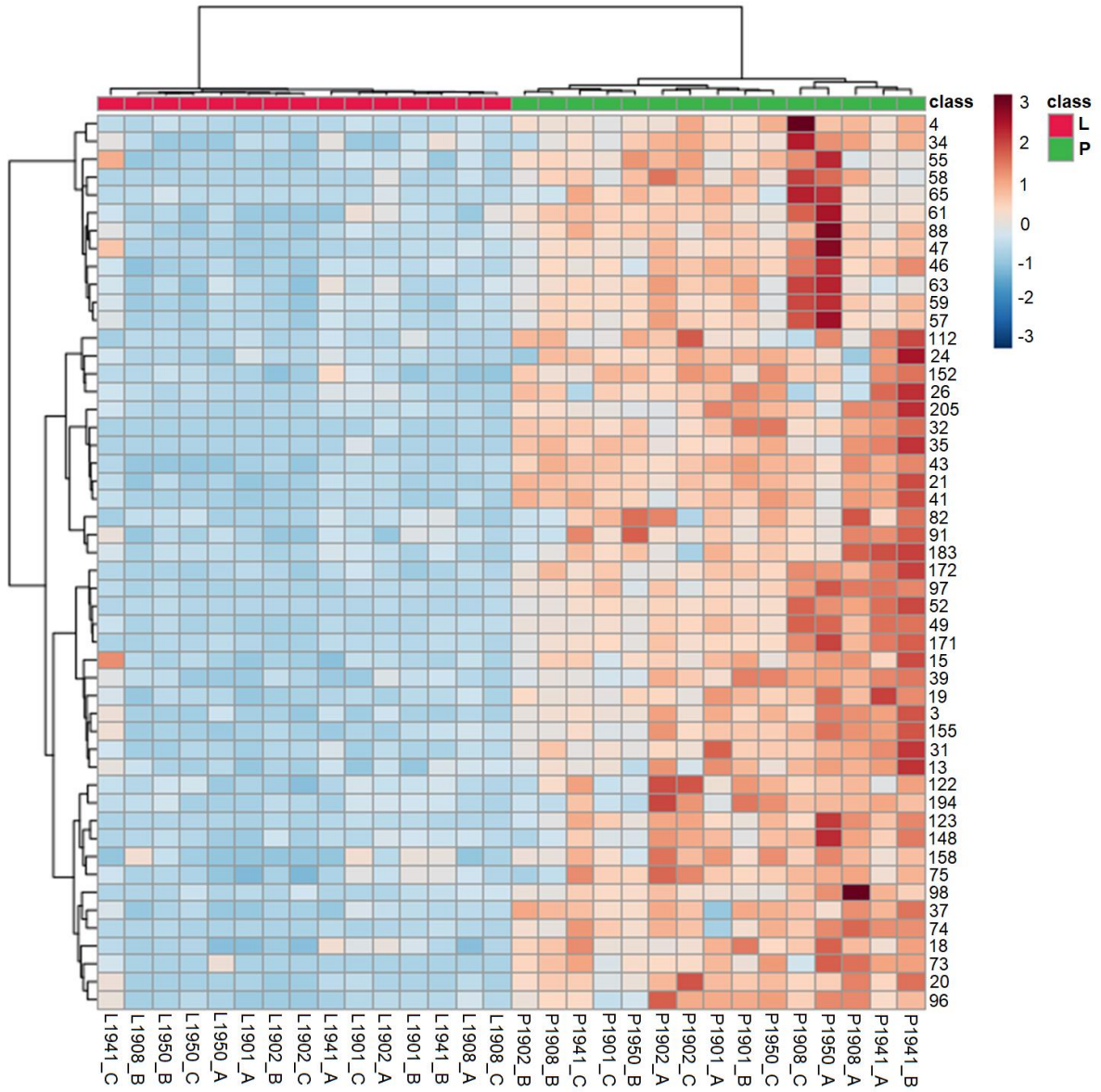

Figure 30 – Heatmap of rhizospheric soil metabolite profile

A heatmap showing 70 most significant metabolites between the rhizospheric soil of each clonal tree variety (1901, 1902, 1908, 1941, and 1950) in three replicates.

5.2.3 Rhizospheric soil microbial community structure

5.2.3.1 Sequencing results

Illumina paired-end amplicon sequencing of the bacterial 16S rRNA gene and fungal ITS2 region from the rhizospheric soil samples of two seed orchards yielded 12,945,042 raw bacterial reads and 8,730,722 raw fungal reads, capturing the microbial diversity in the soils. After quality filtering, 9,630,977 clean bacterial reads (Table 14) and 8,253,265 clean fungal reads (Table 15) were obtained. These clean reads were then processed using bioinformatics pipelines in QIIME2 for further analysis.

Table 14 – Illumina paired-end amplicon sequencing of bacterial 16S in rhizosphere

Collection site	Rhizosphere soil samples	Sample Name	Raw PE reads	Combined reads	Qualified reads	Nochimera	Base [nt]	Average lenght [bp]	Q20	Q30	GC [%]	Effective [%]
L-site	L1901_A	L1901Rz.01	219 572	207 743	199 630	177 043	73 089 632	413	98.06	93.87	55.94	80.63
	L1901_B	L1901Rz.02	201 575	190 262	183 696	161 044	66 703 362	414	98.14	94.08	56.54	79.89
	L1901_C	L1901Rz.03	217 620	207 419	200 213	150 949	62 373 068	413	98.07	93.95	56.23	69.36
	L1901_D	L1901Rz.04	130 455	121 202	116 995	99 366	41 310 202	416	98.02	93.82	56.57	76.17
	L1901_E	L1901Rz.05	206 221	195 728	188 911	162 947	68 121 275	418	97.96	93.62	55.92	79.02
	L1902_A	L1902Rz.01	211 497	200 703	193 912	168 065	69 784 072	415	98.05	93.82	56.44	79.46
	L1902_B	L1902Rz.02	213 522	200 027	192 835	166 905	69 492 815	416	98.1	93.96	56.49	78.17
	L1902_C	L1902Rz.03	207 105	196 253	189 941	168 151	69 506 806	413	98.1	93.94	56.21	81.19
	L1902_D	L1902Rz.04	148 154	142 175	137 997	121 365	50 121 842	413	98.2	94.17	54.49	81.92
	L1902_E	L1902Rz.05	212 827	201 709	194 602	170 727	70 659 457	414	97.94	93.62	56.4	80.22
	L1908_A	L1908Rz.01	145 730	138 342	133 533	115 923	48 027 238	414	97.93	93.63	56.84	79.55
	L1908_B	L1908Rz.02	313 845	280 231	274 529	238 556	99 025 830	415	98.1	93.94	55.95	76.01
	L1908_C	L1908Rz.03	139 975	132 811	128 282	112 435	46 507 214	414	97.96	93.67	56.4	80.33
	L1908_D	L1908Rz.04	107 708	102 229	98 752	87 592	36 316 934	415	98.04	93.71	56.65	81.32
	L1908_E	L1908Rz.05	164 810	156 668	151 544	135 346	55 783 467	412	98.03	93.82	56.43	82.12
	L1941_A	L1941Rz.01	201 665	191 437	185 009	166 927	68 813 526	412	98.01	93.78	56.71	82.77
	L1941_B	L1941Rz.02	107 836	102 325	98 878	85 992	35 607 490	414	97.92	93.38	56.09	79.74
	L1941_C	L1941Rz.03	207 236	193 360	185 527	167 421	69 103 367	413	97.95	93.67	55.92	80.79
	L1941_D	L1941Rz.04	186 231	144 739	137 942	121 124	50 099 539	414	98	93.79	56.71	65.04
	L1941_E	L1941Rz.05	177 887	168 784	163 143	145 264	59 989 948	413	98	93.8	56.51	81.66
	L1950_A	L1950Rz.01	202 247	191 632	184 785	161 301	67 073 758	416	97.87	93.45	57.09	79.75
	L1950_B	L1950Rz.02	133 156	125 189	121 009	110 033	45 423 297	413	98.12	93.95	56.08	82.63
	L1950_C	L1950Rz.03	178 464	168 329	162 435	143 751	59 534 417	414	97.94	93.55	56.23	80.55
	L1950_D	L1950Rz.04	199 519	188 651	181 918	161 933	66 811 207	413	97.9	93.49	56.04	81.16
	L1950_E	L1950Rz.05	189 464	178 460	172 170	151 369	62 719 497	414	97.81	93.21	56.46	79.89
P-site	P1901_A	P1901Rz.01	210 389	199 834	192 992	173 425	71 269 024	411	98.03	93.85	55.9	82.43
	P1901_B	P1901Rz.02	167 027	156 482	151 170	137 473	56 309 068	410	97.96	93.61	55.54	82.31
	P1901_C	P1901Rz.03	155 740	148 238	143 090	126 207	52 104 602	413	98	93.82	55.91	81.04
	P1901_D	P1901Rz.04	307 045	270 987	266 379	242 407	99 490 756	410	98.2	94.16	56.19	78.95
	P1901_E	P1901Rz.05	155 045	147 234	142 154	129 043	52 985 488	411	98.03	93.89	56.57	83.23
	P1902_A	P1902Rz.01	166 843	157 917	152 705	138 568	56 871 030	410	98.08	93.99	56.44	83.05
	P1902_B	P1902Rz.02	200 914	190 718	184 222	167 383	68 761 733	411	98.07	93.94	55.31	83.31
	P1902_C	P1902Rz.03	167 179	158 858	153 624	139 368	57 235 090	411	98.07	93.98	56.58	83.36
	P1902_D	P1902Rz.04	136 287	129 922	125 850	114 360	46 953 519	411	98.16	94.11	56.22	83.91
	P1902_E	P1902Rz.05	419 070	245 168	239 855	220 516	90 389 003	410	97.58	92.75	56.56	52.62
	P1908_A	P1908Rz.01	419 857	261 470	255 924	233 169	95 877 097	411	97.71	93.16	56.21	55.54
	P1908_B	P1908Rz.02	401 657	247 494	241 209	220 483	90 731 901	412	97.48	92.6	55.49	54.89
	P1908_C	P1908Rz.03	382 866	229 885	223 694	204 908	83 950 100	410	97.52	92.73	56.38	53.52
	P1908_D	P1908Rz.04	419 523	260 724	255 853	230 444	94 973 510	412	97.75	93.08	56.77	54.93
	P1908_E	P1908Rz.05	411 180	247 805	242 260	221 585	90 784 639	410	97.68	93.01	56.13	53.89
	P1941_A	P1941Rz.01	412 568	198 908	186 415	170 741	69 927 811	410	97.62	92.92	56.11	41.38
	P1941_B	P1941Rz.02	394 688	250 643	245 028	225 772	92 711 848	411	97.56	92.73	56.15	57.2
	P1941_C	P1941Rz.03	422 785	253 638	247 806	227 086	93 341 028	411	97.64	92.95	56.32	53.71
	P1941_D	P1941Rz.04	430 221	267 685	260 519	229 500	95 282 923	415	97.49	92.61	55.17	53.34
	P1941_E	P1941Rz.05	429 537	266 898	261 049	239 315	98 364 283	411	97.69	93.11	56.45	55.71
	P1950_A	P1950Rz.01	423 446	264 682	258 426	238 153	97 853 834	411	97.56	92.81	56.04	56.24
	P1950_B	P1950Rz.02	414 427	252 270	247 220	224 785	92 390 288	411	97.73	93.04	56.47	54.24
	P1950_C	P1950Rz.03	417 696	261 029	255 690	236 269	96 927 068	410	97.77	93.27	56.29	56.56
	P1950_D	P1950Rz.04	421 433	263 498	257 568	239 323	98 232 448	410	97.61	92.9	56.66	56.79
	P1950_E	P1950Rz.05	433 298	268 118	262 087	242 002	99 501 018	411	97.73	93.17	56.13	55.85

Table 15 – Illumina paired-end amplicon sequencing of fungal ITS in rhizosphere

Collection site	Rhizosphere soil samples	Sample Name	Raw PE reads	Combined reads	Qualified reads	Nochimera	Base [nt]	Average lenght [nt]	Q20	Q30	GC [%]	Effective [%]
L-site	L1901_A	L1901Rz.01	127 337	124 171	123 210	108 464	37 245 711	343	99.05	96.55	46.65	85.18
	L1901_B	L1901Rz.02	144 230	139 980	138 156	117 669	39 345 999	334	99.1	96.72	49.87	81.58
	L1901_C	L1901Rz.03	279 219	274 069	269 619	230 736	72 958 596	316	99.27	97.38	48.38	82.64
	L1901_D	L1901Rz.04	166 144	161 885	160 714	137 034	44 574 328	325	99.06	96.66	48.19	82.48
	L1901_E	L1901Rz.05	143 465	139 549	137 598	115 506	38 787 171	336	99.08	96.77	49.65	80.51
	L1902_A	L1902Rz.01	206 391	201 045	197 642	170 961	55 951 840	327	99.17	97.03	47.78	82.83
	L1902_B	L1902Rz.02	181 085	176 237	175 059	150 557	49 251 192	327	99.19	97.16	51.14	83.14
	L1902_C	L1902Rz.03	207 520	201 882	200 415	173 594	56 876 050	328	99.22	97.19	50.78	83.65
	L1902_D	L1902Rz.04	205 494	200 337	199 420	172 261	56 078 710	326	99.19	97.13	50.4	83.83
	L1902_E	L1902Rz.05	180 154	175 906	174 377	129 648	44 635 033	344	99.11	96.78	45.69	71.97
	L1908_A	L1908Rz.01	173 112	166 913	165 680	137 841	45 545 851	330	99.17	97.03	51.29	79.63
	L1908_B	L1908Rz.02	157 058	153 334	152 444	131 192	44 868 653	342	99.01	96.54	50.7	83.53
	L1908_C	L1908Rz.03	171 795	167 738	166 480	144 605	48 589 829	336	99.18	96.99	47.65	84.17
	L1908_D	L1908Rz.04	166 235	162 780	162 138	139 066	42 864 370	308	99.23	97.37	49.54	83.66
	L1908_E	L1908Rz.05	202 735	197 483	152 594	133 075	46 914 958	353	99.03	96.48	46.84	65.64
	L1941_A	L1941Rz.01	122 323	119 539	118 214	105 712	37 272 988	353	99.05	96.51	45.83	86.42
	L1941_B	L1941Rz.02	202 480	194 602	193 007	168 263	56 493 292	336	99.17	97.03	46.92	83.1
	L1941_C	L1941Rz.03	113 955	112 179	111 196	98 351	32 251 258	328	99.23	97.14	50.09	86.31
	L1941_D	L1941Rz.04	149 203	144 734	143 579	124 087	42 444 438	342	99.1	96.74	47.68	83.17
	L1941_E	L1941Rz.05	138 554	135 352	134 663	111 177	35 783 881	322	99.14	96.94	49.45	80.24
	L1950_A	L1950Rz.01	142 147	139 099	136 167	116 044	40 404 376	348	99.14	96.81	48.66	81.64
	L1950_B	L1950Rz.02	144 276	140 257	139 687	117 057	37 591 416	321	99.18	96.97	50.51	81.13
	L1950_C	L1950Rz.03	152 511	142 553	141 915	120 578	39 806 328	330	98.79	96.06	49.36	79.06
	L1950_D	L1950Rz.04	131 586	128 079	127 011	105 918	34 904 556	330	99.15	96.95	48.38	80.49
	L1950_E	L1950Rz.05	139 452	136 068	135 106	112 174	37 877 797	338	99.09	96.77	49.55	80.44
P-site	P1901_A	P1901Rz.01	202 032	196 488	194 954	167 720	56 008 455	334	99.11	96.78	47.46	83.02
	P1901_B	P1901Rz.02	219 546	214 865	214 204	183 786	55 819 031	304	99.28	97.56	52.22	83.71
	P1901_C	P1901Rz.03	201 055	192 962	134 115	112 378	37 623 659	335	99.12	96.8	48.54	55.89
	P1901_D	P1901Rz.04	172 403	165 455	164 426	139 449	45 719 229	328	99.12	96.98	51.64	80.89
	P1901_E	P1901Rz.05	134 178	130 868	130 132	113 511	37 364 464	329	99.18	97.06	48.74	84.6
	P1902_A	P1902Rz.01	207 244	202 089	200 270	160 916	55 859 045	347	99.04	96.51	47.25	77.65
	P1902_B	P1902Rz.02	180 801	176 889	175 335	142 692	45 823 024	321	99.16	97.05	49.83	78.92
	P1902_C	P1902Rz.03	208 621	201 579	200 724	173 092	55 604 186	321	99.24	97.23	48.82	82.97
	P1902_D	P1902Rz.04	169 391	165 735	165 073	136 873	43 352 643	317	99.21	97.24	50.98	80.8
	P1902_E	P1902Rz.05	219 820	213 488	212 472	187 325	62 923 984	336	99.13	96.89	52.6	85.22
	P1908_A	P1908Rz.01	201 403	193 404	191 537	175 408	61 094 368	348	99.04	96.53	46.83	87.09
	P1908_B	P1908Rz.02	135 344	132 595	131 414	111 096	37 728 235	340	99.12	96.78	45.39	82.08
	P1908_C	P1908Rz.03	200 720	170 669	169 502	149 148	49 886 567	334	99.14	96.89	51.02	74.31
	P1908_D	P1908Rz.04	142 276	134 492	134 046	112 817	36 874 134	327	99.21	97.14	50.2	79.29
	P1908_E	P1908Rz.05	139 725	136 986	136 349	121 067	36 722 113	303	99.33	97.62	50.15	86.65
	P1941_A	P1941Rz.01	188 242	182 456	161 008	145 724	49 546 697	340	99.13	96.8	47.22	77.41
	P1941_B	P1941Rz.02	159 482	153 936	153 070	125 653	40 902 135	326	99.08	96.74	48.13	78.79
	P1941_C	P1941Rz.03	134 679	130 690	130 318	111 353	34 500 496	310	99.29	97.54	49.98	82.68
	P1941_D	P1941Rz.04	169 134	162 537	150 810	131 534	46 188 805	351	98.89	96.09	46.75	77.77
	P1941_E	P1941Rz.05	174 041	168 944	168 249	148 490	47 811 118	322	99.18	97.11	50.46	85.32
	P1950_A	P1950Rz.01	200 322	193 045	191 772	167 474	56 744 018	339	98.9	96.18	47.99	83.6
	P1950_B	P1950Rz.02	210 004	200 937	200 136	171 208	55 983 007	327	99.06	96.75	51.24	81.53
	P1950_C	P1950Rz.03	219 023	210 292	209 279	176 811	59 091 589	334	99	96.53	48.94	80.73
	P1950_D	P1950Rz.04	189 026	183 315	182 579	159 881	51 423 072	322	99.17	97.15	49.23	84.58
	P1950_E	P1950Rz.05	203 749	196 339	195 400	179 602	58 357 655	325	99.08	96.79	51.35	88.15

5.2.3.2 Amplicon Sequence Variants (ASVs) abundance

The rhizospheric soil samples from two seed orchards revealed a total of 29,770 bacterial amplicon sequence variants (ASVs) with 99% similarity. Of these, 15,835 ASVs were found exclusively in the L-site, while 9,576 ASVs were unique to the P-site (Figure 31A). These ASVs were classified into 46 bacterial and 2 archaeal phyla, with the most dominant bacterial phyla being Proteobacteria (39% at L-site, 43% at P-site), Acidobacteriota (25% at L-site, 30% at P-site), Actinobacteria (18% at L-site, 16% at P-site), Verrucomicrobia (5% at L-site, 4% at P-site), and Bacteroidota (3% at L-site, 2% at P-site) (Figure 31B). The evolutionary tree of the top 100 abundant bacterial genera highlighted the presence of *Granulicella, Bradyrhizobium, Acidothermus, Rhodonobacter, Roseiarus, Candidatus Solibacter, Occallatibacter,* and *Burkholderia-Caballeronia-Paraburkholderia.*

For fungi, ITS2 sequencing identified 7,570 ASVs, with 3,778 ASVs specific to the L-site and 2,537 ASVs exclusive to the P-site (Figure 31C). These fungal ASVs were spread across 18 phyla, with Basidiomycota (53% at L-site, 44% at P-site), Ascomycota (35% at L-site, 44% at P-site), and Mortierellomycota (4% at L-site, 5% at P-site) being the most prevalent. The most abundant fungal genera included *Tylospora, Macrolepiota, Hygrophorus, Piloderma, Exophiala*, and *Cenococcum* in the L-site, whereas *Hyaoscypha, Archaeorhizomyces, Amphinema*, and *Amanita* dominated the P-site (Figure 31D).

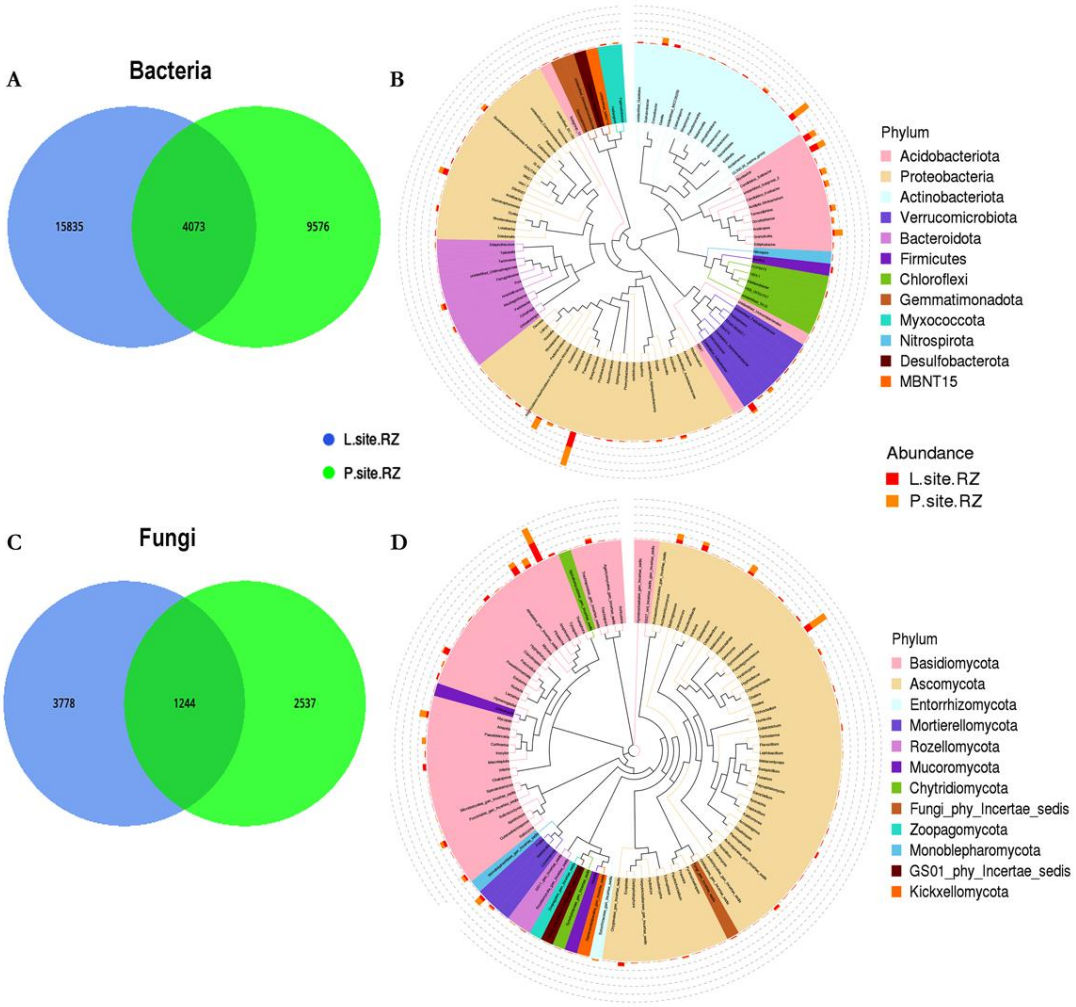

Figure 31 – Amplicon sequence variants (ASVs) abundance

A Venn diagram illustrating the distribution of unique and shared **(A)** bacterial and **(C)** fungal ASVs between the two different rhizospheric soil samples. Additionally, an evolutionary tree representing the top 100 **(B)** bacterial and **(D)** fungal genera in soil samples from the two sites. Different colours of the branches indicate distinct phyla. The relative abundance of each genus in each soil sample is displayed outside the circle, with different colours representing different rhizosphere samples (Source: Zádrapová et al., 2024).

5.2.3.3 Alpha diversity

The completeness of the amplicon sequencing was confirmed by Good's coverage index, which surpassed 99%, demonstrating that the sequencing depth effectively captured nearly all microbial taxa present in the soil samples, with less than 1% of the diversity remaining undetected. Moreover, the rarefaction curves approached a plateau, reinforcing that the Illumina sequencing adequately represented the microbial diversity in the samples (Figure 32). These results underscore the thoroughness of the sequencing in accurately reflecting both bacterial (Figure 32A) and fungal (Figure 32B) communities in the rhizospheric soil.

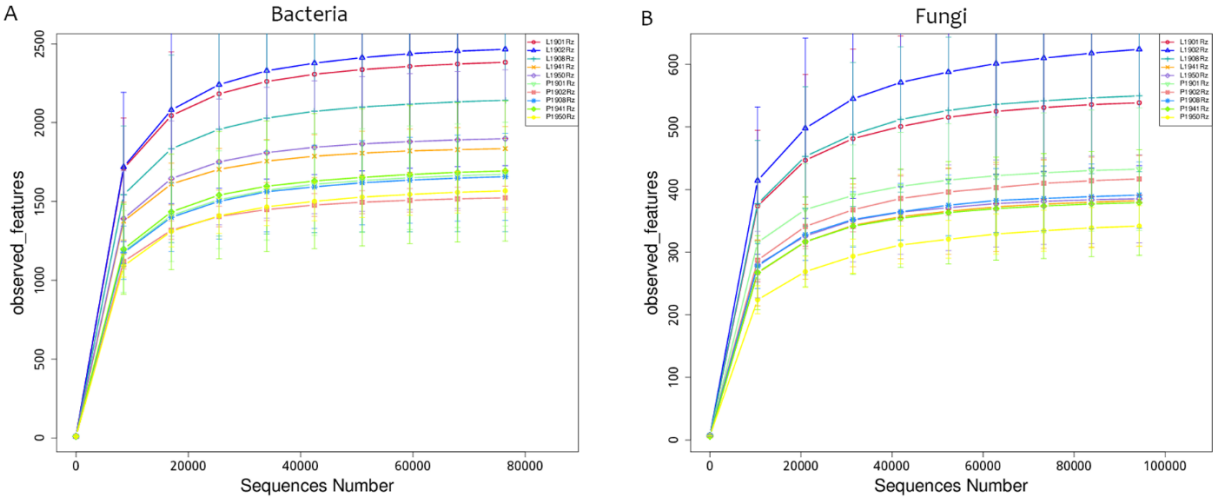

Figure 32 – Rhizosphere rarefaction curves

(A) Bacterial 16S amplicon sequencing and **(B)** fungal ITS sequencing of rhizosphere soil samples collected from L-site and P-site. Different colours and symbols represent different samples (Source: Zádrapová et al., 2024).

The bacterial diversity, richness, and evenness were significantly higher in the L-site soil compared to the P-site soil. The Shannon index, which measures bacterial diversity, was 11.0 in the L-site and 9.66 in the P-site. Similarly, community richness, based on the $Chao_1$ index, was much higher in the L-site (20,460) compared to the P-site (14,308). The Pielou index, which reflects community evenness, was also greater in the L-site (0.77) than in the P-site (0.70). All these differences were statistically significant (Wilcoxon test, $p < 0.001$) (Figure 33A–C).

For fungal communities, the richness ($Chao_1$) was also significantly higher in the L-site (5,184) than in the P-site (3,949) (Wilcoxon test, $p < 0.05$). However, there was no significant difference in fungal diversity (Shannon index, L-site: 7.08; P-site: 6.994) or community evenness (Pielou index, L-site: 0.576; P-site: 0.589) (Figure 33D–F).

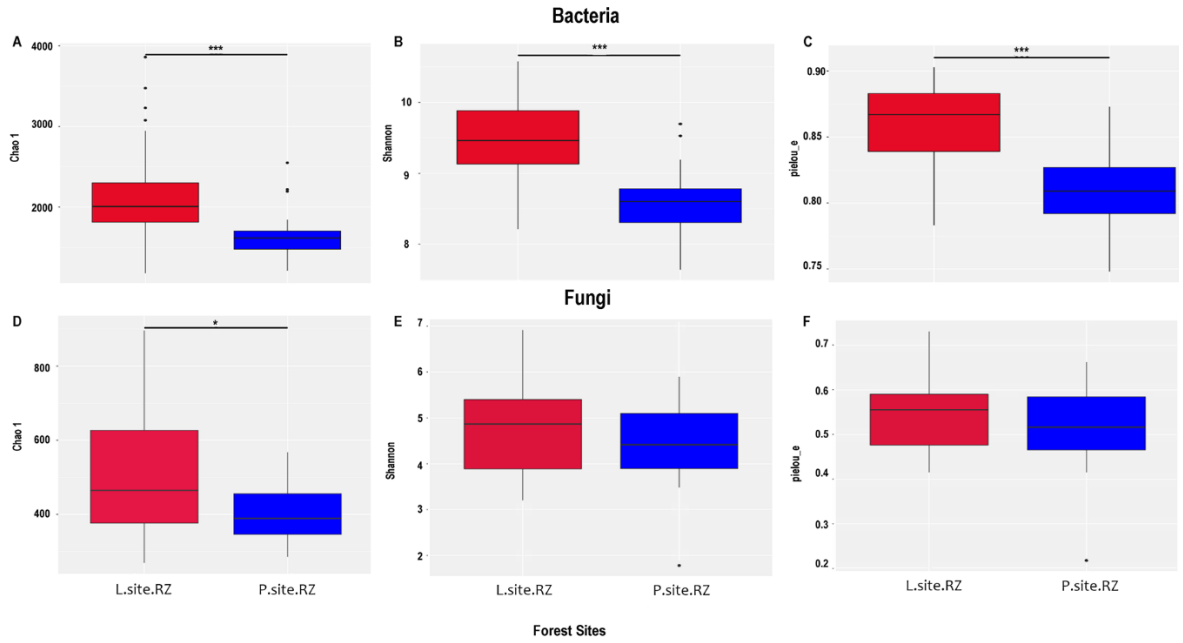

Figure 33 – Alpha diversity indices of rhizospheric soil

The Chao$_1$ index representing **(A)** bacterial and **(D)** fungal richness. The Shannon index estimating **(B)** bacterial and **(E)** fungal diversity. The Pielou index representing **(C)** bacterial and **(F)** fungal evenness in the rhizosphere samples from the two seed orchards. The level of significance was determined using the Wilcoxon test, where "*" denotes p <0.05 and "***" indicates p <0.001 (Source: Zádrapová et al., 2024).

5.2.3.4 Beta diversity

The overall microbial diversity, assessed using unweighted UniFrac distances, revealed clear clustering of bacterial communities from the rhizospheric soil of the two sites. This distinct separation highlights the significant role of site-specific environmental factors in shaping the bacterial populations in the rhizospheric soil (Figure 34A). In comparison, while the fungal populations also formed two distinct clusters based on the site, the clusters were positioned more closely together. This indicates that environmental factors specific to each site had a lesser impact on fungal community structure than on bacterial communities (Figure 34B).

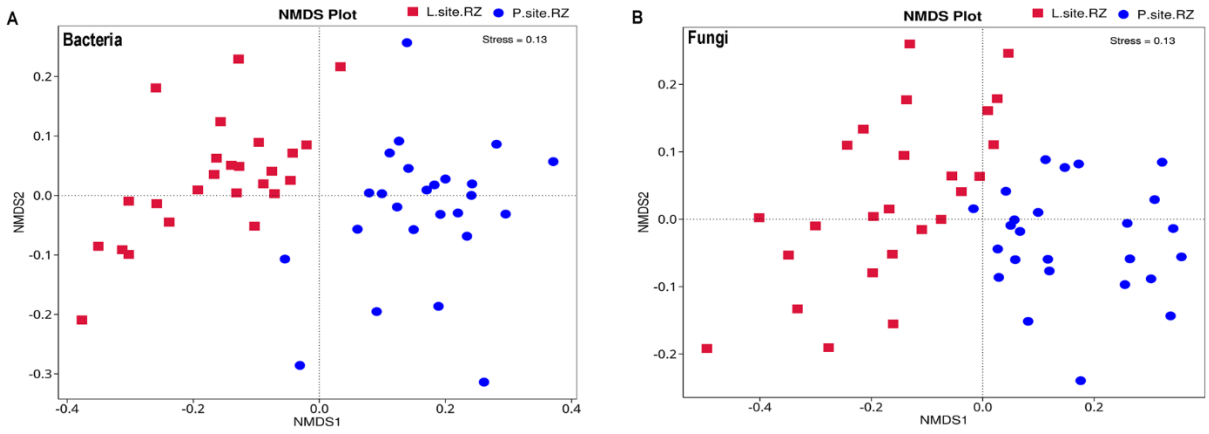

Figure 34 – NMDS analysis of rhizospheric microbiota

Difference in the **(A)** bacterial and **(B)** fungal communities in the rhizospheric soils from L-site and P-site. Data points of the same colour represent soil samples from the same site, while different symbols indicate samples from different locations (Source: Zádrapová et al., 2024).

The ADONIS (Table 16) and ANOSIM (Table 17) analyses demonstrated significant differences in microbial diversity between the soil samples from the two sites. Although these findings suggest a strong environmental influence on the microbial communities, further studies are needed to validate these observations and better understand the specific environmental factors responsible for driving these differences. Additional research could offer more detailed insights into the mechanisms shaping microbial diversity across different environments.

Table 16 – ADONIS rhizosphere

ADONIS						
L-site vs P-site	**Df**	**Sum of Squares**	**Mean Square**	**F.Model**	**R2**	**Pr(>F)**
Bacterial diversity	1 (48)	3.74684 (8.50962)	3.74684 (0.17728)	21.13473	0.3057 (0.6943)	0.001
Fungal diversity	1 (48)	1.45718 (16.17559)	1.45718 (0.33699)	4.32409	0.08264 (0.91736)	0.001

The Bray–Curtis method indicates a significant difference between the bacterial and fungal communities in the soils of the two Norway spruce seed orchards. (Df—degree of freedom, MeanSqs—SS/Df, F. Model—F-test value, R^2—the ratio of group variance to total variance). Values in parentheses denote residual error. The p-value reflects the significance of the variation in microbial community structure.

Table 17 – ANOSIM rhizosphere

ANOSIM				
Comparison	**Bacterial diversity**		**Fungal diversity**	
	R-value	**p-value**	**R-value**	**p-value**
L-site vs P-site	0.87533	0.001	0.37832	0.001

Positive R values indicate significant differences in the microbial communities between the two soils, with p-value <0.05 representing statistically significant differences.

MetaStats and t-test analyses identified that the bacterial genera *Granulicella, Bradyrhizobium, Acidothermus, Roseiarcus, Acidipila, Occallatibacter, Conexibacter, Candidatus Koribacter, Candidatus Xiphinematobacter, Acidisoma*, and *Agathobacter* were significantly more abundant in the P-site (Figure 35 and Figure 37A). In contrast, the genera *Candidatus Udaeobacter, Pseudolabrys, Gaiella, Bacillus, Haliangium, Rhodoplanes, Pedomicrobium, Sphingomonas*, and *Reyranella* were predominantly found in the L-site.

Similarly, several fungal genera were found to be significantly more abundant in the L-site, including *Russula, Thelephora, Keithomyces, Trichocladium, Ilyonectria, Fusarium, Achroistachys, Xanthothecium*, and *Gamsia* (Figure 36 and Figure 37B). In contrast, the fungal genera *Hyaloscypha, Oidiodendron, Cortinarius, Podila, Meliniomyces*, and *Filobasidiella* were predominantly abundant in the P-site.

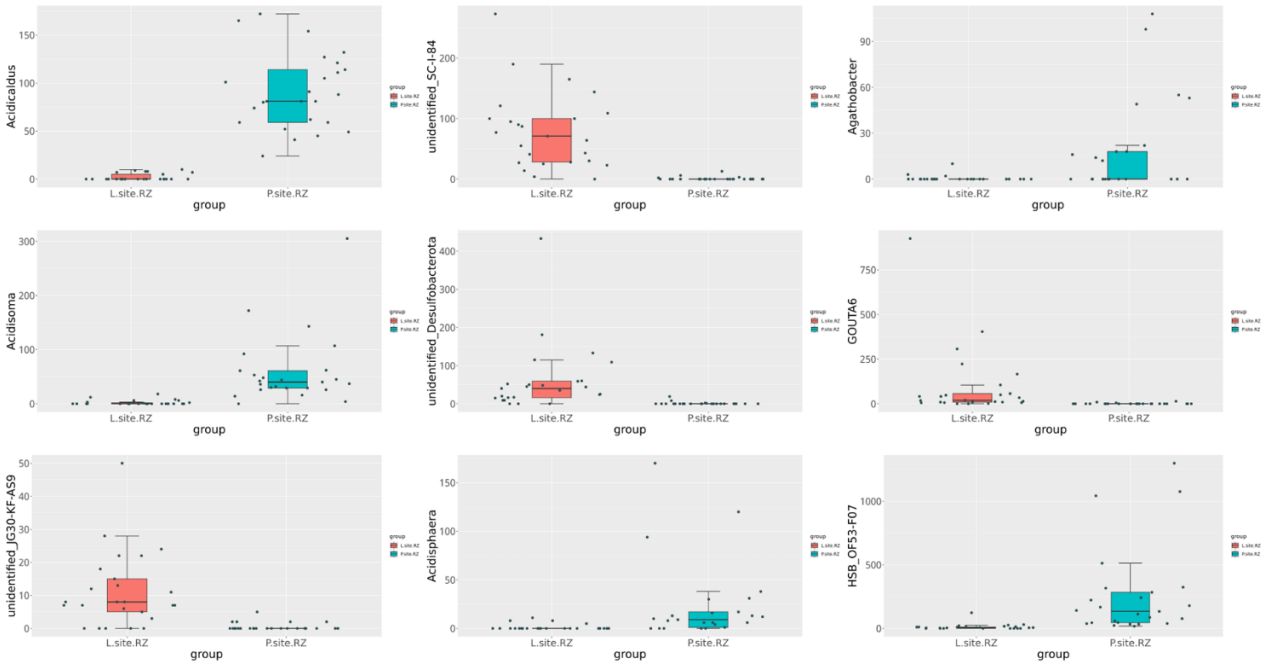

Figure 35 – Bacterial MetaStats analysis of rhizospheric soil

Significantly abundant bacterial species in L-site and P-site. Significant differences in relative abundance were evaluated using the FDR test, where "*" indicates significant variation at q-value <0.05, and "**" denotes highly significant variation at q-value <0.01 (Source: Zádrapová et al., 2024).

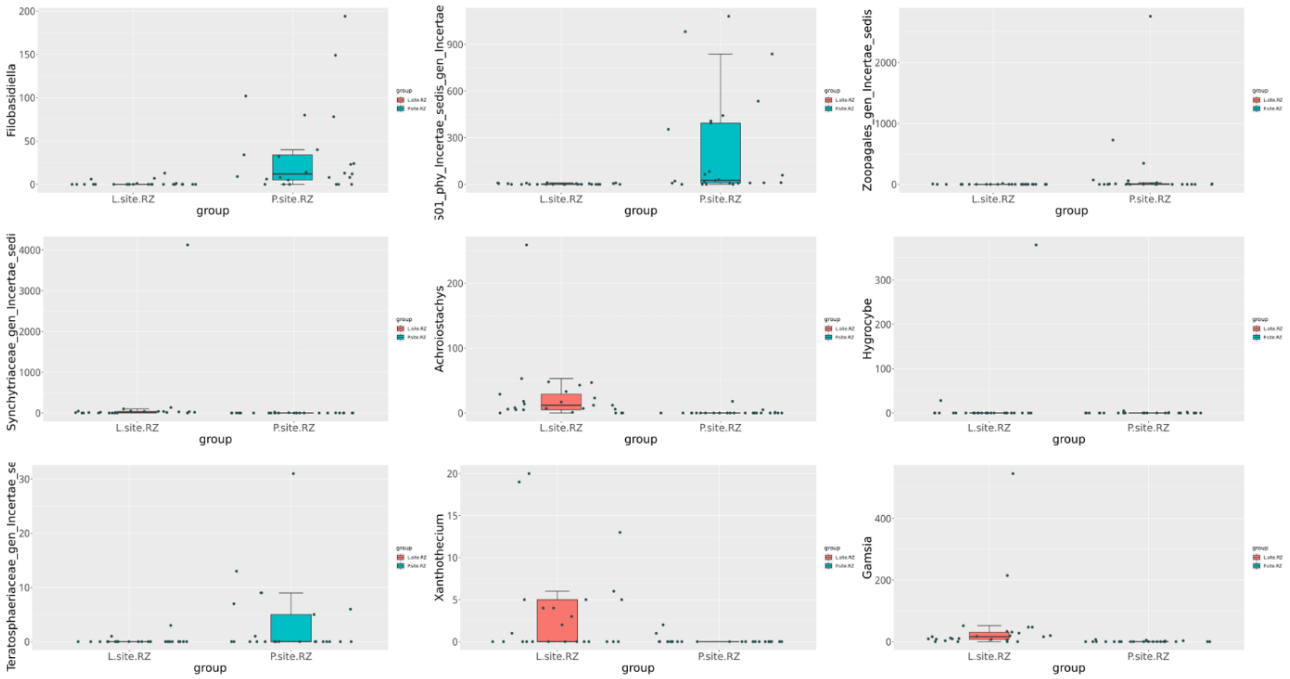

Figure 36 – Fungal MetaStats analysis of rhizospheric soil

Significantly abundant fungal species in L-site and P-site. Significant differences in relative abundance were evaluated using the FDR test, where "*" indicates significant variation at q-value <0.05, and "**" denotes highly significant variation at q-value <0.01 (Source: Zádrapová et al., 2024).

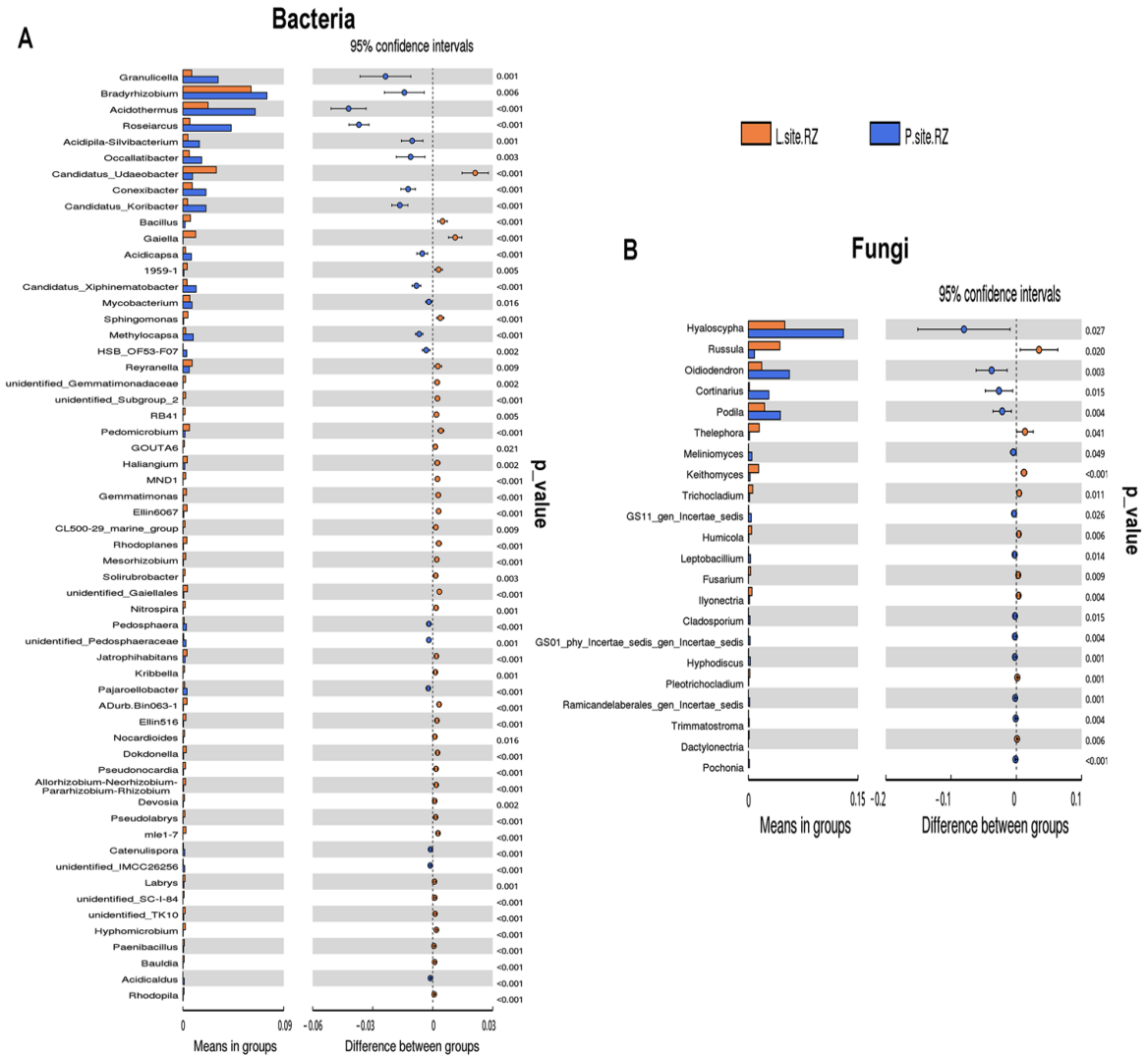

Figure 37 – t-test analysis of rhizospheric soil microbial communities

Significant variation in **(A)** bacterial and **(B)** fungal communities at the genus level. The last panel displays the abundance of genera that significantly differ between the two rhizospheric soils. Each bar represents the mean abundance at the genus level for the genera with significant differences. The right panel illustrates the confidence interval. The left-most part of each circle indicates the lower 95% confidence interval limit, while the right-most part marks the upper limit. The centre of the circle represents the difference in the mean values. The colour of the circle corresponds to the soil sample with the higher mean value. The p-value of the significance test is shown at the far right (Source: Zádrapová et al., 2024).

Bacterial biomarkers (Figure 38A and Figure 39A) determined by the Linear discriminant analysis effect size (LEfSe) with LDA score [log10]>4 showed the presence of significantly abundant and consistent bacterial population, which on P-site belonged to the members of:

- class—Alphaproteobacteria (order—Rhizobiales, family—*Beijerinckiaceae*; order—Acetobacterales, family—*Acetobacteraceae*)
- class—Acidobacteriae (order—Acidobacteriales, family—*Acidobacteriaceae_Subgroup_1*)
- class—Actinobacteria (order—Frankiales, family—*Acidothermaceae*)

Whereas the biomarker from L-site soil were:

- class—Gammaproteobacteria (order—Burkholderiales)
- class—Vicinamibacteria (order—Vicinamibacterales)
- class— Thermoleophilia (order—Gaiellales)

The fungal biomarkers (Figure 38B and Figure 39B) in the rhizospheric soil from P-site belonged to:

- class—Leotiomycetes (order—Helotiales, family—*Hyaloscyphaceae*)
- family—*Myxotrichaceae*, family—*Amanitaceae*, family—*Cortinariaceae*

While on L-site:

- class—Eurotiomycetes
- family—*Agaricaceae*, family—*Hygrophoraceae*, family—*Pilodermataceae*
- order—Thelephorales (family—*Thelephoraceae*)
- order—Russulales (family—*Russulaceae*)

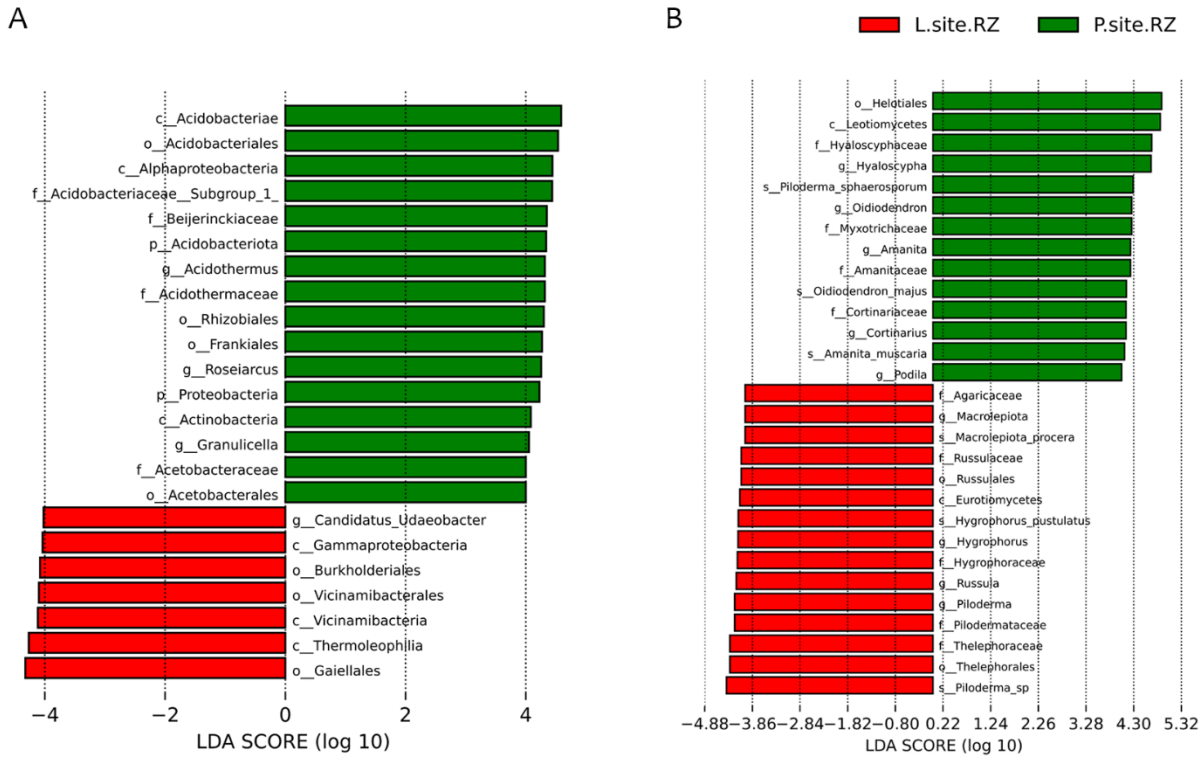

Figure 38 – LEfSe analysis of rhizospheric soil

Presence of **(A)** bacterial and **(B)** fungal biomarker species with significantly different abundances between soils from the L-site and P-site. The length of each bin, represented by the LDA score, indicates the effect, which reflects the extent to which a biomarker species contributes to distinguishing phenotypes between the groups. Only biomarkers with an LDA score above the cutoff threshold of >4 are shown (Source: Zádrapová et al., 2024).

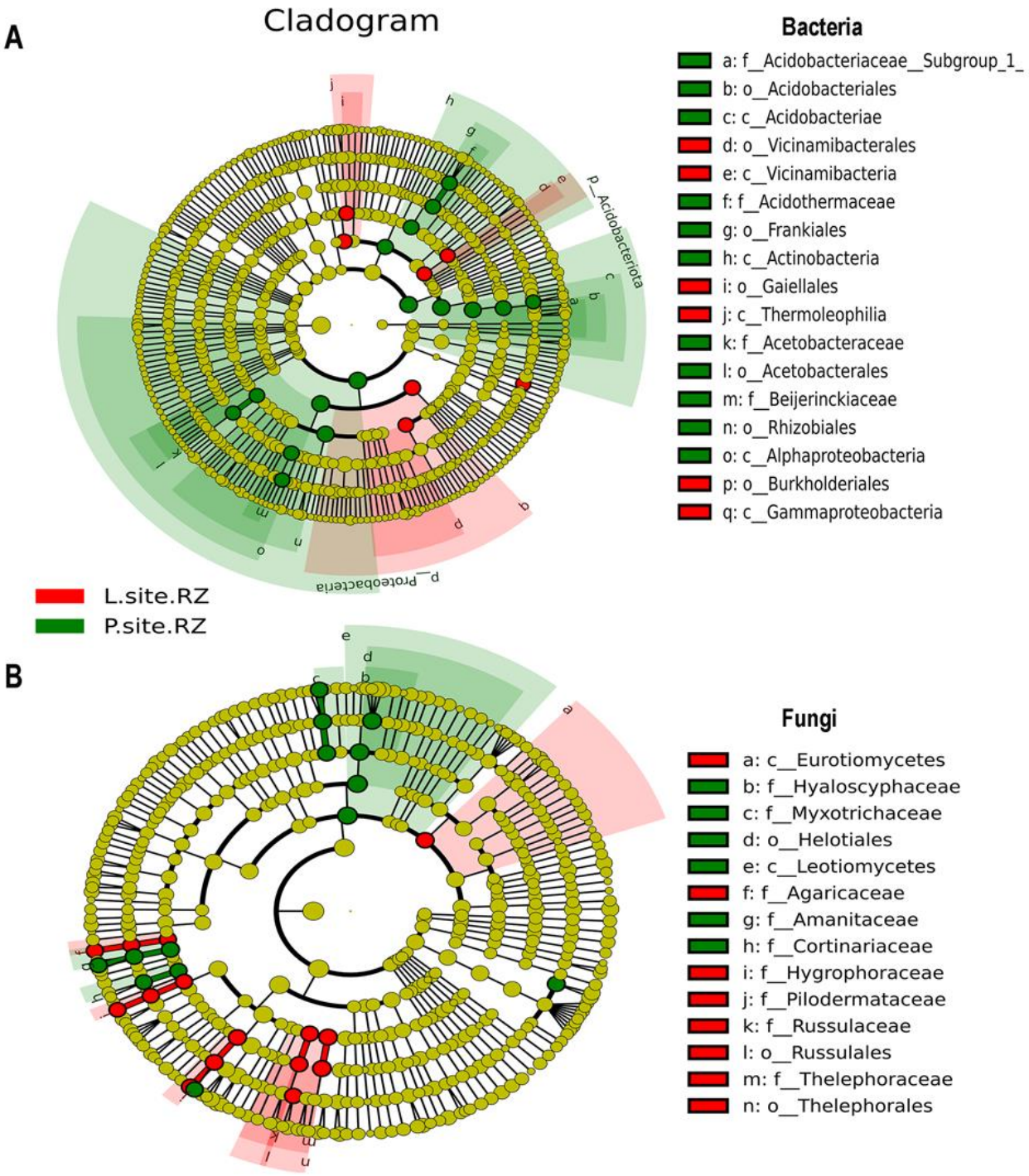

Figure 39 – Cladogram of rhizospheric soil biomarkers obtained by LEfSe

(A) Bacterial and **(B)** fungal biomarkers in the rhizosphere as identified by LEfSe analysis. The circles radiating outwards represent different taxonomic levels, from phylum at the core to genus at the outer edge. Each circle corresponds to a specific taxon at the respective taxonomic level, with the size of each circle proportional to the relative abundance of the taxon. Bacterial and fungal biomarkers with significant differences are color-coded according to the soil sample they are associated with, while yellowish-green circles indicate non-significant species. Red and green nodes highlight species that strongly contribute to group differentiation. Letters above the circles identify the different biomarkers (Source: Zádrapová et al., 2024).

5.2.3.5 Functional composition

The putative metabolic functions of bacterial communities in the rhizospheric soil were predicted by analysing the relative abundance of bacterial 16S rRNA gene sequences, with ASVs mapped to the KEGG database. A bar plot illustrated the top 10 predicted functions, including carbohydrate metabolism, amino acid metabolism, membrane transport, lipid metabolism, cofactor and vitamin metabolism, as well as xenobiotic degradation and metabolism. These functions showed no significant differences between the soil samples from the two orchards, indicating that they are consistent across the bacterial communities (Figure 40A). Furthermore, PICRUSt2 data, visualized in a PCA plot, demonstrated that the predicted functional gene composition of the bacterial communities was similar between the two sites, with no distinct functional clustering (Figure 40B). However, a t-test analysis highlighted certain functions that were significantly more abundant based on KEGG annotations in the rhizospheric soil samples (Figure 41).

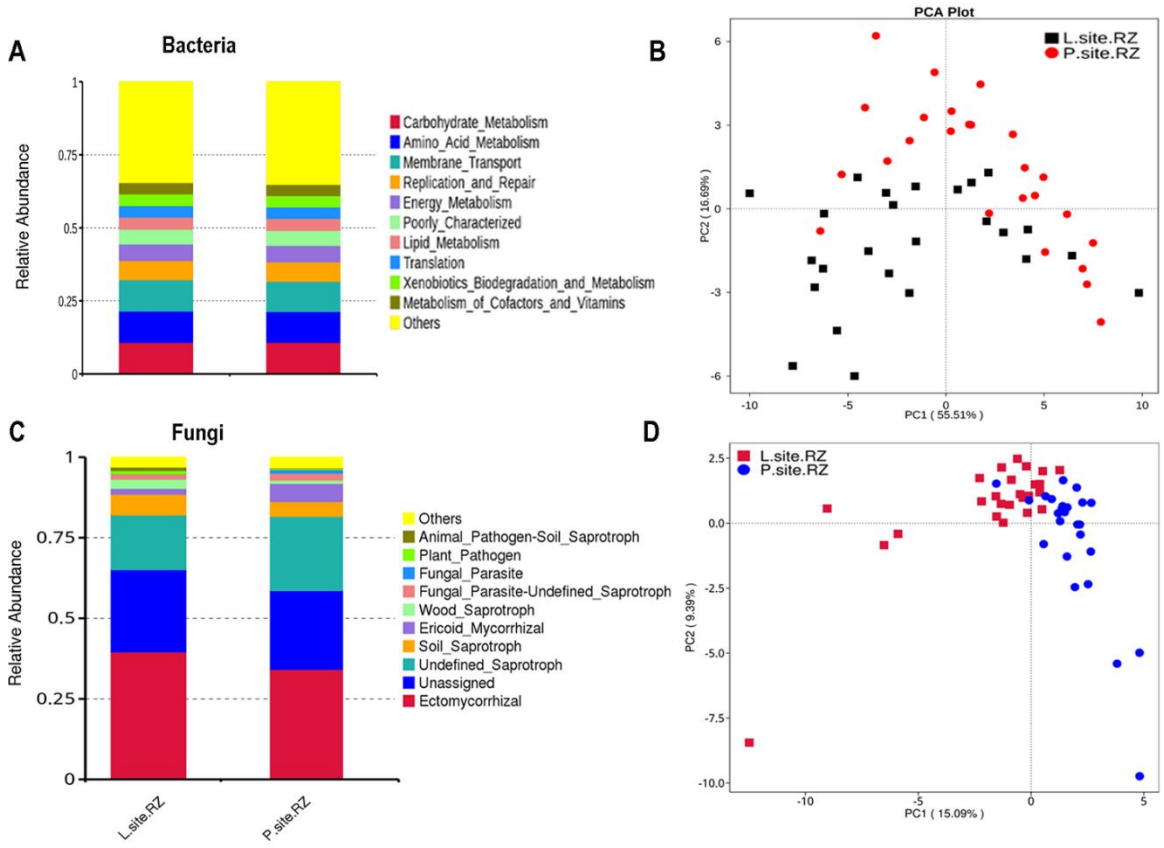

Figure 40 – Functional composition

Barplot illustrating the relative ASV abundance contribution to the top 10 **(A)** bacterial functions and **(C)** fungal guilds in the rhizospheric soil. "Others" represents the cumulative ASV abundance for the remaining gene functions or ecological guilds. The PCA plots depict an overlap in the predicted **(B)** functional contributions of bacterial communities and **(D)** fungal ecological guilds between the L- and P-site soils, based on PICRUSt2 analysis for bacterial functions and FUNGuild classification for fungal guilds (Source: Zádrapová et al., 2024).

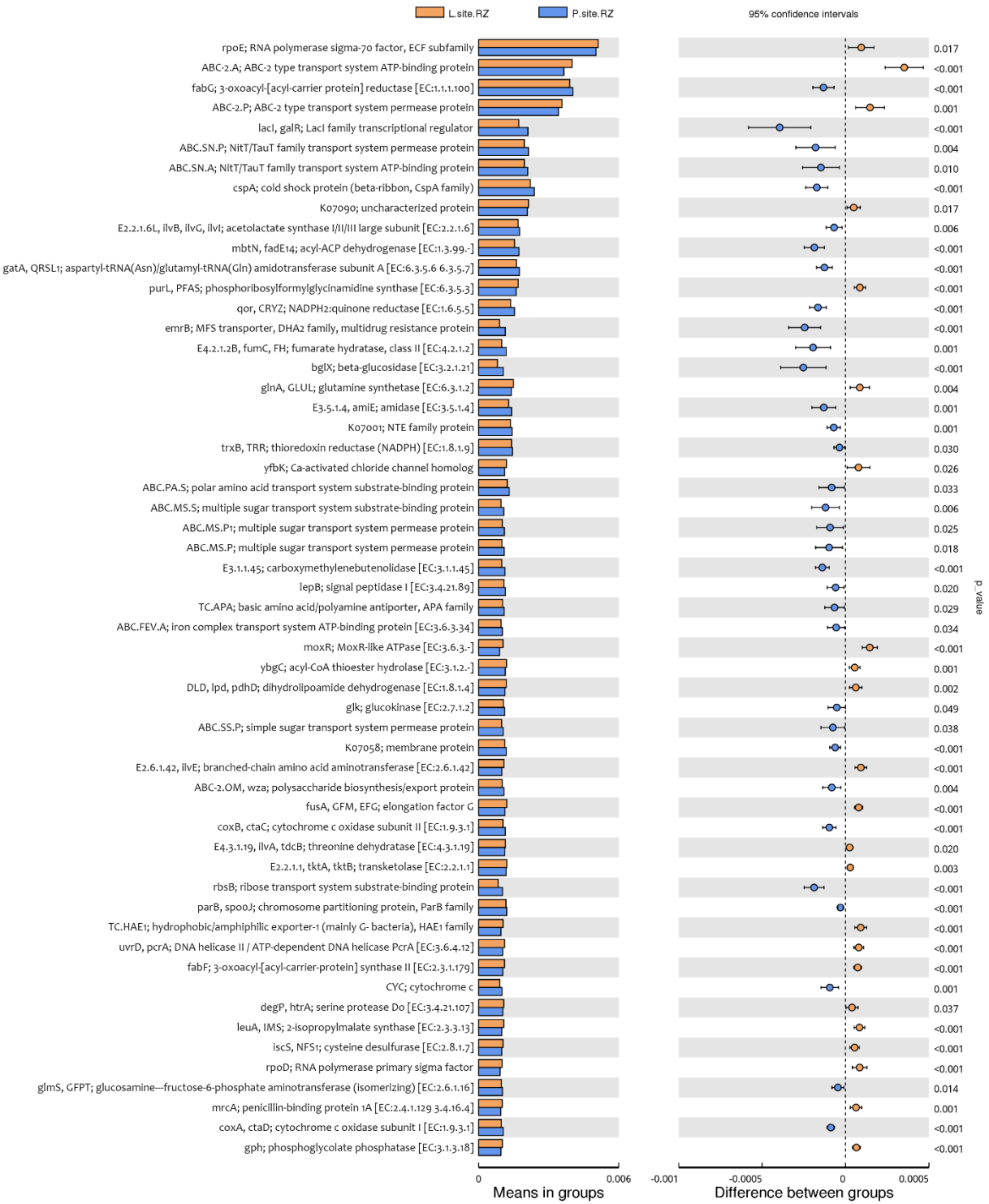

Figure 41 – t-test analysis of predicted functions of rhizospheric bacteria

Significant variation in bacterial putative functions based on the KEGG Orthology (KO) database using PICRUSt2 data in two rhizospheric soil samples (L-site and P-site). Each bar represents the mean abundance of different KOs that significantly differ between the two sites. The right panel illustrates the confidence interval between the soils, with the left-most part of each circle representing the lower 95% confidence interval limit, and the right-most part representing the upper limit. The centre of the circle indicates the difference in the mean value. The colour of the circle corresponds to the soil sample with the higher mean value. The right-most value indicates the p-value of the significance test (Source: Zádrapová et al., 2024).

Similarly, the functional roles of the fungal communities were predicted using FUNGuild software v1.0, which classifies ASVs based on their ecological functions. In both rhizospheric soil samples, the fungal communities were predominantly composed of ectomycorrhizal fungi (Figure 40C). The PCA plot of the overall fungal community functions indicated a significant overlap, suggesting that the functional potential of the fungal populations in the two sites was similar (Figure 40D). Notably, a t-test analysis revealed a significantly higher abundance of Ericoid mycorrhiza in the P-site, while wood saprotrophs were more prevalent in the L-site (Figure 42).

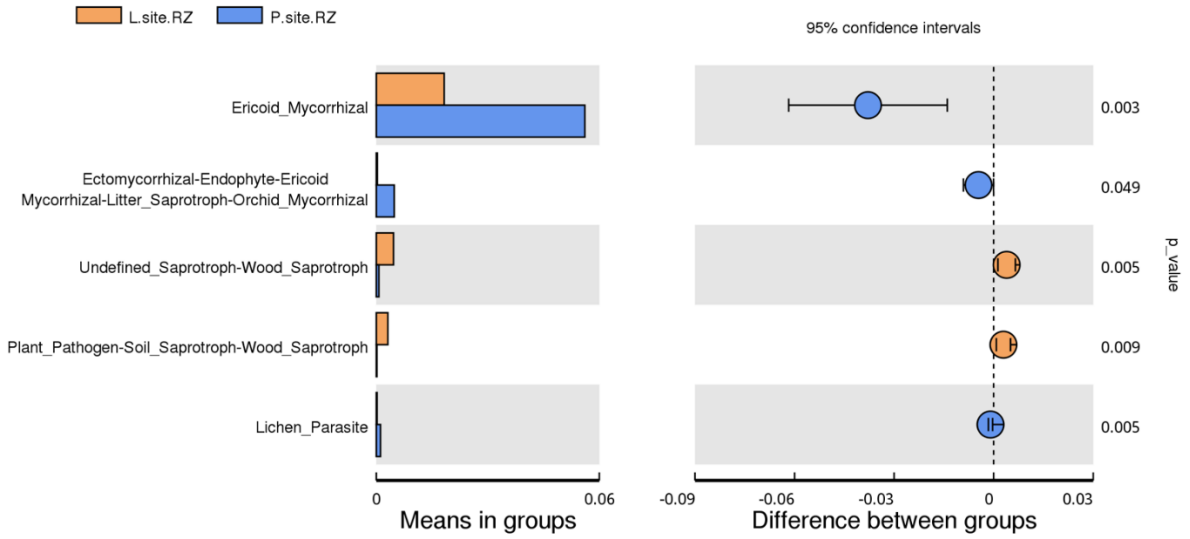

Figure 42 – t-test analysis of predicted guilds of rhizospheric fungi

Significant fungal guilds identified using FUNGuild data in the rhizosphere of L-site and P-site. Each bar represents the mean abundance of different ecological guilds that show significant differences between the two soils. The right panel illustrates the confidence interval between the soils. The left-most part of each circle represents the lower 95% confidence interval limit, while the right-most part represents the upper limit. The centre of the circle indicates the difference in the mean value. The colour of the circle corresponds to the soil sample with the higher mean value. The right-most value shows the p-value of the significance test (Source: Zádrapová et al., 2024).

It is important to note that both FUNGuild and PICRUSt2 are predictive tools, and their results may not fully represent the actual functional roles of the microbial populations. Therefore, additional experimental validation is necessary to confirm the functional capabilities of these microbial communities.

5.2.3.6 Microbial co-occurrence network

The co-occurrence network analysis assists in understanding the complex microbial interactions and their responses to climate change. Bacterial network analysis represented the co-occurrence of dominant bacterial species in two sites with different precipitation regimes (Figure 43).

The rhizosphere soil bacterial network comprises 227 nodes and 3,744 edges with significant correlation in the L-site (Figure 43A). Among them, 2,896 edges showed a positive correlation coefficient, while 848 edges represented a negative correlation coefficient. The major bacterial nodes in L-site belonged to Proteobacteria (37.4%), Actinobacteriota (21.14%), Bacteroidota (10.13%), and Acidobacteriota (7.92%). On the contrary, the bacterial co-occurrence network was simple in the P-site, representing 192 nodes and 1,658 edges with 1,402 positive interactions, while 256 edges constituted negative interactions (Figure 43B). P-site documented the highest positive bacterial interactions (~84%), with the major nodes belonging to Proteobacteria (35.93%), Actinobacteriota (18.75%), Firmicutes (12.5%), and Bacteroidota (6.77%).

The network diameter was 10 for both sites. The average network distance (L-site 2.77; P-site 3.52), clustering coefficient (L-site 0.48; P-site 0.51), network density (L-site 0.07; P-site 0.04), average degree (L-site 33.13; P-site 17.27), and the modularity index (MD) (L-site 0.27; P-site 0.46) were estimated, representing the complexity of the bacterial population in the rhizospheric soil between the two sites. The higher modularity value documented in the P-site bacterial network indicates a modular community structure where the nodes are densely connected within the communities to form modules with similar ecological niches, suggesting a less complex network.

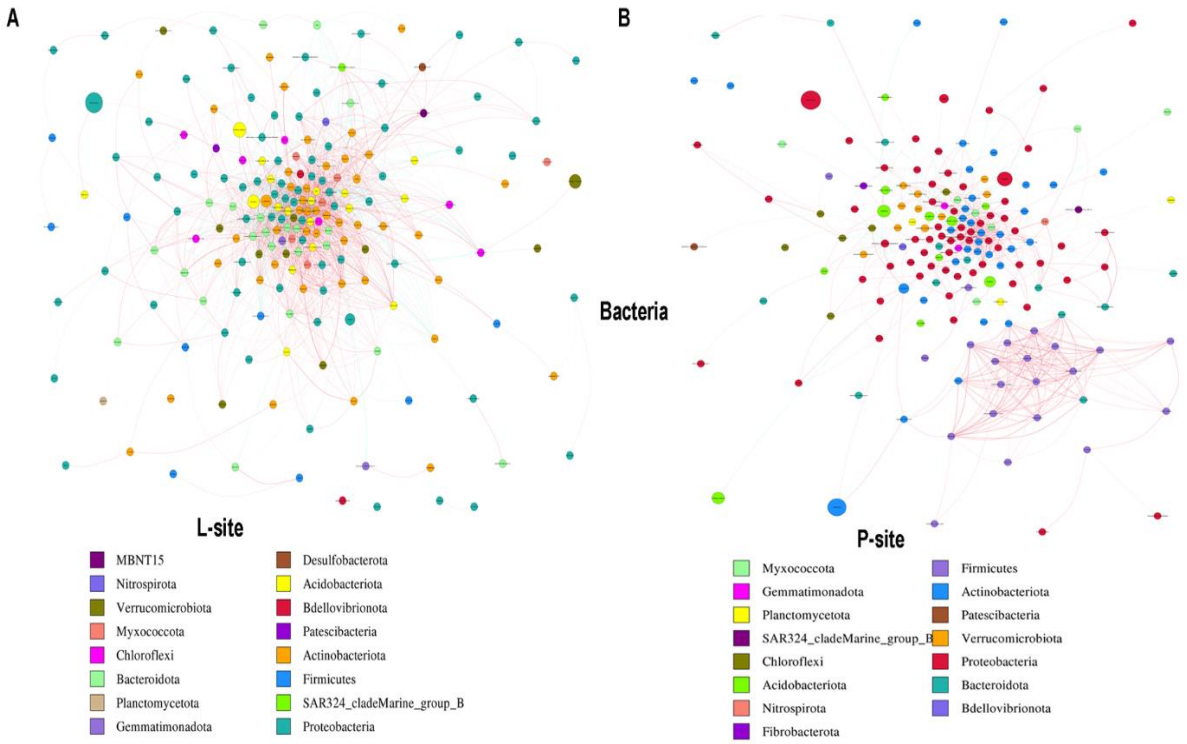

Figure 43 – Co-occurrence network of rhizospheric bacterial communities

Analysis illustrating the interactions among bacterial communities within **(A)** L-site and **(B)** P-site. The connections between nodes indicate significant correlations (Spearman's correlation coefficient cutoff = ±0.6, p <0.05). The size of each circle is proportional to the relative abundance of each taxon, and different colours of the nodes represent different phyla (Source: Zádrapová et al., 2024).

Similarly, the fungal network analysis revealed 227 nodes and 708 edges (692 positive and 16 negative interactions) with significant correlation in L-site (Figure 44A). In contrast, the P-site rhizospheric fungal co-occurrence network documented 185 nodes and 1,280 edges (Figure 44B). Among the fungal interactions, 874 were positive, while 406 were negative. The major fungal nodes include Ascomycota (L-site 66.07%; P-site 60%) and Basidiomycota (L-site 22.46%; P-site 29.18%) in both sites. Although most fungal interactions were positive, L-site documented the highest positive interactions (>97%). The network diameter (L-site 14; P-site 9), average network distance (L-site 4.62; P-site 3.21), clustering coefficient (L-site 0.33; P-site 0.62), network density (L-site 0.01; P-site 0.04), and average degree (L-site 6.23; P-site 13.83) represented the co-occurrence of fungal communities and their interactions in the rhizospheric space between the sites.

In contrast to the bacterial community structure, the fungal community in the L-site documented a higher modularity index (L-site 0.48; P-site 0.34), representing a less complex fungal community structure. The higher average degree of fungal co-occurrence network in the P-site indicates higher interaction with the neighbouring fungal nodes. On the other hand, the L-site documented increased interactions with the neighbouring bacterial nodes. Such observation suggests that variation in the precipitation regime influences fungal and bacterial populations differently.

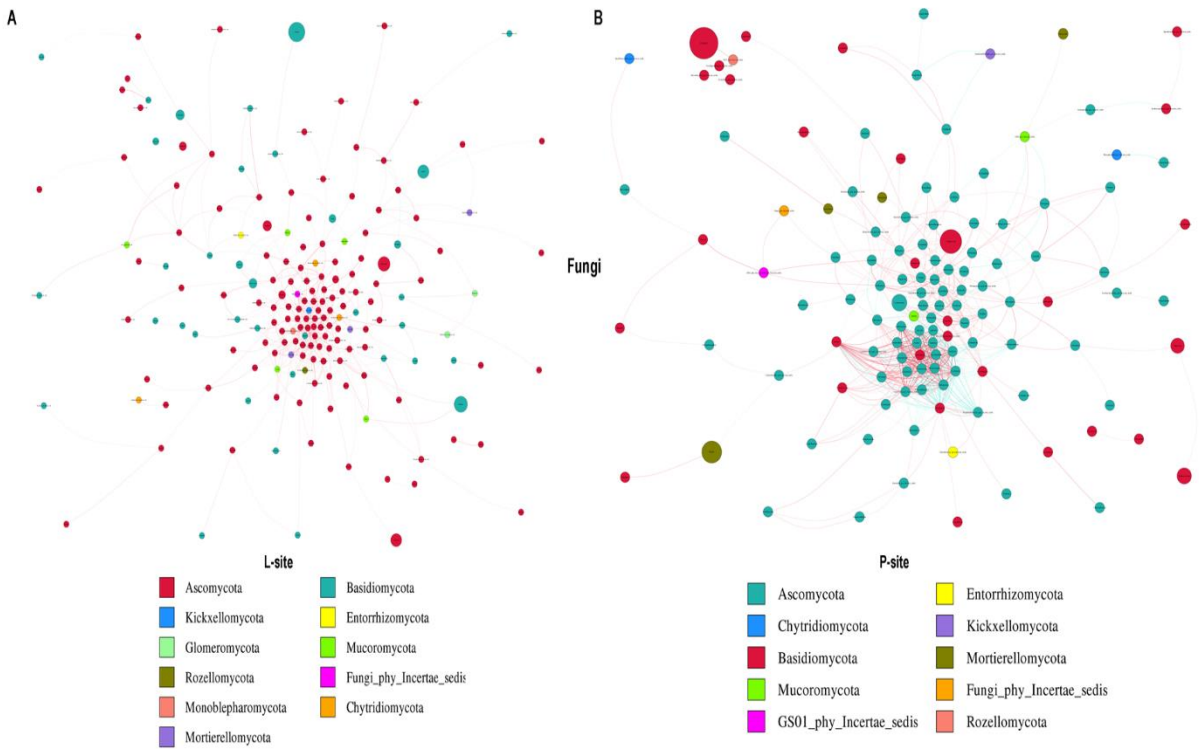

Figure 44 – Co-occurrence network of rhizospheric fungal communities

Analysis illustrating the interactions among fungal communities within **(A)** L-site and **(B)** P-site. The connections between nodes indicate significant correlations (Spearman's correlation coefficient cutoff = ±0.6, $p < 0.05$). The size of each circle is proportional to the relative abundance of each taxon, and different colours of the nodes represent different phyla (Source: Zádrapová et al., 2024).

6. Discussion

Our study explored the connections between precipitation, various soil properties, and the composition of microbial communities at two sites with markedly different precipitation patterns. This section synthesizes and evaluates the findings presented earlier, placing them within the context of prior research on this topic. Additionally, it compares our results to those found in existing literature.

To maintain clarity and continuity, the discussion is organized in two parts: the first focuses on the analysis of bulk soil, while the second addresses the rhizospheric soil.

As in previous sections, the Prenet seed orchard will be referred to as the P-site, and Lipová Lhota as the L-site.

6.1 Bulk soil

6.1.1 Effect of soil physicochemical properties on soil water content

Climatic data indicate that the L-site experiences significantly lower long-term precipitation compared to the P-site, which accounts for the expected lower soil water content (SWC) at the L-site. However, SWC is not solely determined by precipitation; it is also strongly influenced by soil texture, which affects the soil's capacity to retain water (Aina and Periaswamy, 1985; Vereecken et al., 1989). A higher proportion of sand in the soil is associated with reduced water retention, resulting in lower SWC (Li et al., 2009). Conversely, an increase in clay and silt content enhances water retention by reducing permeability, thereby improving the soil's water-holding capacity (Wang et al., 2022). Consequently, the lower water content observed in the L-site soil (9% compared to 32% at the P-site) is linked to its higher sand composition (74.3%) relative to that of the P-site (70.8%).

In addition to enhancing SWC, soil texture, particularly its clay content, plays a crucial role in accumulating soil organic carbon (Franzluebbers et al., 1996; Dexter, 2004). The higher total organic carbon (TOC) levels in the P-site soil, characterized by greater clay and silt content, are likely a result of increased precipitation at that site (Borken and Matzner, 2009; Bell et al., 2014), in contrast to the conditions observed at the L-site.

6.1.2 Effect of precipitation on the soil factors

This study revealed notable differences in total organic carbon (TOC) and total nitrogen (TN) content related to the varying annual precipitation rates between the two sites. The higher levels of TOC and TN observed at the P-site were attributed to increased rainfall at that location (Bell et al., 2014; Borken and Matzner, 2009). Additionally, soil moisture, along with higher clay content, plays a crucial role in the accumulation of soil organic carbon (Franzluebbers et al., 1996; Dexter, 2004). As previously mentioned, the greater percentage of clay and silt, combined with higher water content in the P-site soil, contributed to its increased TOC levels compared to the L-site.

Rising soil moisture levels are expected to accelerate litter decomposition, potentially enhancing soil carbon sequestration. Several studies have reported that reduced water availability can negatively impact soil carbon sequestration (Burke et al., 1989; Zhou et al., 2002). However, this assumption has been recently challenged (Bowden et al., 2014; Fekete et al., 2016). Water availability promotes plant growth, which in turn boosts biomass and litter production. Increased litter decomposition can stimulate microbial activity, leading to enhanced decomposition, soil respiration, and reduced carbon storage (Fontaine et al., 2007; Kuzyakov, 2010). Conversely, it is also possible for lower moisture levels to result in decreased microbial activity and carbon release (Fekete et al., 2014; Fekete et al., 2017). For instance, some studies have documented lower soil carbon accumulation in forests with higher precipitation levels (Meier and Leuschner, 2010; Chen et al., 2016). Nonetheless, higher moisture levels encourage microbial growth, which influences their activity (Liu et al., 2009) and, in turn, contributes to increased carbon release from the soil (Huang et al., 2015). Research has shown that increased rainfall can release more dissolved organic carbon from soil aggregates, providing more accessible substrates for microbes, which leads to heightened activity and higher CO_2 emissions (Wu et al., 2011; Wang B. et al., 2021).

While global studies indicate that changes in precipitation can alter soil pH (Slessarev et al., 2016), our findings showed only minor pH variation between the two sites, likely due to their geographic proximity.

The relationship between soil organic carbon turnover and precipitation is particularly significant in the context of ongoing global climate change, which alters precipitation patterns and consequently reduces soil moisture levels (Zhou et al., 2011). Given that soil moisture is a key factor driving organic carbon turnover (Zhou et al., 2005), understanding the impact of precipitation on soil carbon dynamics becomes increasingly important.

6.1.3 Effect of precipitation on soil metabolite profile

Soil moisture, pH, and the content of soil organic matter (SOM) are key factors that regulate the structure of microbial communities and carbon cycling within soils (Judd et al., 2006; Xu et al., 2020; Collins et al., 2014).

Changes in precipitation affect microbial community structure (Barnard et al., 2013) by altering both soil moisture and organic matter levels (Maestre et al., 2016). The interplay between soil moisture, organic matter content, and microbial community structure is crucial for effective nutrient cycling (Elbert et al., 2012). Microbes utilize dissolved organic carbon in the soil, including root exudates, which also shape microbial community structure (Swenson et al., 2015) and affect plant functions (Pétriacq et al., 2017). Soil metabolites often serve as indicators of microbial responses to various environmental conditions (Lankadurai et al., 2013; Jones et al., 2014). For example, anaerobic soil disinfestation has been shown to alter soil metabolite profiles and shift microbial communities (Johns et al., 2017).

In our research, we identified distinct metabolite profiles in soil samples from two Norway spruce seed orchards exposed to different long-term precipitation patterns over three decades. The P-site exhibited a higher abundance of compounds such as fatty acids, carbohydrates, and alcohols compared to L-site, which correlates with the higher organic carbon content at the P-site. This variation in metabolite composition led to clear clustering of soil samples based on their location. Johns et al. (2017) suggest that soil metabolomics links organic and inorganic compounds with soil microbes. Consequently, our findings reveal differing microbial functions between the soils from the P-site and L-site. The lower moisture content at the L-site likely reduces the decomposition rates of plant materials, such as litterfall and roots (Martin et al., 2004; Ostertag et al., 2008), which could be attributed to diminished microbial biomass and lower activity.

Similarly, soil pH affects the soil metabolite profile. For instance, higher soil pH is associated with increased citrate and decreased malate concentrations, and vice versa (Veneklaas et al., 2003).

Several studies have reported a positive correlation between microbial diversity and soil organic matter across various ecosystems (Berthrong et al., 2013; Maestre et al., 2015).

6.1.4 Effect of precipitation on soil microbial biomass

Soil water availability significantly enhances soil microbial biomass and its activity, as demonstrated in previous studies (Williams and Rice, 2007; Huang et al., 2015). The presence of functionally active microbial communities and their spatial distribution in the soil can be assessed using Phospholipid Fatty Acid (PLFA) analysis, based on differences in microbial cell membrane composition (Zelles, 1999; Cavigelli et al., 1995; Torsvik and Øvreås, 2002). According to the total PLFA estimates, the P-site with higher precipitation levels showed greater microbial biomass. In contrast, the drier L-site soil had lower microbial biomass, indicating fewer functionally active microbial communities. Hueso et al. (2012) suggest that during drought conditions, water scarcity can reduce microbial PLFA levels due to diminished microbial growth as resources are diverted to prevent dehydration, and due to reduced solute mobility and nutrient availability (Harris, 1981; Kieft, 1987; Schimel et al., 2007).

PLFA estimation can serve as an indicator of soil health. For example, changes in the PLFA (fungi/bacteria) ratio can reflect shifts in soil microbial community structure (Zeglin et al., 2013). In our study, while increased precipitation boosted bacterial and fungal PLFA levels in P-site soil, it did not significantly alter the PLFA (fungi/bacteria) ratio between the two sites. Similarly, the PLFA (G^+/G^-) ratio is used as an indicator of water stress (Klamer and Bååth, 1998), with gram-positive bacteria being more resistant to water scarcity due to their thicker cell walls compared to gram-negative bacteria. However, our findings showed no significant effect of increased precipitation on the PLFA (G^+/G^-) ratio between sites. This observation may suggest that soil microbes are adaptable to environmental changes and maintain a stable community structure (Huang et al., 2015; Yang et al., 2017).

Furthermore, both total and specific PLFA contents in the soil were positively correlated with total organic carbon (TOC) and total nitrogen (TN). The availability of organic nutrients is a key factor influencing soil microbial biomass (Wagai et al., 2011; De Vries et al., 2012).

6.1.5 Effect of precipitation on soil microbial enzymatic activity

Soil microbial communities play a key role in nutrient cycling by producing extracellular enzymes (Bowles et al., 2014). These enzymes aid in the breakdown, transformation, and mineralization of soil organic matter (Sinsabaugh, 2010; Xiao et al., 2018), which in turn affects soil quality and ecosystem productivity (Sayer et al., 2013). While microbes are the main producers of extracellular enzymes in soil, specific enzymes are produced by particular microbial taxa. For example, fungi typically produce enzymes that degrade lignocellulose and chitin (Baldrian and Valášková, 2008; Sinsabaugh et al., 2008), allowing them to process recalcitrant nutrient-poor substrates. Bacteria, on the other hand, decompose more easily accessible substrates (Xu et al., 2015; Treseder et al., 2016). Fungi secrete enzymes that break down complex plant organic matter, which then provides bacteria with simpler, more accessible substrates (Romaní et al., 2006). However, the relationship between microbial communities and enzyme activities remains underexplored.

In this study, we focused on extracellular enzymes involved in the decomposition of soil organic carbon (α-glucosidase, β-glucosidase, β-galactosidase, β-xylosidase, cellobiohydrolase), nitrogen (chitinase), and phosphorus (acid phosphatase) into forms that plants can assimilate (Bell et al., 2013).

Our results indicated a significant increase in extracellular enzyme activities with higher microbial biomass in P-site soil under increased precipitation. This suggests that precipitation reduces microbial physiological stress and boosts microbial activity by enhancing nutrient availability (Austin et al., 2004; Tiemann and Billings, 2011; Manzoni et al., 2012). Consequently, the higher levels of organic carbon and nitrogen in P-site soil were positively associated with increased extracellular enzyme activities, consistent with previous studies (Sinsabaugh et al., 1991).

Precipitation is a key factor influencing enzyme production and turnover, affecting soil enzyme responses and ecosystem productivity (Yang et al., 2017). Increased precipitation enhances the activity of soil microbial functional genes involved in biogeochemical cycling (Li et al., 2017).

In summary, our study found notable differences in soil microbial composition between L-site and P-site. The L-site soil exhibited higher bacterial and fungal diversity, while the P-site soil on the other hand had significantly higher levels of extracellular enzyme activities and total PLFA. This suggests a greater abundance of metabolically active microbes at the P-site, which likely play a crucial role in organic matter recycling (Coolen and Overmann, 2000). This observation could be linked to the higher water content at the P-site, which positively influences microbial activity and enzyme production (Borowik and Wyszkowska, 2016).

6.1.6 Effect of precipitation on soil microbial community structure

Soil microbial diversity and biomass are crucial for driving ecosystem processes such as nutrient cycling and organic matter decomposition (Crowther et al., 2016). While numerous studies have explored the influence of various biotic and abiotic factors on soil microbial diversity and biomass (Fierer, 2017; Tedersoo et al., 2014; Delgado-Baquerizo et al., 2018), the specific relationships between microbial diversity, biomass, and their controlling factors remain underexplored.

One key abiotic factor affecting organic matter retention, microbial biomass, and microbial activity is soil texture (Bechtold and Naiman, 2006). Soils with finer particles, such as those with high clay content and low sand percentages, tend to form more stable aggregates. Such soils often accumulate higher levels of organic carbon and total nitrogen, which significantly influences nutrient availability (Raiesi, 2006). Soil texture also impacts the abundance of bacterial and fungal populations. Increased soil organic content generally supports the growth of dominant microbial taxa, leading to higher microbial biomass. However, this increase in biomass can result in reduced diversity among subordinate taxa due to competitive exclusion, leading to a decrease in overall species richness (Bastida et al., 2021). Similar patterns are observed in plant communities, where dominant species can suppress the diversity of other species (Loreau and Hector, 2001; Paquette and Messier, 2011; Rajaniemi, 2003). This aligns with our findings, where the L-site soil, with lower carbon content and reduced microbial biomass, exhibited higher microbial diversity compared to the P-site.

Additionally, soil carbon content is influenced by microbial respiration, which is directly affected by temperature (Frey et al., 2013; Xu et al., 2021). Rising temperatures due to global warming increase microbial activity and accelerate the decomposition of soil organic matter, leading to a depletion of labile carbon substrates (Karhu et al., 2014). In response to such conditions, microbial communities may either acclimate or change in composition, resulting in variations in microbial biomass (Allison and Martiny, 2008; Bradford, 2013). Therefore, the differences observed in microbial structure and activity between the L-site and P-site may also be partially attributed to temperature variations.

6.1.7 Effect of edaphic variables on soil microbial communities

As outlined above, soil organic matter, represented by total organic carbon (TOC) and total nitrogen (TN) content, plays a crucial role in shaping the soil microbiome (Drenovsky et al., 2004; Burns et al., 2015). Numerous studies have shown that the addition of organic carbon and nitrogen to soil significantly alters microbial composition (Drenovsky et al., 2004; Ng et al., 2014; Zhou et al., 2017).

Our findings indicated that edaphic factors such as TOC and TN had a much greater influence on soil microbial communities compared to factors like soil pH and conductivity—37.66% (TOC and TN) compared to 6.5% (pH and EC) for bacteria, and 32.83% (TOC and TN) compared to 6.63% (pH and EC) for fungi. The bacterial genera belonging to the classes Rhizobiales, Acidobacteriales, Chthoniobacterales, Rhodospirillales, Ktedonobacterales, and Planctomycetales showed a significant positive correlation with TOC and TN content. These bacterial orders play key roles in soil carbon and nitrogen cycling (Barton et al., 2014; Jones, 2015; Köberl et al., 2020). For instance, Planctomycetales are facultative chemoorganotrophs that specialize in carbohydrate metabolism (Fuerst, 1995), while Rhodospirillales and Rhizobiales are involved in nitrogen fixation, helping to maintain the carbon-to-nitrogen ratio in the soil (Hayat et al., 2010; Jones, 2015). The relative abundance of these bacterial species is also closely linked to potential carbon mineralization rates (Jones, 2015). Chthoniobacterales contribute to carbon cycling by breaking down complex carbohydrates such as cellulose and xylan (Köberl et al., 2020), while Ktedonobacterales utilize nitrite and nitrate and encode ureases (Barton et al., 2014).

Our study also identified a correlation between bacterial species and soil pH, with these species contributing to nutrient cycling by decomposing organic matter and fixing nitrogen in the soil (Wang et al., 2016). Similarly, the relative abundance of fungal communities was positively correlated with TOC, TN, and soil pH. These fungi play a critical role in carbohydrate degradation, which affects soil organic matter content and helps maintain the nitrogen-to-phosphorus (N:P) ratio (Kottke et al., 1998; Deacon et al., 2006; Avis, 2012; Ohm et al., 2012).

In conclusion, our study highlights the impact of long-term variations in precipitation, along with soil texture and pH, on soil microfauna and their functions in the Norway spruce forest ecosystem. However, further research at the metatranscriptomics and metaproteomics levels is needed to validate these findings at the functional level.

6.2 Rhizosphere

6.2.1 Effect of precipitation on rhizospheric microbial communities

As previously mentioned, soil water content (SWC) plays a critical role in supporting belowground microfauna and soil processes, as water availability boosts microbial activity, facilitates organic matter decomposition, and reduces soil carbon sequestration (Fontaine et al., 2007; Kuzyakov, 2010). Consequently, precipitation events, which directly influence SWC, are key in regulating soil organic matter turnover (Bian et al., 2022; Li et al., 2021). Findings from the bulk soil study revealed that increased precipitation led to higher soil moisture, which in turn resulted in elevated organic matter and total nitrogen (TN) levels at the P-site (Chakraborty et al., 2023). However, there was no significant variation in soil pH or conductivity between the two Norway spruce seed orchards (Chakraborty et al., 2023), despite studies indicating that changes in precipitation can affect soil pH on a global scale (Zhang Y. Y. et al., 2019).

The "root-soil-microbe" triangle is considered one of the most dynamic underground relationships in nature. These interactions, particularly in the rhizosphere, are further amplified through plant-microbe feedback mechanisms (Štraus et al., 2024). Bengough (2012) notes that about 40% of total terrestrial precipitation passes through the narrow volume of rhizosphere soil surrounding plant roots before being transpired, making it a highly active hydrological zone within the biosphere. The differences in precipitation between the study sites led to notable variations in soil metabolite content, specific element concentrations, and microbial community structure. These long-term precipitation changes and their effects on the rhizosphere microbiome at both the L-site and P-site are summarized in the schematic in Figure 45 (source: Zádrapová et al., 2024).

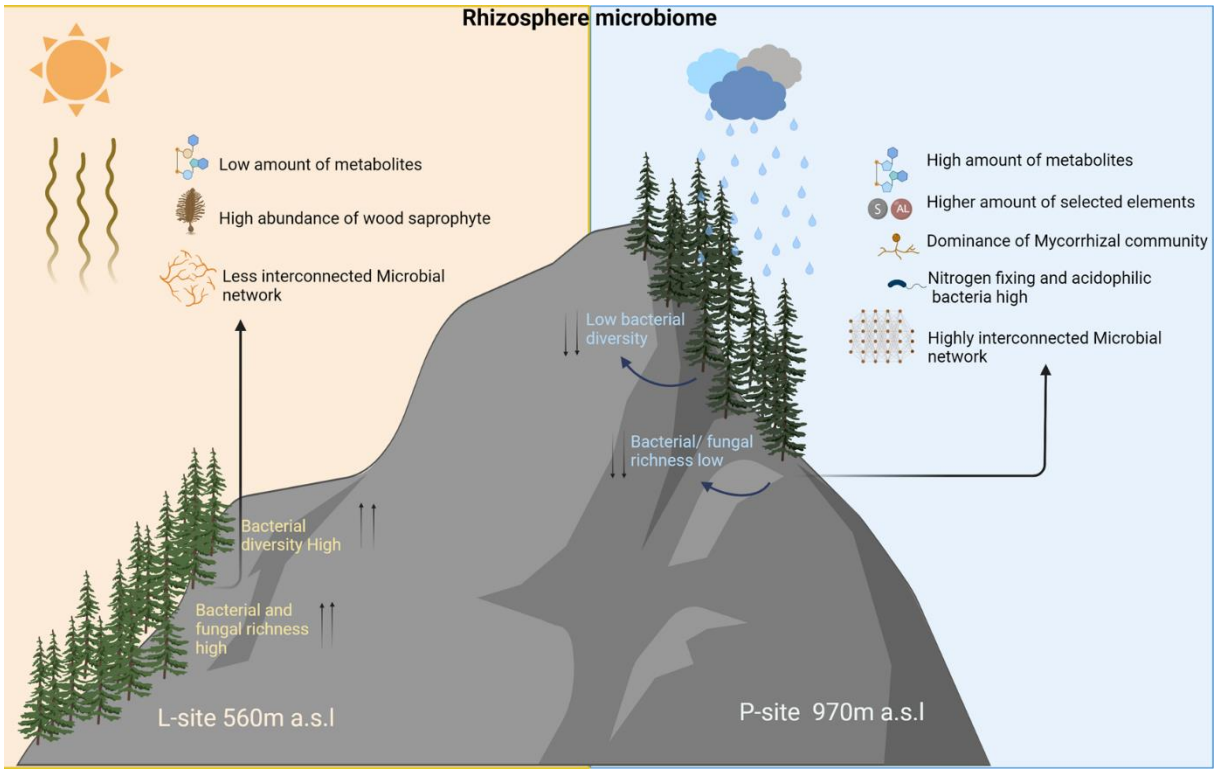

Figure 45 – Impact of long-term precipitation change on rhizosphere microbiome

Source: Zádrapová et al., 2024

6.2.2 Chemistry of rhizospheric soil

The chemistry of the rhizosphere is complex and constantly evolving due to the influence of plant root exudates and microbial secretions (Mashabela et al., 2022). A large proportion of beneficial bacteria found in the rhizosphere are classified as plant growth-promoting rhizobacteria (PGPR), which form a mutual symbiotic relationship with the host plant through biochemical signalling (Grobelak et al., 2015; Mhlongo et al., 2020). In this perspective, rhizosphere can be seen as communication highway that connects the PGPR and the plant's roots. Plants provide a steady stream of nutrients and signalling molecules, such as organic acids, amino acids, vitamins, minerals, and allelochemicals like phenolic acids, terpenoids, and flavonoids, creating a hospitable environment for PGPR to accumulate and proliferate (Miller et al., 2019; Strehmel et al., 2014). In return, PGPR release growth-enhancing and defence-related compounds, including phytohormones, which benefit the plant (Mus et al., 2016; Mhlongo et al., 2018). Certainly, the rhizosphere represents a highly intricate network of interactions involving both plant-microbe and microbe-microbe relationships. These interactions play a critical role in shaping the microbial community and supporting plant growth. A simplified representation of these interactions is shown in Figure 46 (Berendsen et al., 2012).

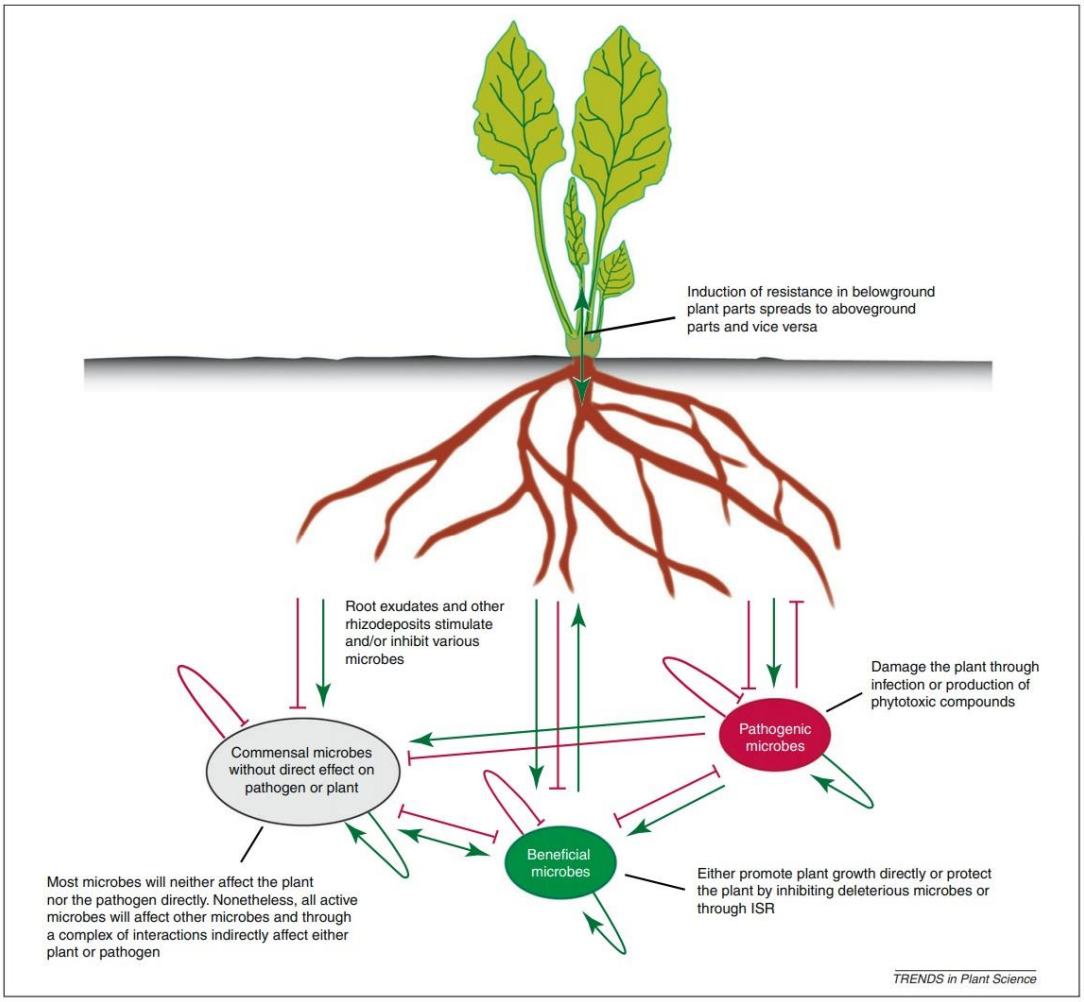

Figure 46 – Interactions in the rhizosphere

Source: Berendsen et al., 2012

In addition, metabolites play a key role in stabilizing carbon within the soil. Compounds like fatty acids, amino acids, lipids, organic acids, sugars, and volatile organic compounds are tightly linked to biogeochemical cycles, which are largely driven by soil microorganisms (Song et al., 2024). Microbial carbon use efficiency is influenced by the diffusional limitations of substrates, which are closely tied to soil water content (Butcher et al., 2020). As a result, soil moisture is a critical factor in regulating microbial activity, which subsequently affects the levels and composition of soil metabolites (Butcher et al., 2020).

This study documented an increased abundance of rhizospheric soil metabolites, including fatty acids, alcohols, acids, and terpenes, in the P-site, while carbohydrates were more prevalent in the L-site. This variation in metabolite profiles may be linked to the higher abundance of microbial phyla such as Proteobacteria, Acidobacteriota, Actinobacteriota, Bacteroidota, and Firmicutes, which play key

eco-physiological roles in cycling essential elements like nitrogen, carbon, and sulphur (Zhao et al., 2022). Notably, the elevated levels of fatty acids and terpenes in the P-site may also be associated with the lower abundance of Actinobacteriota and Chloroflexi (Bi et al., 2021).

Similarly, Shi et al., 2011 found that the addition of carbohydrate metabolites to forest soil significantly boosted the relative abundance of dominant bacterial taxa such as Actinobacteriota, Proteobacteria, and Firmicutes. This supports our findings, indicating that carbohydrates play a key role in shaping the soil bacterial community by enhancing the growth of certain microbial groups. A plausible explanation is that these bacterial taxa may be more efficient at using carbohydrates as a carbon source, providing them with a competitive advantage. However, this relationship warrants further experimental investigation for validation.

In this study, it was not feasible to separately identify the individual contributions of these driving factors to the observed soil metabolite profiles. The mechanisms linking the complex metabolite pools to microbial diversity within the rhizosphere remain unclear and require further exploration. Gaining a deeper understanding of metabolite dynamics in rhizospheric soil could shed light on the intricate interactions between plants and belowground microbial communities in response to environmental shifts (Massalha et al., 2017).

6.2.3 Effect of precipitation on bacterial and fungal diversity in rhizospheric soil

Soil moisture content often influences microbial diversity and function. In this study, higher soil moisture in the P-site was associated with lower bacterial diversity, while fungal diversity remained unaffected. Similar findings were reported by Yang et al. (2021), where precipitation changes significantly impacted bacterial communities but not fungi in a meadow grassland in northeastern China. Bacteria tend to respond more quickly to shifts in soil water availability due to their distinct physiological traits and survival strategies, unlike fungi (Engelhardt et al., 2018). The increased moisture from higher precipitation may have led to osmotic stress, reducing bacterial diversity at the P-site (Kieft, 1987). However, fungal diversity in the rhizosphere remained consistent between the sites, likely due to fungi's resilience and their ability to extend hyphae, allowing them to access nutrient resources even in low-moisture environments (Boer et al., 2005).

In this study, the P-site rhizosphere exhibited a high abundance of Proteobacteria and Acidobacteriota, particularly species like *Granulicella, Roseiarcus, Acidobacteria*, and *Acidipila*. These bacteria are k ey players in decomposing organic matter and enhancing the availability of nutrients such as nitrogen (N), calcium (Ca), and phosphorus (P) in acidic soils (Conradie, 2020; Ren et al., 2021).

The increased presence of acidophilic bacteria may be linked to the elevated levels of fatty acids and organic acid metabolites observed in P-site soil (Bi et al., 2022). According to Bi et al. (2022), high concentrations of fatty acids contribute to soil acidity, significantly influencing the conifer root microbial community structure. Our previous research on bulk soil from these sites confirmed lower pH levels in the P-site compared to the L-site (Chakraborty et al., 2023), though the difference in bulk soil pH between the two sites was not statistically significant.

The elevated presence of *Bradyrhizobium* in the P-site is noted for its significant role in nitrogen fixation and nutrient uptake, particularly nitrogen (N) and phosphorus (P), as well as its interactions with mycorrhizal fungi (Meena et al., 2018). This high abundance of *Bradyrhizobium* is likely linked to the increased total nitrogen content found in soil samples from the P-site, as documented in our previous study (Chakraborty et al., 2023).

Soil moisture and temperature play crucial roles in influencing fungal growth and the functioning of symbiotic relationships (Augé, 2004; Heinemeyer and Fitter, 2004). In the P-site, the combination of high soil moisture and low temperatures likely creates an optimal environment for mycorrhizal development. Studies indicate that changes in precipitation can significantly impact arbuscular mycorrhizal fungi (AMF) communities by altering their interactions among different AMF groups (Wang J. et al., 2021). Additionally, the prevalence of mycorrhizal communities at the P-site may be attributed to their association with various “Mycorrhizae Helper Bacteria” (MHB), which support and enhance the establishment of mycorrhizal symbiosis with the host plant (Frey-Klett et al., 2007). In the rhizosphere microbiota, genera such as *Azospirillum, Burkholderia, Bradyrhizobium, Pseudomonas, Rhizobium, Bacillus*, and *Brevibacillus* were identified as MHBs. Additionally, a high abundance of *Acrodontium, Oidiodendron*, and *Cortinarius* was documented in the rhizosphere of the P-site. *Acrodontium* is known for its inhibitory effects against powdery mildew pathogens (Sharma, 2015), while *Oidiodendron* sp. contributes to the forest ecosystem through its plant cell wall-degrading enzymes (Adnan et al., 2022) and mycorrhizal associations (Morvan et al., 2020). *Cortinarius* sp. is one of the most important symbiont mycorrhizal fungi associated with tree roots in forest ecosystems (Wang et al., 2019).

Interestingly, the L-site, which receives less precipitation compared to the P-site, showed higher bacterial diversity in the rhizospheric soil. Key bacterial genera in the L-site rhizosphere included *Candidatus, Pseudolabrys, Bacillus, Gaiella*, and *Sphingomonas*. These bacteria are known for their role in utilizing plant-derived hydrocarbons and polysaccharides, significantly contributing to soil nutrient cycling (Luo et al., 2019; Dobrovolskaya et al., 2020; Li J. et al., 2020; Zhang X. et al., 2019). Additionally, the L-site rhizosphere supported a diverse community of ectomycorrhizal fungi, such as *Russula* and *Thelephora*. These ectomycorrhizal fungi have been reported to recruit various helper bacteria within the mycosphere to facilitate their growth and maintain mycelium in the soil (Pent et al., 2017; Warmink et al., 2009; Antony-Babu et al., 2014). Additionally, a significant presence of pathogenic fungi was observed at the L-site, including *Ilynocteria*, *Fusarium, Trichocladium*, and *Metarhizium*. *Metarhizium*, known for its role as an entomopathogenic fungus, protects plants from insect pests (Liao et al., 2014). In contrast, *Ilynocteria, Fusarium*, and *Trichocladium* are recognized plant pathogenic fungi (Leslie et al., 2006; Farh et al., 2018; Belosokhov et al., 2022). Interestingly, the lower abundance of pathogenic fungi at the P-site could be linked to the presence of *Occallatibacter*, which is known to hydrolyse chitin and thus offers protection against pathogenic fungal infections (Dobrovolskaya et al., 2020). However, further experimental validation is needed to confirm this hypothesis. Among other fungi significantly abundant at the L-site, *Humicola* is noted for its β-glucosidase gene (bgl4) and β-xylosidase gene (hxylA) coding for β-glucosidase and β-xylosidases, which are involved in cellulose degradation (Benoliel et al., 2010; Cintra et al., 2017).

6.2.4 Predicted functions and network analysis of rhizospheric microorganisms

The rhizosphere soil biomass is predominantly composed of plant materials such as hemicellulose, cellulose, lignin, pectin, and proteins. Microbial communities responsible for cellulose degradation are crucial for nutrient cycling and organic matter decomposition in soil (Datta, 2024). According to the putative functional predictions made by PICRUSt2, there were no distinct clusters in the overall predicted functions of bacterial communities between the two sites, suggesting that the rhizospheric soil bacterial communities from both seed orchards have similar functional potentials. Similarly, the ecological fungal guilds at the two sites were found to overlap, indicating that changes in precipitation have minimal impact on the fungal populations. However, these findings are based on predictions from software and may not fully reflect the actual conditions. Therefore, further experimental validations are necessary to substantiate these observations.

Microorganisms often thrive through intricate association networks rather than existing in isolation. Highly interconnected species can potentially play crucial roles within microbial communities (Liu et al., 2024). In the bacterial network analysis, species belonging to the bacterial phyla such as Proteobacteria, Actinobacteriota, Acidobacteriota, Bacteroidota, and Firmicutes exhibited significantly more connections compared to other phyla. These bacterial groups are likely essential for biogeochemical cycling and carbon mineralization in forest ecosystems (Huang et al., 2023; Zhu et al., 2022; Zhang B. et al., 2019). Notably, these prominent bacterial nodes exhibit varying growth rates; for example, some Proteobacteria taxa grow rapidly, whereas certain Acidobacteria taxa grow are slow growers (Singh et al., 2010; Zhou et al., 2018). The interactions among these nodes indicate that the diverse microbial community optimizes resource utilization and supports the functioning of forest ecosystems (Liu et al., 2024).

In the fungal co-occurrence network, the phyla Ascomycota and Basidiomycota were prominent, reflecting their key role in forming connections. These fungal genera are crucial for breaking down lignin and cellulose, processes that facilitate organic matter decomposition and enhance soil nutrient cycling in forest ecosystems (Lange et al., 2019). The L-site exhibited a higher level of overall microbial interactions compared to the P-site, with bacterial interactions being more than twice as frequent in the L-site. Despite the lower number of microbial interactions in the P-site, its microbial network displayed a higher clustering coefficient, indicating that the community structure in this site is highly interconnected and forms tight clusters. However, further experimental validation is required to confirm the functional implications of these observations.

7. Conclusions

This thesis aimed to achieve three main objectives: to assess soil quality parameters in forest soils under different precipitation regimes, to explore bacterial and fungal diversity in these soils, and to investigate the bacterial and fungal community structure in the rhizosphere of Norway spruce (*Picea abies*). For this study, two clonal Norway spruce seed orchards with distinctly different precipitation regimes were selected.

Our findings revealed that increased precipitation, along with soil texture, enhances water and nutrient availability. As a result, precipitation, combined with the effects of multiple edaphic factors, had a significant impact on microbial community composition and diversity. Higher soil moisture led to increased levels of total organic carbon (TOC) and total nitrogen (TN), which serve as vital nutrients for soil microorganisms. The combined influence of TOC, TN, and soil pH affected both the structure and activity of microbial communities, as evidenced by differences in soil metabolite profiles, extracellular enzyme activities, and phospholipid fatty acid (PLFA) content. Additionally, we observed that while increased soil moisture enhanced microbial biomass and activity, microbial diversity was relatively low, suggesting that soil microbial communities quickly adapt to their environment.

Similarly, variations in the relative abundance of specific rhizospheric microbial classes between sites point to climatic influence. Higher moisture content increased metabolite levels and was associated with a greater relative abundance of acidophilic bacteria, nitrogen-fixing bacteria, and mycorrhizal association. While elevated soil moisture influenced the structure and complexity of the rhizospheric bacterial community network, the diversity of the fungal community remained consistent across sites, indicating that precipitation had a lesser effect on the rhizosphere mycobiome.

This study provides a model for investigating the effects of climate change on belowground forest microbiomes and their implications for sustainable forest growth. It contributes to understanding soil microbial community dynamics towards future global climate change scenarios Understanding belowground processes and dynamics is a critical step toward effectively conserving aboveground ecosystems.

8. Limitations of the study

Several limitations of this study need to be addressed.

Although high-throughput amplicon sequencing is a powerful tool, it is prone to PCR bias (Kebschull and Zador, 2015). PCR amplification may not amplify all sequences equally, leading to variable amplification efficiency across different sequences. This bias can be minimized through alternative approaches such as shotgun sequencing or metatranscriptomics.

Additionally, 16S rRNA gene amplicon sequencing has inherent limitations in taxonomic resolution, often only identifying bacteria to the genus level due to the high similarity between 16S rRNA genes of closely related species (Gupta et al., 2019). As a result, critical functional associations at the species level may be missed. This issue can be addressed by employing techniques such as shotgun sequencing, which provides higher taxonomic resolution.

Functional predictions of microbial taxa, while useful, are based on computational models and may not fully reflect the actual *in situ* conditions in soil. Thus, further experimental validation is often necessary to confirm these predicted functions. The limitations of putative functional predictions can be addressed by using methods such as metatranscriptomics, metaproteomics, and other functional assays.

Regarding metabolite profiling, determining the precise origin of metabolites is challenging, as they may originate from multiple sources such as soil organic matter, plant exudates, or microbial metabolism. Disentangling the contributions of these individual factors to soil metabolite profiles remains difficult. In this study, we used gas chromatography-mass spectrometry (GC-MS), which detects volatile compounds or gases. This limitation could be mitigated by employing more sensitive methods like liquid chromatography-mass spectrometry (LC-MS), which is capable of detecting a broader range of compounds (Zeki et al., 2020).

Despite these limitations, our study provides valuable hypotheses that lay the foundation for future research.

9. References

Abram, F. (2015). Systems-based approaches to unravel multi-species microbial community functioning. *Computational and structural biotechnology journal*, *13*, 24-32.

Adnan, M., Islam, W., Gang, L., & Chen, H. Y. (2022). Advanced research tools for fungal diversity and its impact on forest ecosystem. *Environmental Science and Pollution Research*, *29*(30), 45044-45062.

Aina, P. O., & Periaswamy, S. P. (1985). Estimating available water-holding capacity of western Nigerian soils from soil texture and bulk density, using core and sieved samples. *Soil Science*, *140*(1), 55-58.

Algina, J., & Keselman, H. J. (1999). Comparing squared multiple correlation coefficients: Examination of a confidence interval and a test significance. *Psychological methods*, *4*(1), 76.

Allison, S. D., & Martiny, J. B. (2008). Resistance, resilience, and redundancy in microbial communities. *Proceedings of the National Academy of Sciences*, *105*(supplement_1), 11512-11519.

Allwood, J. W., Ellis, D. I., & Goodacre, R. (2008). Metabolomic technologies and their application to the study of plants and plant–host interactions. *Physiologia plantarum*, *132*(2), 117-135.

Anderson, M. J. (2001). A new method for non-parametric multivariate analysis of variance. *Austral ecology*, *26*(1), 32-46.

Antony-Babu, S., Deveau, A., Van Nostrand, J. D., Zhou, J., Le Tacon, F., Robin, C., ... & Uroz, S. (2014). Black truffle-associated bacterial communities during the development and maturation of T uber melanosporum ascocarps and putative functional roles. *Environmental Microbiology*, *16*(9), 2831-2847.

Augé, R. M. (2004). Arbuscular mycorrhizae and soil/plant water relations. *Canadian Journal of Soil Science*, *84*(4), 373-381.

Augusto, L., Ranger, J., Binkley, D., & Rothe, A. (2002). Impact of several common tree species of European temperate forests on soil fertility. *Annals of forest science*, *59*(3), 233-253.

Ault, T. R. (2020). On the essentials of drought in a changing climate. *Science*, *368*(6488), 256-260.

Austin, A. T., Yahdjian, L., Stark, J. M., Belnap, J., Porporato, A., Norton, U., ... & Schaeffer, S. M. (2004). Water pulses and biogeochemical cycles in arid and semiarid ecosystems. *Oecologia*, *141*, 221-235.

Avis, P. G. (2012). Ectomycorrhizal iconoclasts: the ITS rDNA diversity and nitrophilic tendencies of fetid Russula. *Mycologia*, *104*(5), 998-1007.

Ayres, E., Steltzer, H., Berg, S., Wallenstein, M. D., Simmons, B. L., & Wall, D. H. (2009). Tree species traits influence soil physical, chemical, and biological properties in high elevation forests. *PloS one*, *4*(6), e5964.

Bairoch, A. (2000). The ENZYME database in 2000. *Nucleic acids research*, *28*(1), 304-305.

Bakker, P. A., Berendsen, R. L., Doornbos, R. F., Wintermans, P. C., & Pieterse, C. M. (2013). The rhizosphere revisited: root microbiomics. *Frontiers in plant science*, *4*, 165.

Baldrian, P. (2008). Enzymes of saprotrophic basidiomycetes. In *British mycological society symposia series* (Vol. 28, pp. 19-41). Academic Press.

Baldrian, P. (2009). Microbial enzyme-catalyzed processes in soils and their analysis. *Plant, Soil and Environment*, *55*(9), 370-378.

Baldrian, P. (2014). Distribution of extracellular enzymes in soils: spatial heterogeneity and determining factors at various scales. *Soil Science Society of America Journal*, *78*(1), 11-18.

Baldrian, P. (2017). Forest microbiome: diversity, complexity and dynamics. *FEMS Microbiology reviews*, *41*(2), 109-130.

Baldrian, P., & Štursová, M. (2011). Enzymes in forest soils. *Soil enzymology*, 61-73.

Baldrian, P., & Valášková, V. (2008). Degradation of cellulose by basidiomycetous fungi. *FEMS microbiology reviews*, *32*(3), 501-521.

Baldrian, P., Kolařík, M., Štursová, M., Kopecký, J., Valášková, V., Větrovský, T., ... & Voříšková, J. (2012). Active and total microbial communities in forest soil are largely different and highly stratified during decomposition. *The ISME journal*, *6*(2), 248-258.

Banerjee, M. R., & Chapman, S. J. (1996). The significance of microbial biomass sulphur in soil. *Biology and Fertility of Soils*, *22*, 116-125.

Barberán, A., Bates, S. T., Casamayor, E. O., & Fierer, N. (2012). Using network analysis to explore co-occurrence patterns in soil microbial communities. *The ISME journal*, *6*(2), 343-351.

Barnard, R. L., Osborne, C. A., & Firestone, M. K. (2013). Responses of soil bacterial and fungal communities to extreme desiccation and rewetting. *The ISME journal*, *7*(11), 2229-2241.

Barton, H. A., Giarrizzo, J. G., Suarez, P., Robertson, C. E., Broering, M. J., Banks, E. D., ... & Venkateswaran, K. (2014). Microbial diversity in a Venezuelan orthoquartzite cave is dominated by the

Chloroflexi (Class Ktedonobacterales) and Thaumarchaeota Group I. 1c. *Frontiers in microbiology*, *5*, 615.

Bascompte, J. (2009). Disentangling the web of life. *Science*, *325*(5939), 416-419.

Bastida, F., Eldridge, D. J., García, C., Kenny Png, G., Bardgett, R. D., & Delgado-Baquerizo, M. (2021). Soil microbial diversity–biomass relationships are driven by soil carbon content across global biomes. *The ISME Journal*, *15*(7), 2081-2091.

Bechtold, J. S., & Naiman, R. J. (2006). Soil texture and nitrogen mineralization potential across a riparian toposequence in a semi-arid savanna. *Soil Biology and Biochemistry*, *38*(6), 1325-1333.

Beiko, R. G. (2015). Microbial malaise: how can we classify the microbiome?. *Trends in microbiology*, *23*(11), 671-679.

Bell, C. W., Fricks, B. E., Rocca, J. D., Steinweg, J. M., McMahon, S. K., & Wallenstein, M. D. (2013). High-throughput fluorometric measurement of potential soil extracellular enzyme activities. *JoVE (Journal of Visualized Experiments)*, (81), e50961.

Bell, C. W., Tissue, D. T., Loik, M. E., Wallenstein, M. D., Acosta-Martinez, V., Erickson, R. A., & Zak, J. C. (2014). Soil microbial and nutrient responses to 7 years of seasonally altered precipitation in a Chihuahuan Desert grassland. *Global Change Biology*, *20*(5), 1657-1673.

Belosokhov, A., Yarmeeva, M., Kokaeva, L., Chudinova, E., Mislavskiy, S., & Elansky, S. (2022). Trichocladium solani sp. nov.—A new pathogen on potato tubers causing yellow rot. *Journal of Fungi*, *8*(11), 1160.

Bengough, A. G. (2012). Water dynamics of the root zone: rhizosphere biophysics and its control on soil hydrology. *Vadose Zone Journal*, *11*(2), vzj2011-0111.

Benoliel, B., Poças-Fonseca, M. J., Torres, F. A. G., & de Moraes, L. M. P. (2010). Expression of a glucose-tolerant β-glucosidase from Humicola grisea var. thermoidea in Saccharomyces cerevisiae. *Applied biochemistry and biotechnology*, *160*, 2036-2044.

Berendsen, R. L., Pieterse, C. M., & Bakker, P. A. (2012). The rhizosphere microbiome and plant health. *Trends in plant science*, *17*(8), 478-486.

Berg, G., Opelt, K., Zachow, C., Lottmann, J., Götz, M., Costa, R., & Smalla, K. (2006). The rhizosphere effect on bacteria antagonistic towards the pathogenic fungus Verticillium differs depending on plant species and site. *FEMS Microbiology Ecology*, *56*(2), 250-261.

Berg, M. P., Kniese, J. P., & Verhoef, H. A. (1998). Dynamics and stratification of bacteria and fungi in the organic layers of a Scots pine forest soil. *Biology and Fertility of Soils*, *26*, 313-322.

Berthrong, S. T., Buckley, D. H., & Drinkwater, L. E. (2013). Agricultural management and labile carbon additions affect soil microbial community structure and interact with carbon and nitrogen cycling. *Microbial ecology*, *66*, 158-170.

Bi, B., Wang, K., Zhang, H., Wang, Y., Fei, H., Pan, R., & Han, F. (2021). Plants use rhizosphere metabolites to regulate soil microbial diversity. *Land Degradation & Development*, *32*(18), 5267-5280.

Bi, B., Yuan, Y., Zhang, H., Wu, Z., Wang, Y., & Han, F. (2022). Rhizosphere soil metabolites mediated microbial community changes of Pinus sylvestris var. mongolica across stand ages in the Mu Us Desert. *Applied Soil Ecology*, *169*, 104222.

Bian, H., Li, C., Zhu, J., Xu, L., Li, M., Zheng, S., & He, N. (2022). Soil moisture affects the rapid response of microbes to labile organic C addition. *Frontiers in Ecology and Evolution*, *10*, 857185.

Boer, W. D., Folman, L. B., Summerbell, R. C., & Boddy, L. (2005). Living in a fungal world: impact of fungi on soil bacterial niche development. *FEMS microbiology reviews*, *29*(4), 795-811.

Bokulich, N. A., Kaehler, B. D., Rideout, J. R., Dillon, M., Bolyen, E., Knight, R., ... & Gregory Caporaso, J. (2018). Optimizing taxonomic classification of marker-gene amplicon sequences with QIIME 2's q2-feature-classifier plugin. *Microbiome*, *6*, 1-17.

Bokulich, N. A., Subramanian, S., Faith, J. J., Gevers, D., Gordon, J. I., Knight, R., ... & Caporaso, J. G. (2013). Quality-filtering vastly improves diversity estimates from Illumina amplicon sequencing. *Nature methods*, *10*(1), 57-59.

Bolyen, E., Rideout, J. R., Dillon, M. R., Bokulich, N. A., Abnet, C. C., Al-Ghalith, G. A., ... & Caporaso, J. G. (2019). Reproducible, interactive, scalable and extensible microbiome data science using QIIME 2. *Nature biotechnology*, *37*(8), 852-857.

Bonan, G. B. (2008). Forests and climate change: forcings, feedbacks, and the climate benefits of forests. *science*, *320*(5882), 1444-1449.

Borcard, D., Legendre, P., & Drapeau, P. (1992). Partialling out the spatial component of ecological variation. *Ecology*, *73*(3), 1045-1055.

Borken, W., & Matzner, E. (2009). Reappraisal of drying and wetting effects on C and N mineralization and fluxes in soils. *Global change biology*, *15*(4), 808-824.

Borowik, A., & Wyszkowska, J. (2016). Soil moisture as a factor affecting the microbiological and biochemical activity of soil.

Borowik, A., Wyszkowska, J., & Kucharski, J. (2022). Bacteria and soil enzymes supporting the valorization of forested soils. *Materials*, *15*(9), 3287.

Bowd, E. J., Banks, S. C., Bissett, A., May, T. W., & Lindenmayer, D. B. (2022). Disturbance alters the forest soil microbiome. *Molecular Ecology*, *31*(2), 419-447.

Bowden, R. D., Deem, L., Plante, A. F., Peltre, C., Nadelhoffer, K., & Lajtha, K. (2014). Litter input controls on soil carbon in a temperate deciduous forest. *Soil Science Society of America Journal*, *78*(S1), S66-S75.

Bowles, T. M., Acosta-Martínez, V., Calderón, F., & Jackson, L. E. (2014). Soil enzyme activities, microbial communities, and carbon and nitrogen availability in organic agroecosystems across an intensively-managed agricultural landscape. *Soil Biology and Biochemistry*, *68*, 252-262.

Bradford, M. A. (2013). Thermal adaptation of decomposer communities in warming soils. *Frontiers in microbiology*, *4*, 333.

Bremner, J. M. (1996). Nitrogen-total. *Methods of soil analysis, part*, *3*.

Bukin, Y. S., Galachyants, Y. P., Morozov, I. V., Bukin, S. V., Zakharenko, A. S., & Zemskaya, T. I. (2019). The effect of 16S rRNA region choice on bacterial community metabarcoding results. *Scientific data*, *6*(1), 1-14.

Bundy, J. G., Davey, M. P., & Viant, M. R. (2009). Environmental metabolomics: a critical review and future perspectives. *Metabolomics*, *5*, 3-21.

Bundy, J. G., Ramløv, H., & Holmstrup, M. (2003). Multivariate metabolic profiling using 1H nuclear magnetic resonance spectroscopy of freeze-tolerant and freeze-intolerant earthworms exposed to frost. *Cryoletters*, *24*(6), 347-358.

Burke, I. C., Yonker, C. M., Parton, W. J., Cole, C. V., Flach, K., & Schimel, D. S. (1989). Texture, climate, and cultivation effects on soil organic matter content in US grassland soils. *Soil science society of America journal*, *53*(3), 800-805.

Burns, K. N., Kluepfel, D. A., Strauss, S. L., Bokulich, N. A., Cantu, D., & Steenwerth, K. L. (2015). Vineyard soil bacterial diversity and composition revealed by 16S rRNA genes: differentiation by geographic features. *Soil Biology and Biochemistry*, *91*, 232-247.

Burt, R. (2014). Soil Survey Staff. Soil Survey Field and Laboratory Methods Manual. Soil Survey Investigations Report 51. Washington, DC: US Department of Agriculture.

Butcher, K. R., Nasto, M. K., Norton, J. M., & Stark, J. M. (2020). Physical mechanisms for soil moisture effects on microbial carbon-use efficiency in a sandy loam soil in the western United States. *Soil Biology and Biochemistry*, *150*, 107969.

Cai, L. (2006). Multi-response permutation procedure as an alternative to the analysis of variance: an SPSS implementation. *Behavior Research Methods*, *38*(1), 51-59.

Callahan, B. J., McMurdie, P. J., Rosen, M. J., Han, A. W., Johnson, A. J. A., & Holmes, S. P. (2016). DADA2: High-resolution sample inference from Illumina amplicon data. *Nature methods*, *13*(7), 581-583.

Caporaso, J. G., Kuczynski, J., Stombaugh, J., Bittinger, K., Bushman, F. D., Costello, E. K., ... & Knight, R. (2010). QIIME allows analysis of high-throughput community sequencing data. *Nature methods*, *7*(5), 335-336.

Cavigelli, M. A., Robertson, G. P., & Klug, M. J. (1995). Fatty acid methyl ester (FAME) profiles as measures of soil microbial community structure. *Plant and soil*, *170*, 99-113.

Cesarz, S., Fender, A. C., Beyer, F., Valtanen, K., Pfeiffer, B., Gansert, D., ... & Scheu, S. (2013). Roots from beech (Fagus sylvatica L.) and ash (Fraxinus excelsior L.) differentially affect soil microorganisms and carbon dynamics. *Soil Biology and Biochemistry*, *61*, 23-32.

Chaffron, S., Rehrauer, H., Pernthaler, J., & Von Mering, C. (2010). A global network of coexisting microbes from environmental and whole-genome sequence data. *Genome research*, *20*(7), 947-959.

Chakraborty, A., Zádrapová, D., Dvořák, J., Faltinová, Z., Žáček, P., Cajthaml, T., ... & Roy, A. (2023). Impact of 30 years precipitation regime differences on forest soil physiology and microbial assemblages. *Frontiers in Forests and Global Change*, *6*, 1142979.

Chang, E. H., Tian, G., & Chiu, C. Y. (2017). Soil microbial communities in natural and managed cloud montane forests. *Forests*, *8*(2), 33.

Chang, F., He, S., & Dang, C. (2022). Assisted selection of biomarkers by linear discriminant analysis effect size (LEfSe) in microbiome data. *JoVE (Journal of Visualized Experiments)*, (183), e61715.

Chao, A. (1984). Nonparametric estimation of the number of classes in a population. *Scandinavian Journal of statistics*, 265-270.

Chao, A., & Lee, S. M. (1992). Estimating the number of classes via sample coverage. *Journal of the American statistical Association*, *87*(417), 210-217.

Chao, A., & Yang, M. C. (1993). Stopping rules and estimation for recapture debugging with unequal failure rates. *Biometrika*, *80*(1), 193-201.

Chao, A., Lee, S. M., & Chen, T. C. (1988). A generalized Good's nonparametric coverage estimator. *Chinese Journal of Mathematics*, 189-199.

Chaparro, J. M., Badri, D. V., & Vivanco, J. M. (2014). Rhizosphere microbiome assemblage is affected by plant development. *The ISME journal*, *8*(4), 790-803.

Chaparro, J. M., Sheflin, A. M., Manter, D. K., & Vivanco, J. M. (2012). Manipulating the soil microbiome to increase soil health and plant fertility. *Biology and Fertility of Soils*, *48*, 489-499.

Chapman, M. G., & Underwood, A. J. (1999). Ecological patterns in multivariate assemblages: information and interpretation of negative values in ANOSIM tests. *Marine ecology progress series*, *180*, 257-265.

Che, R., Deng, Y., Wang, F., Wang, W., Xu, Z., Wang, Y., & Cui, X. (2015). 16S rRNA-based bacterial community structure is a sensitive indicator of soil respiration activity. *Journal of Soils and Sediments*, *15*, 1987-1990.

Chen, S., Zhou, Y., Chen, Y., & Gu, J. (2018). fastp: an ultra-fast all-in-one FASTQ preprocessor. *Bioinformatics*, *34*(17), i884-i890.

Chen, X., Zhang, D., Liang, G., Qiu, Q., Liu, J., Zhou, G., ... & Yan, J. (2016). Effects of precipitation on soil organic carbon fractions in three subtropical forests in southern China. *Journal of Plant Ecology*, *9*(1), 10-19.

Chernov, T. I., Zhelezova, A. D., Tkhakakhova, A. K., Ksenofontova, N. A., Zverev, A. O., & Tiunov, A. V. (2021). Soil microbiome, organic matter content and microbial abundance in forest and forest-derived land cover in Cat Tien National Park (Vietnam). *Applied Soil Ecology*, *165*, 103957.

Chiarello, M., McCauley, M., Villéger, S., & Jackson, C. R. (2022). Ranking the biases: The choice of OTUs vs. ASVs in 16S rRNA amplicon data analysis has stronger effects on diversity measures than rarefaction and OTU identity threshold. *PloS one*, *17*(2), e0264443.

Chodak, M., Klimek, B., & Niklińska, M. (2016). Composition and activity of soil microbial communities in different types of temperate forests. *Biology and Fertility of Soils*, *52*, 1093-1104.

Chong, J., Wishart, D. S., & Xia, J. (2019). Using MetaboAnalyst 4.0 for comprehensive and integrative metabolomics data analysis. *Current protocols in bioinformatics*, *68*(1), e86.

Cintra, L. C., Fernandes, A. G., Oliveira, I. C. M., Siqueira, S. J. L., Costa, I. G. O., Colussi, F., Jesuíno, R. S. A., Ulhoa, C. J., & Faria, F. P. (2017). Characterization of a recombinant xylose tolerant β-xylosidase from Humicola grisea var. thermoidea and its use in sugarcane bagasse hydrolysis. *International journal of biological macromolecules*, *105*(Pt 1), 262–271.

Clarke, K. R. (1993). Non-parametric multivariate analyses of changes in community structure. *Australian journal of ecology*, *18*(1), 117-143.

Clauset, A., Newman, M. E., & Moore, C. (2004). Finding community structure in very large networks. *Physical Review E—Statistical, Nonlinear, and Soft Matter Physics*, *70*(6), 066111.

Clemmensen, K. E., Bahr, A., Ovaskainen, O., Dahlberg, A., Ekblad, A., Wallander, H., ... & Lindahl, B. (2013). Roots and associated fungi drive long-term carbon sequestration in boreal forest. *Science*, *339*(6127), 1615-1618.

Collins, S. L., Belnap, J., Grimm, N. B., Rudgers, J. A., Dahm, C. N., D'odorico, P., ... & Wolf, B. O. (2014). A multiscale, hierarchical model of pulse dynamics in arid-land ecosystems. *Annual Review of Ecology, Evolution, and Systematics*, *45*(1), 397-419.

Conradie, T., & Jacobs, K. (2020). Seasonal and agricultural response of Acidobacteria present in two fynbos rhizosphere soils. *Diversity*, *12*(7), 277.

Cook, B. I., Mankin, J. S., & Anchukaitis, K. J. (2018). Climate change and drought: From past to future. *Current Climate Change Reports*, *4*, 164-179.

Cook, R. J., Thomashow, L. S., Weller, D. M., Fujimoto, D., Mazzola, M., Bangera, G., & Kim, D. S. (1995). Molecular mechanisms of defense by rhizobacteria against root disease. *Proceedings of the National Academy of Sciences*, *92*(10), 4197-4201.

Coolen, M. J., & Overmann, J. (2000). Functional exoenzymes as indicators of metabolically active bacteria in 124,000-year-old sapropel layers of the eastern Mediterranean Sea. *Applied and Environmental Microbiology*, *66*(6), 2589-2598.

Coûteaux, M. M., Raubuch, M., & Berg, M. (1998). Response of protozoan and microbial communities in various coniferous forest soils after transfer to forests with different levels of atmospheric pollution. *Biology and fertility of soils*, *27*, 179-188.

Crowther, T. W., Glick, H. B., Covey, K. R., Bettigole, C., Maynard, D. S., Thomas, S. M., ... & Bradford, M. A. (2015). Mapping tree density at a global scale. *Nature*, *525*(7568), 201-205.

Crowther, T. W., Todd-Brown, K. E., Rowe, C. W., Wieder, W. R., Carey, J. C., Machmuller, M. B., Snoek, B. L., Fang, S., Zhou, G., Allison, S. D., Blair, J. M., Bridgham, S. D., Burton, A. J., Carrillo, Y., Reich, P. B., Clark, J. S., Classen, A. T., Dijkstra, F. A., Elberling, B., Emmett, B. A., … Bradford, M. A. (2016). Quantifying global soil carbon losses in response to warming. *Nature*, *540*(7631), 104–108.

Csardi, G., & Nepusz, T. (2006). The igraph software. *Complex syst*, *1695*, 1-9.

D'Argenio, V., Casaburi, G., Precone, V., & Salvatore, F. (2014). Comparative metagenomic analysis of human gut microbiome composition using two different bioinformatic pipelines. *BioMed research international*, *2014*(1), 325340.

Dai, A., Zhao, T., & Chen, J. (2018). Climate change and drought: a precipitation and evaporation perspective. *Current Climate Change Reports*, *4*, 301-312.

Datta R. (2024). Enzymatic degradation of cellulose in soil: A review. *Heliyon*, *10*(1), e24022.

De Feudis, M., Cardelli, V., Massaccesi, L., Lagomarsino, A., Fornasier, F., Westphalen, D. J., ... & Agnelli, A. (2017). Influence of altitude on biochemical properties of European beech (Fagus sylvatica L.) forest soils. *Forests*, *8*(6), 213.

De Vries, F. T., Manning, P., Tallowin, J. R., Mortimer, S. R., Pilgrim, E. S., Harrison, K. A., ... & Bardgett, R. D. (2012). Abiotic drivers and plant traits explain landscape-scale patterns in soil microbial communities. *Ecology letters*, *15*(11), 1230-1239.

Deacon, L. J., Pryce-Miller, E. J., Frankland, J. C., Bainbridge, B. W., Moore, P. D., & Robinson, C. H. (2006). Diversity and function of decomposer fungi from a grassland soil. *Soil Biology and Biochemistry*, *38*(1), 7-20.

DeAngelis, K. M., Brodie, E. L., DeSantis, T. Z., Andersen, G. L., Lindow, S. E., & Firestone, M. K. (2009). Selective progressive response of soil microbial community to wild oat roots. *The ISME journal*, *3*(2), 168-178.

Delgado-Baquerizo, M., Oliverio, A. M., Brewer, T. E., Benavent-González, A., Eldridge, D. J., Bardgett, R. D., ... & Fierer, N. (2018). A global atlas of the dominant bacteria found in soil. *Science*, *359*(6373), 320-325.

Deng, R., Chen, X., Qiu, L. P., Chen, J. Z., & Meng, S. L. (2021). Bacterial community structure and diversity in the aqueous environment of Shihou Lake and its relationship with environmental factors. *Indian Journal of Microbiology*, *61*(4), 475-486.

Dexter, A. R. (2004). Soil physical quality: Part I. Theory, effects of soil texture, density, and organic matter, and effects on root growth. *Geoderma*, *120*(3-4), 201-214.

Diamond, S., Andeer, P. F., Li, Z., Crits-Christoph, A., Burstein, D., Anantharaman, K., ... & Banfield, J. F. (2019). Mediterranean grassland soil C–N compound turnover is dependent on rainfall and depth, and is mediated by genomically divergent microorganisms. *Nature microbiology*, *4*(8), 1356-1367.

Dietzen, C. A., Larsen, K. S., Ambus, P. L., Michelsen, A., Arndal, M. F., Beier, C., ... & Schmidt, I. K. (2019). Accumulation of soil carbon under elevated CO2 unaffected by warming and drought. *Global Change Biology*, *25*(9), 2970-2977.

Diniz-Filho, J. A. F., Soares, T. N., Lima, J. S., Dobrovolski, R., Landeiro, V. L., Telles, M. P. D. C., ... & Bini, L. M. (2013). Mantel test in population genetics. *Genetics and molecular biology*, *36*, 475-485.

Dobrovolskaya, T. G., Golovchenko, A. V., Lysak, L. V., & Yurchenko, E. N. (2020). Taxonomic structure of bacterial communities of Rhizospheric soil under Bogs' plants. *Moscow University Soil Science Bulletin*, *75*, 93-100.

Donn, S., Kirkegaard, J. A., Perera, G., Richardson, A. E., & Watt, M. (2015). Evolution of bacterial communities in the wheat crop rhizosphere. *Environmental microbiology*, *17*(3), 610-621.

Douglas, G. M., Maffei, V. J., Zaneveld, J. R., Yurgel, S. N., Brown, J. R., Taylor, C. M., ... & Langille, M. G. (2020). PICRUSt2 for prediction of metagenome functions. *Nature biotechnology*, *38*(6), 685-688.

Douglas, G., Beiko, R., and Langille, M. (2018). Microbiome Analysis. Berlin: Springer.

Drenovsky, R. E., Vo, D., Graham, K. J., & Scow, K. M. (2004). Soil water content and organic carbon availability are major determinants of soil microbial community composition. *Microbial ecology*, *48*, 424-430.

Edgar, R. C. (2004). MUSCLE: multiple sequence alignment with high accuracy and high throughput. *Nucleic acids research*, *32*(5), 1792-1797.

Edgar, R. C. (2013). UPARSE: highly accurate OTU sequences from microbial amplicon reads. *Nature methods*, *10*(10), 996-998.

Edgar, R. C., Haas, B. J., Clemente, J. C., Quince, C., & Knight, R. (2011). UCHIME improves sensitivity and speed of chimera detection. *Bioinformatics*, *27*(16), 2194-2200.

Edwards, J., Johnson, C., Santos-Medellín, C., Lurie, E., Podishetty, N. K., Bhatnagar, S., ... & Sundaresan, V. (2015). Structure, variation, and assembly of the root-associated microbiomes of rice. *Proceedings of the National Academy of Sciences*, *112*(8), E911-E920.

Elbert, W., Weber, B., Burrows, S., Steinkamp, J., Büdel, B., Andreae, M. O., & Pöschl, U. (2012). Contribution of cryptogamic covers to the global cycles of carbon and nitrogen. *Nature Geoscience*, *5*(7), 459-462.

Engelhardt, I. C., Welty, A., Blazewicz, S. J., Bru, D., Rouard, N., Breuil, M. C., ... & Barnard, R. L. (2018). Depth matters: effects of precipitation regime on soil microbial activity upon rewetting of a plant-soil system. *The ISME journal*, *12*(4), 1061-1071.

Fadeev, E., Cardozo-Mino, M. G., Rapp, J. Z., Bienhold, C., Salter, I., Salman-Carvalho, V., ... & Boetius, A. (2021). Comparison of two 16S rRNA primers (V3–V4 and V4–V5) for studies of arctic microbial communities. *Frontiers in microbiology*, *12*, 637526.

Fang, X., Zhou, G., Li, Y., Liu, S., Chu, G., Xu, Z., & Liu, J. (2016). Warming effects on biomass and composition of microbial communities and enzyme activities within soil aggregates in subtropical forest. *Biology and Fertility of Soils*, *52*, 353-365.

Farh, M. E. A., Kim, Y. J., Kim, Y. J., & Yang, D. C. (2018). Cylindrocarpon destructans/Ilyonectria radicicola-species complex: Causative agent of ginseng root-rot disease and rusty symptoms. *Journal of ginseng research*, *42*(1), 9-15.

Fekete, I., Kotroczó, Z., Varga, C., Nagy, P. T., Várbíró, G., Bowden, R. D., ... & Lajtha, K. (2014). Alterations in forest detritus inputs influence soil carbon concentration and soil respiration in a Central-European deciduous forest. *Soil Biology and Biochemistry*, *74*, 106-114.

Fekete, I., Lajtha, K., Kotroczó, Z., Várbíró, G., Varga, C., Tóth, J. A., ... & Berki, I. (2017). Long-term effects of climate change on carbon storage and tree species composition in a dry deciduous forest. *Global Change Biology*, *23*(8), 3154-3168.

Fekete, I., Varga, C., Biró, B., Tóth, J. A., Várbíró, G., Lajtha, K., ... & Kotroczó, Z. (2016). The effects of litter production and litter depth on soil microclimate in a central european deciduous forest. *Plant and soil*, *398*, 291-300.

Fiehn, O. (2002). Metabolomics—the link between genotypes and phenotypes. *Functional genomics*, 155-171.

Fierer, N. (2017). Embracing the unknown: disentangling the complexities of the soil microbiome. *Nature Reviews Microbiology*, *15*(10), 579-590.

Fierer, N., & Jackson, R. B. (2006). The diversity and biogeography of soil bacterial communities. *Proceedings of the National Academy of Sciences*, *103*(3), 626-631.

Fierer, N., Strickland, M. S., Liptzin, D., Bradford, M. A., & Cleveland, C. C. (2009). Global patterns in belowground communities. *Ecology letters*, *12*(11), 1238-1249.

Fontaine, S., Barot, S., Barré, P., Bdioui, N., Mary, B., & Rumpel, C. (2007). Stability of organic carbon in deep soil layers controlled by fresh carbon supply. *Nature*, *450*(7167), 277-280.

Forzieri, G., Dakos, V., McDowell, N. G., Ramdane, A., & Cescatti, A. (2022). Emerging signals of declining forest resilience under climate change. *Nature*, *608*(7923), 534-539.

Franzluebbers, A. J., Haney, R. L., Hons, F. M., & Zuberer, D. A. (1996). Active fractions of organic matter in soils with different texture. *Soil Biology and Biochemistry*, *28*(10-11), 1367-1372.

Frey, B., Carnol, M., Dharmarajah, A., Brunner, I., & Schleppi, P. (2020). Only minor changes in the soil microbiome of a sub-alpine forest after 20 years of moderately increased nitrogen loads. *Frontiers in Forests and Global Change*, *3*, 77.

Frey, S. D., Lee, J., Melillo, J. M., & Six, J. (2013). The temperature response of soil microbial efficiency and its feedback to climate. *Nature Climate Change*, *3*(4), 395-398.

Frey-Klett, P., Garbaye, J., & Tarkka, M. (2007). The mycorrhiza helper bacteria revisited. *New phytologist*, *176*(1), 22-36.

Frostegård, Å., Tunlid, A., & Bååth, E. (2011). Use and misuse of PLFA measurements in soils. *Soil Biology and Biochemistry*, *43*(8), 1621-1625.

Fu, F., Li, Y., Zhang, B., Zhu, S., Guo, L., Li, J., ... & Li, J. (2024). Differences in soil microbial community structure and assembly processes under warming and cooling conditions in an alpine forest ecosystem. *Science of The Total Environment*, *907*, 167809.

Fuerst, J. A. (1995). The planctomycetes: emerging models for microbial ecology, evolution and cell biology. *Microbiology*, *141*(7), 1493-1506.

Fujita, A., Sato, J. R., Demasi, M. A. A., Sogayar, M. C., Ferreira, C. E., & Miyano, S. (2009). Comparing Pearson, Spearman and Hoeffding's D measure for gene expression association analysis. *Journal of bioinformatics and computational biology*, *7*(04), 663-684.

Gao, W., Kou, L., Zhang, J., Müller, C., Wang, H., Yang, H., & Li, S. (2016). Enhanced deposition of nitrate alters microbial cycling of N in a subtropical forest soil. *Biology and Fertility of Soils*, *52*, 977-986.

Glassman, S. I., & Martiny, J. B. (2018). Broadscale ecological patterns are robust to use of exact sequence variants versus operational taxonomic units. *MSphere*, *3*(4), 10-1128.

Gomez, E. J., Delgado, J. A., & Gonzalez, J. M. (2021). Influence of water availability and temperature on estimates of microbial extracellular enzyme activity. *PeerJ*, *9*, e10994.

Gomoryova, E. (2004). Small-scale variation of microbial activities in a forest soil under a beech [Fagus sylvatica L.] stand. *Polish Journal of Ecology*, *3*(52).

Gottel, N. R., Castro, H. F., Kerley, M., Yang, Z., Pelletier, D. A., Podar, M., ... & Schadt, C. W. (2011). Distinct microbial communities within the endosphere and rhizosphere of Populus deltoides roots across contrasting soil types. *Applied and environmental microbiology*, *77*(17), 5934-5944.

Graham, E. B., Crump, A. R., Kennedy, D. W., Arntzen, E., Fansler, S., Purvine, S. O., ... & Stegen, J. C. (2018). Multi'omics comparison reveals metabolome biochemistry, not microbiome composition or gene expression, corresponds to elevated biogeochemical function in the hyporheic zone. *Science of the total environment*, *642*, 742-753.

Grobelak, A., Napora, A., & Kacprzak, M. J. E. E. (2015). Using plant growth-promoting rhizobacteria (PGPR) to improve plant growth. *Ecological Engineering*, *84*, 22-28.

Gupta, S., Mortensen, M. S., Schjørring, S., Trivedi, U., Vestergaard, G., Stokholm, J., ... & Sørensen, S. J. (2019). Amplicon sequencing provides more accurate microbiome information in healthy children compared to culturing. *Communications biology*, *2*(1), 291.

Guseva, K., Darcy, S., Simon, E., Alteio, L. V., Montesinos-Navarro, A., & Kaiser, C. (2022). From diversity to complexity: Microbial networks in soils. *Soil Biology and Biochemistry*, *169*, 108604.

Haas, B. J., Gevers, D., Earl, A. M., Feldgarden, M., Ward, D. V., Giannoukos, G., ... & Human Microbiome Consortium. (2011). Chimeric 16S rRNA sequence formation and detection in Sanger and 454-pyrosequenced PCR amplicons. *Genome research*, *21*(3), 494-504.

Haas, J. C., Street, N. R., Sjödin, A., Lee, N. M., Högberg, M. N., Näsholm, T., & Hurry, V. (2018). Microbial community response to growing season and plant nutrient optimisation in a boreal Norway spruce forest. *Soil Biology and Biochemistry*, *125*, 197-209.

Haichar, F. E. Z., Marol, C., Berge, O., Rangel-Castro, J. I., Prosser, J. I., Balesdent, J., ... & Achouak, W. (2008). Plant host habitat and root exudates shape soil bacterial community structure. *The ISME journal*, *2*(12), 1221-1230.

Han, B., Gan, X., Shi, S., Hu, X., Mu, X., Yu, Q., ... & Li, H. (2024). Gravesoil fungi are more sensitive than bacteria in response to precipitation. *Soil Ecology Letters*, *6*(3), 230225.

Hardoim, P. R., Van Overbeek, L. S., Berg, G., Pirttilä, A. M., Compant, S., Campisano, A., ... & Sessitsch, A. (2015). The hidden world within plants: ecological and evolutionary considerations for defining functioning of microbial endophytes. *Microbiology and molecular biology reviews*, *79*(3), 293-320.

Harris, R. F. (1981). Effect of water potential on microbial growth and activity. *Water potential relations in soil microbiology*, *9*, 23-95.

Hättenschwiler, S., Tiunov, A. V., & Scheu, S. (2005). Biodiversity and litter decomposition in terrestrial ecosystems. *Annu. Rev. Ecol. Evol. Syst.*, *36*(1), 191-218.

Hayat, R., Ali, S., Amara, U., Khalid, R., & Ahmed, I. (2010). Soil beneficial bacteria and their role in plant growth promotion: a review. *Annals of microbiology*, *60*, 579-598.

He, R., Yang, K., Li, Z., Schädler, M., Yang, W., Wu, F., ... & Xu, Z. (2017). Effects of forest conversion on soil microbial communities depend on soil layer on the eastern Tibetan Plateau of China. *PloS one*, *12*(10), e0186053.

He, Y., Caporaso, J. G., Jiang, X. T., Sheng, H. F., Huse, S. M., Rideout, J. R., ... & Zhou, H. W. (2015). Stability of operational taxonomic units: an important but neglected property for analyzing microbial diversity. *Microbiome*, *3*, 1-10.

Heinemeyer, A., & Fitter, A. H. (2004). Impact of temperature on the arbuscular mycorrhizal (AM) symbiosis: growth responses of the host plant and its AM fungal partner. *Journal of Experimental Botany*, *55*(396), 525-534.

Held, I. M., & Soden, B. J. (2000). Water vapor feedback and global warming. *Annual review of energy and the environment*, *25*(1), 441-475.

Hiltner, L. (1904). Über neuere Erfahrungen und Probleme auf dem Gebiet der Bodenbakteriologie und unter besonderer Berücksichtigung der Gründüngung und Brache. *Arbeiten der deutschen landwirtschaftlichen gesellschaft*, *98*, 59.

Hofrichter, M. (2002). lignin conversion by manganese peroxidase (MnP). *Enzyme and Microbial technology*, *30*(4), 454-466.

Hongoh, Y., & Toyoda, A. (2011). Whole-genome sequencing of unculturable bacterium using whole-genome amplification. *High-Throughput Next Generation Sequencing: Methods and Applications*, 25-33.

Horz, H. P., Barbrook, A., Field, C. B., & Bohannan, B. J. (2004). Ammonia-oxidizing bacteria respond to multifactorial global change. *Proceedings of the National Academy of Sciences*, *101*(42), 15136-15141.

Hu, Y., Ganjurjav, H., Hu, G., Wang, X., Wan, Z., & Gao, Q. (2023). Seasonal patterns of soil microbial community response to warming and increased precipitation in a semiarid steppe. *Applied Soil Ecology*, *182*, 104712.

Huang, G., Li, Y., & Su, Y. G. (2015). Effects of increasing precipitation on soil microbial community composition and soil respiration in a temperate desert, Northwestern China. *Soil Biology and Biochemistry*, *83*, 52-56.

Huang, J., Gao, K., Yang, L., & Lu, Y. (2023). Successional action of Bacteroidota and Firmicutes in decomposing straw polymers in a paddy soil. *Environmental Microbiome*, *18*(1), 76.

Hueso, S., García, C., & Hernández, T. (2012). Severe drought conditions modify the microbial community structure, size and activity in amended and unamended soils. *Soil Biology and Biochemistry*, *50*, 167-173.

Huhta, V., & Setälä, H. (1990). Laboratory design to simulate complexity of forest floor for studying the role of fauna in the soil processes. *Biology and Fertility of Soils*, *10*, 155-162.

Hungate, B. A., Hart, S. C., Selmants, P. C., Boyle, S. I., & Gehring, C. A. (2007). Soil responses to management, increased precipitation, and added nitrogen in ponderosa pine forests. *Ecological Applications*, *17*(5), 1352-1365.

IPCC (2023). Summary for Policymakers. In: Climate Change 2023: Synthesis Report. Contribution of Working Groups I, II and III to the Sixth Assessment Report of the Intergovernmental Panel on Climate Change [Core Writing Team, H. Lee and J. Romero (eds.)]. IPCC, Geneva, Switzerland, pp. 1-34.

Iyer, S., Killingback, T., Sundaram, B., & Wang, Z. (2013). Attack robustness and centrality of complex networks. *PloS one*, *8*(4), e59613.

Jeanbille, M., Buée, M., Bach, C., Cébron, A., Frey-Klett, P., Turpault, M. P., & Uroz, S. (2016). Soil parameters drive the structure, diversity and metabolic potentials of the bacterial communities across temperate beech forest soil sequences. *Microbial ecology*, *71*, 482-493.

Johns, C. W., Lee, A. B., Springer, T. I., Rosskopf, E. N., Hong, J. C., Turechek, W., ... & Finley, N. L. (2017). Using NMR-based metabolomics to monitor the biochemical composition of agricultural soils: A pilot study. *European Journal of Soil Biology*, *83*, 98-105.

Jones, O. A., Maguire, M. L., Griffin, J. L., Dias, D. A., Spurgeon, D. J., & Svendsen, C. (2013). Metabolomics and its use in ecology. *Austral Ecology*, *38*(6), 713-720.

Jones, O. A., Sdepanian, S., Lofts, S., Svendsen, C., Spurgeon, D. J., Maguire, M. L., & Griffin, J. L. (2014). Metabolomic analysis of soil communities can be used for pollution assessment. *Environmental toxicology and chemistry*, *33*(1), 61-64.

Jones, R. T. (2015). A comprehensive survey of soil rhizobiales diversity using high-throughput DNA sequencing. *Biological nitrogen fixation*, 769-776.

Jovel, J., Patterson, J., Wang, W., Hotte, N., O'Keefe, S., Mitchel, T., ... & Wong, G. K. S. (2016). Characterization of the gut microbiome using 16S or shotgun metagenomics. *Frontiers in microbiology*, *7*, 459.

Judd, K. E., Crump, B. C., & Kling, G. W. (2006). Variation in dissolved organic matter controls bacterial production and community composition. *Ecology*, *87*(8), 2068–2079.

Kamble, A., Sawant, S., & Singh, H. (2020). 16S ribosomal RNA gene-based metagenomics: A review. *Biomedical Research Journal*, *7*(1), 5-11.

Kanehisa, M., Goto, S., Sato, Y., Furumichi, M., & Tanabe, M. (2012). KEGG for integration and interpretation of large-scale molecular data sets. *Nucleic acids research*, *40*(D1), D109-D114.

Karhu, K., Auffret, M. D., Dungait, J. A., Hopkins, D. W., Prosser, J. I., Singh, B. K., ... & Hartley, I. P. (2014). Temperature sensitivity of soil respiration rates enhanced by microbial community response. *Nature*, *513*(7516), 81-84.

Kebschull, J. M., & Zador, A. M. (2015). Sources of PCR-induced distortions in high-throughput sequencing data sets. *Nucleic acids research*, *43*(21), e143-e143.

Kennedy, P. G., & Maillard, F. (2023). Knowns and unknowns of the soil fungal necrobiome. *Trends in Microbiology*, *31*(2), 173-180.

Khaine, I., & Woo, S. Y. (2015). An overview of interrelationship between climate change and forests. *Forest Science and Technology*, *11*(1), 11-18.

Kieft, T. L. (1987). Microbial biomass response to a rapid increase in water potential when dry soil is wetted. *Soil Biology and Biochemistry*, *19*(2), 119-126.

Klamer, M., & Bååth, E. (1998). Microbial community dynamics during composting of straw material studied using phospholipid fatty acid analysis. *FEMS Microbiology Ecology*, *27*(1), 9-20.

Klindworth, A., Pruesse, E., Schweer, T., Peplies, J., Quast, C., Horn, M., & Glöckner, F. O. (2013). Evaluation of general 16S ribosomal RNA gene PCR primers for classical and next-generation sequencing-based diversity studies. *Nucleic acids research*, *41*(1), e1-e1.

Köberl, M., Wagner, P., Müller, H., Matzer, R., Unterfrauner, H., Cernava, T., & Berg, G. (2020). Unraveling the complexity of soil microbiomes in a large-scale study subjected to different agricultural management in Styria. *Frontiers in microbiology*, *11*, 1052.

Koek, M. M., Muilwijk, B., van der Werf, M. J., & Hankemeier, T. (2006). Microbial metabolomics with gas chromatography/mass spectrometry. *Analytical chemistry*, *78*(4), 1272-1281.

Kokalis-Burelle, N., McSorley, R., Wang, K. H., Saha, S. K., & McGovern, R. J. (2017). Rhizosphere microorganisms affected by soil solarization and cover cropping in Capsicum annuum and Phaseolus lunatus agroecosystems. *Applied Soil Ecology*, *119*, 64-71.

Kottke, I., Qian, X. M., Pritsch, K., Haug, I., & Oberwinkler, F. (1998). Xerocomus badius–Picea abies, an ectomycorrhiza of high activity and element storage capacity in acidic soil. *Mycorrhiza*, *7*, 267-275.

Krashevska, V., Klarner, B., Widyastuti, R., Maraun, M., & Scheu, S. (2015). Impact of tropical lowland rainforest conversion into rubber and oil palm plantations on soil microbial communities. *Biology and fertility of soils*, *51*, 697-705.

Kuzyakov, Y. (2010). Priming effects: interactions between living and dead organic matter. *Soil Biology and Biochemistry*, *42*(9), 1363-1371.

Lange, L., Pilgaard, B., Herbst, F. A., Busk, P. K., Gleason, F., & Pedersen, A. G. (2019). Origin of fungal biomass degrading enzymes: evolution, diversity and function of enzymes of early lineage fungi. *Fungal Biology Reviews*, *33*(1), 82-97.

Lankadurai, B. P., Nagato, E. G., & Simpson, M. J. (2013). Environmental metabolomics: an emerging approach to study organism responses to environmental stressors. *Environmental Reviews*, *21*(3), 180-205.

Lê Cao, K. A., Boitard, S., & Besse, P. (2011). Sparse PLS discriminant analysis: biologically relevant feature selection and graphical displays for multiclass problems. *BMC bioinformatics*, *12*, 1-17.

LeBrun, E. S., King, R. S., Back, J. A., & Kang, S. (2018). Microbial community structure and function decoupling across a phosphorus gradient in streams. *Microbial ecology*, *75*, 64-73.

Lechevalier, M. P. (1989). Lipids in bacterial taxonomy. *Practical handbook of microbiology*, 57-67.

Legendre, P. (2008). Studying beta diversity: ecological variation partitioning by multiple regression and canonical analysis. *Journal of plant ecology*, *1*(1), 3-8.

Legendre, P., & Anderson, M. J. (1999). Distance-based redundancy analysis: testing multispecies responses in multifactorial ecological experiments. *Ecological monographs*, *69*(1), 1-24.

Leslie, J. F., & Summerell, B. A. (2008). *The Fusarium laboratory manual*. John Wiley & Sons.

Li, C., Liu, L., Zheng, L., Yu, Y., Mushinski, R. M., Zhou, Y., & Xiao, C. (2021). Greater soil water and nitrogen availability increase C: N ratios of root exudates in a temperate steppe. Soil Biology and Biochemistry, 161, 108384.

Li, H., Xu, Z., Yang, S., Li, X., Top, E. M., Wang, R., ... & Jiang, Y. (2016). Responses of soil bacterial communities to nitrogen deposition and precipitation increment are closely linked with aboveground community variation. *Microbial ecology*, *71*, 974-989.

Li, H., Yang, S., Xu, Z., Yan, Q., Li, X., van Nostrand, J. D., ... & Jiang, Y. (2017). Responses of soil microbial functional genes to global changes are indirectly influenced by aboveground plant biomass variation. *Soil Biology and Biochemistry*, *104*, 18-29.

Li, H., Ye, D., Wang, X., Settles, M. L., Wang, J., Hao, Z., ... & Ma, Z. (2014). Soil bacterial communities of different natural forest types in Northeast China. *Plant and Soil*, *383*, 203-216.

Li, J., Chen, X., Li, S., Zuo, Z., Zhan, R., & He, R. (2020). Variations of rhizospheric soil microbial communities in response to continuous Andrographis paniculata cropping practices. *Botanical studies*, *61*, 1-13.

Li, J., Li, Z., Wang, F., Zou, B., Chen, Y., Zhao, J., ... & Xia, H. (2015). Effects of nitrogen and phosphorus addition on soil microbial community in a secondary tropical forest of China. *Biology and Fertility of Soils*, *51*, 207-215.

Li, M., Shao, D., Zhou, J., Gu, J., Qin, J., Chen, W., & Wei, W. (2020). Signatures within esophageal microbiota with progression of esophageal squamous cell carcinoma. *Chinese Journal of Cancer Research*, *32*(6), 755.

Liao, X., O'Brien, T. R., Fang, W., & St. Leger, R. J. (2014). The plant beneficial effects of Metarhizium species correlate with their association with roots. *Applied microbiology and biotechnology*, *98*, 7089-7096.

Lindahl, B. D., Ihrmark, K., Boberg, J., Trumbore, S. E., Högberg, P., Stenlid, J., & Finlay, R. D. (2007). Spatial separation of litter decomposition and mycorrhizal nitrogen uptake in a boreal forest. *New phytologist*, *173*(3), 611-620.

Lindahl, B. D., Nilsson, R. H., Tedersoo, L., Abarenkov, K., Carlsen, T., Kjøller, R., ... & Kauserud, H. (2013). Fungal community analysis by high-throughput sequencing of amplified markers–a user's guide. *New phytologist*, *199*(1), 288-299.

Ling, N., Wang, T., & Kuzyakov, Y. (2022). Rhizosphere bacteriome structure and functions. *Nature communications*, *13*(1), 836.

Linn, D. M., & Doran, J. W. (1984). Effect of water-filled pore space on carbon dioxide and nitrous oxide production in tilled and nontilled soils. *Soil Science Society of America Journal*, *48*(6), 1267-1272.

Lisá, L., Bajer, A., Pacina, J., McCool, J. P., Cílek, V., Rohovec, J., ... & Gottvald, Z. (2017). Prehistoric dark soils/sediments of Central Sudan; case study from the Mesolithic landscape at the Sixth Nile Cataract. *Catena*, *149*, 273-282.

Liu, W., Zhang, Z. H. E., & Wan, S. (2009). Predominant role of water in regulating soil and microbial respiration and their responses to climate change in a semiarid grassland. *Global Change Biology*, *15*(1), 184-195.

Liu, Y., Jin, X., Huang, S., Liu, Y., Kong, Z., Wu, L., & Ge, G. (2024). Co-Occurrence Patterns of Soil Fungal and Bacterial Communities in Subtropical Forest-Transforming Areas. *Current Microbiology*, *81*(2), 64.

Liu, Y., Liu, S., Wan, S., Wang, J., Luan, J., & Wang, H. (2016). Differential responses of soil respiration to soil warming and experimental throughfall reduction in a transitional oak forest in central China. *Agricultural and Forest Meteorology*, *226*, 186-198.

Lladó, S., López-Mondéjar, R., & Baldrian, P. (2017). Forest soil bacteria: diversity, involvement in ecosystem processes, and response to global change. *Microbiology and Molecular Biology Reviews*, *81*(2), 10-1128.

López-Mondéjar, R., Voříšková, J., Větrovský, T., & Baldrian, P. (2015). The bacterial community inhabiting temperate deciduous forests is vertically stratified and undergoes seasonal dynamics. *Soil Biology and Biochemistry*, *87*, 43-50.

Loreau, M., & Hector, A. (2001). Partitioning selection and complementarity in biodiversity experiments. *Nature*, *412*(6842), 72-76.

Lozupone, C. A., Hamady, M., Kelley, S. T., & Knight, R. (2007). Quantitative and qualitative β diversity measures lead to different insights into factors that structure microbial communities. *Applied and environmental microbiology*, *73*(5), 1576-1585.

Lozupone, C., & Knight, R. (2005). UniFrac: a new phylogenetic method for comparing microbial communities. *Applied and environmental microbiology*, *71*(12), 8228-8235.

Lozupone, C., Lladser, M. E., Knights, D., Stombaugh, J., & Knight, R. (2011). UniFrac: an effective distance metric for microbial community comparison. *The ISME journal*, *5*(2), 169-172.

Lu, W., Bennett, B. D., & Rabinowitz, J. D. (2008). Analytical strategies for LC–MS-based targeted metabolomics. *Journal of chromatography B*, *871*(2), 236-242.

Lugtenberg, B., & Kamilova, F. (2009). Plant-growth-promoting rhizobacteria. *Annual review of microbiology*, *63*(1), 541-556.

Lundberg, D. S., Lebeis, S. L., Paredes, S. H., Yourstone, S., Gehring, J., Malfatti, S., ... & Dangl, J. L. (2012). Defining the core Arabidopsis thaliana root microbiome. *Nature*, *488*(7409), 86-90.

Luo, Y., Wang, F., Huang, Y., Zhou, M., Gao, J., Yan, T., ... & An, L. (2019). Sphingomonas sp. Cra20 increases plant growth rate and alters rhizosphere microbial community structure of Arabidopsis thaliana under drought stress. *Frontiers in Microbiology*, *10*, 1221.

Maestre, F. T., Delgado-Baquerizo, M., Jeffries, T. C., Eldridge, D. J., Ochoa, V., Gozalo, B., ... & Singh, B. K. (2015). Increasing aridity reduces soil microbial diversity and abundance in global drylands. *Proceedings of the National Academy of Sciences*, *112*(51), 15684-15689.

Maestre, F. T., Eldridge, D. J., Soliveres, S., Kéfi, S., Delgado-Baquerizo, M., Bowker, M. A., ... & Berdugo, M. (2016). Structure and functioning of dryland ecosystems in a changing world. *Annual review of ecology, evolution, and systematics*, *47*(1), 215-237.

Magoč, T., & Salzberg, S. L. (2011). FLASH: fast length adjustment of short reads to improve genome assemblies. *Bioinformatics*, *27*(21), 2957-2963.

Maitra, P., Hrynkiewicz, K., Szuba, A., Jagodziński, A. M., Al-Rashid, J., Mandal, D., & Mucha, J. (2024). Metabolic niches in the rhizosphere microbiome: dependence on soil horizons, root traits and climate variables in forest ecosystems. *Frontiers in Plant Science*, *15*, 1344205.

Mantel, N. (1967). The detection of disease clustering and a generalized regression approach. *Cancer research*, *27*(2_Part_1), 209-220.

Manzoni, S., Taylor, P., Richter, A., Porporato, A., & Ågren, G. I. (2012). Environmental and stoichiometric controls on microbial carbon-use efficiency in soils. *New Phytologist*, *196*(1), 79-91.

Marschner, P., Crowley, D., & Yang, C. H. (2004). Development of specific rhizosphere bacterial communities in relation to plant species, nutrition and soil type. *Plant and soil*, *261*(1), 199-208.

Martin, P. H., Sherman, R. E., & Fahey, T. J. (2004). Forty years of tropical forest recovery from agriculture: Structure and floristics of secondary and old-growth riparian forests in the Dominican Republic. *Biotropica*, *36*(3), 297-317.

Martinović, T., Mašínová, T., López-Mondéjar, R., Jansa, J., Šťursová, M., Starke, R., & Baldrian, P. (2022). Microbial utilization of simple and complex carbon compounds in a temperate forest soil. *Soil Biology and Biochemistry*, *173*, 108786.

Mashabela, M. D., Tugizimana, F., Steenkamp, P. A., Piater, L. A., Dubery, I. A., & Mhlongo, M. I. (2022). Untargeted metabolite profiling to elucidate rhizosphere and leaf metabolome changes of wheat cultivars (Triticum aestivum L.) treated with the plant growth-promoting rhizobacteria Paenibacillus alvei (T22) and Bacillus subtilis. *Frontiers in Microbiology*, *13*, 971836.

Massalha, H., Korenblum, E., Tholl, D., & Aharoni, A. (2017). Small molecules below-ground: the role of specialized metabolites in the rhizosphere. *The Plant Journal*, *90*(4), 788-807.

Matthews, A., Pierce, S., Hipperson, H., & Raymond, B. (2019). Rhizobacterial community assembly patterns vary between crop species. *Frontiers in microbiology*, *10*, 581.

Mavrodi, D. V., Mavrodi, O. V., Elbourne, L. D., Tetu, S., Bonsall, R. F., Parejko, J., ... & Thomashow, L. S. (2018). Long-term irrigation affects the dynamics and activity of the wheat rhizosphere microbiome. *Frontiers in Plant Science*, *9*, 345.

Meena, R. S., Vijayakumar, V., Yadav, G. S., & Mitran, T. (2018). Response and interaction of Bradyrhizobium japonicum and arbuscular mycorrhizal fungi in the soybean rhizosphere. *Plant Growth Regulation*, *84*, 207-223.

Mehlich, A. (1984). Mehlich 3 soil test extractant: A modification of Mehlich 2 extractant. *Communications in soil science and plant analysis*, *15*(12), 1409-1416.

Meier, I. C., & Leuschner, C. (2010). Variation of soil and biomass carbon pools in beech forests across a precipitation gradient. *Global Change Biology*, *16*(3), 1035-1045.

Mercado-Blanco, J., Abrantes, I., Barra Caracciolo, A., Bevivino, A., Ciancio, A., Grenni, P., ... & Proença, D. N. (2018). Belowground microbiota and the health of tree crops. *Frontiers in Microbiology*, *9*, 1006.

Mhlongo, M. I., Piater, L. A., Madala, N. E., Labuschagne, N., & Dubery, I. A. (2018). The chemistry of plant–microbe interactions in the rhizosphere and the potential for metabolomics to reveal signaling related to defense priming and induced systemic resistance. *Frontiers in plant science*, *9*, 112.

Mhlongo, M. I., Piater, L. A., Steenkamp, P. A., Labuschagne, N., & Dubery, I. A. (2020). Metabolic profiling of PGPR-treated tomato plants reveal priming-related adaptations of secondary metabolites and aromatic amino acids. *Metabolites*, *10*(5), 210.

Mielke Jr, P. W. (1991). The application of multivariate permutation methods based on distance functions in the earth sciences. *Earth-Science Reviews*, *31*(1), 55-71.

Miller, S. B., Heuberger, A. L., Broeckling, C. D., & Jahn, C. E. (2019). Non-targeted metabolomics reveals sorghum rhizosphere-associated exudates are influenced by the belowground interaction of substrate and sorghum genotype. *International Journal of Molecular Sciences*, *20*(2), 431.

Minchin, P. R. (1987). An evaluation of the relative robustness of techniques for ecological ordination. In *Theory and models in vegetation science: Proceedings of Symposium, Uppsala, July 8–13, 1985* (pp. 89-107). Springer Netherlands.

Mishra, A., Singh, L., & Singh, D. (2022). Unboxing the black box—one step forward to understand the soil microbiome: a systematic review. *Microbial ecology*, *85*(2), 669-683.

Mistry, J., Chuguransky, S., Williams, L., Qureshi, M., Salazar, G. A., Sonnhammer, E. L., ... & Bateman, A. (2021). Pfam: The protein families database in 2021. *Nucleic acids research*, *49*(D1), D412-D419.

Mohanram, S., & Kumar, P. (2019). Rhizosphere microbiome: revisiting the synergy of plant-microbe interactions. *Annals of Microbiology*, *69*, 307-320.

Moore-Kucera, J., & Dick, R. P. (2008). PLFA profiling of microbial community structure and seasonal shifts in soils of a Douglas-fir chronosequence. *Microbial ecology*, *55*, 500-511.

Morales-Rodríguez, C., Martín-García, J., Ruiz-Gómez, F. J., Poveda, J., & Diez, J. J. (2024). Relationships between rhizosphere microbiota and forest health conditions in Pinus pinaster stands at the Iberian Peninsula. *Applied Soil Ecology*, *193*, 105142.

Morvan, S., Meglouli, H., Lounès-Hadj Sahraoui, A., & Hijri, M. (2020). Into the wild blueberry (Vaccinium angustifolium) rhizosphere microbiota. *Environmental Microbiology*, *22*(9), 3803-3822.

Mus, F., Crook, M. B., Garcia, K., Garcia Costas, A., Geddes, B. A., Kouri, E. D., ... & Peters, J. W. (2016). Symbiotic nitrogen fixation and the challenges to its extension to nonlegumes. *Applied and environmental microbiology*, *82*(13), 3698-3710.

Nelson, D. W., & Sommers, L. E. (1982). Total carbon, organic carbon, and organic matter. *Methods of soil analysis: Part 2 chemical and microbiological properties*, *9*, 539-579.

Ng, E. L., Patti, A. F., Rose, M. T., Schefe, C. R., Wilkinson, K., Smernik, R. J., & Cavagnaro, T. R. (2014). Does the chemical nature of soil carbon drive the structure and functioning of soil microbial communities?. *Soil Biology and Biochemistry*, *70*, 54-61.

Nguyen, N. H., Song, Z., Bates, S. T., Branco, S., Tedersoo, L., Menke, J., ... & Kennedy, P. G. (2016). FUNGuild: an open annotation tool for parsing fungal community datasets by ecological guild. *Fungal ecology*, *20*, 241-248.

Nielsen, U. N., & Ball, B. A. (2015). Impacts of altered precipitation regimes on soil communities and biogeochemistry in arid and semi-arid ecosystems. *Global change biology*, *21*(4), 1407-1421.

Nilsson, R. H., Larsson, K. H., Taylor, A. F. S., Bengtsson-Palme, J., Jeppesen, T. S., Schigel, D., ... & Abarenkov, K. (2019). The UNITE database for molecular identification of fungi: handling dark taxa and parallel taxonomic classifications. *Nucleic acids research*, *47*(D1), D259-D264.

O'Brien, H. E., Parrent, J. L., Jackson, J. A., Moncalvo, J. M., & Vilgalys, R. (2005). Fungal community analysis by large-scale sequencing of environmental samples. *Applied and environmental microbiology*, *71*(9), 5544-5550.

O'Brien, S. L., Jastrow, J. D., Grimley, D. A., & Gonzalez-Meler, M. A. (2010). Moisture and vegetation controls on decadal-scale accrual of soil organic carbon and total nitrogen in restored grasslands. *Global Change Biology*, *16*(9), 2573-2588.

Ohm, R. A., Feau, N., Henrissat, B., Schoch, C. L., Horwitz, B. A., Barry, K. W., ... & Grigoriev, I. V. (2012). Diverse lifestyles and strategies of plant pathogenesis encoded in the genomes of eighteen Dothideomycetes fungi. *PLoS pathogens*, *8*(12), e1003037.

Oksanen, J. (2010). Vegan: community ecology package. *http://vegan. r-forge. r-project. org/*.

Ostertag, R., Marín-Spiotta, E., Silver, W. L., & Schulten, J. (2008). Litterfall and decomposition in relation to soil carbon pools along a secondary forest chronosequence in Puerto Rico. *Ecosystems*, *11*, 701-714.

Pan, Y., Birdsey, R. A., Fang, J., Houghton, R., Kauppi, P. E., Kurz, W. A., ... & Hayes, D. (2011). A large and persistent carbon sink in the world's forests. *science*, *333*(6045), 988-993.

Paquette, A., & Messier, C. (2011). The effect of biodiversity on tree productivity: from temperate to boreal forests. *Global Ecology and Biogeography*, *20*(1), 170-180.

Parada, A. E., Needham, D. M., & Fuhrman, J. A. (2016). Every base matters: assessing small subunit rRNA primers for marine microbiomes with mock communities, time series and global field samples. *Environmental microbiology*, *18*(5), 1403-1414.

Park, I., Seo, Y. S., & Mannaa, M. (2023). Recruitment of the rhizo-microbiome army: assembly determinants and engineering of the rhizosphere microbiome as a key to unlocking plant potential. *Frontiers in Microbiology*, *14*, 1163832.

Patel, K. F., Fansler, S. J., Campbell, T. P., Bond-Lamberty, B., Smith, A. P., RoyChowdhury, T., ... & Bailey, V. L. (2021). Soil texture and environmental conditions influence the biogeochemical responses of soils to drought and flooding. *Communications Earth & Environment*, *2*(1), 127.

Patti, G. J., Yanes, O., & Siuzdak, G. (2012). Metabolomics: the apogee of the omics trilogy. *Nature reviews Molecular cell biology*, *13*(4), 263-269.

Paulson, J. N., Pop, M., & Bravo, H. C. (2011). Metastats: an improved statistical method for analysis of metagenomic data. *Genome Biology*, *12*, 1-27.

Pent, M., Põldmaa, K., & Bahram, M. (2017). Bacterial communities in boreal forest mushrooms are shaped both by soil parameters and host identity. *Frontiers in microbiology*, *8*, 836.

Peñuelas, J., & Sardans, J. (2009). Ecological metabolomics. *Chemistry and Ecology*, *25*(4), 305-309.

Peres-Neto, P. R., Legendre, P., Dray, S., & Borcard, D. (2006). Variation partitioning of species data matrices: estimation and comparison of fractions. *Ecology*, *87*(10), 2614-2625.

Pétriacq, P., Williams, A., Cotton, A., McFarlane, A. E., Rolfe, S. A., & Ton, J. (2017). Metabolite profiling of non-sterile rhizosphere soil. *The Plant Journal*, *92*(1), 147-162.

Philippot, L., Raaijmakers, J. M., Lemanceau, P., & Van Der Putten, W. H. (2013). Going back to the roots: the microbial ecology of the rhizosphere. *Nature reviews microbiology*, *11*(11), 789-799.

Pielou, E. C. (1966). The measurement of diversity in different types of biological collections. *Journal of theoretical biology*, *13*, 131-144.

Poisot, T., Stouffer, D. B., & Kéfi, S. (2016). Describe, understand and predict. *Functional Ecology*, *30*(12), 1878-1882.

Quast, C., Pruesse, E., Yilmaz, P., Gerken, J., Schweer, T., Yarza, P., ... & Glöckner, F. O. (2012). The SILVA ribosomal RNA gene database project: improved data processing and web-based tools. *Nucleic acids research*, *41*(D1), D590-D596.

Quince, C., Walker, A. W., Simpson, J. T., Loman, N. J., & Segata, N. (2017). Shotgun metagenomics, from sampling to analysis. *Nature biotechnology*, *35*(9), 833-844.

R Core Team. (2013). R: A language and environment for statistical computing. *Foundation for Statistical Computing, Vienna, Austria*.

Raiesi, F. (2006). Carbon and N mineralization as affected by soil cultivation and crop residue in a calcareous wetland ecosystem in Central Iran. *Agriculture, ecosystems & environment*, *112*(1), 13-20.

Rajaniemi, T. K. (2003). Explaining productivity-diversity relationships in plants. *Oikos*, *101*(3), 449-457.

Raynaud, X., & Nunan, N. (2014). Spatial ecology of bacteria at the microscale in soil. *PloS one*, *9*(1), e87217.

Rellstab, C., Gugerli, F., Eckert, A. J., Hancock, A. M., & Holderegger, R. (2015). A practical guide to environmental association analysis in landscape genomics. *Molecular ecology*, *24*(17), 4348-4370.

Ren, H., Wang, H., Qi, X., Yu, Z., Zheng, X., Zhang, S., ... & Li, B. (2021). The damage caused by decline disease in bayberry plants through changes in soil properties, rhizosphere microbial community structure and metabolites. *Plants*, *10*(10), 2083.

Riedl, J., Kluender, C., Sans-Piché, F., Heilmeier, H., Altenburger, R., & Schmitt-Jansen, M. (2012). Spatial and temporal variation in metabolic fingerprints of field-growing Myriophyllum spicatum. *Aquatic botany*, *102*, 34-43.

Rivas-Ubach, A., Pérez-Trujillo, M., Sardans, J., Gargallo-Garriga, A., Parella, T., & Penuelas, J. (2013). Ecometabolomics: optimized NMR-based method. *Methods in Ecology and Evolution*, *4*(5), 464-473.

Rochfort, S., Ezernieks, V., Mele, P., & Kitching, M. (2015). NMR metabolomics for soil analysis provide complementary, orthogonal data to MIR and traditional soil chemistry approaches–a land use study. *Magnetic Resonance in Chemistry*, *53*(9), 719-725.

Roesch, L. F., Fulthorpe, R. R., Riva, A., Casella, G., Hadwin, A. K., Kent, A. D., ... & Triplett, E. W. (2007). Pyrosequencing enumerates and contrasts soil microbial diversity. *The ISME journal*, *1*(4), 283-290.

Rognes, T., Flouri, T., Nichols, B., Quince, C., & Mahé, F. (2016). VSEARCH: a versatile open source tool for metagenomics. *PeerJ*, *4*, e2584.

Romaní, A. M., Fischer, H., Mille-Lindblom, C., & Tranvik, L. J. (2006). Interactions of bacteria and fungi on decomposing litter: differential extracellular enzyme activities. *Ecology*, *87*(10), 2559–2569.

Röttjers, L., & Faust, K. (2018). From hairballs to hypotheses–biological insights from microbial networks. *FEMS microbiology reviews*, *42*(6), 761-780.

Rousk, J., Bååth, E., Brookes, P. C., Lauber, C. L., Lozupone, C., Caporaso, J. G., ... & Fierer, N. (2010). Soil bacterial and fungal communities across a pH gradient in an arable soil. *The ISME journal*, *4*(10), 1340-1351.

Saetre, P., & Bååth, E. (2000). Spatial variation and patterns of soil microbial community structure in a mixed spruce–birch stand. *Soil Biology and Biochemistry*, *32*(7), 909-917.

Sanders, H. L. (1968). Marine benthic diversity: a comparative study. *The American Naturalist*, *102*(925), 243-282.

Sardans, J., Peñuelas, J., & Rivas-Ubach, A. (2011). Ecological metabolomics: overview of current developments and future challenges. *Chemoecology*, *21*, 191-225.

Sayer, E. J., Wagner, M., Oliver, A. E., Pywell, R. F., James, P., Whiteley, A. S., & Heard, M. S. (2013). Grassland management influences spatial patterns of soil microbial communities. *Soil Biology and Biochemistry*, *61*, 61-68.

Schimel, J. (2016). Microbial ecology: Linking omics to biogeochemistry. *Nature microbiology*, *1*(2), 1-2.

Schimel, J. P. (2018). Life in dry soils: effects of drought on soil microbial communities and processes. *Annual review of ecology, evolution, and systematics*, *49*(1), 409-432.

Schimel, J., Balser, T. C., & Wallenstein, M. (2007). Microbial stress-response physiology and its implications for ecosystem function. *Ecology*, *88*(6), 1386-1394.

Schoch, C. L., Seifert, K. A., Huhndorf, S., Robert, V., Spouge, J. L., Levesque, C. A., ... & White, M. M. (2012). Nuclear ribosomal internal transcribed spacer (ITS) region as a universal DNA barcode marker for Fungi. *Proceedings of the national academy of Sciences*, *109*(16), 6241-6246.

Schreiter, S., Ding, G. C., Heuer, H., Neumann, G., Sandmann, M., Grosch, R., ... & Smalla, K. (2014). Effect of the soil type on the microbiome in the rhizosphere of field-grown lettuce. *Frontiers in microbiology*, *5*, 144.

Segata, N., Izard, J., Waldron, L., Gevers, D., Miropolsky, L., Garrett, W. S., & Huttenhower, C. (2011). Metagenomic biomarker discovery and explanation. *Genome biology*, *12*, 1-18.

Seppälä, R. (2009). A global assessment on adaptation of forests to climate change. *Scandinavian Journal of Forest Research*, *24*(6), 469-472.

Shang, Y. (2014). Unveiling robustness and heterogeneity through percolation triggered by random-link breakdown. *Physical Review E*, *90*(3), 032820.

Shannon, C. E. (1948). A mathematical theory of communication. *The Bell system technical journal*, *27*(3), 379-423.

Sharma, P. (2015). Bio fungicides: their role in plant disease management. In *WINTER SCHOOL* (p. 113).

Sheik, C. S., Mitchell, T. W., Rizvi, F. Z., Rehman, Y., Faisal, M., Hasnain, S., ... & Krumholz, L. R. (2012). Exposure of soil microbial communities to chromium and arsenic alters their diversity and structure. *PloS one*, *7*(6), e40059.

Shi, S., Nuccio, E., Herman, D. J., Rijkers, R., Estera, K., Li, J., ... & Firestone, M. (2015). Successional trajectories of rhizosphere bacterial communities over consecutive seasons. *MBio*, *6*(4), 10-1128.

Shi, S., Richardson, A. E., O'Callaghan, M., DeAngelis, K. M., Jones, E. E., Stewart, A., ... & Condron, L. M. (2011). Effects of selected root exudate components on soil bacterial communities. *FEMS microbiology ecology*, *77*(3), 600-610.

Shulaev, V., Cortes, D., Miller, G., & Mittler, R. (2008). Metabolomics for plant stress response. *Physiologia plantarum*, *132*(2), 199-208.

Silver, W. L., Neff, J., McGroddy, M., Veldkamp, E., Keller, M., & Cosme, R. (2000). Effects of soil texture on belowground carbon and nutrient storage in a lowland Amazonian forest ecosystem. *Ecosystems*, *3*, 193-209.

Simpson, E. H. (1949). Measurement of Diversity. *Nature*, *163*.

Sinclair, L., Osman, O. A., Bertilsson, S., & Eiler, A. (2015). Microbial community composition and diversity via 16S rRNA gene amplicons: evaluating the illumina platform. *PloS one*, *10*(2), e0116955.

Singh, B. K., Bardgett, R. D., Smith, P., & Reay, D. S. (2010). Microorganisms and climate change: terrestrial feedbacks and mitigation options. *Nature Reviews Microbiology*, *8*(11), 779-790.

Sinsabaugh, R. L. (2010). Phenol oxidase, peroxidase and organic matter dynamics of soil. *Soil Biology and Biochemistry*, *42*(3), 391-404.

Sinsabaugh, R. L., Antibus, R. K., & Linkins, A. E. (1991). An enzymic approach to the analysis of microbial activity during plant litter decomposition. *Agriculture, Ecosystems & Environment*, *34*(1-4), 43-54.

Sinsabaugh, R. L., Lauber, C. L., Weintraub, M. N., Ahmed, B., Allison, S. D., Crenshaw, C., ... & Zeglin, L. H. (2008). Stoichiometry of soil enzyme activity at global scale. *Ecology letters*, *11*(11), 1252-1264.

Six, J. A. E. T., Elliott, E. T., & Paustian, K. (2000). Soil macroaggregate turnover and microaggregate formation: a mechanism for C sequestration under no-tillage agriculture. *Soil Biology and Biochemistry*, *32*(14), 2099-2103.

Six, J., Conant, R. T., Paul, E. A., & Paustian, K. (2002). Stabilization mechanisms of soil organic matter: implications for C-saturation of soils. *Plant and soil*, *241*, 155-176.

Slessarev, E. W., Lin, Y., Bingham, N. L., Johnson, J. E., Dai, Y., Schimel, J. P., & Chadwick, O. A. (2016). Water balance creates a threshold in soil pH at the global scale. *Nature*, *540*(7634), 567-569.

Smalla, K., Wieland, G., Buchner, A., Zock, A., Parzy, J., Kaiser, S., ... & Berg, G. (2001). Bulk and rhizosphere soil bacterial communities studied by denaturing gradient gel electrophoresis: plant-dependent enrichment and seasonal shifts revealed. *Applied and environmental microbiology*, *67*(10), 4742-4751.

Šnajdr, J., Valášková, V., Merhautová, V., Herinková, J., Cajthaml, T., & Baldrian, P. (2008). Spatial variability of enzyme activities and microbial biomass in the upper layers of Quercus petraea forest soil. *Soil Biology and Biochemistry*, *40*(9), 2068-2075.

Sokal, R. R., & Michener, C. D. (1958). A statistical method for evaluating systematic relationships.

Song, Y., Li, X., Yao, S., Yang, X., & Jiang, X. (2020). Correlations between soil metabolomics and bacterial community structures in the pepper rhizosphere under plastic greenhouse cultivation. *Science of the Total Environment*, *728*, 138439.

Song, Y., Yao, S., Li, X., Wang, T., Jiang, X., Bolan, N., ... & Chang, S. X. (2024). Soil metabolomics: Deciphering underground metabolic webs in terrestrial ecosystems. *Eco-Environment & Health*.

Sorensen, P. O., Germino, M. J., & Feris, K. P. (2013). Microbial community responses to 17 years of altered precipitation are seasonally dependent and coupled to co-varying effects of water content on vegetation and soil C. *Soil Biology and Biochemistry*, *64*, 155-163.

Spearman, C. (1904). The proof and measurement of association between two things. *The American Journal of Psychology, 15*(1), 72–101.

Sridhar, B., Lawrence, G. B., Debenport, S. J., Fahey, T. J., Buckley, D. H., Wilhelm, R. C., & Goodale, C. L. (2022). Watershed-scale liming reveals the short-and long-term effects of pH on the forest soil microbiome and carbon cycling. *Environmental Microbiology*, *24*(12), 6184-6199.

Stat, M., Pochon, X., Franklin, E. C., Bruno, J. F., Casey, K. S., Selig, E. R., & Gates, R. D. (2013). The distribution of the thermally tolerant symbiont lineage (S ymbiodinium clade D) in corals from H awaii: Correlations with host and the history of ocean thermal stress. *Ecology and evolution*, *3*(5), 1317-1329.

Stella, T., Covino, S., Burianová, E., Filipová, A., Křesinová, Z., Voříšková, J., ... & Cajthaml, T. (2015). Chemical and microbiological characterization of an aged PCB-contaminated soil. *Science of the Total Environment*, *533*, 177-186.

Stocker, T. (Ed.). (2014). *Climate change 2013: the physical science basis: Working Group I contribution to the Fifth assessment report of the Intergovernmental Panel on Climate Change*. Cambridge university press.

Štraus, D., Redondo, M. Á., Castaño, C., Juhanson, J., Clemmensen, K. E., Hallin, S., & Oliva, J. (2024). Plant–soil feedbacks among boreal forest species. *Journal of Ecology*, *112*(1), 138-151.

Strehmel, N., Böttcher, C., Schmidt, S., & Scheel, D. (2014). Profiling of secondary metabolites in root exudates of Arabidopsis thaliana. *Phytochemistry*, *108*, 35-46.

Štursová, M., Bárta, J., Šantrůčková, H., & Baldrian, P. (2016). Small-scale spatial heterogeneity of ecosystem properties, microbial community composition and microbial activities in a temperate mountain forest soil. *FEMS Microbiology Ecology*, *92*(12), fiw185.

Su, X., Su, X., Yang, S., Zhou, G., Ni, M., Wang, C., ... & Deng, J. (2020). Drought changed soil organic carbon composition and bacterial carbon metabolizing patterns in a subtropical evergreen forest. *Science of the Total Environment*, *736*, 139568.

Suseela, V., & Dukes, J. S. (2013). The responses of soil and rhizosphere respiration to simulated climatic changes vary by season. *Ecology*, *94*(2), 403-413.

Swenson, T. L., & Northen, T. R. (2019). *Untargeted soil metabolomics using liquid chromatography–mass spectrometry and gas chromatography–mass spectrometry* (pp. 97-109). Springer New York.

Swenson, T. L., Jenkins, S., Bowen, B. P., & Northen, T. R. (2015). Untargeted soil metabolomics methods for analysis of extractable organic matter. *Soil Biology and Biochemistry*, *80*, 189-198.

Taguchi, Y. H., & Oono, Y. (2005). Relational patterns of gene expression via non-metric multidimensional scaling analysis. *Bioinformatics*, *21*(6), 730-740.

Tautenhahn, R., Cho, K., Uritboonthai, W., Zhu, Z., Patti, G. J., & Siuzdak, G. (2012). An accelerated workflow for untargeted metabolomics using the METLIN database. *Nature biotechnology*, *30*(9), 826-828.

Tedersoo, L., Bahram, M., Põlme, S., Kõljalg, U., Yorou, N. S., Wijesundera, R., ... & Abarenkov, K. (2014). Global diversity and geography of soil fungi. *science*, *346*(6213), 1256688.

Ter Braak, C. J. (1986). Canonical correspondence analysis: a new eigenvector technique for multivariate direct gradient analysis. *Ecology*, *67*(5), 1167-1179.

Tiemann, L. K., & Billings, S. A. (2011). Changes in variability of soil moisture alter microbial community C and N resource use. *Soil Biology and Biochemistry*, *43*(9), 1837-1847.

Toole, D. R., Zhao, J., Martens-Habbena, W., & Strauss, S. L. (2021). Bacterial functional prediction tools detect but underestimate metabolic diversity compared to shotgun metagenomics in southwest Florida soils. *Applied Soil Ecology*, *168*, 104129.

Torsvik, V., & Øvreås, L. (2002). Microbial diversity and function in soil: from genes to ecosystems. *Current opinion in microbiology*, *5*(3), 240-245.

Torsvik, V., Goksøyr, J., & Daae, F. L. (1990). High diversity in DNA of soil bacteria. *Applied and environmental microbiology*, *56*(3), 782-787.

Treseder, K. K., Marusenko, Y., Romero-Olivares, A. L., & Maltz, M. R. (2016). Experimental warming alters potential function of the fungal community in boreal forest. *Global change biology*, *22*(10), 3395-3404.

Trivedi, P., Leach, J. E., Tringe, S. G., Sa, T., & Singh, B. K. (2020). Plant–microbiome interactions: from community assembly to plant health. *Nature reviews microbiology*, *18*(11), 607-621.

Turner, T. R., James, E. K., & Poole, P. S. (2013). The plant microbiome. *Genome biology*, *14*, 1-10.

Uroz, S., Ioannidis, P., Lengelle, J., Cébron, A., Morin, E., Buée, M., & Martin, F. (2013). Functional assays and metagenomic analyses reveals differences between the microbial communities inhabiting the soil horizons of a Norway spruce plantation. *PloS one*, *8*(2), e55929.

Uroz, S., Oger, P., Tisserand, E., Cébron, A., Turpault, M. P., Buée, M., ... & Frey-Klett, P. (2016). Specific impacts of beech and Norway spruce on the structure and diversity of the rhizosphere and soil microbial communities. *Scientific reports*, *6*(1), 27756.

Van Hees, P. A., Jones, D. L., Finlay, R., Godbold, D. L., & Lundström, U. S. (2005). The carbon we do not see—the impact of low molecular weight compounds on carbon dynamics and respiration in forest soils: a review. *Soil Biology and Biochemistry*, *37*(1), 1-13.

Veneklaas, E. J., Stevens, J., Cawthray, G. R., Turner, S., Grigg, A. M., & Lambers, H. (2003). Chickpea and white lupin rhizosphere carboxylates vary with soil properties and enhance phosphorus uptake. *Plant and Soil*, *248*, 187-197.

Vepsäläinen, M., Kukkonen, S., Vestberg, M., Sirviö, H., & Niemi, R. M. (2001). Application of soil enzyme activity test kit in a field experiment. *Soil Biology and Biochemistry*, *33*(12-13), 1665-1672.

Vereecken, H., Maes, J., Feyen, J., & Darius, P. (1989). Estimating the soil moisture retention characteristic from texture, bulk density, and carbon content. *Soil science*, *148*(6), 389-403.

Viant, M. R. (2008). Recent developments in environmental metabolomics. *Molecular Biosystems*, *4*(10), 980-986.

Vinayavekhin, N., & Saghatelian, A. (2010). Untargeted metabolomics. *Current protocols in molecular biology*, *90*(1), 30-1.

Wagai, R., Kitayama, K., Satomura, T., Fujinuma, R., & Balser, T. (2011). Interactive influences of climate and parent material on soil microbial community structure in Bornean tropical forest ecosystems. *Ecological Research*, *26*, 627-636.

Walters, W. A., Jin, Z., Youngblut, N., Wallace, J. G., Sutter, J., Zhang, W., ... & Ley, R. E. (2018). Large-scale replicated field study of maize rhizosphere identifies heritable microbes. *Proceedings of the National Academy of Sciences*, *115*(28), 7368-7373.

Wang, B., Chen, Y., Li, Y., Zhang, H., Yue, K., Wang, X., ... & Wu, Q. (2021). Differential effects of altered precipitation regimes on soil carbon cycles in arid versus humid terrestrial ecosystems. *Global change biology*, *27*(24), 6348-6362.

Wang, J., Zhang, J., Wang, C., Ren, G., Yang, Y., & Wang, D. (2021). Precipitation exerts a strong influence on arbuscular mycorrhizal fungi community and network complexity in a semiarid steppe ecosystem. *European Journal of Soil Biology*, *102*, 103268.

Wang, Q., Garrity, G. M., Tiedje, J. M., & Cole, J. R. (2007). Naive Bayesian classifier for rapid assignment of rRNA sequences into the new bacterial taxonomy. *Applied and environmental microbiology*, *73*(16), 5261-5267.

Wang, W., Wang, H., Feng, Y., Wang, L., Xiao, X., Xi, Y., ... & Cui, Z. (2016). Consistent responses of the microbial community structure to organic farming along the middle and lower reaches of the Yangtze River. *Scientific Reports*, *6*(1), 35046.

Wang, X. Q., Zhang, X. C., Pei, X. J., & Ren, G. F. (2022). Effect of the particle size composition and dry density on the water retention characteristics of remolded loess. *Minerals*, *12*(6), 698.

Wang, Y. L., Gao, C., Chen, L., Ji, N. N., Wu, B. W., Li, X. C., ... & Guo, L. D. (2019). Host plant phylogeny and geographic distance strongly structure Betulaceae-associated ectomycorrhizal fungal communities in Chinese secondary forest ecosystems. *FEMS Microbiology Ecology*, *95*(4), fiz037.

Wang, Y., & Qian, P. Y. (2009). Conservative fragments in bacterial 16S rRNA genes and primer design for 16S ribosomal DNA amplicons in metagenomic studies. *PloS one*, *4*(10), e7401.

Warmink, J. A., Nazir, R., & Van Elsas, J. D. (2009). Universal and species-specific bacterial 'fungiphiles' in the mycospheres of different basidiomycetous fungi. *Environmental Microbiology*, *11*(2), 300-312.

Watts, D. J., & Strogatz, S. H. (1998). Collective dynamics of 'small-world'networks. *nature*, *393*(6684), 440-442.

Wentworth, C. K. (1922). A scale of grade and class terms for clastic sediments. *The journal of geology*, *30*(5), 377-392.

White, J. R., Nagarajan, N., & Pop, M. (2009). Statistical methods for detecting differentially abundant features in clinical metagenomic samples. *PLoS computational biology*, *5*(4), e1000352.

White, R. A. III., Rivas-Ubach, A., Borkum, M. I., Köberl, M., Bilbao, A., Colby, S. M., Hoyt, D. W., Bingol, K., Kim, Y.-M., Wendler, J. P., Hixson, K. K., & Jansson, C. (2017). The state of rhizospheric science in the era of multi-omics: a practical guide to omics technologies. *Rhizosphere*, 3(2), 212-221.

White, T. J., Bruns, T., Lee, S. J. W. T., & Taylor, J. (1990). Amplification and direct sequencing of fungal ribosomal RNA genes for phylogenetics. *PCR protocols: a guide to methods and applications*, *18*(1), 315-322.

Williams, M. A., & Rice, C. W. (2007). Seven years of enhanced water availability influences the physiological, structural, and functional attributes of a soil microbial community. *Applied Soil Ecology*, *35*(3), 535-545.

Withers, E., Hill, P. W., Chadwick, D. R., & Jones, D. L. (2020). Use of untargeted metabolomics for assessing soil quality and microbial function. *Soil Biology and Biochemistry*, *143*, 107758.

Wu, K., Xu, W., & Yang, W. (2020). Effects of precipitation changes on soil bacterial community composition and diversity in the Junggar desert of Xinjiang, China. *PeerJ*, *8*, e8433.

Wu, X., Rensing, C., Han, D., Xiao, K. Q., Dai, Y., Tang, Z., ... & Zhang, F. (2022). Genome-resolved metagenomics reveals distinct phosphorus acquisition strategies between soil microbiomes. *Msystems*, *7*(1), e01107-21.

Wu, Z., Dijkstra, P., Koch, G. W., Peñuelas, J., & Hungate, B. A. (2011). Responses of terrestrial ecosystems to temperature and precipitation change: A meta-analysis of experimental manipulation. *Global change biology*, *17*(2), 927-942.

Xia, Y., & Sun, J. (2023). *Bioinformatic and statistical analysis of microbiome data: from raw sequences to advanced modeling with QIIME 2 and R*. Springer Nature.

Xiao, W., Chen, X., Jing, X., & Zhu, B. (2018). A meta-analysis of soil extracellular enzyme activities in response to global change. *Soil Biology and Biochemistry*, *123*, 21-32.

Xu, G., Chen, J., Berninger, F., Pumpanen, J., Bai, J., Yu, L., & Duan, B. (2015). Labile, recalcitrant, microbial carbon and nitrogen and the microbial community composition at two Abies faxoniana forest elevations under elevated temperatures. *Soil Biology and Biochemistry*, *91*, 1-13.

Xu, J., Zhang, Y., Zhang, P., Trivedi, P., Riera, N., Wang, Y., ... & Wang, N. (2018). The structure and function of the global citrus rhizosphere microbiome. *Nature communications*, *9*(1), 4894.

Xu, M., Li, X., Kuyper, T. W., Xu, M., Li, X., & Zhang, J. (2021). High microbial diversity stabilizes the responses of soil organic carbon decomposition to warming in the subsoil on the Tibetan Plateau. *Global Change Biology*, *27*(10), 2061-2075.

Xu, Z., Zhang, T., Wang, S., & Wang, Z. (2020). Soil pH and C/N ratio determines spatial variations in soil microbial communities and enzymatic activities of the agricultural ecosystems in Northeast China: Jilin Province case. *Applied Soil Ecology*, *155*, 103629.

Yan, L., Chen, S., Huang, J., & Lin, G. (2011). Water regulated effects of photosynthetic substrate supply on soil respiration in a semiarid steppe. *Global Change Biology*, *17*(5), 1990-2001.

Yan, Y., Kuramae, E. E., de Hollander, M., Klinkhamer, P. G., & van Veen, J. A. (2017). Functional traits dominate the diversity-related selection of bacterial communities in the rhizosphere. *The ISME journal*, *11*(1), 56-66.

Yang, S. L., Zhang, J., & Xu, X. J. (2007). Influence of the Three Gorges Dam on downstream delivery of sediment and its environmental implications, Yangtze River. *Geophysical Research Letters*, *34*(10).

Yang, S., Xu, Z., Wang, R., Zhang, Y., Yao, F., Zhang, Y., ... & Li, H. (2017). Variations in soil microbial community composition and enzymatic activities in response to increased N deposition and precipitation in Inner Mongolian grassland. *Applied soil ecology*, *119*, 275-285.

Yang, X., Zhu, K., Loik, M. E., & Sun, W. (2021). Differential responses of soil bacteria and fungi to altered precipitation in a meadow steppe. *Geoderma*, *384*, 114812.

Yao, H., Chapman, S. J., Thornton, B., & Paterson, E. (2015). 13 C PLFAs: a key to open the soil microbial black box?. *Plant and Soil*, *392*, 3-15.

Yu, Z., Yang, J., Yu, X., Liu, L., & Tian, Y. (2014). Aboveground vegetation influences belowground microeukaryotic community in a mangrove nature reserve. *Wetlands*, *34*, 393-401.

Zádrapová, D., Chakraborty, A., Žáček, P., Korecký, J., Bhar, A., & Roy, A. (2024). Exploring the Rhizospheric Microbial Communities under Long-Term Precipitation Regime in Norway Spruce Seed Orchard. *International Journal of Molecular Sciences*, *25*(17), 9658.

Zak, D. R., Pregitzer, K. S., Curtis, P. S., Teeri, J. A., Fogel, R., & Randlett, D. L. (1993). Elevated atmospheric CO 2 and feedback between carbon and nitrogen cycles. *Plant and soil*, *151*, 105-117.

Zak, D. R., Tilman, D., Parmenter, R. R., Rice, C. W., Fisher, F. M., Vose, J., ... & Martin, C. W. (1994). Plant production and soil microorganisms in late-successional ecosystems: A continental-scale study. *Ecology*, *75*(8), 2333-2347.

Zbíral, J. (2016). Determination of plant-available micronutrients by the Mehlich 3 soil extractant-a proposal of critical values.

Zeglin, L. H., Bottomley, P. J., Jumpponen, A., Rice, C. W., Arango, M., Lindsley, A., ... & Myrold, D. D. (2013). Altered precipitation regime affects the function and composition of soil microbial communities on multiple time scales. *Ecology*, *94*(10), 2334-2345.

Zeki, Ö. C., Eylem, C. C., Reçber, T., Kır, S., & Nemutlu, E. (2020). Integration of GC–MS and LC–MS for untargeted metabolomics profiling. *Journal of Pharmaceutical and Biomedical Analysis*, *190*, 113509.

Zelles, L. (1999). Fatty acid patterns of phospholipids and lipopolysaccharides in the characterisation of microbial communities in soil: a review. *Biology and fertility of soils*, *29*, 111-129.

Zhang, B., Wu, X., Tai, X., Sun, L., Wu, M., Zhang, W., ... & Dyson, P. (2019). Variation in actinobacterial community composition and potential function in different soil ecosystems belonging to the arid Heihe River Basin of Northwest China. *Frontiers in microbiology*, *10*, 2209.

Zhang, H., Liu, H., Zhao, J., Wang, L., Li, G., Huangfu, C., ... & Yang, D. (2017). Elevated precipitation modifies the relationship between plant diversity and soil bacterial diversity under nitrogen deposition in Stipa baicalensis steppe. *Applied Soil Ecology*, *119*, 345-353.

Zhang, X., Gao, G., Wu, Z., Wen, X., Zhong, H., Zhong, Z., ... & Gai, X. (2019). Agroforestry alters the rhizosphere soil bacterial and fungal communities of moso bamboo plantations in subtropical China. *Applied Soil Ecology*, *143*, 192-200.

Zhang, Y. Y., Wu, W., & Liu, H. (2019). Factors affecting variations of soil pH in different horizons in hilly regions. *Plos one*, *14*(6), e0218563.

Zhang, Y., Zheng, N., Wang, J., Yao, H., Qiu, Q., & Chapman, S. J. (2019). High turnover rate of free phospholipids in soil confirms the classic hypothesis of PLFA methodology. *Soil Biology and Biochemistry*, *135*, 323-330.

Zhao, Y., Yao, Y., Xu, H., Xie, Z., Guo, J., Qi, Z., & Jiang, H. (2022). Soil metabolomics and bacterial functional traits revealed the responses of rhizosphere soil bacterial community to long-term continuous cropping of Tibetan barley. PeerJ, 10, e13254.

Zheng, H., Liu, Y., Chen, Y., Zhang, J., Li, H., Wang, L., & Chen, Q. (2020). Short-term warming shifts microbial nutrient limitation without changing the bacterial community structure in an alpine timberline of the eastern Tibetan Plateau. *Geoderma*, *360*, 113985.

Zhou, C. Y., Zhou, G. Y., Zhang, D. Q., Wang, Y., & Liu, S. (2005). CO2 efflux from different forest soils and impact factors in Dinghu Mountain, China. *Sci. China Ser. D*, *48*, 198-206.

Zhou, G., Guan, L., Wei, X., Tang, X., Liu, S., Liu, J., ... & Yan, J. (2008). Factors influencing leaf litter decomposition: an intersite decomposition experiment across China. *Plant and Soil*, *311*, 61-72.

Zhou, G., Wang, Y., & Wang, S. (2002). Responses of grassland ecosystems to precipitation and land use along the Northeast China Transect. *Journal of Vegetation Science*, *13*(3), 361-368.

Zhou, G., Wei, X., Wu, Y., Liu, S., Huang, Y., Yan, J., ... & Liu, X. (2011). Quantifying the hydrological responses to climate change in an intact forested small watershed in Southern China. *Global Change Biology*, *17*(12), 3736-3746.

Zhou, S. X., Huang, C. D., Han, B. H., Xiao, Y. X., Tang, J. D., Xiang, Y. B., & Luo, C. (2017). Simulated nitrogen deposition significantly suppresses the decomposition of forest litter in a natural evergreen broad-leaved forest in the Rainy Area of Western China. *Plant and Soil*, *420*, 135-145.

Zhou, Z., Wang, C., & Luo, Y. (2018). Effects of forest degradation on microbial communities and soil carbon cycling: a global meta-analysis. *Global Ecology and Biogeography*, *27*(1), 110-124.

Zhu, H. Z., Jiang, C. Y., & Liu, S. J. (2022). Microbial roles in cave biogeochemical cycling. *Frontiers in Microbiology*, *13*, 950005.

Žifčáková, L., Větrovský, T., Howe, A., & Baldrian, P. (2016). Microbial activity in forest soil reflects the changes in ecosystem properties between summer and winter. *Environmental microbiology*, *18*(1), 288-301.